PHD

Characterisation of SHIP-1 as a Regulator of T Lymphocyte Function

Harris, Stephanie

Award date:
2010

Awarding institution:
University of Bath

Characterisation of SHIP-1 as a Regulator of T Lymphocyte Function

Stephanie Jean Harris

A thesis submitted for the degree of Doctor of Philosophy

University of Bath
Department of Pharmacy and Pharmacology

September 2010

Declaration of work done in conjunction with others

The work shown in Figure 8.1 was performed by Matthew Thomas of Novartis

Acknowledgements

I would like to thank my supervisor, Prof. Steve Ward for his help and support throughout my PhD. I would also like to thank Richard Parry for all his help. I am very grateful to the other members of the Ward lab past and present for their help and friendship.

I would also like to thank the other occupants of the postgrad office for help and entertainment. I would like to thank my Industrial supervisor, John Westwick for advice, support and funding. I would also like to thank Matt Thomas and his group at Novartis for their help and encouragement.

In addition I would like to thank Adrian Rogers for his help with confocal microscopy and flow cytometry and to acknowledge Lai Wei for help with optimisation of CD8+ T cell cytotoxicity protocols.

Finally, I would like to thank Matt Hanna for his help.

Publications

Parry RV, Harris SJ, Ward SG. (2010) Fine tuning T lymphocytes: A role for the lipid phosphatase SHIP-1. *Biochim Biophys Acta*. *Proteins and Proteomics* **1804:** 592-7.

Harris SJ, Foster JG, Ward SG. (2009) PI3K isoforms as drug targets in inflammatory diseases: lessons from pharmacological and genetic strategies. *Curr Opin Investig Drugs.* **10**:1151-62.

Harris SJ, Parry RV, Westwick J, Ward SG. (2008) Phosphoinositide lipid phosphatases: natural regulators of phosphoinositide 3-kinase signaling in T lymphocytes. *J Biol Chem*. **283**:2465-9.

Abstract

PI3Ks have been shown to have many important functions in T cells, including in cell growth and survival, chemotaxis and differentiation; however, the role of SHIP-1 as a negative regulator of PI3K signalling has not been so thoroughly investigated. The use of knockout mouse models has given an insight into the role of SHIP-1 in murine T cells, but these are compromised by loss of function during development which impinges upon mature T cell function. In addition, some work has been undertaken to investigate the role of SHIP-1 in human leukaemic T cell lines, but it is not clear how these findings might translate to SHIP-1's function in normal cells.

Therefore the work in this thesis was undertaken to investigate the role of SHIP-1 in primary human T lymphocytes. Initial experiments demonstrated that SHIP-1 was active both in unstimulated cells and in response to a variety of stimuli. Using a lentiviral method to deliver shRNA against SHIP-1 and a constitutively active form of SHIP-1 it was found that whilst constitutive activation of SHIP-1 led to cell death, silencing of SHIP-1 expression resulted in viable cells which failed to proliferate. Furthermore, silencing of SHIP-1 revealed its crucial role in the regulation of basal PI3K signalling, actin polymerisation, cell morphology and basal motility. Interestingly, there was no additional defect in chemotaxis, in agreement with findings that SHIP-1 and TAPP PH domain probes did not localise to specific regions of the cell membrane during chemotaxis. In addition, silencing of SHIP-1 caused an abnormal profile of cytokine production and in particular, CD4+ T cells were skewed towards becoming Tregs.

The observations in this study suggest that whilst the role of SHIP-1 in primary human T cells has some similarities to its role in both murine T cells and leukaemic cell lines, there are also significant differences which it will be crucial to take into account when designing drugs to target SHIP-1.

The final results section comprises work completed for Novartis, the sponsor of this PhD. In this section it was found that knockout of PI3Kγ in mice resulted in elevated production of IL-17A and IL-17F along with abberant expression of IL-17 receptors and loss of PI3K signalling in response to IL-17A. These findings are of particular relevance for PI3Kγ inhibitors that are in clinical trials for inflammation and autoimmune diseases.

Table of Contents

List of Figures

Chapter 4

Chapter 5

Chapter 8

Chapter 9

List of Tables

Chapter 1

Chapter 2

List of Abbreviations

aa	Amino acid
ACAD	Activated T cell autonomous death
ADAP	Adhesion and degranulation promoting adaptor protein
AICD	Activation induced cell death
AML	Acute myeloid leukaemia
AP-1	Activator protein 1
APC	Antigen presenting cell
A-TLL	Adult T cell leukaemia/lymphoma
Bcl-xl	B-cell lymphoma-extra large
BCR	B cell receptor
CD	Cluster of differentiation
CDC42	Cell division control 42 kDa
CIA	Collagen induced arthritis
CTL	Cytotoxic T lymphocyte
CTLA-4	Cytotoxic T-Lymphocyte Antigen 4
DAG	Di acyl glycerol
DC	Dendritic cell
DOCK	Dedicator of cytokinesis 2
DOK	Downstream of tyrosine kinase 2
ER	Endoplasmic reticulum
Fc	Fragment crystalisable
FOXO	Forkhead box
FOXP3	Forkhead box P3

GAB2	Grb2-asociated binding protein 2
GADS	Grb2-related adaptor downstream of Shc
GEF	Guanine nucleotide exchange factor
GM-CSF	Granulocyte macrophage-colony stimulating factor
GPCR	G protein coupled receptor
Grb2	Growth factor receptor bound protein 2
GvHD	Graft vs. host disease
HEK 293T	Human embryonic kidney cell line strain 293T
HEPES	4-(2-hydroxyethyl)-1-piperazineethanesulfonic acid
HEV	High endothelial venules
IBD	Inflammatory bowel disease
ICOS	Inducible costimulator
IFN	Interferon
Ig	Immunoglobulin
IKK	IκB kinase
IL	Interleukin
IP3	Inositol trisphosphate
IPEX	Immunodeficiency, polyendocrinopathy and enteropathy, X-linked syndrome
ITAM	Immunoreceptor tyrosine based activation
iTreg	Induced regulatory T cell
KI	Knockin
KO	Knockout
LAT	Linker of activated T cells

LFA-1	Lymphocyte function-associated antigen 1
MDF	Mouse Dermal Fibroblast
MFI	Mean fluorescence intensity
MHC	Major histocompatibility complex
miR	Micro RNA
MMP	Matrix mettaloproteinase
MTOC	Microtubular organizing center
mTOR	Mammalian target of rapamycin
mTORC2	mTOR complex 2
NFAT	Nuclear factor of activated T cells
NFκB	Nuclear factor κB
NK	Natural killer cell
nTreg	Natural regulatory T cell (thymus derived)
OVA	Ovalbumin
PD-1	Programmed death-1
PH	Pleckstrin homology
PI3K	Phosphatidylinositol 3-kinase
$PI(3,4,5)P_3$	Phosphatidylinositol (3,4,5) tris phosphate
PKA	Cyclic AMP dependent protein kinase
PKG	Cyclic GMP dependent protein kinase
p-Rex-1	$PI(3,4,5)P_3$-dependent Rac exchange factor 1
PTEN	Phosphatase and tensin homologue
RA	Rheumatoid arthritis
RBC	Red blood cell

RBD	Ras binding domain
RIAM	Rap1-GTP interacting adaptor molecule
ROR	RAR- related orphan receptor
S1P	Sphingosine 1 phosphate
S6K	S6 kinase
SAP	SLAM associated molecule
SEB	Staphylococcal enterotoxin B
SF	Steel factor
SGK	Serum-and glucocorticoid-induced protein kinase
SHIP	SH2 domain containing inositol phosphatase
SKAP-55	Src kinase associated phosphoprotein 55 kDa
SLAM	Signalling lymphocytic activation molecule
SLE	Systemic lupus erythromatosis
SLO	Secondary lymphoid organs
SLP-76	SH2 domain containing leukocyte protein 76 kDa
SOCS	Suppressor of cytokine signalling 1
SOS	Son of sevenless
s-SHIP	Stem cell SHIP
STAT	Signal transducer and activator of transcription
T-ALL	T cell acute lymphoblastic leukaemia
Tbet	T box expressed in T cells
TCR	T cell receptor
Tfh	Follicular T helper cell
TGF	Transforming growth factor

Th	T helper cell
TIAM	T cell lymphoma invasion and metastasis
TNF	Tumour necrosis factor
TRAIL	TNF-related apoptosis-inducing ligand
Treg	Regulatory T cell
UTR	Untranslated region
VLA-4	Very late antigen 4
WT	Wild Type
ZAP70	Zeta chain associated protein kinase 70kDa

Chapter 1: Introduction

In this section, the immune system will be introduced and the various components of the innate and adaptive immune systems discussed. The Introduction will then focus upon T cells, examining the range of T cells subsets, their activation and chemotaxis. Next the phosphatidylinositol -3 kinase (PI3K) signalling pathway will be described, with an emphasis on its role in immune cells and its regulation by lipid phosphatases, including SH2 domain containing inositol phosphatase-1 (SHIP-1). In addition, the role of the PI3K signalling pathway in inflammation and disease will also be covered, using the example of airway inflammation, including the potential of PI3Ks and lipid phosphatases as targets for drug discovery.

1.1 The immune system

1.1.1 Innate immunity

The immune system serves two main roles in the body. Firstly its searches for and neutralises pathogens, including extracellular pathogens, intracellular pathogens, fungi, and parasites such as worms. The second function of the immune system is to remove unhealthy, dead or cancerous cells. The immune system can be broadly divided into two branches; innate and adaptive immunity. The innate immune system consists of phagocytes (i.e. macrophages, neutrophils and dendritic cells) as well as mast cells, eosinophils basophils and natural killer cells. Common motifs on pathogens can be recognised by pattern recognition receptors on cells of the innate immune system (2). Phagocytes can engulf pathogens, whilst mast cells, eosinophils and basophils release inflammatory mediators such as histamine to trigger inflammation and initiate further leukocyte recruitment. Natural killer (NK) cells kill tumour cells or cells infected with virus that fail to present major histocompatibility complex I (MHCI) (3). γδ T cells may also be considered to be part of the innate immune system as the T cell receptor (TCR) can function as a pattern recognition receptor (4, 5).

1.1.2 Adaptive immunity

Dendritic cells can be described as a bridge between innate and adaptive immunity as they are professional antigen presenting cells (APCs)(6). The main components of the adaptive immune system are B cells and T cells. T cells may be either CD (cluster of differentiation) 8+ T cells, which recognise antigen presented by MHC I (found on all cells) and primarily kill cancerous or virally infected cells, or they can be CD4+ and recognise antigen presented by MHC II which is found on macrophages, dendritic cells and B cells (7). CD4+ T cells differentiate into a number of effector cell

subtypes that can be classified according to their transcription factor and cytokine expression profile (3, 8) (Figure 1.1).

1.2 CD4+ T cell subsets and CD8+ T cells

1.2.1 Overview of T cell subsets

Mosmann and Coffman were the first to describe how T helper cells could be of either Th1 or Th2 phenotypes (8). Broadly, Th1s, which are characterised by the secretion of IFNγ, aid cell mediated killing, by directing B cells' production of opsonising antibodies and supporting macrophage-mediated killing. Th2s help B cells to make neutralising antibodies and are characterised by the production of IL-4 (9). More recently another subset of T helper cells has been identified, namely the Th17 subset, which produce the signature cytokine IL-17 and encourage tissue based immunity, for example by triggered IL-6 production by fibroblasts (10, 11). Further T cells subsets include the recently identified Th9 (12, 13), and Th22s (14), which produce IL-9 and IL-22 respectively. Although niche functions of these cells have been identified their overall significance is as yet unclear. Tregs are a further subset of T helper cells which are suppressive upon other cell types. Tregs may develop in the thymus or can be developed from naïve T cells in the periphery. They may release signature cytokines including TGFβ and IL-10. Some would also consider follicular T cells to be a separate class of T helper cells (Tfh)(9).The CD4+ T cell subsets will now be considered in more detail.

1.2.2 Th1 cells

Th1 cells produce IFNγ and IL-12. In addition they produce lymphotoxin, tumour necrosis factor α (TNFα) and substantial quantities of IL-2. They aid B cell class switching to immunoglobulin G2a (IgG2a) and stimulate macrophage activity, thus promoting the destruction of cells infected with intracellular pathogens such as *Listeria monocytogenes*. Th1 cells are implicated in the pathology of autoimmune diseases, for example multiple sclerosis (15, 16).

Th1 differentiation is initiated by IFNγ or the IL-12 family member IL-27 (whose receptors are expressed on naive cells) triggering the activation of signal transducer and activator of transcription 1 (STAT1) which upregulates the T-box transcription factor Tbet. Tbet induces production of IFNγ, remodels the ifnγ gene locus and also

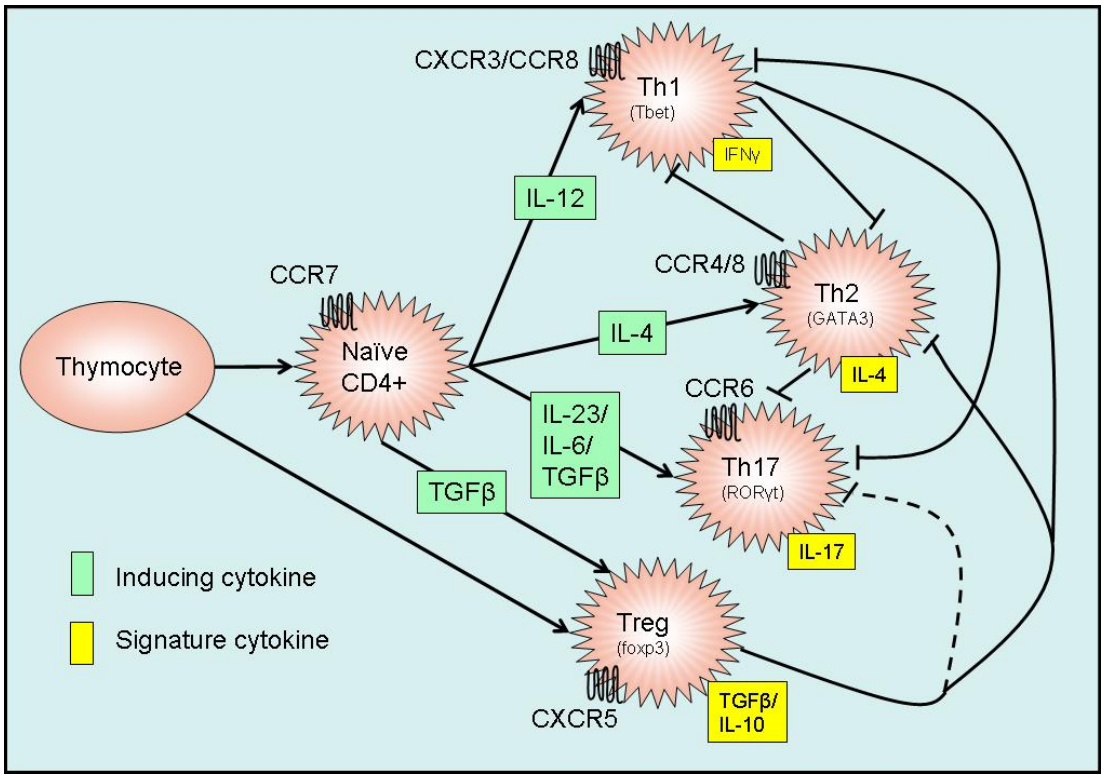

Figure 1.1: CD4+ T cell subsets

Tregs can be induced from thymocytes or from naive cells in the periphery. All other CD4+ subsets are induced in the periphery. T helper 1 (Th1) differentiation is induced by interleukin -12 (IL-12), Th2 differentiation by IL-4, and Th17 most likely by a combination of IL-23, IL-6 and transforming growth factor β (TGFβ). They then produce their signature cytokines, amongst others: interferon γ (IFNγ) is produced by Th1, IL-4 by Th2, IL-17 by Th17 and IL-10 and TGFβ by regulatory T cells (Tregs). IFNγ suppresses Th2 and Th17 differentiation and function, IL-4 suppresses Th1 and Th17, Treg cytokines suppress Th1, Th2 and probably Th17s. It is not clear whether IL-17 has suppressive actions on particular CD4+ subsets (17) although there is some evidence that it may regulate Th1 function (18). Signature chemokine receptors and transcription factors are also shown.

increases transcription of the β chain of the receptor for IL-12 (19). In some limited circumstances, STAT1 signalling may be dispensable for the generation of IFNγ producing Th cells (20). The transcription factor Eomes also plays an important role in the control of the Th1 lineage (21) as do STAT2 and STAT4. Tbet and STAT4 contribute to a positive feed back loop by upregulating IFNγ and IL-12Rβ2, but also inhibit Th2 responses by downregulating the transcription factor GATA3. TCR signalling controls activation of the transcription factors nuclear factor of activated T cells (NFAT), nuclear factor κB (NfκB) and activator protein 1 (AP-1), and strong TCR signalling biases towards Th1 development (22).

1.2.3 Th2 cells

Th2 cells produce IL-4, IL-5 and IL-13: these aid B cell class switching to produce IgE and IgG1, help eosinophil recruitment and promote mucosal defence. Therefore Th2 cells play a role in defence against extracellular pathogens such as helminths (23). Aberrant Th2 responses are implicated in allergic diseases such as asthma (9).

Naive CD4+ T cells express the IL-4 receptor, and IL-4 stimulates the receptor to activate STAT6. In combination with IL-2 mediated activation of STAT5, this causes the cells to differentiate into Th2s as well as causing production of the transcription factor GATA3. GATA3 remodels the il-4 locus to facilitate increased IL-4 transcription upon restimulation (24), although it does not directly bind the IL-4 promoter itself (25). However, it can bind the IL-5 and IL-13 promoters (26). Activation of the transcription factors AP-1, NFAT and NFκB also aids the differentiation of Th2 cells, although NFAT1 also plays a part in a negative feedback loop to inhibit IL-4 production (27).

The Th2 phenotype is reinforced by cytokine feed back loops. IL-4 induces its own expression, whilst the cells become unresponsive to IFNγ and IL-12. In human cells, some degree of plasticity remains, for example if Th1 cells are cultured under Th2 skewing conditions, then a proportion of the cells will start to express both IFNγ and IL-4 (28).

1.2.4 Th17 cells

In order to induce differentiation towards a Th17 phenotype, TGFβ and IL-6 are required in mice, and IL-1 and TNFα may also play a role (29-31). Whilst IL-23 is not

required for the generation of murine Th17 cells it is thought to aid in their expansion and maintenance once differentiated (31). Human Th17 generation is thought to require at least IL-1β, IL-23 and TGFβ, although a consensus has not been reached (protocols for generation of human Th17 cells are comprehensively reviewed by de Jong *et al.* (32)).

Th17 cells are believed to be generated using STAT3 signalling, whilst STAT1 and 5 are inhibitory upon Th17 development (33). STAT3 also binds IL-17 and IL-17F promoters (34). Retinoic Acid Receptor- related orphan receptor γt (RORγt) (which is expressed in response to STAT3) and RORα are both involved in Th17 differentiation and RORγt is required for the production of IL-17 and IL-17F (35). Similarly, an absence of RORα reduces IL-17 expression, whilst interferon regulatory factor (IRF) is also thought to aid Th17 differentiation (33). Development of Th17 is inhibited by other cytokines for example IL-2 and IFNγ (29). TGFβ facilitates expression of the IL-23R. Note that in the absence of IL-6, TGFβ induces Tregs rather than Th17 (33).

The Th17 cells produce IL-17A, IL-17F, IL-21 and IL-22 as well as the Th1-expressed cytokines TNFα and lymphotoxin β (36). Th17 cells also preferentially express the chemokine receptor CCR6 and its ligand, the chemokine CCL20 (also known as MIP3α) (37). However, Th17 cells express neither IFNγ nor IL-4 (33). Furthermore both IFNγ and IL-4 inhibit Th17 differentiation (11) (however there is some evidence of CD4+ cells that express both IFNγ and IL-17 (33)). IL-27 also negatively regulates IL-17 production. IL-2 signalling has been shown in mice to reduce IL-17 production and increase generation of Tregs (38).

IL-17A drives a tissue based immune response to combat extracellular pathogens such as bacteria and fungi via the production of IL-6, IL-8, granulocyte macrophage colony stimulating factor (GM-CSF), matrix metalloproteinases (MMPs) and chemokines including CXCL1 and CXCL10 (31) to orchestrate the recruitment of macrophages and neutrophils to tissues (33). IL-17F has about 50% homology to IL-17A with similar functions (31, 36, 39). IL-17A and IL-17F have been implicated in airway inflammation (36, 40, 41) as well as diseases including multiple sclerosis, psoriasis, inflammatory bowel disease (IBD), rheumatoid arthritis (RA) and systemic

lupus erythromatosis (SLE) (36, 42). Furthermore, IL-17A and IL-17F are thought to have both pro- and anti- tumour functions, with IL-17F in particular exacerbating tumour growth by facilitating angiogenesis (43).

1.2.5 Treg cells

Tregs can be broadly divided into natural Tregs (nTregs), which are generated in the thymus, and inducible T regs (iTregs), which can be generated from naive T cells in the periphery or *in vitro* (44 - 46). Tregs can be generated *in vitro* by TGFβ, and express the transcription factor forkhead box P3 (foxp3). Mutations in foxp3 in mice or humans, leads to Scurfy mice and IPEX syndrome (immunodeficiency, polyendocrinopathy, and enteropathy, X-linked syndrome) respectively (47). A key target of Foxp3 is the micro RNA miR155. miR155 suppresses suppressor of cytokine signalling 1 (SOCS1) and increases proliferation of Tregs in response to IL-2 (48). miR155 is also upregulated in naive T cells upon activation and when miR155 is lost, cells are skewed towards a Th2 phenotype (49). In addition, there are several reports of the lipid phosphatase SHIP-1 being negatively regulated by miR155, indicating that loss of SHIP may have opposite effects of miR155 loss (50). The control of SHIP-1 by miR155 will be covered in the Discussion.

Tregs may be further subdivided, with some researchers considering TGFβ-producing cells as a separate class of T helper cells termed Th3, whilst those producing IL-10 are described as Tr1 cells. Interestingly, some cells can also express both foxp3 and RORγt and are therefore Tregs with the ability to produce IL-17 (51-53). In addition, subpopulations of foxp3 positive cells have also been shown to express GATA3 (15) and Tbet (54) with the latter playing a particular role in the suppression of Th1 responses.

1.2.6 CD8+ T cells

CD8+ T cells are also known as cytotoxic T lymphocytes (CTLs). The main function of CD8+ T cells is to lyse cells that are either cancerous or infected with viruses, using perforins and granzymes. Granzymes are a family of serine proteases and CTLs produce granzyme A and granzyme B (55). CTLs also release the antiviral cytokines IFNγ and TNFα (although CTLs have recently been shown to secrete IL-17 as well (56-58)). However, individual cells do not necessarily express all granzymes, perforins and cytokines (59). Eomesodermin drives the production of cytokines and cytotoxic products, although T-bet is also thought to play a role (60, 61). TCR

stimulation and signalling from cytokines such as IL-2 are also important in initiation of granzyme production (62).

Granzymes and perforins bound to serglycin are stored in cytotoxic granules, a type of secretory lysosome (63). Upon TCR ligation, the secretory granules move to the supramolecular activation cluster (SMAC) at the immunological synapse (64). The granzymes enter target cells through the actions of perforins (58). The exact process is not clearly understood but is thought to involve perforins making pores in the target cell that allow calcium influx and trigger endocytosis (65). Once in the target cell, granzyme A can initiate caspase independent cell death by initiating mitochondrial damage leading to DNA damage and subsequent apoptosis (66). Granzyme B can activate caspases, including caspase 3 to initiate apoptosis (67).

1.3 T cell trafficking

1.3.1 Immune surveillance and T cell trafficking

T cells generally encounter antigens presented by professional APCs in secondary lymphoid organs (SLOs) such as lymph nodes. In order for this to occur during normal immune surveillance, T cells must be directed to leave the blood and to migrate through the SLO in a manner which encourages them to encounter their cognate antigen, followed by egress from the lymph node, across a further endothelial cell barrier, to re-enter the vascular system (68). This process is orchestrated by chemokines (see below), selectins, integrins and sphingosine 1 phosphate (S1P).

Lymphocytes in the blood express selectins and α4 integrins (e.g. Very Late Antigen -4, VLA-4) on the tips of their microvilli. These tether to their ligands (e.g. vascular cell adhesion molecule-1 (VCAM-1)) on the endothelial cell wall, in the face of shear flow, allowing rolling to occur. This can occur spontaneously, without need of integrin activation. T lymphocytes also use LFA-1 during rolling, but not in making the initial tethering contact (69-71). Once tethered or rolling, T cells can come into contact with chemokines associated with the endothelium. If they express a cognate receptor for these chemokines, the T cell will arrest and undergo firm adhesion via LFA-1 and α4 integrins. It will then extravasate from the blood vessel using CD31, LFA-1 and α4 integrins. Expression of a variety of chemokine receptors allows the correct T cell to

be recruited and if necessary retained in a particular tissue. For example; lymphocytes expressing CCR7 and L-selectin will home to secondary lymphoid tissues by virtue of their expression of the CCR7 ligands CCL21 and CCL19. Expression of L-selectin and the CCR7 ligand CCL21 (and possibly CCL19) by the high endothelial venules (HEVs) promotes diapedis of the naïve T cells as illustrated in Figure 5 (72), whilst central memory T cells may undergo diapedis in response to CXCL12/CXCR4 signalling (73). CCL21 gradients then direct the T cell to migrate through the SLO for 6-24 hours, where it can interact with dendritic cells (DC), which may bear its cognate antigen (74), although random movement of T cells within SLOs has also been observed (75). Sphingosine-1 phosphate gradients promote the egress of T cells from SLOs, a process which is antagonised by CCR7 ligands (76).

During an adaptive immune response, the above process is facilitated by upregulation of ICAM-1 and CCL21 on the HEV to encourage migration into lymph nodes (77). Once activated, expression of specific chemokine receptors facilitates migration to sites of peripheral inflammation; for example CCR9 allows homing to the small intestine and CCR4 and CCR10 to the skin (78). Furthermore, subsets of T helper cells express characteristic chemokine receptors (Th1 CXCR3 and CCR5, Th2 CCR4 and CCR8 (79), Th17 CCR6 (37), Th22 CCR10 (14, 80) and Tfh CXCR5. Tregs express a variety of chemokine receptors, but change from expressing CCR7 to CXCR5 upon activation (81)). The signature cytokines released by these cells encourage tissue resident cells to release appropriate chemokines to recruit more cells from the same T helper subtype, thus contributing to a positive feedback loop during the adaptive immune response (82).

1.3.2 The role of chemokines in the immune system

Chemokines (*chemo*tactic cyto*kines*) are small proteins, approximately 8-10kDa, which derive their names from characteristic cysteine residues in CC, CXC C or CXXXC motifs at the amino terminus. There are over 50 chemokines and 18 chemokines receptors (83, 84). Most chemokine receptors can bind different chemokines, and some chemokines can also act at several different receptors. Although some chemokines have homeostatic functions (such as CCR7 ligands), the majority are released from cells upon inflammation in order to recruit leukocytes (85). Chemokine receptors are 7 transmembrane GPCRs, coupled to Gαi (84). Classically viewed as forming a chemokine gradient in order to direct chemotaxis, in fact a key role of chemokines is to induce arrest of leukocytes on the endothelium and firm

adhesion through intergrin clustering and affinity changes (86, 87). In addition to the functional chemokine receptors, two non-signalling receptors, D6 and duffy antigen receptor for chemokines (DARC) have been identified. D6 serves to scavenge and endocytose excess inflammatory chemokines, whilst DARC scavenges excess chemokines and also aids the uptake of chemokines by endothelial cells for subsequent display to leukocytes (88, 89).

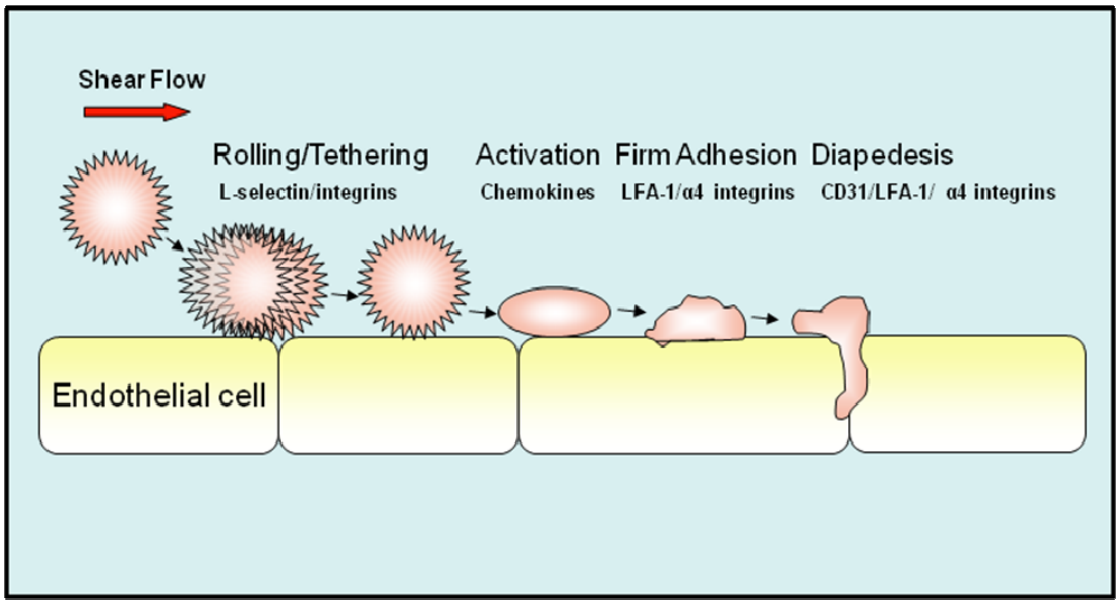

Figure 1.2: T cell extravasation from the blood

T cells in the blood make temporary contact with endothelial cell through the interaction of L-selectin and integrins with their ligands presented on the surface of endothelial cells. Chemokines activate multiple pathways within the cell to cause flattening and firm adhesion, which is mediated by the actions of LFA-1 and α4 integrins. The cell may then crawl along the endothelial cell until it reaches a junction between endothelial cells, at which point it will extravasate from the blood vessel in a process known as diapedesis (90).

1.3.3 T cell activation

T cell activation is described by a two signal model. “Signal 1” occurs when an antigen presenting cell presents antigen on an MHC. The MHC and antigen are bound by the T cell’s TCR. The MHC protein is also bound by either CD4 or CD8 on the T cell. “Signal 2” is initiated by the binding of costimulatory molecule on the T cell (typically CD28) by an appropriate ligand such as CD80/CD86 (B7) on the antigen presenting cell. Without signal 2, signal 1 induces anergy in the T cell, a protective mechanism which prevents aberrant response to self-antigen (91) (Figure 1.3). Other molecules can also provide a costimulatory signal, for example, ICOS, an inducible costimulator which is expressed on activated T cells, Lymphocyte function-associated antigen 1 (LFA-1) and some β1 integrins including Very late antigen-4 (VLA-4). Negative regulation of TCR signalling also occurs, firstly through termination of the existing signals, for example by the actions of phosphatase and tensin homolog (PTEN) or though recruitment of negative regulators of signalling such as the Dok adaptor proteins of SH2-domain-containing tyrosine phosphatase 1 (SHP1) to the TCR signalosome, and secondly through the actions of inhibitory co-receptors such as Cytotoxic T-Lymphocyte Antigen 4 (CTLA-4) and Programmed Death 1 (PD-1) (92, 93). Signal 1 and 2 initiate a range of intracellular signalling pathways in the T cell including PLCγ and PI3K signalling pathways (Figure 1.4). These have a number of crucial roles in T cell activation, perhaps the most important of which is the production of IL-2. IL-2 is a key factor in the survival and proliferation of T cells (94). Furthermore, activated T cells upregulate expression of CD25 (the IL-2 receptor α chain) via NFAT transcription factors, in order to increase the positive feedback loop (95).

The signalling pathways that control T cell activation will now be considered in more detail. The T cell receptor consists of α and β chains, (which are variable in nature and can recognise and bind their cognate antigen), associated non-covalently with dimers of different CD3 proteins. Antigen binding, in the context of MHC presentation, leads to the phosphorylation of immunoreceptor tyrosine based activation (ITAM) motifs on CD3 molecules by Src kinases, thus initiating the formation of signalling complexes. This starts with recruitment of the adaptor protein zeta chain associated protein kinase 70 kDa (ZAP-70) which in turn recruits linker of activated T cells (LAT) (96). LAT can bind phospholipase Cγ (PLCγ), SH2 domain containing leukocyte protein 76 kDa (SLP-76) and the p85 adaptor subunit of PI3Ks as well as growth factor receptor bound protein 2 (Grb2) and Grb2-Related Adaptor

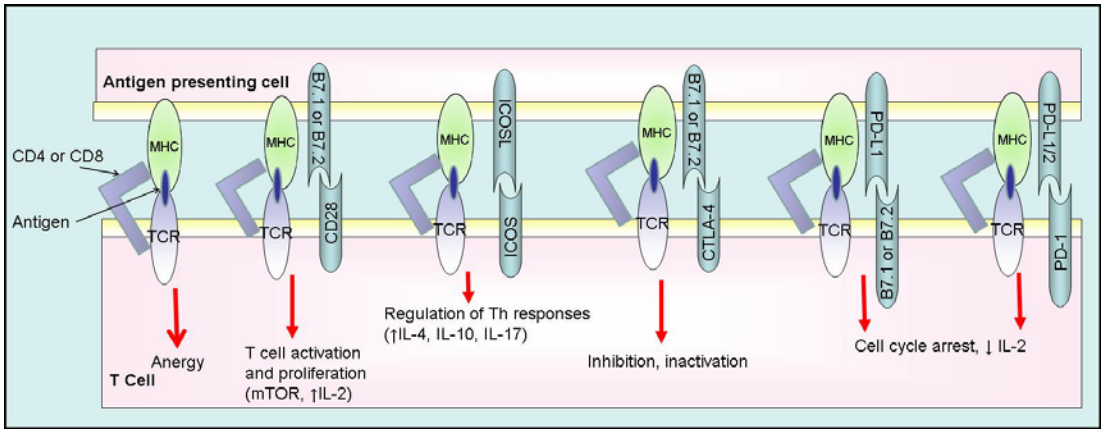

Figure 1.3: T cell activation and costimulation
The TCR recognises a peptide antigen when it is presented by MHC complexes. CD4 recognises class II MHC, expressed by professional antigen presenting cells, whilst CD8 recognises class I MHC, which is expressed on all cells. This signal alone (signal 1) induces anergy, or even death of the T cell. However, signal 2 can be provided by B7.1 or B7.2 on the antigen presenting cell (APC) binding CD28. CD28 is widely expressed on T cells and direct the cell towards activation and proliferation (e.g. IL-2 production). ICOS is upregulated upon T cell activation, and therefore serves to modulate the functions of the active cell through interactions with ICOSL. Negative regulation of T cell responses is achieved via the interaction of B7.1 or B7.2 with CTLA4 (the expression of which is also upregulated upon activation of T cells), or via Programmed Death ligand (PD-L) costimulation (97-99).

Downstream of Shc (GADS). Thus PI3K, inositol trisphosphate (IP_3) (which leads to Ca^{2+} flux) and diacyl glycerol (DAG) signalling pathways are all controlled by the TCR (Figure 1.4). CD28 initiates PI3K signalling by recruitment of the p85 adaptor to the pYMNM motif (100). The $PI(3,4,5)P_3$ generated serves to recruit PDK1 and Akt. In the case of T cell activation, two Akt signalling pathways are of particular importance. Firstly, inhibition of GSK3β prolongs nuclear localisation of NFAT and hence increases IL-2 production. Akt also activates NFκB, causing the transcription of pro survival genes such as Bcl-xl (B-cell lymphoma-extra large). $PI(3,4,5)P_3$ also recruits Itk, thus regulating the ERK signalling pathway (101).

Full T cell activation requires polarisation of the cell, with movement of the microtubular organizing center (MTOC) towards the site of contact with the APC and the formation of a strong synapse, in the form of a supramolecular activation cluster (SMAC) (102). The central SMAC is rich in TCRs, whilst the peripheral SMAC has a high density of integrins to facilitate adhesion (103).

Adhesion of T cells to the endothelium or to antigen presenting cells requires actin polymerisation and inside-out signalling from the TCR to integrins to increase their affinity for their ligands. This involves the formation of signalling complexes initiated by recruitment of adhesion and degranulation promoting adaptor protein (ADAP) to SLP-76 (104, 105). ADAP binds Src kinase associated phosphoprotein 55 kDa (SKAP-55) and Rap1-GTP interacting adaptor molecule (RIAM) and translocates to the cell membrane, possibly through the interaction of RIAM's pleckstrin homology (PH) domain with phosphatidylinositol 3,4 bisphosphate ($PI(3,4)P_2$) (106). This complex facilitates the recruitment of Talin to the tails of the integrins. Lastly, PLCγ1 stimulated PKD1 association with Rap1 causes its activation and hence the recruitment of RAPL (107, 108). RAPL initiates the clustering of integrins and changes in their conformation to improve their affinity for their ligands (Figure 1.5). Furthermore, TCR signalling can itself mediate integrin activation, whilst LFA-1 contributes to T cell adhesion to antigen presenting cells, allowing a stable contact to form at the synapse (90).

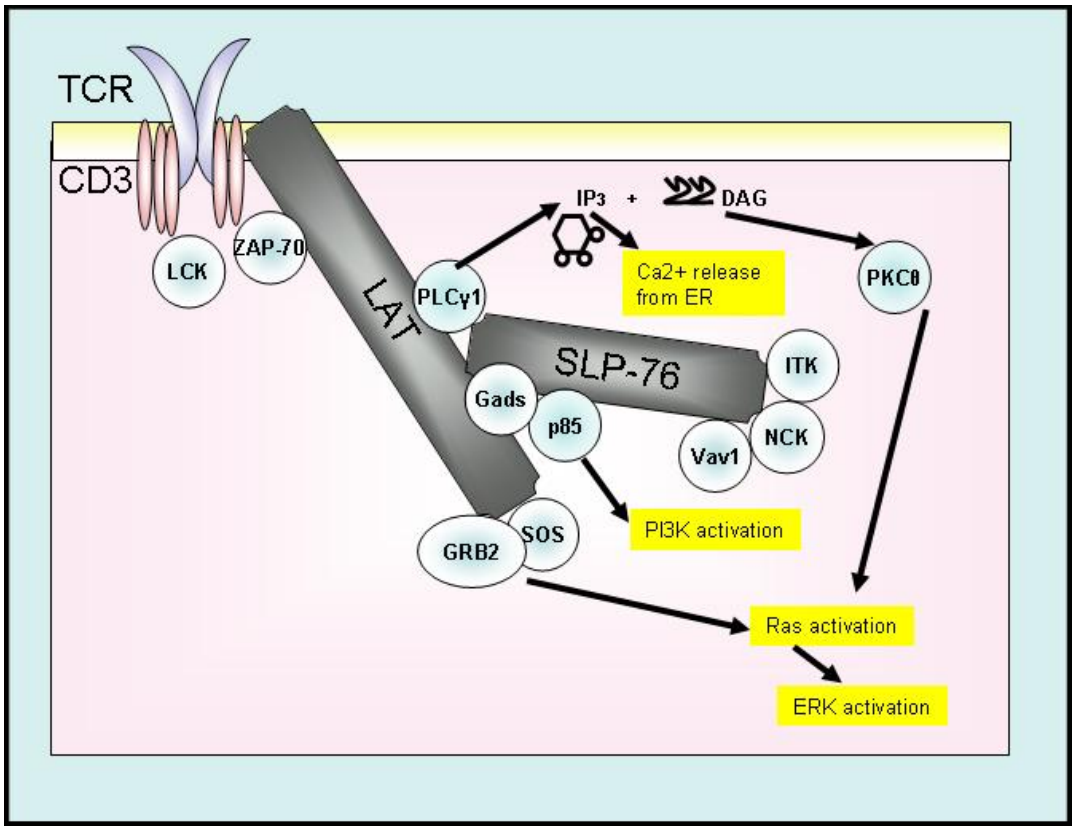

Figure 1.4: Signalling initiated by T cell activation
Upon TCR activation, leukocyte-specific protein tyrosine kinase (LCK) activates ZAP-70 which phosphorylates tyrosine residues on LAT, facilitating recruitment of GADS and SLP-76. ZAP-70 further phosphorylates SLP-76, allowing the recruitment of more SH2 domain containing proteins. SLP-76 also has a proline rich domain which allows recruitment of SH3 domain containing proteins including PLCγ1 and ITK. The involvement of Gads in the signalling complex allows the recruitment of PI3K, whilst PLCγ1 cleaves $PI(4,5)P_2$ to yield IP_3 and DAG. IP_3 acts on its receptors on the endoplasmic reticulum (ER) to initiate Ca^{2+} release, this leads to colocalisation of STIM with CRAC channels to allow extracellular Ca^{2+} to enter the cell. In addition, DAG triggers PKCθ activation and recruitment of RasGRP (guanyl nucleotide-releasing protein). Protein kinase Cθ (PKCθ) activates RasGRP, which removes GDP from Ras, allowing it to bind GTP and thus activating it (92).

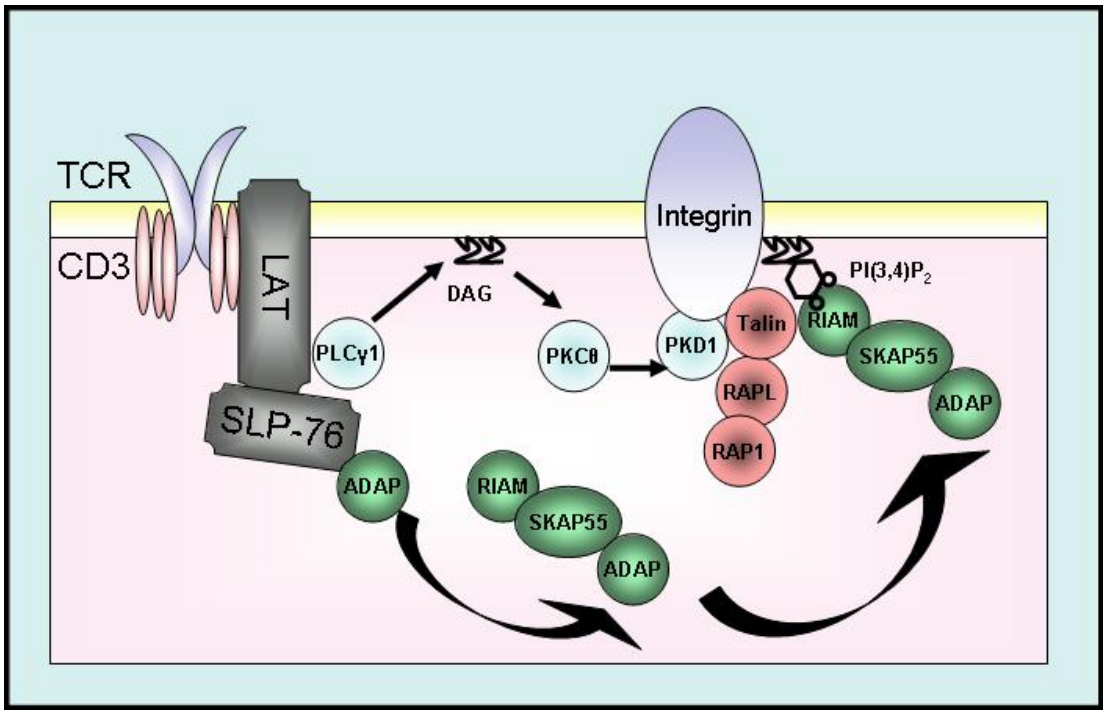

Figure 1.5: Integrin activation by TCR signalling
The LAT/SLP-76 complex is assembled as described in Figure 1.4. ADAP is recruited to SLP-76 and complexes with RIAM and SKAP55. These then localise the membrane where RIAM is thought to bind $PI(3,4)P_2$ by virtue of its PH domain. The complex recruits RAP1 (Repressor Activator Protein) and RAPL (regulator of cell adhesion and polarization enriched in lymphoid tissues) and subsequently Talin. PLCγ1 is recruited to the TCR signalosome, and mediates generation of DAG which activates PKCθ and in turn PKD1, which contributes to the recruitment and activation of Rap1. Talin and RAPL mediate the clustering of integrins and the conformational changes required to increase their affinity.

1.3.4 Reactive oxygen species in cell signalling

Thus far, an examination of signalling pathways has focussed on the role of proteins and phospholipids. Yet other molecules can also play a key role in cell signalling. For example it is well known that reactive oxygen species (ROS) are generated by a range of phagocytic cells and have a key role in mediating microbial killing (109). However, ROS are also generated in a range of other cell signalling pathways, including TCR signalling (110, 111) and death receptor signalling (112), where they are key mediators of apoptosis.

1.3.5 Resolution of the T cell response

During the adaptive immune response there is a large proliferation of T cells (the expansion phase). However, as infection is resolved, many of these cells will become surplus to requirement and die. This can happen in two main ways: activation induced cell death (AICD) and activated T cell autonomous death (ACAD). AICD relies upon TCR stimulation and also upon cytokines particularly IL-2 (113). It is not currently clear how IL-2, which generally increases the survival and expansion of T cells, switches during the contraction phase to sensitise to AICD, although it has been hypothesised that IL-2 signalling drives the expression of CD95L (FasL) (114). TCR signals also generate ROS which can initiate a mitochondrial dependent death pathway and aid expression of CD95L (115).

Death receptors can play a key role in AICD. Three main receptors are implicated: Fas, TNFα, and TNF-related apoptosis-inducing ligand (TRAIL) receptors (116). Knockout of the Fas receptor (CD95) in mice results in accumulation of T cells and autoimmunity (116, 117). The involvement of TNF signalling in AICD is less well characterised but inhibition of TNF signalling can reduce TCR-mediated cell death (118). Knockout of TRAIL on its own does not result in a strong phenotype, but in conjunction with knockout of FasL show a severe pathology (119). ACAD, also known as death by neglect, is a cell intrinsic process that does not require TCR stimulation or death receptor ligation. Instead it is triggered by Bim signalling (120) and a decrease in levels of Bcl-2 (through a ROS dependent mechanism (121-123)). Thus ACAD has been hypothesised to be the dominant mechanism at the end of the immune response when levels of foreign antigen are low (116).

1.4 The PI3K pathway

1.4.1 PI3K in health and disease

Phosphoinositide 3-kinases (PI3K) were discovered in the late 1980s (124, 125) and it is now understood that they play many important roles, including the control of cell growth and survival, transcriptional and translational responses, glucose and nutrient uptake, proliferation, migration and differentiation. However, dysregulation of PI3K in these processes contributes to a range of diseases including diabetes, cardiovascular disease, autoimmune diseases as well as cancer and inflammation (126-128).

1.4.2 Structure, function and distribution of PI3K isoforms

The class 1 PI3Ks are composed of a regulatory subunit and a constitutively associated catalytic subunit. The three class 1A catalytic isoforms p110α, p110β and p110γ each pair with one of five regulatory subunits encoded by three genes: p85α, its alternative transcripts p55α and p50α, p85β and p55γ (Figure 1.6). The regulatory subunits modulate enzymatic activity and degradation of the catalytic subunits and are responsible for recruitment of the complex to the plasma membrane upon receptor ligation. Class 1A isoforms are activated downstream of immune cell receptors including the TCR, B cell receptor (BCR), costimulatory molecules and cytokine receptors that are phosphorylated by tyrosine kinases upon cognate stimulus (129, 130) (Figure 1.7).

The class 1B catalytic isoform p110γ pairs with either of the regulatory subunits p84/p87 or p101 (131, 132) and is activated by G protein βγ subunits and signals downstream of G protein coupled receptors (GPCRs). However, there is now substantial evidence that some GPCRs including chemokine receptors activate class IA PI3Ks, particularly PI3Kβ (133-135). Regulation of PI3K signalling is mediated by the 3' phosphatase PTEN and the 5' phosphatases SHIP-1 and SHIP-2 (136). Whereas PI3Kα and PI3Kβ appear to have a ubiquitous tissue distribution, PI3Kδ and PI3Kγ are predominantly expressed in immune cells, although PI3Kγ is also expressed in the heart and endothelium (137, 138) and PI3Kδ is found in neurons and in some cancers including melanoma and breast cancer (139, 140). Similarly, PTEN and SHIP-2 are ubiquitously expressed, whilst SHIP-1 is mainly restricted to

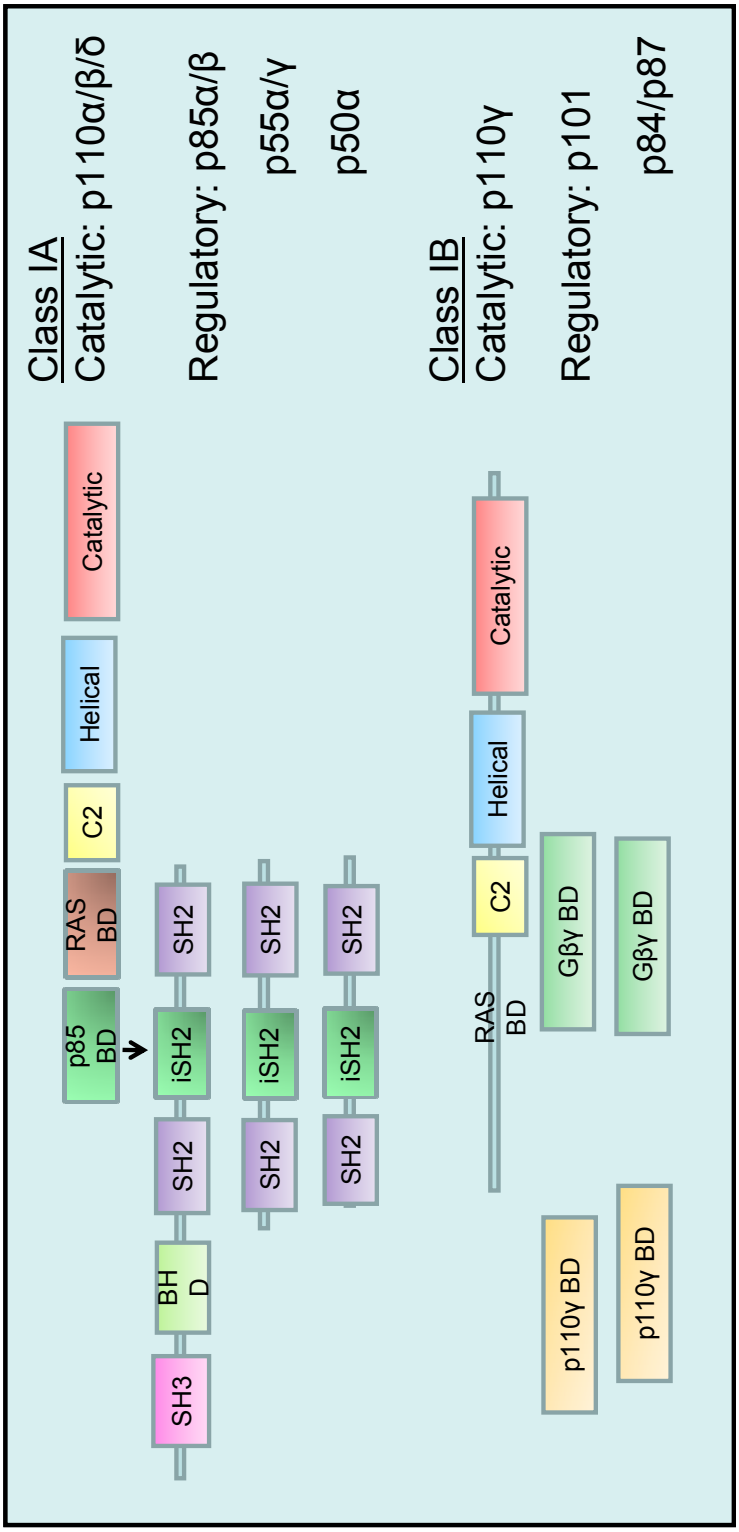

Figure 1.6: Structures of the class I PI3Ks
There are four class I PI3Ks. Class IA consists of PI3Kα, PI3Kβ and PI3Kδ, each of which has a catalytic p110 isoform, bound to one of several regulatory/adaptor domains (p85 p55 or p50). PI3Kα and PI3Kβ are ubiquitously expressed, whilst PI3Kδ is restricted to the immune system. Class IB has only one member, PI3Kγ, which has a p110 catalytic subunit bound to a p101 or p84/87 regulatory/adaptor subunit. PI3Kγ is mainly restricted to the immune system, but is also found in some other tissues, notably the heart. BD-binding domain, SH- Src Homology domain iSH- inter SH domain C2- calcium binding domain (the C2 domain is thought to bind the cell membrane).

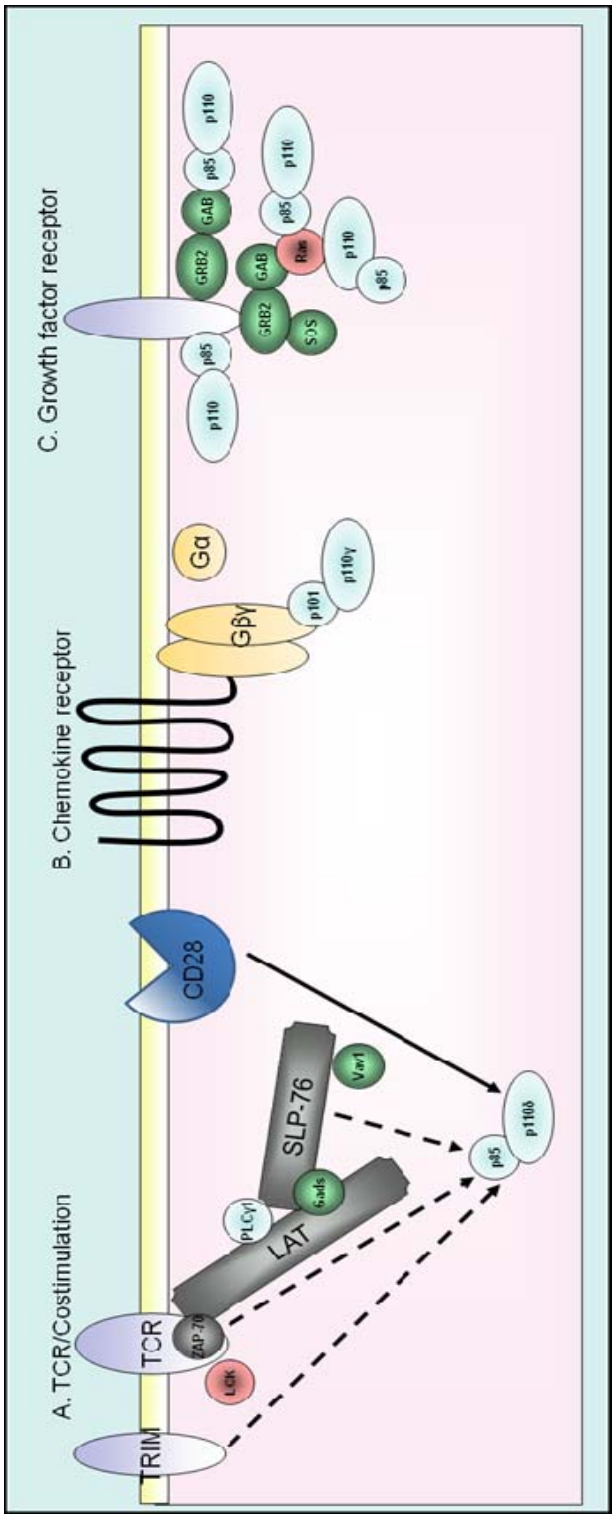

Figure 1.7: Recruitment of PI3Ks to receptors
A. Upon TCR stimulation, PI3K (predominantly PI3Kδ)(1), is recruited to pYxxM motifs which are present on a variety of scaffolding and adaptor proteins, which it binds via the SH2 domains on its regulatory/adaptor subunit, illustrated by dashed lines. In addition, CD28 can directly bind PI3K, again via interaction with the SH2 domain. B. Chemokine receptors recruit PI3Kγ, by virtue of the Gβγ binding domain on the regulatory/adaptor subunit. PI3Kβ has also been reported to be activated in response to GPCRs. C. Growth factor receptors can activate PI3Ks in a variety of ways. Receptor tyrosine kinases (RTKs) can autophosphorylate and then recruit p85 to pYxxM motifs. The GRB2/GAB/SOS (son of sevenless) complex can recruit Ras, which then binds the regulatory subunit of PI3Ks, or the catalytic subunits via their Ras binding domains (RBDs). In addition, Grb2-asociated binding protein 2 (GAB2) can directly bind the adaptor subunit.

leukocytes (136), although it is also found in spermatids (141) and has recently been reported to be expressed in the endothelium (142).

1.4.3 PI3K signalling

Phosphatidyl Inositol 3' Kinases (PI3Ks) catalyse the addition of a phosphate group to the 3' position of the inositol ring in phosphatidyl inositides. The Class I PI3Ks convert $PI(4,5)P_2$ to $PI(3,4,5)P_3$ (Figure 1.7). $PI(3,4,5)P_3$ remains associated with the cell membrane and recruits proteins containing pleckstrin homology (PH) domains, thus initiating signalling cascades. PI3Ks are found in all cells of the body and play essential roles in processes such as proliferation and survival. In addition, PI3Ks have unique functions in immune cells, playing a part in chemotaxis to chemokines as well as antigen, cytokine and co-receptor signalling. PI3K signalling can be terminated by the actions of the lipid phosphatase PTEN, a 3' phosphatase which hydrolyses $PI(3,4,5)P_3$ back to $PI(4,5)P_2$. However, $PI(3,4,5)P_3$ is also a substrate for the SHIPs which covert $PI(3,4,5)P_3$ to $PI(3,4)P_2$. PI3K signalling activates a multitude of signalling pathways (Figure 1.8). Some key pathways will now be considered in detail.

1.4.4 The importance of PDK-1 and other AGC family kinases in PI3K signalling

The AGC family of kinases are all serine/threonine or tyrosine kinases, consisting of 60 members, including cyclic AMP dependent protein kinase (PKA), cyclic GMP dependent protein kinase (PKG) and protein kinase C (PKC) from which their name is derived (143). There are also several members with key roles in PI3K signalling including PDK1 and protein kinase B (PKB/ Akt). PDK1 is constitutively active as it can trans autophosphorylate its activation motif and upon recruitment to $PI(3,4,5)P_3$, phosphorylates many other AGC family kinases on their activation motifs, which lie within the catalytic domain (144). For example, Akt is recruited to $PI(3,4,5)P_3$ and then phosphorylated upon Thr308 by PDK1(145). mTOR complex 2 (mTORC2) then phosphorylates Akt on Ser473, to allow full activation (146). S6 kinase (S6K), serum- and glucocorticoid-induced protein kinase (SGK) and PKC, all members of the AGC family of kinases, also depend upon PDK1 for activation (147, 148). Therefore it can be seen that PDK1 serves as a master regulator of PI3K signalling.

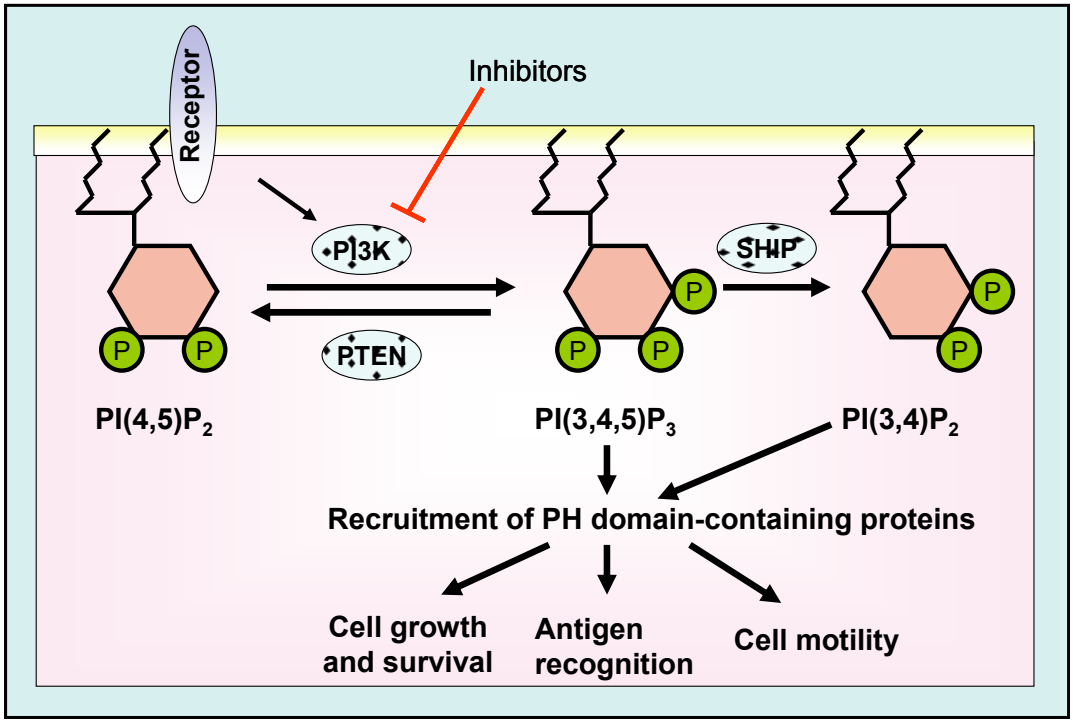

Figure 1.8: Phosphatidylinositol signalling by PI3K, PTEN and SHIP
Phosphatidylinositol (4,5) bisphosphate ($PI(4,5)P_2$) is associated with the inner cell surface membrane. Upon receptor stimulation, PI3K catalyses the addition of a phosphate group to the 3 prime position of the inositol ring to yield Phosphatidylinositol (3,4,5) trisphosphate ($PI(3,4,5)P_3$), which remains associated with the membrane and recruits proteins containing pleckstrin homology (PH) domains, the classical example of which is Akt (149). This initiates a number of signalling pathways as illustrated in Figure 9. Regulation of PI3K signalling is achieved by the actions of the lipid phosphatases PTEN and the SHIPs. PTEN removes the phosphate from the 3 prime position to give the original substrate $PI(4,5)P_2$, whilst the SHIPs remove a phosphate group from the 5 prime position to generate $PI(3,4)P_2$. Many small molecule ATP-competitive inhibitors of PI3K have been developed in order to control the PI3K signalling pathway.

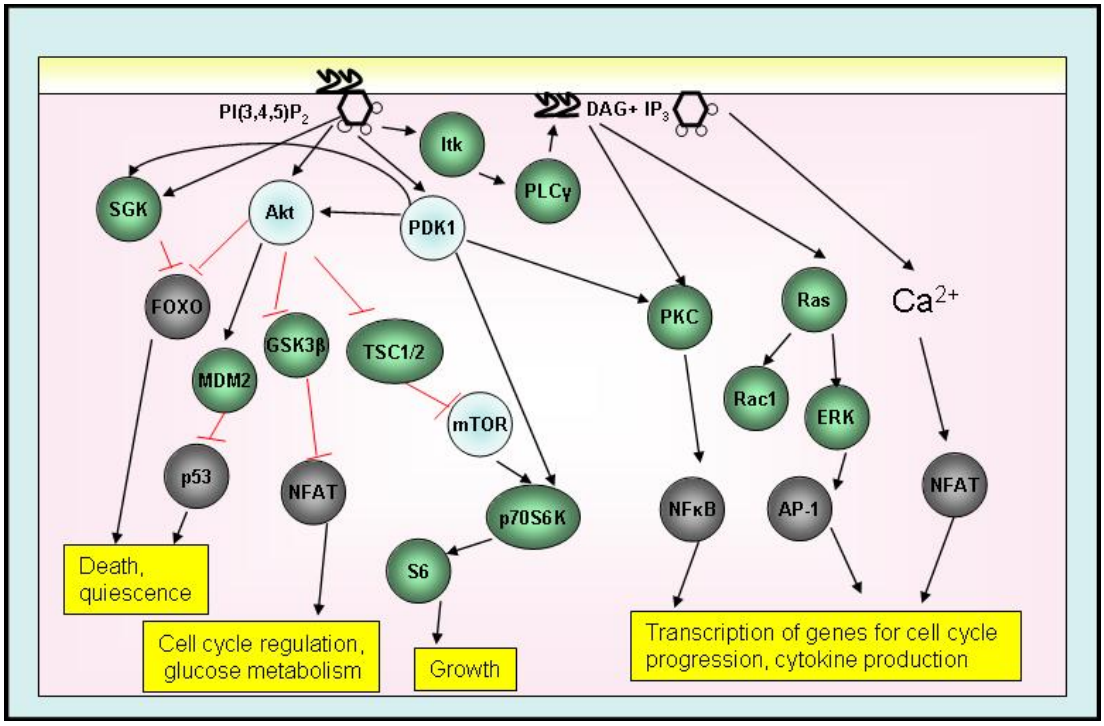

Figure 1.9: PI3K signalling pathways

$PI(3,4,5)P_3$, the product of PI3K, remains associated with the membrane and recruits proteins containing pleckstrin homology domains. Akt is one such protein: an AGC family kinase, it adds phosphate groups to wide variety of proteins to modulate their action. For example, it inhibits the transcription factor p53 and forkhead box (FOXO), to inhibit cell death, it inhibits GSK3β to promote the cell cycle and metabolism and it activates the mammalian target of rapamycin (mTOR) to initiate cell growth. Other PH domain containing proteins that are recruited to $PI(3,4,5)P_3$ include SGK and Tec. The latter, through activation of PLCγ, activates DAG and IP_3 signalling pathways. Thus PI3K signalling can also regulate Ras, PKC and Ca^{2+} signalling pathways (150, 151).

1.4.5 Akt as a second messenger of PI3K signalling

Akt is another key protein in the PI3K signalling cascade: an AGC family kinase, it adds phosphate groups to wide variety of proteins to modulate their action. For example, it inhibits the transcription factor p53 and forkhead box (FOXO), to inhibit cell death, it inhibits GSK3β to promote the cell cycle and metabolism and it activates the mammalian target of rapamycin (mTOR) to initiate cell growth. Other PH domain containing proteins that are recruited to $PI(3,4,5)P_3$ include SGK and Tec. The latter, through activation of PLCγ, activates DAG and IP_3 signalling pathways. Thus PI3K signalling can also activate Ras, PKC and Ca^{2+} signalling pathways (150, 151). Interestingly, Akt has also been shown to have equal or greater affinity for $PI(3,4)P_2$ as it does for $PI(3,4,5)P_3$ (152, 153).

1.4.6 mTOR signalling downstream of PI3K

Another downstream target of PI3K is mTOR, a kinase with a wide variety of substrates. There are two distinct complexes formed by mTOR; TORC1 and TORC2. TORC1 consists of Rheb (a GTPase), the GβL adaptor subunit, mLST8, PRAS40 and the regulatory associated protein of TOR (Raptor). TORC2 consists of mSin1, mLST8, and protor and rapamycin-insensitive companion of TOR (Rictor) (154) (although recent evidence has suggested that Rictor is something of a misnomer, as long incubations in rapamycin (hours) can also reduce TORC2 activity (155)). mTOR has a host of downstream targets. In the case of TORC1, the most notable are S6K and 4E-BP1, with important roles in nutrient sensing, integrating signals from insulin, amino acids and growth factors (156-158) to prevent apoptosis and autophagy and to promote G_0 to G_1 transition, transcription and cell growth (159). A major role of TORC2 is to phosphorylate Akt on Ser473 conferring maximum activity (146). Akt phosphorylates and inactivates tuberous sclerosis complex protein 2 (TSC2), which, through its actions as a GAP for Rheb, is a negative regulator of TORC1 (160). Furthermore TORC1/S6K-mediated phosphorylation of Rictor increases phosphorylation of Akt by TORC2 (161). Thus mTOR signalling is both up and downstream of Akt and plays a key role in PI3K signalling.

In T cells mTOR signalling has specific roles. Notably, when mTOR is inhibited, T cells become anergic (162). mTOR inhibition or deletion can also promote the generation of Treg cells and their selective expansion (163) and inhibits development of Th1, Th2 and Th17 effector T cells (164).

1.4.7 PI3Ks in innate and adaptive immunity

PI3K signalling occurs in response to activation of a diverse array of receptors that are expressed on leukocytes and are responsible for both innate and adaptive immune responses. PI3Ks are activated by antigen receptors, costimulatory receptors, Fc (fragment crystallisable) receptors, adhesion molecules, Toll-like receptors and cytokines receptors as well as receptors for a variety of chemoattractants including C5a, fMLP, chemokines and sphingosine-1-phosphate (S1P) (165). Given their leukocyte-restricted expression, PI3Kγ and PI3Kδ are thought to be the main isoforms involved in inflammatory and autoimmune diseases. Mice in which PI3Kδ or PI3Kγ have been either knocked out (KO) or replaced with kinase-inactive mutants (e.g. PI3Kδ^{D910A}) are viable, fertile and generally healthy (134). However, as detailed in Table 1.1, when their immune system is challenged, they exhibit severely altered phenotypes demonstrating that PI3Kδ and PI3Kγ have key functions in immune cells. Whilst they serve important functions during an immune response to pathogens, they also play a role in many inflammatory diseases (134, 166). There is evidence of considerable redundancy between PI3Kδ and PI3Kγ as mice with a dual knockout of PI3Kγ and point mutation of PI3Kδ have a very severe immune phenotype, with impairment of thymocyte development and T cell lymphopenia as well as T cell and eosinophil infiltration of mucosal organs, elevated IgE levels, and a skewing toward Th2 immune responses (167). However, use of isoform selective PI3K inhibitors (AS-604850 and IC87114) on wild type cells *in vitro* did not increase production of Th2 cytokines, indicating that in mature T cells deletion of these is not sufficient to skew cells to Th2. Therefore the exact role of PI3K signalling in Th1/Th2 differentiation remains undetermined, particularly as Akt activation can induce differentiation of both subsets (168).

PI3K signalling has a number of essential functions in cell growth, survival proliferation and differentiation. However, PI3K signalling also has cell-type specific roles. In T cells PI3K is required for activation induced by T cell receptor signalling, particularly when affinity for the antigen is low or costimulation is weak (reviewed (169)). It is not clear whether PI3K signalling is essential for CD28 signalling (reviewed (170)). However, some researchers have shown that the p110δ isoform is important in CD28-mediated expansion and differentiation, although CD28 has also been shown to activate PI3K independently of its ability to recuit PI3Kδ (171). Co-inhibitory receptors have been demonstrated to interact with the p85 regulatory

subunit of PI3Ks, and to downregulate Akt activation. PI3K signalling is also involved in IL-2 production by T cells (172) as well as Th1, Th2 and Th17 cytokines (173).

1.4.8 The role of PI3Kγ in T lymphocytes

Loss of PI3Kγ causes some defects in thymocyte development (168, 174-176). In CD4+ T cells PI3Kγ is dispensable for activation and proliferation, with generally normal TCR signalling (177), however some studies have indicated a role for PI3Kγ in TCR signalling and T cell activation (178). Both *in vitro* and *in vivo* activation are normal, though PI3Kγ$^{-/-}$ effector CD4+ T cells fail to migrate to sites of peripheral inflammation, and *in vitro* they fail to migrate to CCL22 despite normal expression of its receptor (CCR4), and their ability to polarise F-actin in response to chemokine is reduced (177). PI3Kγ aides chemotaxis of other leukocytes including neutrophils and eosinophils (175), however, it is often dispensable for T cell chemotaxis (135). A lack of PI3Kγ prevents hyperresponsiveness, inflammation and remodelling of the airways in an ovalbumin (OVA) based model of asthma, with a reduction in the levels of IL-4 IL-5 and IL-13 (175). Furthermore, loss of PI3Kγ reduces the severity of autoimmune disease models such as collagen induced arthritis (CIA) and Systemic lupus erythematosus (SLE) (127).

1.4.9 The role of PI3Kδ in T lymphocytes

Loss of PI3Kδ results in murine T cells that have defective TCR signalling (179) and reduced proliferation (180) and differentiation to Th1 and Th2 (180). *In vivo* this results in reduced immune responses, and reduced recruitment of T cells to sites of inflammation (181) although on some backgrounds loss of PI3Kδ results in an inflammatory bowel disease (179). PI3Kδ is also important for Treg maintenance in the periphery, and for their suppressive functions (182) as well as the regulation of T helper cytokines such as IL-4, IFNγ and IL-17 (173).

1.5 Lipid phosphatases in the immune system

Genetic loss of PTEN or SHIP-1 can also influence the immune system. Mice heterozygous for PTEN and the lymphocyte-specific PTEN null mouse have a tendency towards overactive immune responses (Table 1.1). Similarly, knockout of SHIP-1 results in an inflammatory phenotype while cell-specific gene targeting of SHIP-1 in T cells leads to altered Th1/Th2 cytokine production (183, 184). SHIP-1 is also thought to control the ratio of Tregs vs Th17 differentiation (185, 186). Together, this evidence underlines the importance of PI3K in maintaining a balanced and functional immune response and the necessity of keeping PI3K-dependent signalling

Table 1.1: The effect of genetic manipulation of the PI3K pathway on immune cell function

Cell Type	PI3Kδ KO or KD	PI3Kγ KO	Dual PI3KδKD/ PI3KγKO	SHIP-1 KO	PTEN KO[i]
T cell	• Defective TCR signalling (179) • ↓proliferation (180) • ↓ migration to sites of inflammation (181) • Decreased differentiation to Th1 and Th2 (180) • ↓peripheral Treg number and function (189) • Abberant Th1, Th2 and Th17 cytokine production (173)	• ↓DP T cell number (190) • ↑ proportion of CD8+ (190) • ↑ apoptosis ↓ survival of memory T cells(191) • ↓ *in vivo* cytotoxic response (176) • Impaired TCR signalling (178) • Small ↓ in polarisation and F-actin polymerisation (192) • ↓ in effector CD4+ migration to sites of inflammation (177)	• Severe lymphopenia(167) • ↓ maturation(167) • ↑ peripheral proliferation(167) • ↑Th2 cytokine(167) • ↓ T reg function (167)	• ↓ in progenitor number (184) • ↑ In Th2 cytokines in lung (193) • ↑ numbers in lung (193) • ↑ T reg numbers (185, 194) • ↑Treg and ↓Th17 *in vitro*(186) • T cell specific KO ↓ in Th2 response, skewed to Th1,↑ in CD8+ cytotoxicity (183)	• Heterozygote has lymphoproliferative autoimmune disorder (195) • ↑ motility (196) • Loss in CD8+ causes CNS disease and ↑suceptibilty to EAE (197) • Autoreactive T cells , no CD28 costimulation req'd (198)
B cell	• ↑IgE production (199) • Aberrant BCR signalling (179, 200) • ↓ B cell numbers(179) • ↓ proliferation (180) • ↑ apoptosis (180)	• No strong phenotype (176)	• ↓ B cell numbers(167) • ↓ Ig production(167)	• ↓ in progenitor number (201) • ↑ in B cell number (201) • B cell specific KO=no phenotype (202)	• ↑proliferation, (203) • ↓apoptosis (203) • Defective class switch recombination (203) • Heterozygote has immune-complex mediated glomerular nephritis (195)
Neutro-phil	• ↓ chemotaxis to some ligands (204)	• ↓ GPCR (e.g. fMLP and C5a) signalling (176) • ↑ numbers (176) • Defects in respiratory burst (176) • ↓ chemotaxis (176, 204)	• ↑ Infiltration and inflammation (probably result of lymphopenia)(167) • ↓ chemotaxis (204)	• Spontaneous infiltration to lung (184) • ↑ numbers in blood (184)	• ↑ motility (205) • ↓ability to prioritise chemotactic cues (206) • ↑ numbers in lung (207)
Eosino-phil		• ↑ numbers(176) • ↓ infiltration *in vivo* (208) • ↓ chemotaxis to eotaxin *in vitro*(208)	• ↑ Infiltration and inflammation (probably result of lymphopenia)(167)	• ↑ numbers in lung (193)	
Mono-cyte/ Macrop-hage	• ↓ chemotaxis(209) • ↓ proliferation (209)	• ↑monocyte numbers (176) • ↓motility and chemotaxis(210, 211)		• Spontaneous infiltration to lung (184) • ↑circulating monocyte numbers (184) • Skewed to M2 (alternatively activated) (212) • ↑FcR mediated	• ↑ numbers in lung (207)

				phagocytosis (213) • ↓NADPH oxidase activity and early oxidative burst (214) • macrophage specific KO: myeloproliferative disease and ↑in both Treg and Th17 (202)	
Mast cell	• Fail to degranulate *in vitro* and *in vivo* in response to FcεRI signaling(215) • No IgE/Antigen-dependent hypersensitivity(215) • ↓ proliferation, adhesion and migration, (216) • Protected against passive cutaneous anapylaxis(216)	• Fail to amplify activation via GPCR stimulation (e.g. adenosine ATP MIP1α) (215) • ↓IgE and antigen induced migration (217) • Fail to mediate formation of edema upon passive immunisation and antigen challenge (218) • Fail to degranulate *in vitro* in response to FcεRI (215)		• Spontaneous infiltration to lung and degranulation (219) • ↑degranulation, (220) • ↑hyperplasia, cytokine production and asthma pathology(219)	• ↑survival (human[ii]) (221) ↑cytokine production (human[ii]) (221)
NK	• ↓migration to inflammation and chemokines and S1P(222)	• ↓migration to inflammation and chemokines (222) • Impaired development (223)	• ↓numbers in spleen (223) • Impaired development (223) • ↓ cytotoxicity (223)	• ↑ numbers(224) • Altered repertoire, (224) • ↑ expression of inhibitory receptors leading to ↓GVHD (224)	• Vα14*i*NKT cells have ↓ development ↓ proliferation, cytokine secretion, tumor surveillance(225)
Dendritic cell	• ↓ IL-6 production (226)	• Defective *in vitro* chemotaxis (227) • ↓ numbers (227) • Fail to migrate to draining lymph nodes(227) • ↓ contact hypersensitivity due to ↓migration of cutaneous DC (227)		• ↑splenic DC(228) • ↑ myeloid DC from BMDC(228) • ↓ ability to induce T cell proliferation (228)	• In humans, ↑ expression during aging implicated in ↓ DC function (229)
Basophil				• In humans low expression correlates with increased histamine release (230)	

[i] Whole animal KO of PTEN is embryonic lethal, models indicated here are cell type specific KO, except for the whole animal heterozygote where indicated

[ii] Using shRNA

in check. The lipid phosphatases will be discussed in greater detail in subsequent sections.

1.5.1 PTEN

PTEN was initially identified as a tumour suppressor that is lost in a wide variety of tumours (187). PTEN dephosphorylates the 3' position of the inositol ring, and *in vitro* can act upon PI(3)P, PI(3,4)P_2 and PI(3,4,5)P_3 (188). However, most interest is concerned with its role in modulating the PI3K pathway and hence its actions upon PI(3,4,5)P_3.

The phosphatase domain of PTEN contains many residues in common with protein phosphatases, including a conserved catalytic cysteine residue, but in addition it has two lysine residues which are thought to aid binding to negatively charged phosphatidylinositides. PTEN also contains a lipid-binding C2 domain and a C terminal PDZ- binding domain (Figure 1.10). The actions of PTEN are regulated in a number of ways. Binding to the membrane is facilitated by the phosphatase and C2 domains and is enhanced by an electrostatic interaction, whilst phosphorylation of the C terminal region of PTEN may inhibit its recruitment to the membrane. The presence of PI(4,5)P_2 at the membrane aids PTEN phosphatase activity, possibly by bringing it into proximity with PI(3,4,5)P_3 and also by facilitating a conformational change (231). Phosphorylation of PTEN on serine residues can stabilise the enzyme and modify its ability to interact with the membrane and other proteins. For example, phosphorylation of PTEN in its C terminal region results in an altered conformation with impaired binding to PDZ domains (55). Reversible inhibition of PTEN is mediated by oxidation by reactive oxygen species (ROS), resulting in the formation of a disulphide bond between the catalytic cysteine (cys124) with a neighbouring cysteine residue (cys71) (232).

PTEN interacts with a number of proteins, for example interaction with PDZ-containing proteins such as MAGI can reduce the degradation of PTEN. PTEN can also interact with certain receptors, for example the sphingosine-1-phosphate receptor 2 (233). Despite its ability to interact with the membrane, PTEN is predominantly found in the cytoplasm of unstimulated cells, where it is suggested that interaction with cytoplasmic structures (234) or a closed conformation may

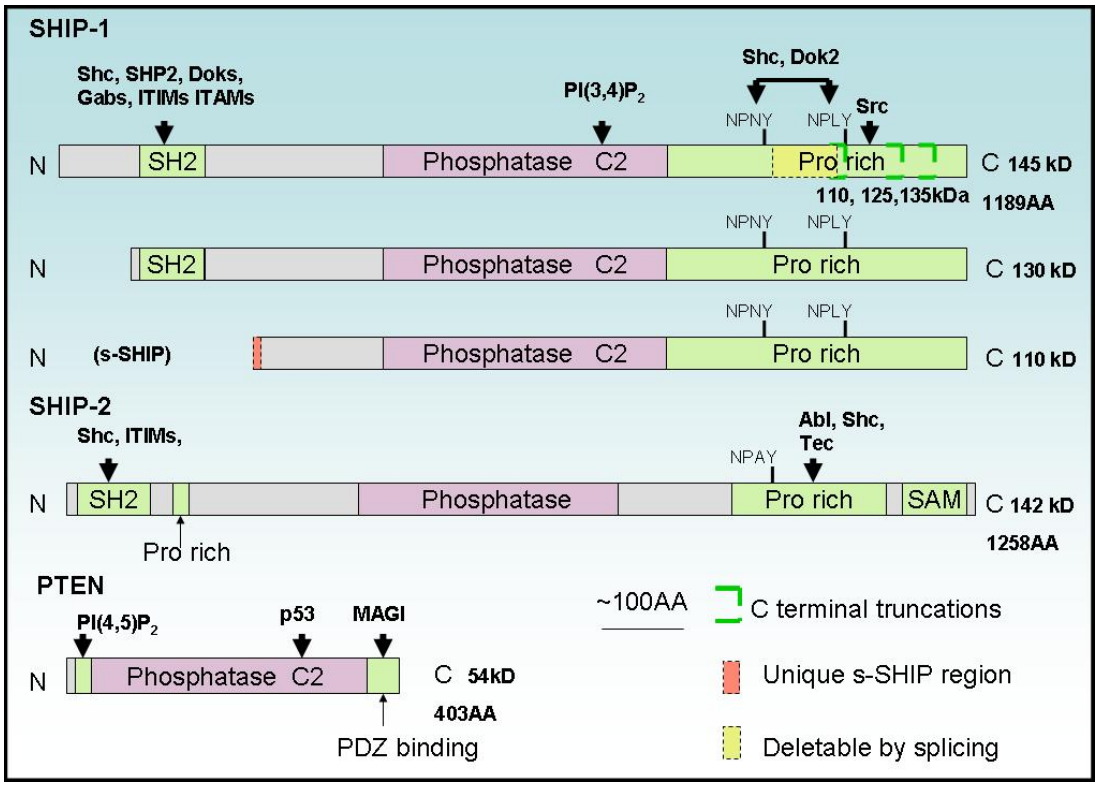

Figure 1.10: Structures of PTEN and the SHIPs
The protein interaction motifs are indicated, along with their binding partners. Regions lost in SHIP-1 due to alternative splicing and proteolytic cleavage of the protein are also shown, along with the approximate molecular weights of the resulting proteins. Splice variants of SHIP-1 with molecular weights of 145 and 130 kDa, have been reported with truncations occurring at the N terminal. In humans, the 110kDa protein which lacks an SH2 domain (SIP-110) was originally hypothesised to be a splice variant (237), but it has been postulated that this is in fact the human ortholog of s-SHIP which arises from use of an internal promoter and contains a unique amino acid sequence at the N terminal (238). However, whilst s-SHIP is reported to be restricted to stem cells, antibodies raised against SIP-110 also detected a 110kDa protein in the mature mouse B-cell lymphoma line Bal 17 (237).

Note that in mice, a SHIP isoform with a molecular weight of 110kDa also arises from an out of frame splice in the C terminal region ((239) not shown). C terminal truncations of SHIP-1, possibly due to cleavage by calpain, result in proteins with molecular weights of 135,125 and 110 kDa (240). Finally, murine SHIP-1 mRNA can contain a 183bp deletion (282bp in humans). This results in a 135kDa protein with the deletion occurring in the proline rich region between the two NPXY motifs (241). Whilst the SHIP-1 genomic locus has been extensively characterised in mice, such a comprehensive study has not been undertaken for human SHIP-1. It has also been hypothesised that SHIP-2 splice variants may also occur (239).

prevent free association with the membrane. PTEN contains two PEST motifs and ubiquitination by Nedd 4 can target it to the nucleus or towards degradation pathways (235). PTEN is found in the nucleus of many cells, particularly during the G_0-G_1 phase, and both $PI(4,5)P_2$ and $PI(3,4,5,)P_3$ have also been detected in the nucleus (236).

Whilst a ubiquitous PTEN knockout is embryonic lethal, tissue specific and heterozygous knockouts have elucidated the functions of PTEN, many of them in the immune system. For example, PTEN heterozygous mice develop an autoimmune lymphoproliferation by 9 months of age whilst mice heterozygous for both PTEN and SHIP-1 exhibit a more rapid progression of lymphoproliferation (242). Furthermore both PTEN and SHIP-1 are frequently lost in leukaemias (243) and many immortalised leukaemic cell lines such as Jurkats lack one or both of these phosphatases (244). T cell-specific PTEN KO mice exhibit splenomegaly and an enlargement of the thymus. They have increased numbers of T cells and die due to CD4+ lymphomas. The mice display a defect in negative selection and have reduced positive selection of CD8+ cells. Furthermore, PTEN plays a role in peripheral tolerance as $PTEN^{-/-}$ T cells are autoreactive. They also display an increase in proliferation and cytokine production and a decrease in apoptosis compared to wild-type cells (245).

PTEN is crucial to many lymphocyte functions. Notably PTEN inhibits T cell receptor (TCR) signalling, necessitating a requirement for CD28 costimulation in order to generate a response to TCR stimulation. In addition, PTEN null T cells fail to become anergic in response to TCR stimulation without CD28 stimulation (246). However, other researchers have shown that PTEN may be more important in maintaining low levels of $PI(3,4,5)P_3$ and $PI(3,4)P_2$ in the absence of TCR signalling (247). PTEN expression has been shown to limit TCR and CD3-dependent phosphorylation of phospholipase Cγ1 (PLCγ1) and ERK and to limit Itk kinase activity. Basal levels of $PI(3,4,5)P_3$ are high in PTEN null leukaemic cell lines, with a corresponding high level of phosphorylation of Akt (248).

PTEN also has a role in Th2 driven inflammation, for instance its expression is decreased in murine models of allergic inflammation. In asthmatic mice introduction of PTEN cDNA via adenovirus can reduce levels of cytokines such as IL-4 and CCL5

(RANTES) (which are secreted by T cells), contributing to a reduction in bronchial inflammation and airway hyperresponsiveness (249, 250).

1.5.2 SHIP-1

Three forms of SHIP have been identified. SHIP-1 is confined to haematopoietic cells and spermatids, whilst SHIP-2 is widely expressed with high levels in the brain, heart and skeletal muscles (and is coexpressed with SHIP-1 in haematopoietic cells) and s-SHIP is limited to stem cells. SHIP-1 can metabolise the 5' phosphate from inositol (1,3,4,5) tetraphosphate and PI(3,4,5)P_3, and so can terminate PI3K-dependent signalling pathways. However, whilst many proteins containing pleckstrin homology (PH) domains are recruited to PI(3,4,5)P_3, some, such as DAPP1 (dual adaptor of phosphotyrosine and 3-phosphoinositides), can interact with both PI(3,4,5)P_3 and PI(3,4)P_2, whilst the TAPPs (tandem PH domain containing protein) are recruited exclusively to PI(3,4)P_2 (251).

SHIP-1 possesses an N terminal SH2 domain and a C terminal proline rich domain as well as two NPXY motifs and a C2 domain that can bind its product PI(3,4)P_2 (Figure 1.10). The SH2 domain has been demonstrated to bind tyrosine phosphorylated Shc, SHP-2, Doks, Gabs and some ITIMs and ITAMs (immunoreceptor tyrosine-based inhibition/activation motif). The proline rich region can bind selected SH3 domain-containing proteins such as Src and is essential to SHIP-1 function (252). Meanwhile the NPXY motifs can bind PTB (phosphotyrosine binding) domains of Shc and Dok2 (201, 253, 254), and mutating the NPXY motifs to NPXF partially reduced SHIP-1 activity. NPXY motif binding requires phosphorylation by the Src family kinase Lyn and this phosphorylation plays a key role in its recruitment to the membrane and activity (255, 256). It has also been proposed that SHIP-1 activity is regulated by cAMP-dependent protein kinase (257).

Multiple variants of SHIP-1 are produced. Splice variants with molecular weights of 145, 130 and 110 kDa, have been reported with truncations occurring at the N terminal. This results in different binding specificities between SHIP-1 proteins. For example, the Grb2 SH3 domain binds exclusively to the 110kDa splice variant which lacks an SH2 domain, whilst Shc can bind the 145 and 135 kDa proteins (237). The 110kDa protein is postulated by others (238) to be the human ortholog of sSHIP (see below), as it contains a unique N terminal amino acid sequence. C terminal

truncations of SHIP-1 have also been reported, possibly due to cleavage by calpain, resulting in SHIP1- proteins with molecular weights of 135,125 and 110 kDa. Finally, murine SHIP-1 mRNA can contain a 183bp deletion (282bp in humans). This results in a 135kDa protein with the deletion occurring in the proline rich region between the two NPXY motifs (241) .These truncations also result in variation in binding partners, for example, only 145kDa SHIP-1 can be immunoprecipitated with Shc (240).

SHIP-1 can also aid formation of signalling complexes, for example following stimulation of the TCR, SHIP-1 recruits Dok2 (downstream of tyrosine kinase 2) to a complex containing LAT, Dok1 and Grb2, facilitating the inhibitory effects of Dok2 on TCR signalling (258).

SHIP-1 KO mice have an increased proportion of CD4+ vs CD8+ cells in the spleen. Their peripheral CD4+ T cells display a higher percentage of the activation markers CD25 and CD69 but fail to produce IL-2 in response to PMA/ionomycin stimulation. They also produce TGFβ and express Foxp3. Finally, these lymphocytes also inhibit the production of IL-2 by CD4+CD25- T cells, indicating that they are Tregs (194). others have also found that a lack of SHIP-1 causes an increase in Treg numbers and this was found to limit graft vs. host disease (GvHD) (185, 259, 260). Different groups have variously reported that SHIP-1 KO T cells proliferate normally in response to TCR signalling (261) or are anergic (194).

A substantial proportion of SHIP-1$^{-/-}$ mice succumb to a fatal myeloid cell infiltration of the lungs by 14 weeks of age, which is thought to be Th2 driven (184, 262). In addition, SHIP-1 null haematopoietic stem cells are hyper-responsive, for example to IL-3, GM-CSF and steel factor (SF). However, a T cell specific deletion of SHIP-1 resulted in mice that failed to skew towards Th2 responses, possibly due to an increase in basal levels of T-bet. In addition these mice have a more efficient CD8+ cytotoxic response. In contrast to the mice with complete deletion of SHIP-1, T cell specific deletion did not result in an increased number of Tregs and the mice had a normal lifespan, without leukocyte infiltration of the lungs (183). Further controversy on this subject came from experiments using naïve T cells from whole animal SHIP-1 knockout mice. These were found to differentiate *in vitro* into Tregs more easily than

WT cells, but failed to differentiate into Th17s under appropriate conditions. This was attributed to a decreased ability of IL-6 to mediate STAT3 signalling in the KO cells, thus biasing them away from Th17 development.

SHIP-1 has also been shown to have a key role in controlling the response of T lymphocytes to oxidative stress. Leukaemic T cells which lack SHIP-1 have higher levels of cell death in response to reactive oxygen species than those which express SHIP-1, as they fail to activate the NFκB survival pathway through IKK (IκB kinase) mediated serine phosphorylation of IκBα, and instead must rely upon a less effective mechanism involving tyrosine phosphorylation of IκBα (263). In this manner, SHIP-1 can reduce apoptosis in response to both H_2O_2 and signalling pathways that involve generation of reactive oxygen species such as Fas signalling (264).

1.5.3 A note on SHIP-1 null mouse models

The Krystal laboratory utilises SHIP-1 null mice with a deletion of the transcriptional start site and the first exon on a C57BL/6-129Sv background. C57BL/6 mice are generally prone to Th1 type inflammation (265), as are 129/sv (although to a lesser extent (266)), (whereas balb/c are prone to Th2 driven inflammation (267, 268)). Despite this, the group feels that the severe lung inflammation seen in the SHIP-1 knockout mice may be due to the strain used and therefore are in the process breeding the SHIP-1 deletion onto different backgrounds (A. Ming Lum personal communication).

Workers at the John Hopkins School of medicine, Baltimore use SHIP-1 null mice on a C57BL/6-129Sv (262) background or 129/J (261) backgrounds through deletion of the first coding exon and part of the following intron. The Kerr group used SHIP-1 null mice on a C57BL/6J background, either by knockout of the enzymatic domain (exons 10-13) or by deletion of the promoter and first exon of SHIP-1. MxCreSHIP-$1^{flox/flox}$ on a C57BL/6J background were also used so that SHIP-1 could be deleted in mature animals (185).

Finally the Bolland group generated a T cell specific knockout mouse by crossed mice containing a loxP-flanked SHIP-1 gene (covering exons 10-13, encoding the

entire enzymatic domain) with mice transgenic for Cre recombinase driven by the CD4 promoter (183). These mice had a C57BL/6 background. Thus it can be seen that a variety of models have been used to characterise the role of SHIP-1 in mice, albeit on a limited range of backgrounds.

1.5.4 SHIP-1 in health and disease

A dominant negative mutation of SHIP-1 has been reported in some acute myeloid leukaemia (AML) cases (269) and multilobulated nuclear formation of adult T cell leukaemia/lymphoma (ATLL) (270, 271) whilst SHIP-1 (along with PTEN) is reported to be widely inactivated in T lymphoblastic leukaemia (T-ALL). In T-ALL cell lines, SHIP-1 is frequently lost at the protein level (including in Jurkats). Even in the T-ALL cell line CEM, where SHIP-1 has been previously reported (244), it has a conservative mutation and protein levels are reduced. In primary T-ALL a variety of mutations have been reported in the SHIP-1 gene, often resulting in reduced expression, or expression of lower molecular weight forms (272).

The measles virus drives expression of 110kDa splice variant of SHIP-1 (SIP110) (237) in order to reduce Akt activity and cell proliferation, thus facilitating suppression of the immune system during infection (273). SHIP-1 is also a key effector in the SLAM-SAP (signaling lymphocytic activation molecule/SLAM associated molecule) signalling pathway, and loss of the latter leads to X-linked lymphoproliferative disease (274).

1.5.6 Stem cell SHIP

Stem cell SHIP (s-SHIP) is expressed in totipotent embryonic stem cells and haematopoietic stem cells, whilst full length SHIP-1 is not present in stem cells. s-SHIP is also encoded by the SHIP-1 gene Inpp5d and its transcription is controlled by an internal promoter. It lacks the N-terminal SH2 region of SHIP-1, but its mRNA has a unique 44 nucleotide sequence at the 5' end. As with SHIP-1 (241), a 183 nucleotide sequence can be spliced out, resulting in a doublet of 104 and 97 kDa being detected in western blots (928 amino acids (aa) and 867 aa rather than the full 1191 aa of SHIP-1) (238). It has been demonstrated that s-SHIP associates with gp130, most probably through its interactions with Grb2. This interaction may inhibit both the PI3K pathway and the Ras/Mek/Erk pathway by preventing association of SOS with Grb2. In this way s-SHIP could modulate signalling through the leukaemic

inhibitory factor receptor (LIFR), which is required for growth and survival of both embryonic and haematopoietic stem cells (275).

SHIP-1 null haematopoietic stem cells (HSCs) have a lower rate of spontaneous apoptosis than wild type cells and SHIP-$1^{-/-}$ mice have a larger number of HSCs. However, these stem cells are more likely to differentiate to myeloid cells and have a reduced ability to differentiate to B lymphocytes. In addition, SHIP-$1^{-/-}$ HSCs home less efficiently to the bone marrow, and this is associated with a decrease in expression of CXCR4 and VCAM-1 (276).

1.5.7 SHIP-2

SHIP-2 is a 142kDa protein with high homology to SHIP-1. Most variation occurs in the proline rich domain and it has only one NPXY motif, but also has a sterile alpha motif (SAM) domain (277). SHIP-2 can metabolise PI(3,4,5)P_3 and PI(3,5)P_2 as well as some inositol phosphates (278) and is widely expressed, with high levels found in a disparate range of tissues including the heart, skeletal muscle, placenta and fibroblasts (279). Notably SHIP-2 is coexpressed with SHIP-1 in haematopoietic cells and has also been detected in leukaemic cell lines.

SHIP-2 is tyrosine phosphorylated in response to insulin and a variety of growth factors (280) and is known to play a role in the negative regulation of lymphocyte signalling. For example in T cell lines both forms of SHIP can associate with Tec and inhibit its activity following TCR stimulation (281). In addition, SHIP-1 and SHIP-2 SH2 domains recognise very similar pY sequences (pY[S/Y][L/Y/M][L/M/I/V]), but their binding kinetics are different, with SHIP-1 having much faster association and dissociation rates than SHIP-2, contributing to their different actions in immune cells (282).

1.5.8 The role of PTEN and SHIP-1 in T lymphocyte migration

Directional sensing and ordered cell migration are essential to leukocyte function and are mediated by a variety of G-protein coupled receptors. These activate second messenger systems, including PI3K, resulting in the generation of PI(3,4,5)P_3. During the process of T lymphocyte chemotaxis, chemokines, or other GPCR ligands such as S1P, stimulate their cognate GPCR, causing activation of G proteins (usually

Gαi/o) (283). This initiates polarisation of the cell, with the formation of a leading edge (pseudopod) and tail (uropod).

The intracellular signalling processes leading to polarisation have mainly been studied in neutrophils, but are thought to occur in T cells as well. The Rac GEFS (guanine nucleotide exchange factor), Dedicator of cytokinesis 2 (DOCK2), Tiam1 (T cell lymphoma invasion and metastasis) Vav1, and p-Rex1 (phosphatidylinositol-3,4,5-trisphosphate-dependent Rac exchange factor 1) are localised to the pseudopod leading to Rac1 activation and hence F-actin polymerisation (85). PI3Kγ also accumulates at the leading edge and regulates the activity of RacGEFs as either they, or their associates proteins (e.g. ELMO proteins (284)), have PH domains to facilitate their colocalisation (285). Loss of DOCK2 causes a reduction in the chemotactic ability of the cells. The effect of PI3Kγ loss or inhibition is less clear cut, but it is thought to reduce the chemokinetic activity of the cell (85). In activated T cells it has been shown to be required for basal motility but not chemotaxis whereas in freshly isolated T cells its inhibition has also been shown to reduce directional chemotaxis (286). Others have found that PI3K signalling is important for chemotaxis in shallow gradients, but is dispensable at higher concentrations of chemoattractant (287, 288).

Reciprocal distributions of PTEN and SHIP-1 allow the maintenance of polarisation and facilitate directional sensing, with PTEN being distributed to the sides and back of the cell (289, 290) and enabling prioritisation of certain chemotactic cues (206) (however, even if a chemokine is uniform in distribution, the cell will still polarise and undergo chemokinesis). Loss of PTEN results in neutrophils with mildly increased actin polymerisation and speed, but slightly impaired directionality (291). Chemotaxis of leukocytes has been most extensively studied in neutrophils. In agreement with the findings in *Dictylostelium*, the distribution of PTEN to the uropod during chemotaxis has also been observed in human neutrophils. Concurrent with this, it is reported that PTEN-null neutrophils have increased Akt phosphorylation in response to chemokines and increased F-actin polymerisation in response to fMLP. PTEN null neutrophils are more sensitive to chemoattractants and they exhibit enhanced chemotaxis with increased speed, although directional sensing is impaired, whilst *in vivo* PTEN-null neutrophils are recruited more efficiently in a mouse model of peritonitis (291). A similar situation is believed to occur in T lymphocytes, for example

PTEN negatively regulates CXCR4- mediated chemotaxis to CXCL12 as well as chemotaxis to insulin-like growth factor 1 (IGF-1) (292).

Other researchers have found a limited role for PTEN in neutrophil chemotaxis and consider that SHIP-1 is key for the formation of the leading edge and polarisation of the cell. SHIP-1 null neutrophils fail to localise $PI(3,4,5)P_3$ to the front of the cell, thus reducing polarity of the cell. Basal actin polymerisation is increased, and motility is decreased. However, during chemotaxis, whilst the speed is reduced, the ability to sense direction was not impaired (293). In Jurkats (which lack SHIP-1 and PTEN), introduction of constitutively active SHIP-1 reduces CXCL12- mediated chemotaxis. (294).

1.6 Pharmacological targeting of the PI3K pathway

The above paragraphs have outlined some of the normal physiological roles of the PI3K pathway in the immune system and the effects of genetic manipulation on individual cell function. The introduction will now examine the role of PI3Ks in disease.

1.6.1 The development of PI3K inhibitors

Initially, interest in the PI3K pathway focused on its role in cancer. PI3Kα frequently has activating point mutations in solid tumours, and PTEN is a well known tumour suppressor. Therefore early work was concerned with small molecule ATP competitive inhibitors of PI3Kα (295). The first compound shown to target PI3K was the fungal product wortmannin, which is an irreversible inhibitor (296). LY294002 was then developed as a specific, ATP competitive reversible inhibitor (297). The first isoform selective inhibitor was IC87114, which was developed by the ICOS

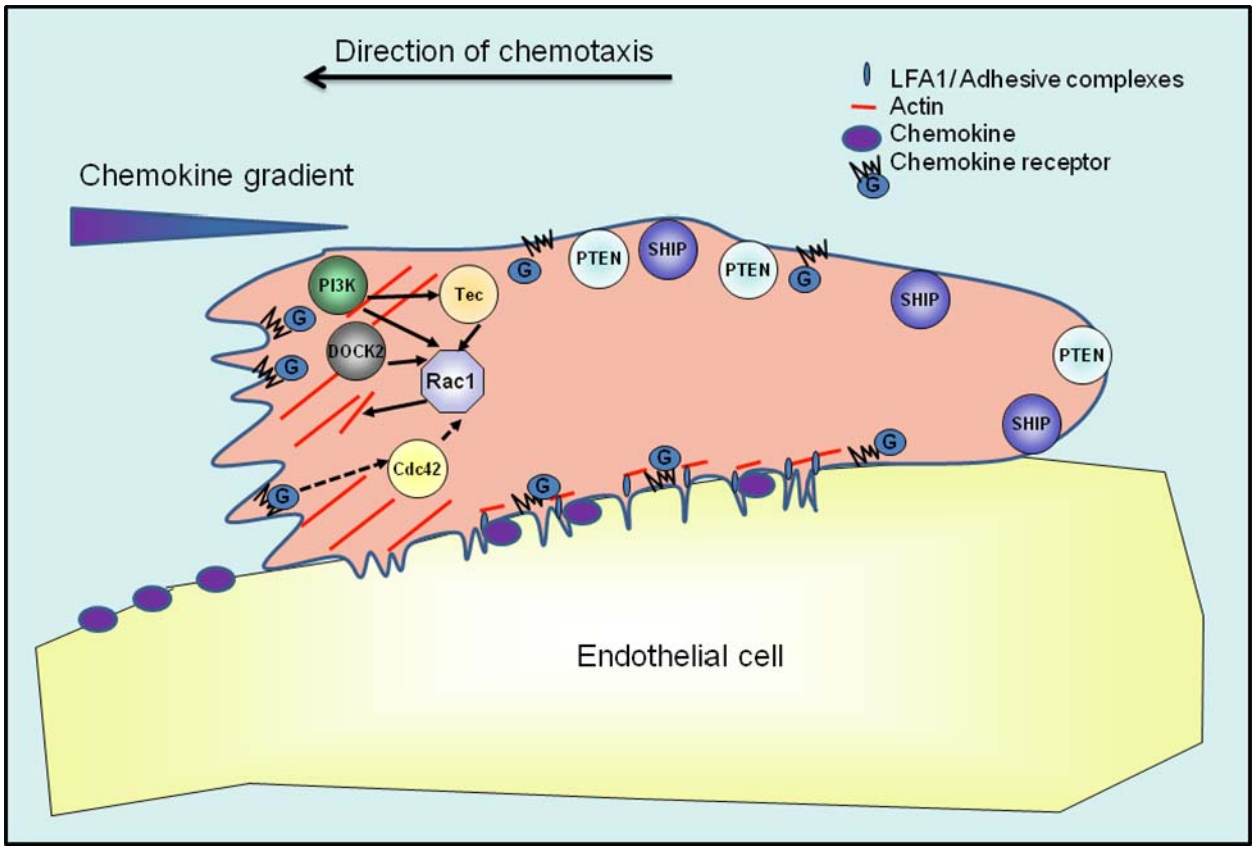

Figure 1.11: The chemotaxing cell
Chemokines can be presented on the surface of endothelial cells. These trigger firm adhesion of T cells, which flatten and polarise. LFA-1 clusters in filapodia which protrude into the endothelial cell, helping to anchor the T cell. The T cell polarises, with PI3K, DOCK2 and Cdc42 (cell division control 42 kDa) signalling pathways all contributing to Rac1 activation and actin polymerisation at the leading edge. PI3K activity is confined to the pseudopod by the distribution of SHIP-1 and PTEN to the side and uropod (85, 283, 289).

Corporation. This compound has an IC_{50} of ~100 nM for inhibition of PI3Kδ but does not target the other class I PI3K isoforms (298). Class 1A selective compounds, with a slight selectivity for the alpha isoform, were developed by Piramed Ltd, based upon a compound developed by Yamanouchi Pharmaceutical Company Ltd, PI-103, and culminating in the development of GDC-0941, an orally available compound that has entered clinical trials for cancer (299).

However, because of its important role in the immune system, it has also become clear that the PI3K signalling pathway plays an important part in many inflammatory conditions, for example in autoimmune diseases such as rheumatoid arthritis and multiple sclerosis, in transplant rejection, in the clearance of pathogens and even in myocardial infarction (300). To target the PI3K isoforms involved in inflammation, selective inhibition of PI3Kγ has been achieved with compounds from Serono, AS252424, AS605240 and AS604850 (210). Meanwhile dual inhibition of PI3Kγ and PI3Kδ has also been achieved with TG100-115 developed by TargeGen Inc, (301). Lung inflammation and allergy will now be examined in detail as an illustration of the role of PI3K in inflammation. Much research has been done on murine models of disease, both using genetic models, and small molecule pharmacological inhibitors.

1.6.2 PI3Kγ and PI3Kδ selective inhibitors

PI3Kδ KD mice are protected in an OVA model of asthma as they have a decreased production of Th2 cytokines and mucus, and are resistant to OVA-induced airway hyper-responsiveness, whilst PI3Kδ KD eosinophils fail to infiltrate the lungs, even if transferred into wildtype recipients (302). The PI3Kδ inhibitor IC87114 (developed by ICOS and the first isoform specific inhibitor of PI3K to be described), was also effective in this model, reducing eosinophil, lymphocyte and neutrophil infiltration into the lungs. It also decreased Th2 cytokines, IgE, eotaxin and mucus, vascular permeability and hyper-responsiveness (16, 17). In addition, IC87114 has been shown to be effective in a canine model of allergic rhinitis (176), whilst the PI3Kδ selective inhibitor CAL-101 developed by Calistoga pharmaceuticals has been tested in a clinical trial for allergic rhinitis (303).

In response to an OVA challenge, PI3Kγ KO mice had a greatly reduced number of infiltrating eosinophils, neutrophils, lymphocytes and macrophages in their

bronchoalveolar lavage (BAL) (304). PI3Kγ KO mice also had a decreased hyper-responsiveness and less peribronchial smooth muscle and fibrosis compared to WT mice. Whilst a decrease in Th2 cytokines in the KO had been reported by some (175), others found no difference in IL-5 and eotaxin levels, and mucus levels that were comparable to those in WT mice (305).

TG100-115 is a dual PI3Kδ/PI3Kγ inhibitor that has been successful in models of asthma and COPD (306). The compound was administered by aerosol as a preventative treatment in an OVA model of asthma and reduced infiltration of eosinophils and other leukocytes into the lungs. It also decreased airway hyper-responsiveness, IL-13 levels and mucin accumulation. TG100-115 also showed promise as an intervention treatment in asthma models, reduced neutrophilia and TNFα in response to lipopolysaccharide (LPS), and was effective as an intervention after cigarette smoke exposure (307).

1.6.3 Caveats of PI3K inhibition in inflammation

It can be seen that PI3Ks have a role in driving pathological inflammation and there are benefits of their inhibition in inflammatory diseases. However, it is important to remember that they are required in normal inflammation during an immune response: for example PI3Kγ KO mice, or mice treated with AS605240, failed to recruit macrophages to the lung in response to *S. pneumoniae* and had impaired clearance resulting in progressive pneumococcal pneumonia and decreased survival (308).

In addition, the crucial role of PI3Ks in the development and maintenance of immune cells may result in adverse effects of inhibitors. PI3Kδ KD (kinase dead) mice are skewed towards Th1 (302) and have a decrease in peripheral Treg numbers and function, secreting less IL-10 and failing to suppress inflammation in a colitis model (189) leading to the possibility that inhibition of PI3Kδ may decrease peripheral tolerance (309) (an additional concern with a PI3Kδ inhibitor might be spontaneous inflammatory bowel disease as were seen in some mouse models (179)). As mentioned above, mice with a dual PI3Kγ knockout and PI3Kδ inactivating point mutation were prone to inflammation. Pharmacological inhibiton of PI3Kδ did not promote T cell skewing *in vitro* but instead reduced production of all cytokines, and a PI3Kγ inhibitor had no effect either alone or in combination with a PI3Kδ inhibitor.

However, the authors still caution that dual inhibition of PI3Kδ and PI3Kγ may increase the risk of eosinophil-mediated inflammation (167, 190).

However, recent data from preclinical trials of a PI3Kδ inhibitor CAL101 suggest that no adverse effects were seen in a 28 day toxicity study in dogs, although with prolonged treatment in rats a decrease in the size of lymph nodes, including Peyer's patches, was noted (310). CAL-101, developed by Calistoga pharmaceuticals has also shown promise in phase I clinical trials treating haematological malignancies. Mostly mild or moderate side effects have so far been observed in an expanded study of 24 patients, with only one patient showing dose-limiting toxicity (311, 312).

In the heart, the kinase activity of PI3Kγ is required for its role in regulating β-adrenergic signalling. However PI3Kγ also binds phosphodiesterase 3B (PDE3B) and facilitates it's degradation of cyclic adenosine monophosphate (cAMP) and in doing so negatively regulates contractility. Therefore PI3Kγ KO but not KD mice have an increase in basal cardiac contractility and are more susceptible than wildtype controls to cardiomyopathy, ventricular dilation and heart failure (138). However, the fact that the kinase function of PI3Kγ is not crucial for its role in the heart bodes well for ATP-competitive inhibitors of PI3Kγ as immunomodulators, as they would not be predicted to have cardiac side effects.

Interestingly, recent research identifies differing roles for the two regulatory/adaptor subunits p84 and p101: the p84 subunit was first identified in the heart (which has low levels of the p101 subunit), where it associates with PDE3B and may therefore help to mediate the interaction of PI3Kγ with this protein. However both subunits were expressed in a variety of leukocytes and both could mediate interaction with $G_{\beta\gamma}$ (132) although p84/p110γ is recruited less efficiently (131).

Finally, many of the current small molecule ATP-competitive inhibitors also hit other enzymes such as mTOR or DNA dependent protein kinase (DNA-PK), which could potentially lead to off target side effects (reviewed (313)).

1.6.4 Modulation of Lipid phosphatase function

Overexpression of PTEN (i.e. lowering the levels of $PI(3,4,5)P_3$), was protective against OVA-induced asthma (25-27), and in toluene diisocyanate-induced airway disease, overexpression of PTEN (or use of LY294002) decreased IL-17 production, leukocyte infiltration, epithelial thickening, airway hyperresponsiveness and mucus secretion (314). In contrast, in a model of pneumonia, loss of PTEN increased the ability of the neutrophils to kill bacteria. Macrophage and neutrophil numbers in the lung were increased as were levels of chemokines and cytokines such as TNF, IL-1 and IL-6, whilst damage to the lung and mortality were reduced (207).

PTEN has also been suggested as a pharmacological target, although most interest is focussed on its role in insulin signalling, rather than in inflammation. Based on the fact that vanadates, particularly the bisperoxovanadiums, are potent inhibitors of PTEN, several selective small molecule inhibitors have been described (315). A possible drawback to the use of a PTEN inhibitor in the clinic is its potentially oncogenic action, although it will certainly be useful as a pharmacological tool (316). Intriguingly, thalidomide has been reported to cause limb deformities in developing foetuses through its actions on PTEN. It indirectly stabilises PTEN, protecting it from proteasomal degradation and thus suppresses Akt signalling, which in turn leads to increased caspase-dependent cell death. The phenotype could be rescued by either inhibition of PTEN or by insulin (317). Hence it can be seen that it would be desirable to avoid targeting non-immune cells when suppressing the PI3K pathway.

Therefore, when seeking a target for modulation of the immune system, the leukocyte-restricted expression of SHIP-1 makes it an especially attractive target (318). Of particular note is the identification of pelorol, a meroterpenoid originally isolated from the marine sponge *Dactylospongia elegans* (319) as an activator of SHIP-1. A chemical synthesis from (+)-sclareolide has also been devised for pelerol and more potent analogues. One of the derivatives, AQX-MN100, has been shown to reduce mast cell and macrophage activation *in vitro*, whilst *in vivo* it has an anti-inflammatory action in mouse ear oedema and is effective in reducing serum TNFα in a murine model of endotoxic shock (320).

It has been indicated that structural analogues of pelorol act through allosteric activation of SHIP-1. It was found that $PI(3,4)P_2$ and pelorol derivatives activate SHIP-1 by binding the C2 domain at the C terminal end of its phosphatase domain. The possibility of using an allosteric regulator reduces the chances of off-target effects compared to compounds that target the active site, and concurrent with this, the SHIP-1 activators were ineffective in SHIP-$1^{-/-}$ mast cells and macrophages, and did not affect SHIP-2 activity (321) (322). AQX-MN100 has also been shown to inhibit growth and trigger the apoptosis of multiple myeloma cell lines (323). A related compound AQX1125 is expected to enter clinical trials in 2011 as an anti-inflammatory, with preclinical studies indicating its use in asthma and other allergic disease (324).

However, the role of SHIP-1 in asthma remains unclear: knockout of SHIP-1 in mice caused death in up to half of mice by 10 weeks of age due to macrophage, neutrophil, lymphocyte, degranulating mast cell and eosinophil infiltration of the lungs. The KO mice had airway epithelial hypertrophy and fibrosis along with excessive mucus, IL-4, IL-13, eotaxin and CCL2 (30, 31), indicating the importance of tightly controlled PI3K signalling. However, other researchers have found that using an OVA model of asthma, loss of SHIP-1 *decreases* disease severity, with knockout animals having less eosinophil infiltration and decreased IgE, IL-4 and IL-13 (325).

1.7 Summary

In summary, it can be seen that the immune system is a highly complicated and delicately balanced system. Whilst much is known about the role of T cells and the PI3K pathway within the immune system, there are still fundamental gaps in our knowledge. Firstly there is significantly less information available about SHIP-1 than about PI3Ks themselves, partly because SHIP-1 has been considered a less attractive drug target than kinases. Secondly, much of the information about PI3K signalling in general, and SHIP-1 in particular, has been gathered using knockout mice, or pharmacological tools studied in murine disease models. Therefore, the aim of this thesis is to investigate the role of SHIP-1 in human T cells.

1.8 Aims of the research

The overall aim of the thesis was to characterise the role of SHIP-1 in human T lymphocytes. This could be subdivided into two main aims:

1) To set up a lentiviral delivery system for the modulation of SHIP-1 expression in primary human T cells.

2) To investigate the role of SHIP-1 in leukaemic T cell lines and in primary human T cells using the lentiviral expression system. In particular, there were a number of key objectives:

- To characterise phosphorylation of SHIP-1 as a marker for its activation in response to a variety of stimuli in leukaemic cells lines and primary human T cells
- To investigate the effects of SHIP-1 expression on survival of leukaemic cell lines
- To investigate the role of SHIP-1 in primary human T cell viability, proliferation and signalling
- To investigate the role of SHIP-1 on morphology and adhesion of primary human T cells
- To investigate the role of SHIP-1 in chemotaxis of primary human T cells
- To investigate the role of SHIP-1 on cytokine production and differentiation to T helper subsets
- To investigate the role of SHIP-1 in CD8+ T cell cytotoxicity

Chapter 2: Materials and Methods

2.1 Cell culture

2.1.1 Leukaemic T Cell Lines

Leukaemic cell lines (J6 Jurkats (Cancer Research UK), CCRF CEMs (Novartis) and HUT78s (unknown provenance) were cultured in T175 flasks at 37˚C in 95% air /5% CO_2. The culture medium was RPMI 1640 supplemented with 10% FCS, 10 µg/ml penicillin and 10µg/ml streptomycin (complete media/ complete RPMI). All cell culture reagents were from Invitrogen unless otherwise specified. All cell culture plasticware was from Nunc unless otherwise specified. Cells were cultured every 2-3 days. Cells were maintained at a confluency of 0.5-1x10^6/ml and discarded after 3 months.

2.1.2 rCD2:SHIP Jurkats

rCD2:SHIP was previously made in the lab by ligating DNA encoding the extracellular and transmembrane domains of rat CD2 with the catalytic core of human SHIP, which was cloned into the pUHD10-3-hygromycin regulatory plasmid and stably transfected into Jurkats expressing a tetracycline (tet) controlled transactivator, allowing a tet-off inducible expression system (Figure 2.1). The expression of rCD2:SHIP results in the constitutive membrane localisation of the catalytic core of SHIP and hence its constant phosphatase activity, which depletes the cell membrane of PI(3,4,5)P_3 and generated PI(3,4)P_2 (244) (Figure 2.1). SHIP 11 Jurkat clones (which express rCD2:SHIP) were cultured in the presence of 2 µg/ml tetracycline. rCD2:SHIP Jurkats and J6 Jurkats which were to be used in the same assays as rCD2:SHIP Jurkats, were not allowed to exceed a density of 5x10^5/ml during cell culture.

To induce expression of CD2:SHIP, cells were washed into complete media without tet and incubated for 24 hr. Samples of both were lysed and western blotted for rat CD2 using the monoclonal antibody OX34. However, the expression system appeared “leaky” with high levels of rCD2 expressed even in the presence of tet, with some further expression in the absence of the antibiotic. Therefore when the actions of CD2:SHIP are to be compared to cells lacking expression, the parental J6 cell line is used, rather than rCD2:SHIP Jurkats cultured in the presence of tet.

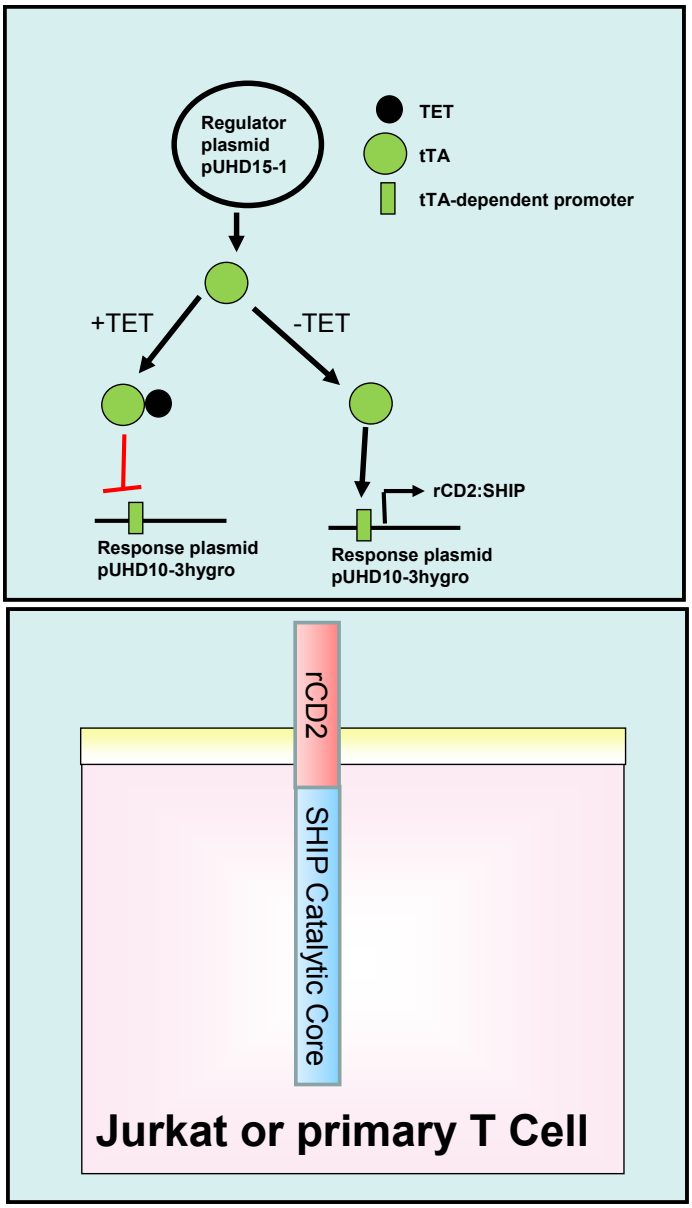

Figure 2.1 The tetracycline inducible gene system and rCD2:SHIP.
Top panel: Two plasmids are stably expressed in Jurkats. The regulator plasmid produces a tetracycline-sensitive transactivator (tTA) which in the absence of tetracycline binds the tTA-dependent promoter and induces the production of rCD2:SHIP. If tetracycline is present, it binds the tTA and alters its conformation so that it is unable to bind the promoter. Redrawn from Curnock *et al* (326).
Bottom panel: The chimeric protein, consisting of the catalytic core of human SHIP-1 fused to the extracellular and transmembrane domains of rat CD2 was stably expressed in clones derived from the J6 Jurkat cell line, under the control of a Tetracycline-regulated expression system as previously described (244). Alternatively, it was cloned into the lentiviral pCLPS expression vector for expression in primary human T cells. The SHIP-1 catalytic core is located next to the cell surface membrane where it can metabolise $PI(3,4,5)P_3$ to $PI(3,4)P_2$. Expression of the construct can be verified by western blotting for expression of rat CD2 in human cells. In addition live cells can be selected for expression of the chimeric protein on the basis of cell surface expression of rat CD2.

2.1.3 HEK 293T

Human embryonic kidney (HEK) 293T cells (A gift from Carl June, University of Pennsylvania, USA, hereafter, HEKs) were cultured in complete media. Cells were passaged every 2-3 days and allowed to reach no greater than 80% confluency.

To passage, media was removed, cells were washed once in PBS then trypsinised for 1 minute at room temperature. The media was put back onto detached cells and centrifuged. Cells were resuspended in fresh media and seeded into a new T175 flask. Cells were discarded after 30 passages.

2.1.4 A20

The A20 Mouse B lymphoma cell line (unknown provenance) was cultured in complete media, as for the human leukaemic T cell lines above, supplemented with 2-mercaptoethanol (50 μM, Sigma) to provide reduced cysteines. Cells were maintained at a density of $1x10^6$/ml by passaging every 2-3 days.

2.1.5 Isolation of Peripheral Blood Mononuclear Cells

Peripheral blood mononuclear cells (PBMCs) were isolated from the heparinised blood of healthy volunteers, by separation in Lymphoprep (Greiner Bio One). Briefly, 10-100 ml blood was collected in heparinised (final concentration of 10 Units/ml) syringes. Blood was diluted 1:1 in plain RPMI and layered onto Lymphoprep in 50ml falcon tubes. Tubes were centrifuged at 250xg for 30 min without braking upon deceleration and the middle (PBMC) layer removed with a Pasteur pipette. Cells were washed three times in plain RPMI to remove Lymphoprep.

2.1.6 Culture of T cells using SEB

PBMCs obtained as above were resuspended in the initial blood volume of complete RPMI plus 1 μg/ml of the superantigen Staphylococcal enterotoxin B (SEB, Sigma) for 72hrs. Cells were then washed into double the volume of complete RPMI and 36 U/ml IL-2 added to generate activated peripheral blood derived T lymphocytes (PBLs). Cells were cultured every two days, with the volume doubled each time and fresh IL-2 added at each passage. PBLs were used for experiments at days 9-12.

2.1.7 Isolation of CD4+, CD8+ and naive CD4+ T cells

PBMCs were isolated as previously described. The final wash was done in ice cold MACS buffer (PBS/ 0.5% BSA/ 2mM EDTA). The manufacture's protocol was then followed: briefly, cells were resuspended in 40 μL MACS buffer per 10^7 cells and

antibody cocktail at 10 µl/10^7 cells was added, incubated at 4°C for 15 minutes then a further 30 µl/10^7 cells MACS buffer added, then 20 µl anti-biotin microbeads. Following a further 10 minute incubation at 4°C the cells were washed once, resuspended in 500 µl and applied to an LS column (Miltenyi Biotec). The column was washed three times and the cells that passed though were collected, and their purity verified by flow cytometry. Kits used were from Miltenyi Biotec MACS: naïve CD4+ T cell isolation kit, human 130-091-894, pan T cell, human 130-053-001, CD8+ T cell isolation kit II, human 130-091-154, CD4+ T cell isolation kit II human 130-091-155.

2.1.8 Culture of isolated T cells using CD3/CD28 beads (Th0 conditions)

Cells were isolated with CD4+ T cell isolation kit II human (Miltenyi Biotec) or naïve CD4+ T cell isolation kit as required. Cells were cultured in RPMI 1640/10% FCS/ 10µg/ml penicillin /10µg/ml streptomycin (complete RPMI). Anti-CD3, anti-CD28 antibody coated activating beads (hereafter CD3/CD28 beads) were used at a ratio of three beads to one cell (Dynabeads Invitrogen 111.31D) and IL-2 at 36 U/ml. Cells were cultured every 2-3 days with further media and IL-2, to maintain them at 1 x10^6/ ml. Cells were discarded after 14 days

2.1.9 Culture of T cells under Th1 polarising conditions

Following isolation, naive CD4+ T cells were washed twice into complete RPMI at 1 x10^6/ml. CD3/CD28 beads were used at a ratio of three beads to one cell, IL-2 at 36 units/ml, IL-12 2 ng/ml and anti IL-4 200ng/ml. Cells were cultured every 2-3 days with further media and half quantities of cytokines, to maintain them at 1 x10^6/ ml.

2.1.10 Culture of T cells under Th2 polarising conditions

Following isolation, naive CD4+ T cells were washed twice into complete RPMI at 1 x10^6/ml. CD3/CD28 beads were used at a ratio of three beads to one cell, IL-2 at 36 units/ml, IL-4 20 ng/ml, anti-IFNγ 5 µg/ml and anti IL-12 5 µg/ml. Cells were cultured every 2-3 days with further media and half quantities of cytokines, to maintain them at 1 x10^6/ ml.

2.1.11 Culture of T cells under Th17 polarising conditions

Following isolation, naive CD4+ T cells were washed twice into complete RPMI at 1 x10^6/ml. CD3/CD28 beads were used at a ratio of three beads to one cell, IL-1β at 10 ng/ml, IL-6 50ng/ml, anti-IFNγ 10µg/ml, anti IL-4 10µg/ml and IL-23 10ng/ml. Cells

were cultured every 2-3 days with further media and half quantities of cytokines, to maintain them at 1 x10^6/ ml. All cytokines were from Peprotech and all antibodies were from R&D.

2.2 Electroporation and Lentiviral Methods

2.2.1 Electroporation

Electroporation was performed using a Microporator MP-100 and following the manufacturer's instruction (Figure 2.2). Cells (either freshly isolated CD4+ T cells or PBMCs cultured for 10 days in the presence of SEB and IL-2) were washed in Mg^{2+} Ca^{2+} free PBS. Immediately before electoporation cells were washed into the manufacturer's resuspension buffer R at a concentration of 2x10^7/ml. 0.5 µg pCLPS GFP plasmid was added and the mixture was pipetted into a supplied capillary pipette tip. A variety of parameters were used during optimisation and are indicated in the results. For subsequent electroporation of PH domain expression plasmids in freshly isolated CD4+ T cells parameter 8 was used with a single pulse of 2300V, with a pulse width of 20ms. Electroporation was performed using the supplied gold electrodes and electroporation buffer. Immediately following electroporation cells suspended in buffer R were pipetted into prewarmed complete media with IL-2. For the CD4+ T cells CD3/CD28 beads at a 1:1 ratio were also supplied. Cells were cultured for 48 hours before use in experiments.

2.2.2 Overview of the lentiviral expression system

Lentiviral expression systems are ideal for expressing proteins in difficult to transfect cells, when long term expression is required or when it is important that cells are not subjected to harsh conditions (e.g. electroporation, chemical transfection), which might alter their function (327, 328). Based on the HIV-1 virus, the lentiviral expression system utilises four plasmids. When these are simultaneously transfected into a HEK "packaging" cell line three of the plasmids supply the DNA necessary for manufacture of a viral particle, whilst the fourth plasmid is packaged into the viral particle (329). These viruses can then be used to infect the target cell. As they only contain the fourth plasmid, the infected target cell can only make proteins encoded by that one plasmid, and can't assemble a viral particle (Figure 2.2).

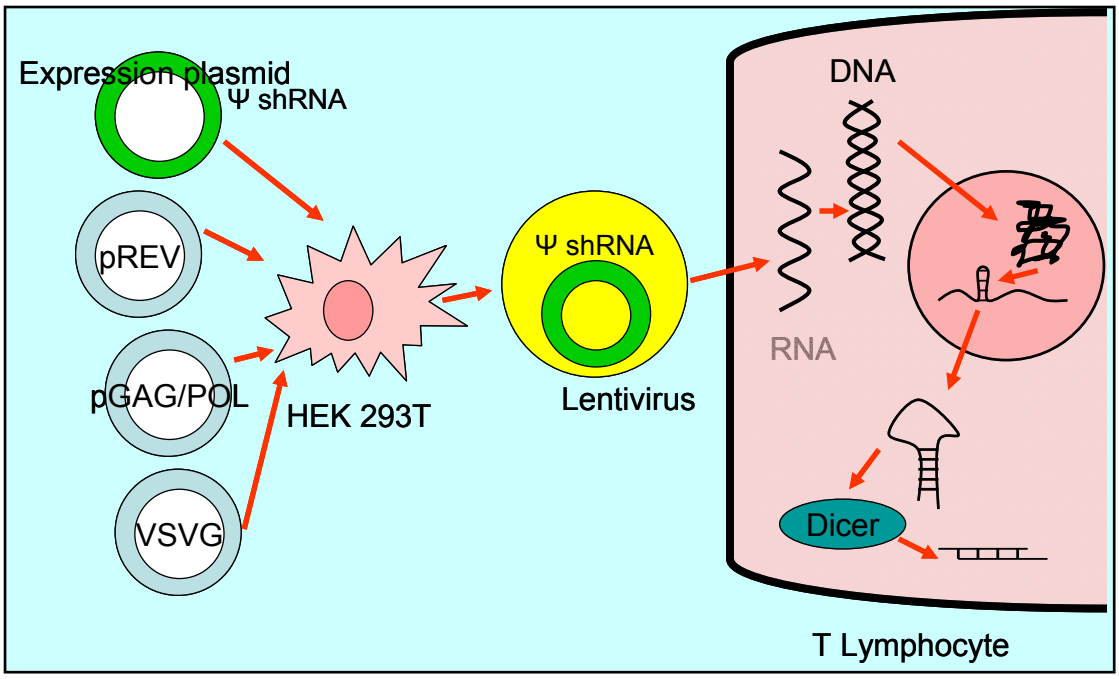

Figure 2.2 The Microporator MP-100 and the lentiviral method of gene delivery
Top panel: These images are taken from the manufacturer's website (www.microporator.com). On the left is the microporator equipment. On the right is the pipette tip in which cells are electroporated, showing the gold electrode that is used to conduct electricity. The microporator is reported to offer the benefits of electroporation with decreased cell death.

Bottom panel: Lentiviral plasmids were chemically transfected into HEK293T cells. VSVG, pREV and pGAG/POL code for the proteins necessary for the production of lentiviruses, which takes place in the HEK293T cells. During the construction of lentivirus, RNA is packaged into the virus when it includes a packaging signal (ψ). Hence only the expression plasmid, encoding shRNA (or rCD2:SHIP or GFP) is packaged into the lentivirus. This means that the lentivirus is incapable of reproducing. The lentivirus infects the target cell and the RNA from the expression plasmid is transcribed into DNA. The DNA integrates into the host cell DNA, and thus will be passed to daughter cells. The DNA encoding shRNA or protein can also be transcribed back to RNA. In the case of shRNA this is cleaved by Dicer as targets complementary RNA for destruction. In the case of proteins the RNA is translated into protein.

2.2.3 Use of transfer plasmids

When using the lentiviral expression system as described above, the fourth plasmid, the transfer or "expression" plasmid can be any appropriate plasmid that contains a ψ packaging sequence. Hence, the lentiviral delivery system can be used to deliver DNA cloned into an expression vector or commercially available expression plasmids can be used with the packaging system. The following plasmids were used as indicated in Table 2.1: The shRNA sequences against SHIP-1 (raised against either the 3' untranslated region (3'UTR) or the coding sequence (CDS) of the gene) and the shRNA scrambled control, (which contains at lease 4 base pair mismatches to any known human or mouse gene) were obtained from SIGMA and all the sequences are inserted into a pLKO.1-puro backbone plasmid (Table 2.1, Figure 2.3). The plasmid contains an ampicillin resistance element, to allow selection in *E. coli* and a puromycin resistance element to allow selection in mammalian cells. The pCLPS expression plasmid was used for the expression of GFP (green fluorescent protein). In addition rCD2:SHIP was cloned into this vector in place of GFP, as described in Section 2.16.4.

2.2.4 Transfection of packaging cell line with Lentiviral plasmids

The packaging plasmids used were: pRSV.Rev (Addgene No 12253), pMDLg/pRRE (Addgene No 12251) from Addgene and pVSVG (a gift from David Baltimore (California Institute of Technology, California, USA)). HEK 293T cells were cultured the day before transfection to give cells that were approximately 60% confluent on the day of transfection. Four hours before transfection the media on the flask was exchanged for 20 ml complete RPMI. Plasmids were transfected following a protocol provided by Olga Liu and Richard Carroll (University of Pennsylvania, Philadelphia, USA). On the day of transfection 1.3 ml RPMI/ 12.5 mM HEPES (4-(2-hydroxyethyl)-1-piperazineethanesulfonic acid, Invitrogen), and Mirus LT1 Transit (219 µl) (in earlier optimisation experiments Fugene 6 was used as the chemical transfection agent) were combined without letting the transfection reagent touch the side of the tube. The tube was immediately vortexed for 1 second and incubated at room temperature for at least 5 minutes. Plasmid DNA (73 µg total: comprised of 18 µg pRev, 18 µg pMDLg/pRRE, 7 µg VSVG and 30 µg expression plasmid) was combined with H_2O to take the final concentration of DNA to 0.5 µg/ml. The plasmid mix was then added slowly to the RPMI/HEPES/Mirus and then the tube was vortexed again for one second. The tube was incubated at room temperature for 30-45 minutes. The solution was then gently pipetted up and down twice, then added to

Table 1.1 Lentiviral expression plasmids

Plasmid	Source	Reference number	Product
pCLPS	J. Riley, Uni. Of Pennsylvania, USA		GFP or rCD2:SHIP
TRCN0000039893	Sigma MISSION shRNA	1	SHIP-1 shRNA CCGGGCTAAGTGCTTTACGAAC ATTCTCGAGAATGTTCGTAAAGCACTTAGCTTTTTG (3UTR)
TRCN0000039894	Sigma MISSION shRNA	2	SHIP-1 shRNA CCGGGCTCATTAAGTCACAGAAATTCTCGAGAATTTCTGTGACTTAATGAGCTTTTTG (CDS)
TRCN0000039895	Sigma MISSION shRNA	3	SHIP-1 shRNA CCGGGCCCATATCACCCAAGAAGTTCTCGAG AACTTCTTGGGTGATATGGGCTTTTTG (CDS)
TRCN0000039896	Sigma MISSION shRNA	4	SHIP-1 shRNA CCGGGCAGAAGGTCTTCCTACACTTCTCGA GAAGTGTAGGAAGACCTTCTGCTTTTTG (CDS)
TRCN0000039897	Sigma MISSION shRNA	5	SHIP-1 shRNA CCGGGCCTTCCAGATCGGAAATCAACTCGA GTTGATTTCCGATCTGGAAGGCTTTTTG (CDS)
SHC002	Sigma MISSION Non-Target shRNA Control Vector		Non-targeting shRNA CCGGCAACAAGATGAAGAGCACCAACTCGAG TTGGTGCTCTTCATCTTGTTGTTTTT

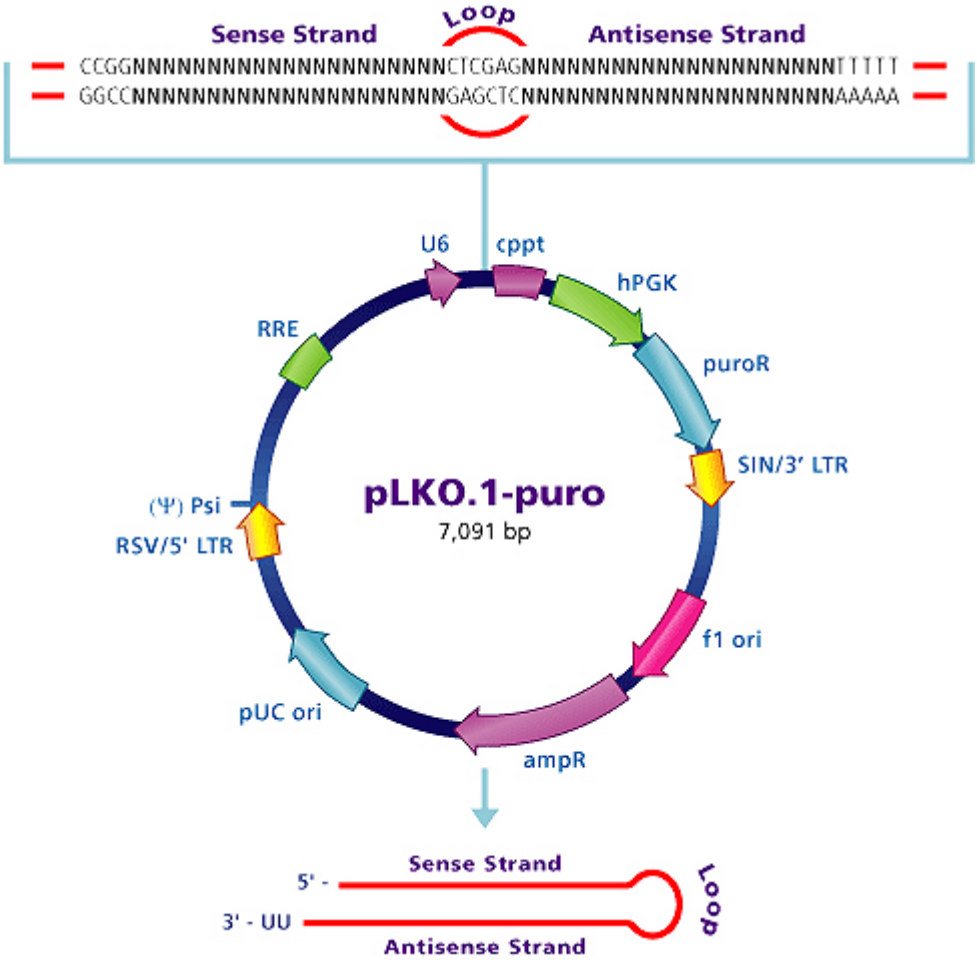

Figure 2.3 The Mission shRNA vector map
This diagram is from the Sigma website (www.sigma.com). This plasmid was used to express the shRNA control and SHIP-1 shRNA. The main backbone is a pLKO.1-puro vector and indicated on the diagram are the ampicillin (ampR) and puromycin (puroR) resistance elements, as well as the site for shRNA coding, the ψ packaging sequence and the long terminal repeats (LTR) that facilitate integration into the host cell DNA.

the flask of HEK293T. The flask was rocked gently to disperse the mixture. Cells were incubated for 48 hours, media containing the virus was harvested and replaced with fresh media. After a further 24 hours this media was also harvested and cells were discarded. Media was clarified by centrifugation, and then filtered using a 0.45 µm pore filter, aliquoted into 2ml Nunc vials and stored at -80˚C.

2.2.5 Determination of viral titre and MOI

To determine multiplicity of infection (MOI), supernatant from GFP-virus producing HEKS was harvested and serial dilutions used to culture HEKS seeded at 50% confluency in 6 well plates 18 hours previously. After 48 hours the supernatant was removed, cells were trypsinised from the plate, resuspended in Fluorescence Analyser and Cells Sorter (FACS) buffer (PBS 0.5% BSA) and the proportion that were GFP positive were assessed by flow cytometry (see section 2.5.1). This was then used to calculate the initial number of cells infected per ml of supernatant applied and from that a viral titre per ml of supernatant was used to calculate the volume of viral supernatant required to give the desired MOI. The MOI is the number of viral particles per target cell. Generally, there needs to be more than one virus per cell as some will be degraded before infection and sometimes two viruses may infect a single cell. E.g. 5ml of supernatant at $1x10^6$ virus particles /ml would be required to infect $5x10^5$ cells at an MOI of 10.

2.2.6 Construction of puromycin kill curve

Primary CD4+ T cells cultured as above for four days were exposed to escalating concentrations of puromycin (Sigma). The minimum concentration required to cause 100% cell death (verified by trypan blue staining) was assessed after 48 hours. This was found to be 0.3 µg/ml, Sigma's shRNA plasmid literature suggested a range between 1 and 10 µg/ml, in order to select cell on the basis of puromycin resistance. However, the lower concentration was always found to be effective at killing uninfected populations.

2.2.7 Infection of cell lines with lentivirus

CEMs were passaged the day before transduction. $5x10^5$ cells in 1 ml complete RPMI were added to a 6 well plate and 2 ml of media containing the virus was added. Cells were incubated overnight then media was washed and replaced with complete media and cells were incubated for a further 48 hours at a density of $1x10^6$ /ml and then assessed for GFP by flow cytometry if required. Alternatively, in the case of infection with shRNA encoding lentivirus, puromycin at 10 µg/ml was used to select

infected cells which were then assessed for expression of SHIP-1 by Western blotting after a further 72 hours.

2.2.8 Infection of primary CD4+ T cells

PBMCs were isolated from the blood of human volunteers as described above. CD4+ or CD8+ T cells were then purified from the PBMCs using a Miltenyi Biotec MACs kit, according to the manufacturer's instructions. The CD4+ cells were resuspended at $1x10^6$ /ml in complete RPMI and CD3/CD28 beads were added at a ratio of 3 beads/cell. Cells were incubated for 24 hours. Cells were then gently pipetted to break up clumps, and added to 6 well plates at $1x10^6$ cells/ well. Lentivirus was thawed on ice if required, then added to the T cells. Infection was performed in the presence of polybrene at 5 µg/ml, and in complete media supplemented with 36 U/ml IL-2. Cells were spinoculated for the first 90 minutes of infection by centrifugation at 300xg. Plates were then returned to the incubator for 24 hours. The media was then exchanged for complete RPMI supplemented with 36 U/ml IL-2 and cells were cultured for a further 48 hours. At this point GFP positive cells were assessed for expression by flow cytometry, rCD2:SHIP expressing cells were sorted by rCD2 expression, and shRNA expressing cells were selected by culture with puromycin (0.3 µg/ml) for 72 hours. Cells were used for experiments up to 14 days after isolation.

2.2.9 Isolation of rCD2 positive cells

Positive selection or rCD2:SHIP expressing primary CD4+ T cells was performed on the basis of cell surface expression of rat CD2 using a MACs kit according to manufacturer's instructions. Briefly: three days post infection, cells were washed twice into MACS buffer. They were incubated for 1 hour at 4°C with anti-rat CD2 (AbD serotec MCA154G 1:30), then washed and incubated for 15 minutes at 4°C with rat anti-mouse IgG2a+b microbeads (Miltenyi Biotec 130-047-201) at 20 µl/10^7 cells. Cells were then washed and resuspended in 500 µL MACs buffer. Cells were applied to an LS column against a magnet and washed three times. The rCD2 positive cells were retained by the column. The column was removed from the magnet and flushed with 5 ml MACs buffer to recover the cells.

2.3 Cell stimulations

Unless otherwise specified, the day before cell stimulation, primary T cells were removed from CD3/CD28 beads and were cultured overnight in complete RPMI in the absence of IL-2. SEB expanded T cells were also cultured overnight in complete

RPMI in the absence of IL-2. Cell lines were cultured overnight as normal. On the day of stimulation, cells were washed into RPMI at a concentration of $2x10^6$ /ml in a volume of 0.5 ml in eppendorf tubes and incubated for an hour at 37˚C. Cells were stimulated as appropriate in a waterbath at 37˚C, then centrifuged for 30 seconds to pellet the cells, the media was aspirated and 100 µl of an appropriate lysis buffer was added, or an appropriate volume of fixative.

2.4 Measurement of phosphoinositide levels

2.4.1 PI(3,4,5)P_3

To extract lipids $5x10^6$ CD4+ T cells (day 9-10) were used, and stimulations were performed as in Section 2.3. After stimulation, cells were rinsed with 0.5 M TCA then twice with 5% TCA /1 mM EDTA. Neutral lipids were extracted by washing twice in MeOH:$CHCl_3$ (2:1) with a 10 minute incubation each time. Acidic lipids were then extracted by incubating for 15 minutes in MeOH: $CHCl_3$:12 M HCl (80:40:1) followed by centrifugation. The pellet was discarded and the supernatant was phase split by addition of $CHCl_3$ and 0.1 M HCl. After centrifugation, the lower, organic phase was dried in a vacuum dryer. For the PI(3,4,5)P_3 ELISA, dried lipids were resuspended in 120 µL of the supplied PIP_3 buffer and the competitive ELISA was performed according to the manufacturer's instructions (Echelon Bioscience cat # K-2500). All chemicals used were from Sigma.

2.4.2 PI(3,4)P_2

For assessment of PI(3,4)P_2 levels, the above protocol was followed for extraction of lipids. After drying, lipids were resuspended in 10 µL of $CHCl_3$:MeOH: H_2O (1: 2: 0.8) and sonicated in an icy waterbath. The solution was spotted onto mass strip nitrocellulose paper (Echelon Bioscience cat # K-3400) which was prestained with appropriate controls, and the manufacturers instructions were followed to label PI(3,4)P_2 with antibody and HRP-conjugated secondary antibody. The results were captured on X-ray film.

2.5 Measurement of phospho- and total protein levels

2.5.1 Western blotting

Cells were stimulated as described in Section 2.3 and lysed in 100µL lysis buffer (50 mM Tris-HCL pH 7.5, 150 mM NaCl, 1% Nonidet P40 (BioRad), 5 mM EDTA, 1 mM

sodium vanadate, sodium molybdate, 10 mM sodium fluoride, 40 μg/ml PMSF, 0.7 μg/ml pepstatin A, 10 μg/ml aprotinin, 10 μg/ml leupeptin, 10 μg/ml soyabean trypsin inhibitor) on a rotator at 4˚C for a minimum of 1hr and then centrifuged at 600 g for 10 minutes. 25 μl 5x sample buffer was added and samples were heated to 85˚C on a hot block for 10 min. Samples were briefly centrifuged then either loaded directly onto gels or stored at -20˚C. 10% or 7.5% (for clearer resolution of SHIP-1 variants) gels were poured. 15 μl of sample was loaded per lane, (5 μl for the molecular weight marker). Samples were stacked at 80 V and resolved at 180 V. Gels were then transferred onto nitrocellulose membrane (BioRad) for 1 hr at 0.8 mA per cm^2 in semi-dry buffer. Membranes were blocked for 1 hr in TBS Tween (TBST, 20 mM Tris-HCl, 150 mM NaCl, 0.1% Tween)/ 5% milk (Marvel). Membranes were briefly washed in TBST, then incubated in primary antibody overnight at 4˚C. Primary antibodies were used at 1:1000 dilution of stocks, in TBST with 5% BSA, 0.01% sodium azide, with the exception of the pY^{1020} SHIP-1 antibody, which was used at 1:2500 in TBST with 1% BSA, 0.01% sodium azide (Table 2.2). The following day, membranes were washed 3 times in TBST then incubated for at least 1 hour at room temperature in secondary antibody at 1:10,000 in TBST /1% milk. Membranes were then washed a further 3 times in TBST, then shaken gently for 1 minute in ECL or ECL Advance (Amersham Bioscience), and exposed to X-ray film (Fuji) to visualise antibody binding.

All membranes were assessed for equal protein loading. If required, membranes were stripped of the original antibodies by rehydrating in TBST then incubating at 60°C for 20 minutes in stripping buffer (100mM 2-mercaptoethanol, 2% SDS, 62.5nM Tris-HCl pH 6.7). Membranes were then washed for 3x 15 minutes in TBST, and reblocked, before incubation with a second primary antibody. If stripping was not required (because the molecular weights of the two proteins being examined were sufficiently different), then membranes were washed for 10 min in TBST then reblocked before incubation with a second primary antibody. All chemicals were from Sigma except where otherwise stated.

Table 2.2 Antibodies for western blotting and cell stimulations

Reagent	Manufacturer	Product code
SHIP-1 antibody	Santa Cruz	6244
pY^{1020}SHIP antibody	Stem Cell Technologies	01507
AKT antibody	Santa Cruz	1618
pS^{473} AKT antibody	Cell Signalling	9271
ERK antibody	Santa Cruz	93
pERK antibody	Cell Signalling	4377
β-actin –HRP conjugate	Cell Signalling	5125
rCD2 antibody (OX34)	AbD Serotec	MCA154GA
Anti-CD3 (UCHT1)	eBioscience	16-0038
Anti-CD28 (9.3)	Gift from Carl June, University of Pennsylvania, USA	-
HRP conjugated anti-rabbit	Dako	P0448
HRP conjugated anti-goat	Dako	P0160
HRP conjugated anti-mouse	Dako	P0447

Table 2.3 Flow cytometry antibodies*

Antigen	Antibody #	Supplier	Dilution used	Fluorophore
CD4	555346	BD Pharmingen	1:20	FITC
CD8	FAB1509F	R&D	1:10	FITC
CD25	555431	BD Pharmingen	1:20	FITC
CD11a	2120114	Immunotools	1:20	PE
CD49d	21488494	Immunotools	1:20	PE
CXCR3	FAB160P	R&D	1:10	PE
CXCR3	550967	BD Pharmingen	1:20	APC
rCD2	MCA154F	AbD Serotec	1:20	FITC
Annexin V	10040-15	Southern Biotec	10µL/ 10^6 cells	Cy-5
IL-17	IC317IP	eBioscience	1:10	PE
IL-4	12-7049-41	eBioscience	1:10	PE
IFNγ	12-7319-41	eBioscience	1:10	PE
pERM	3141	Cell Signal Technology	1:20	Unconjugated
ERM	3142	Cell Signal Technology	1:20	Unconjugated

*Dilutions used are of the supplied stock (which generally did not provide a concentration in µg/ml)

2.5.3 Mesoscale plate analysis of phospho- and total proteins

In addition to western blotting, levels of phosphorylated proteins in the PI3K pathway were quantified, using the MSD mesoscale system (Figure 2.4). To prepare lysates, day 9 cells were removed from beads and cultured in complete media overnight. The following day they were washed into plain RPMI and incubated at 37°C for 1 hour. They were then stimulated as required and then lysed in the supplied Tris-based lysis buffer. The mesoscale plate assay was then performed according to the manufacturer's instructions, with phospho (K11115D-1) and total proteins plates (K11133D-1) being performed in parallel. Briefly; plate were blocked for 1 hour in the supplied blocking buffer, then 25 µL lysate/well was placed onto the 96-well assay plate, pre-coated with capture antibody and incubated for 1 hour at room temperature before washing. Detection antibody was diluted in the supplied diluent and incubated for 1 hour at room temperature before washing. The supplied Read Buffer was added to each well and plates were read on a Mesoscale Sector 6000.

2.6 Flow cytometry of live cells

All flow cytometry was performed on a BD FACs Canto, using a FACs buffer of PBS/0.5% BSA. Cells were gated on viable population based on FSC and SSC and 10,000 events in this population were acquired.

2.6.1 Flow cytometric analysis of GFP expression

For analysis of GFP expression, cell were washed once in PBS and resuspended in 200µl PBS and assessed on a FACSCanto II with BDFacs DiVa software for fluorescence with excitation at 488nm, emission at 518nm.

2.6.2 Antibody staining

For cell surface staining by conjugated antibodies, beads were magnetically removed from cells. $1x10^6$ cells were then washed twice in ice cold FACs buffer (PBS +1% BSA) than the conjugated antibody was added at the recommended dilution (Table 2.3) in a volume of 50µL and incubated on ice in the dark for 30 minutes. Cells were then washed once and resuspended in FACs buffer on ice. For unconjugated antibodies, the same procedure was followed, but after washing, cells were resuspended in a minimum volume FACs buffer, and a conjugated secondary was added at 1:100 for 30 minutes,

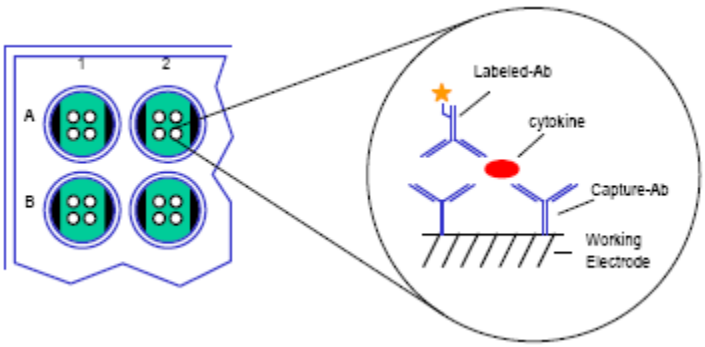

Figure 2.4 The MSD mesoscale technology
This figure is taken from the manufacturer's website (www.mesoscale.com). Capture antibody is bound to dots in the bottom of wells on a 96 well plate. There are up to 10 dots per well, allowing form 10 different analytes to be examined in a single well. Protein is bound by the capture antibody then detected with a labelled antibody. The Label emits light when excited by electricity passing through the base of the plate. This is recorded by a camera in the MSD sector imager machine and is automatically quantified.

before washing and final resuspension. For analysis of apoptotic cells see apoptosis assay.

2.6.3 CFSE labelling

Carboxyfluorescein succinimidyl ester (CFSE) is a fluorescent dye that covalently binds to intracellular proteins (330). As cells proliferate, the dye is equally partitioned between daughter cells and thus each daughter cell will have half the fluorescence intensity of the original cell when assessed by flow cytometry. To perform CFSE assays the manufacturer's protocol was followed. Briefly, freshly isolated CD4+ T cells were resuspended at $1x10^6$ /ml in PBS /0.1% BSA. 2 µL of 5 mM CFSE solution (Invitrogen) was added per ml and cells were incubated at 37°C for 15 minutes. Cells were then washed twice in complete media, followed by another wash after 30 minutes. Cells were then cultured as desired for seven days, before CFSE fluorescence was assessed by flow cytometry. For labelling of previously activated cells, day 7 cells were rested overnight off CD3/CD28 beads in complete media. Cells were resuspended at $1x10^6$ /ml in PBS /5% BSA. 1 µL of 5 mM CFSE solution was added per ml and cells were incubated at 37°C for 15 minutes. Cells were then washed twice in complete media, followed by another wash after 30 minutes. Cells were cultured as required for 48 hours before CFSE fluorescence was assessed by flow cytometry.

2.7 Flow cytometry of fixed cells

Flow cytometry was performed essentially as for live cells. Cells were prepared using a BD cytofix/cytoperm kit (554715) which causes some alterations to FSC and SSC, but still allows intact cells to be distinguished from debris when gating. $1x10^5$ cells were acquired from each sample with obvious debris excluded from the acquisition.

2.7.1 Intracellular staining of pSTAT3

Cells were stimulated as required then immediately fixed in BD cytofix for 1 hour. They were washed twice in BD perm/wash and incubated in 100µL volume ($1 x10^6$ cells) for 15 minutes before addition of antibody or isotype control (1:100) overnight (all incubations at 4°C). Cells were then washed three times and resuspended in FACs buffer for flow cytometry.

2.7.2 Intracellular staining of actin

Cells were stimulated as required then immediately fixed in BD cytofix for 1 hour. They were washed twice in BD perm/wash and incubated in 100 µL volume ($1x10^6$ cells) for 15 minutes before addition of 50 ng/ml Phalloidin TRITC (Sigma) for 3 hours (all incubations at 4°C). Cells were then washed three times and resuspended in FACs buffer.

2.7.3 Intracellular staining of pERM and ERM

pERM or ERM antibody was applied as for pSTAT3, but following the last wash, were resuspended in 100µL BDperm/wash. Secondary antibody (Goat anti-rabbit FITC, Dako) was added (1:100 dilution) Cells were incubated at 4°C for 3 hours before being washed three times and resuspended in FACs buffer.

2.7.4 Intracellular staining of cytokines

On day nine-ten post isolation $1x10^6$ cells were restimulated for 6 hours using PMA (50ng/ml)/Ionomycin (1 µg/ml) in the presence of Golgistop (BD), to cause the retention of cytokines. Cells were then fixed and the desired cytokine was stained using conjugated antibodies for IL-4, IFNγ or IL-17 as described for pSTAT

2.7.5 Triple Treg stain

For identification of Tregs the Human Regulatory T cell Staining Kit #3 (w/ PE-Cy5 Foxp3 PCH101, FITC CD4, PE CD25; Treg Kit) from eBioscience (cat #88-8995) was used according to the manufacturer's instructions. Briefly, $1x10^6$ cells were resuspended in 100µL eBioscience staining buffer, and 20 µL anti-CD4 anti-CD25 cocktail (or appropriate isotype controls) was added and cells incubated at 4°C for 30 minutes. Cells were washed once in buffer then resuspended in 1ml eBioscience Fixation/permeabilization buffer for 1 hour at 4°C. Cells were then washed twice in Permeabilization buffer, resuspended in 100µL Permeabilization buffer/2% normal rat serum for 15 minutes, then 5µL anti-Foxp3 or appropriate isotype control was added for 1 hour. Cells were washed twice in permeabilisation buffer and resuspended in staining buffer for flow cytometry. Appropriate single stains were also done to allow manual compensation on the flow cytometer.

2.7.6 Cell cycle analysis

$1x10^6$ cells were washed once in PBS then fixed in 70% ice cold ethanol. Cells were incubated at 4°C for 1 hour then washed twice in PBS. Cells were resuspended in

PBS/1µg/ml RNase (Qiagen) for 30 minutes at room temperature then DNA was stained using PI (50 µg/ml, Sigma) for 1 hour at 4°C in PBS. Cells were washed twice and resuspended in PBS for flow cytometry.

2.8 Confocal microscopy of live cells

All confocal microscopy was performed on a Zeiss LSM 510 Meta at room temperature (except for chemotaxis assay, see later). To stain for rCD2, a FITC conjugated antibody was used at 1:100, as for flow cytometry. $1x10^6$ cells were labelled for 1 hour at 4°C in PBS/ 1% BSA. Cells were then washed twice and resuspended in Annexin labelling buffer (10 mM HEPES pH 7.4, 140 mM NaCl, 2.5 mM CaCl2, 0.1% BSA). Annexin-cy5 (1:100) and PI (1 µg/ml final concentration) were added 5 minutes prior to imaging, at 4°C. Imaging was performed at room temperature.

2.9 Confocal microscopy of Fixed Cells

2.9.1 pERM, Actin and nuclear triple stain

pERM was stained as for flow cytometry: $1x10^6$ cells were stimulated as required then immediately fixed in BD cytofix for 1 hour. They were washed twice in BD perm/wash and incubated in 100µL volume (1 $x10^6$ cells) for 15 minutes before addition of antibody or isotype control (1:20) overnight (all incubations at 4°C). Cells were then washed twice in BDperm/wash and following the last wash, cells were resuspended in 100 µL BDperm/wash. Secondary antibody (Goat anti-rabbit FITC 1:100 dilution), DAPI, for nuclear staining (1 µg/ml) and Phalloidin TRITC (50 ng/ml) for staining of polymerised actin were also used. When actin only was stained, this was done for three hours immediately after the fixative was washed off. Cells were then washed twice in BD perm/wash and once in MilliQ. They were resuspended in 100 µL MilliQ and spun onto coverslips using a Shandon Cytospin 3 (10 minutes at 500 rpm, low acceleration). Coverslips were adhered to slides using Mowoil and allowed to set overnight. Cells were then visualised on a confocal microscope. All chemicals were from Sigma.

2.9.2 ERM and nuclear dual stain

ERM was stained as for pERM above at a 1:20 dilution of the stock antibody. During incubation with the secondary antibody, DAPI was used to stain the nucleus and cells were mounted and visualised as above.

2.10 Scanning Electron Microscopy

$2x10^6$ cells were removed from beads and cultured in complete media overnight. They were then washed into plain RPMI for 1 hour. They were then transferred to 24 well plates with Thermanox coverslips at the bottom of each well. They were incubated for a further hour, in inhibitors as necessary. Cells were fixed by replacing the media with RPMI /2.5% glutaraldehyde/1% tannic acid. Plates were incubated for 2 hours at 37˚C. Coverslips were then washed with plain RPMI. Cells were postfixed in aqueous 1% osmium tetroxide for 1 hour at room temperature. Cells were washed twice in distilled water, each time incubating for 5 minutes. Coverslips were transferred to glass petri dishes. Cells were stained with aqueous 2% uranyl acetate for 1 hour in the dark. Cells were dehydrated in acetone by washing twice in 50%, 70%, 90 % and 100% acetone, each time incubating for 5 minutes. They were then incubated in 1:1 Acetone: hexamethyldisilazane (HMDS) for 15 minutes, then twice in 100% HMDS for 15 minutes. HMDS was then pipetted off, and coverslips were dried in a fume hood overnight. Coverslips with cells were coated in gold and cells were visualised on a JEOL JSM6480LV scanning electron microscope. All chemicals were from Sigma.

2.11 Cell viability assays

2.11.1 MTT assay

Serial dilutions of H_20_2 in RPMI were made in 96 well plates to give a volume of 100µl. Cells at $1x10^6$/ml in RPMI were added at 10^5 cells/ well (i.e. 100 µL/well), and incubated for 30 minutes. Plates were centrifuged for 5 min at 300 xg and the media was aspirated and replaced with complete media. Plates were returned to the incubator for 20 hours, then 20µl of MTT (Sigma) at 5 mg/ml was added to each well. After a further 4 hours at 37˚C media was aspirated and cells were lysed in 100 µl/well DMSO 100%. The plate was read for absorbance at 550 nm on a Versamax microplate reader.

2.11.2 Trypan Blue exclusion assay

Cells were seeded in 96 well plates at 10^5 cells/well in 100µl in RPMI. TRAIL (Immunotools) or TNFα (Peprotech) at appropriate dilution was added in RPMI supplemented with 0.2% FCS (final FCS concentration 0.1%). Plates were incubated at 37˚C and samples were taken at 6 and 24 hours. Samples were diluted with

Trypan blue (1:10, Invitrogen) and 100 cells from each well were counted in a haemocytometer.

2.11.3 Apoptosis assay

Cells were treated as described in the trypan blue exclusion assay. At 6 hours, plates were centrifuged at 250g for 5 min, the media was aspirated and cells were resuspended in Annexin binding buffer (10 mM HEPES pH 7.4, 140 mM NaCl, 2.5 mM CaCl2, 0.1% BSA) plus AnnexinV-FITC (25 ng/test Apoptest A700 Dako) and propidium iodide (2.5 µg/ml). After a 10 minute incubation on ice cells were analysed by flow cytometry for emission at 518nm (FITC) and 617nm (propidium iodide). Compensation was performed manually.

2.12 Cytokine assays

2.12.1 Mesoscale 10-plex cytokine assay

Naïve CD4+ T cells were incubated under Th0, Th1 or Th2 conditions as described above. After nine days the cells were washed into complete RPMI without cytokines, and restimulated with CD3/CD28 beads at 1:1 ratio for 16 hours in a volume of 100µL and at a concentration of $1x10^6$ cells/ml. After this the supernatant was collected and the cytokines present were analysed on an MSD mesoscale plate (K11010B-1) and absolute amounts calculated using a standard curve of known concentrations. The cytokines examined were IFN-γ, IL-1β, IL-10, IL-12 p70, IL-13, IL-2, IL-4, IL-5, IL-8 and TNF-α . Briefly, the protocol was as follows: Wells were blocked for 1 hour at room temperature with 1% w/v MSD blocker B, washed in PBS/ 0.05% Tween-20, and 25 µL sample was added to the well. The plate was incubated on an orbital shaker for 2 hours and then 25 µL of the supplied detection antibody cocktail was added without removing the sample. The plate was incubated with shaking for a further two hours then washed three times with PBS/ 0.05% Tween-20 and 150 µL of 2x MSD Read buffer T was added and the plate was read on an MSD Sector imager 6000.

2.12.2 IL-17 ELISA

Naïve CD4+ T cells were cultured under Th0, or Th17 conditions as appropriate. After nine days the cells were washed into complete RPMI without cytokines, and restimulated with CD3/CD28 beads at 1:1 ratio for 16 hours at a concentration of $1x10^6$ cells/ml. After this the supernatant was collected and the cytokines present

were analysed using an IL-17A ELISA (eBioscience cat #88-7176) and absolute amounts calculated using a standard curve of known concentrations.

2.13 Adhesion assay

The adhesion assay was based on a protocol from Vielkind *et al.* (331) Briefly, Flat-bottom Maxisorp 96-well plates (Nunc) were coated overnight at 4°C with recombinant human ICAM-1 (CD54, 12.5µg/ml) (R&D ADP4-050) or fibronectin (10µg/ml R&D 1918-FN-02M) in PBS. Wells were washed once with PBS and blocked with 2% BSA /PBS for 1 h at 37°C. The wells were washed once with PBS and once with plain RPMI. CD4+ T cells (day 9-10 post isolation) were labelled with CFSE as above. The labelled cells were added to the precoated plates at $5x10^5$ cells/well (input cells) in 100 µl of RPMI without phenol red supplemented with 0.1% BSA and were collected at the bottom of the well by centrifugation (1 minute 300xg). UCHT1 was added at 10µg/ml for the entire incubation or CXCL11 at 10nM for the last 15 minutes. The plates were incubated at 37°C for 30 min. The wells were filled with chemotaxis media (37°C) and covered with a plate sealer (Costar) and the sealed plate was turned upside down for 15 min at 37°C allowing the nonadherent cells to detach. While leaving the plate turned upside down, the plate sealer was removed. Adherent cells were then detached using 10mM EDTA and transferred to flat 96-well black plates (Sterilin 611F96BK). Adhesion was quantified by a multidetection plate reader (FLUOstar OPTIMA, BMG labtech) and the background adhesion (adhesion to BSA coated wells) was subtracted from the reading for each well.

2.14 Migration assays

2.14.1 Neuroprobe

CD4+ T cells (day 8-9) were removed from CD3/CD28 beads and washed into complete media without IL-2 and incubated overnight. The following day they were washed into plain RPMI without phenol red supplemented with 0.1% BSA (chemotaxis media) at $3.2x10^6$/ml and rested for 1 hour. Neuroprobe chemotaxis plates (ChemoTx®101-5) were preincubated with chemotaxis media for 1 hour then aspirated. Chemokine dilute in chemotaxis media was placed in the well in volumes of 29µL. A membrane with 5µm pores was placed on top. Cell suspension was dotted in bubbles on top of the membrane, in volumes of 25µL (Figure 2.5). The plate was incubated at 37°C for three hours. The bubbles were wiped from the membrane and the plate was centrifuged for 10 minutes at 300xg. Contents of the wells were

pipette into FACs tubes in a total volume of 300µL in PBS and cells were counted by flow cytometry.

2.14.2 Ibidi slide videomicroscopy

Hydrophobic uncoated µ-slides for chemotaxis (Ibidi #80301, obtained from Thistle Scientific) were coated with fibronectin at 45 µg/ml in PBS for 1 hour at room temperature and then washed twice with Milliq. This was indicated by the manufacturer to give a coating density of 1.5 µg/cm^2. The slide and all reagents were warmed to 37°C to prevent formation of bubbles. The slide was filled with chemotaxis media, chemokine was added to the top chamber as required, in a volume of 18 µL, and cells (prepared as above, for the neuroprobe chemotaxis assay, but to a concentration of 5x10^6 /ml), were pipetted onto the bridge in a volume of 6µL (Figure 2.5). A chemokine gradient was allowed to form for 15 minutes at 37°C, after which the cells were recorded for 15 minutes at 37°C on the LSM 510 Meta, with an image being taken every 15 seconds. The paths of 20 individual cells were tracked using the imageJ manual tracker and analysed using the imageJ chemotaxis tool.

2.15 CD8 cytotoxicity assay

This protocol was modified from that published by Van Gool *et al.* (332). Briefly CD8+ T cells were isolated and cultured as described above. On day 7-8 they were removed from beads and rested for 1 hour in complete media in the presence of Wortmannin (100 nM, Sigma) LY294002 (20 µM, Sigma) or ZSTK474 (1 µM, Zenyaku) if necessary. They were then washed into complete media without inhibitors. Meanwhile A20 cells were loaded with CFSE, following the protocol for freshly isolated T cells. In complete media, CD8+ T cells (effector cells) were combined in varying ratios with A20 cells (target cells) to give a total of 1x10^6 cells in a volume of 200 µL. The addition of UCHT1 at 10 µg/ml directed killing of A20 cells as indicated in Figure 2.6. The cells were incubated together for three hours at 37°C at which point cell were washed into annexin labelling buffer and incubated with annexin V-cy-5 (1:100) for 15 minutes. Cells were then assessed by flow cytometry for CFSE (i.e. discrimination of effector and target cells) and cy-5 (identification of apoptotic cells).

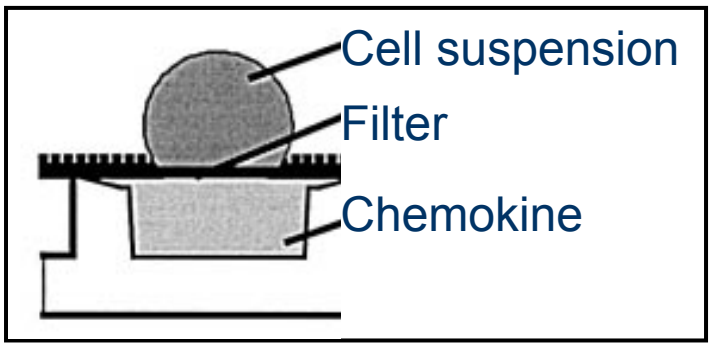

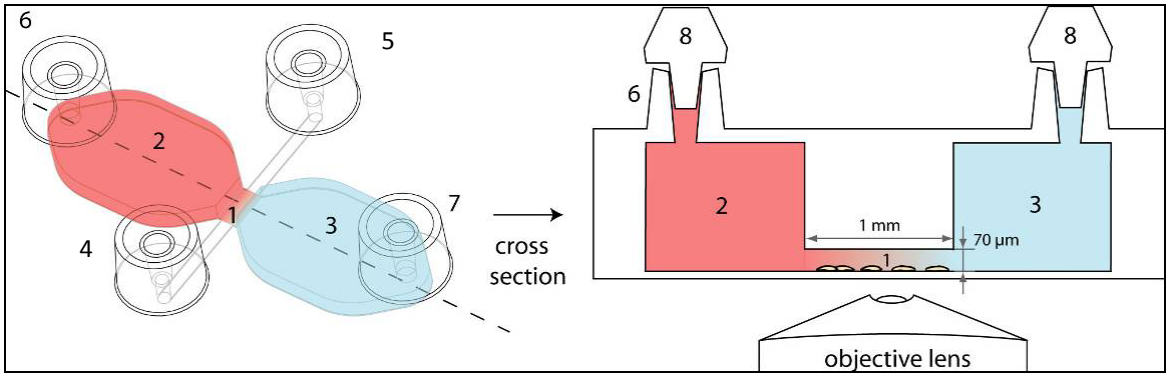

Figure 2.5. Set up of the Neuroprobe chemotaxis chamber and Ibidi chemotaxis slide

Top panel; This image was taken from the manufacturer's website (www.neuroprobe.com). Chemokine is placed in the well, a filter with pores is placed on top and then a cell suspension is pipetted onto it. Hydrophobic rings on the filter keep the cell suspension focussed over the well.

Bottom panel: This image was taken from the manufacturer's website (www.ibidi.de). 1. Bridge on which cells are placed. 2. Upper reservoir with chemokine 3. Lower reservoir without chemokine. 4. and 5. Channels through which cells are pipetted. 6. Channel into which chemokine is pipetted. 7. Channel through which excess media is aspirated. 8. Stoppers to prevent evaporation. A chemokine gradient between the two reservoirs forms across the bridge. Cells are recorded as they move on the bridge.

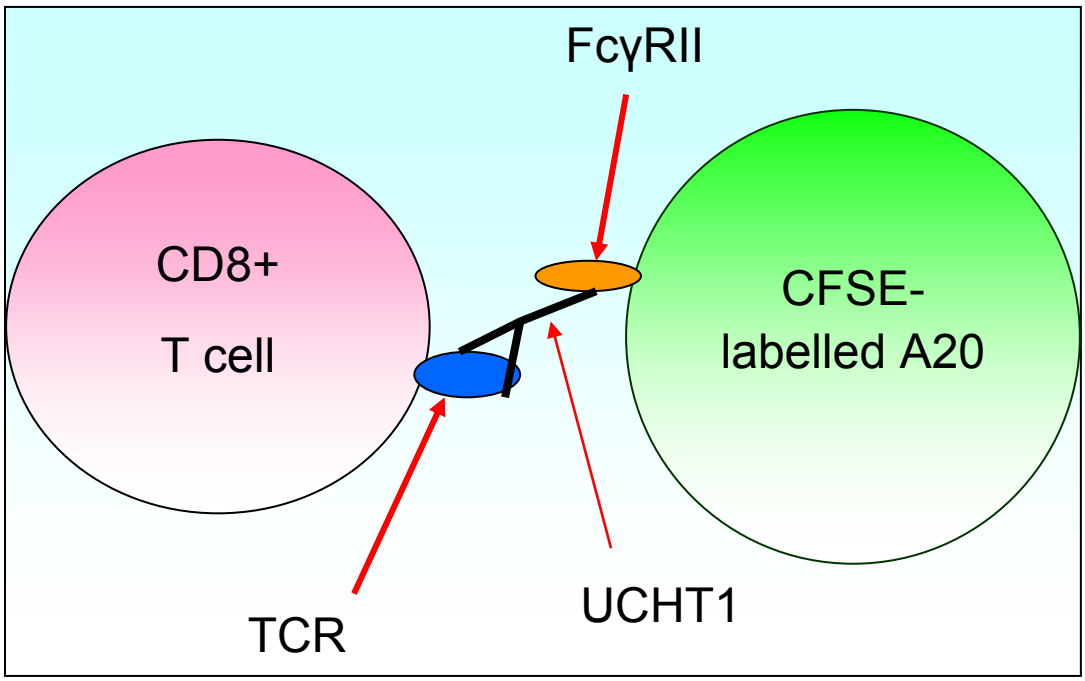

Figure 2.6 CD8+ T cell cytotoxicity assay
The human CD8+ T cell expresses a TCR which is bound and activated by UCHT1. UCHT1 is an antibody raised in mice, and hence is bound by FcγRII which is expressed upon the murine B cell lymphoma A20 cells. Hence the activated CD8+ T cell is directed to kill the A20 cell via release of granzymes and perforins. The A20 cells are labelled with CFSE to distinguish them from the CD8+ T cells by flow cytometry. Labelling with an annexin cy-5 antibody (not shown) identifies apoptotic cells.

2.16 Molecular techniques

2.16.1 PCR

Conditions varied according to the DNA to be copied, but in brief, all reactions unless otherwise indicated were performed in a volume of 20µl, using Standard Taq buffer to 1x final concentration, 1 µl Taq (500units/ml), 1 µl dNTPs (10 mM of each dNTP) (all NEB) and primers at 0.5 µM (2.5 µM for mutation). Primers were from Invitrogen custom primers. Initial denaturation was for 10 min, followed by 20-30 cycles of denaturation for 1 minute, annealing at 55˚C for 1 minute and extension at 72˚C (1 min/ kilobase). Following PCR 5 µl of the reaction mix was diluted with 6x loading buffer (NEB B7021S) and visualised on a 1% agarose gel stained with ethidium bromide. If required PCR products were cleaned by running on a 1% agarose gel, the DNA band excised and purified with a gel purification kit (Qiagen). Alternatively a Wizard PCR cleanup kit was used.

2.16.2 Restriction enzyme digestion and ligation of DNA

Conditions varied according to the enzymes used, but in general digests were performed in reaction volumes of 10 µl with 1 µl enzyme(s) in appropriate buffer and BSA if required, for at least 1 hour. All enzymes and buffers were from NEB. Products were cleaned using gel purification. Ligations were performed in reaction volumes of 10 µl with 1 µl T4 ligase, 1 µl ligase buffer (both Promega) and ratios of insert: vector between 1:1 and 3:1 for at least 4 hours at room temperature.

2.16.3 Transfection of *E. Coli* and isolation of plasmids

For expression of most plasmids competent DS5α *E. coli*, were thawed from -80˚C on ice for 10 minutes. 5µl plasmid at 1 µg/µL was added and left on ice for a further 20 minutes. Bacteria were then heat shocked at 42˚C for 30 seconds, then 250 µl SOC media was added and tubes were shaken at 200 rpm at 37˚C for 1 hour. 200 µl of the bacteria were plated onto ampicillin agar (100 µg/ml), and incubated overnight. The following day colonies were screened for appropriate plasmids using PCR. Colonies were used to seed 5ml of LB broth with ampicillin (100 µg/ml, Sigma) for 8 hours, which in turn was used to seed 100 ml of LB broth with ampicillin. Plasmids were isolated according to manufacturer's instructions with Qiagen mini (5 ml) or maxi prep (100 ml) spin columns.

For expression of lentiviral expression plasmids, which contain LTR and have a tendency to recombine with host cell DNA, Stbl3 *E. coli* (C7373-03 Invitrogen) were used. These were heat shocked as above, but for 45 seconds. After addition of SOC and plating, plates were incubated at 30°C for 24 hours before colonies were picked and screened. Colonies were then used to seed 5 ml of LB broth which was incubated overnight at 30°C. This was then expanded to 100 ml culture volume during the following day and 300 ml culture the next night. Finally, plasmids were isolated with a Machery Nagel Nucleobond Xtra Maxi plus kit according to the manufacturer's instructions.

2.16.4 Ligation of CD2:SHIP into lentiviral plasmid pCLPS

In order to use this system to express rCD2:SHIP in human T cells it was necessary to ligate the DNA coding for rCD2:SHIP into an expression plasmid. The pCLPS expression plasmid encodes GFP which has previously been successfully excised using the BamH1 and Sal1 restriction sites. Therefore the following primers were designed to introduce these restriction sites to the rCD2:SHIP

F (5' to 3') GCA A**GG ATC C**AT GAG ATG TAA ATT CCT AGG GAG

Underlined = BamH1 restriction sequence

R (5' to 3') CCA A**GT CGA C**TC ATG TGG CCT CTA ACC G

Underlined = Sal1 restriction sequence

25 cycles of PCR were performed as described in the methods and the product was double digested (with BamH1 and Sal1 at 37˚C with BSA in BamH1 buffer) and cleaned using a Wizard PCR clean up kit. The pCLPS vector was also double digested and ligated in a 1:1 ratio with the insert either overnight at room temperature or for 4 hours at room temperature. The plasmids were then transfected into DH5α E.Coli and colonies screened by PCR using the above primers for the presence of rCD2:SHIP.

2.16.5 RT-PCR and semi-quantitative PCR

RNA was isolated with Trizol reagent (Invitrogen) and converted to cDNA with an Omniscript RT kit (Qiagen) following the manufacturer's instructions. 1ml of Trizol was used to lyse $5x10^6$ cells per point. The phases were separated using chloroform and RNA was precipitated using propan-2-ol, then washed in 75% ethanol. The pellet of RNA was air dried and then resuspended in sterile, endonuclease free water. RNA was quantified then quantified and 100ng reverse transcribed with Omniscript. Reverse transcriptase (RT) buffer, dNTP mix (final concentration 0.5mM each dNTP), Oligo-dT primer (final concentration 1μM) RNase inhibitor (10Units/ reaction) and Omniscript Reverse Transcriptase (4Units/ reaction) were combined with 100ng RNA and reverse transcribed at 37°C for 1 hour. Negative controls contained no RT. PCR for SHIP-1 was performed at 55°C and for β-actin at 60°C, each at 30 cycles, as described above, the primers used were

SHIP-1 5'-AAGAGAGAAGGCTTCTGCCA-3' (F),

5'- CAGGAACCGGAGAATGTTCA-3' (R).

β Actin 5'- TAGGCACCAGGGTGTGATGG-3' (F),

5'-CATGGCTGGGGTGTTGAAGG-3' (R).

2.17 Materials and Methods for murine experiments

2.17.1 Animals

PI3Kγ$^{-/-}$ mice on both 129sv and BALB/c backgrounds were bred under specific pathogen free conditions at Charles River (UK), or under comparable conditions at Novartis, UK (Horsham) (333). PI3Kγ kinase dead mice were bred at the University of Basel (138). Control wild-type mice were produced at Charles River (UK). Animals were housed at 24^{o}C in a 12 hours light-dark cycle. Food and water were accessible *ad libitum*. The studies reported here conformed to the UK Animals (scientific procedures) Act 1986.

2.17.2 In vivo challenge and assessment of BAL cytokines

Animals were lightly anaesthetised with gaseous isofluorane, then instilled with 50μl of LPS (Sigma) at 0.1 mg/kg intra-nasally. Bronchoalveolar lavage with 4 x 0.3 ml

PBS was performed at various time points following challenge, and IL-17 content determined via ELISA (R&D). Further studies used 1 mg/ml recombinant IL-17A (Peprotech) as a stimulus, resulting in a 50 µg challenge, 5hrs after which bronchoalveolar lavage was analysed for cell influx and KC, MIP2, IL-6 and IL-5 content via ELISA (R&D). **N.B. This experiment was performed by Matt Thomas.**

2.17.3 Splenocyte isolation and culture

Splenocytes were isolated from the spleens of mice and disrupted by passing through a 40µm cell stainer (BD Falcon). Mononuclear cells were obtained by density gradient centrifugation (Ficoll Paque Plus, Sigma), and cultured in complete growth medium (RPMI supplemented with 10% FCS, 100 U/ml streptomycin, 100 µg/ml penicillin, and 2mM L-glutamine and 50µM 2-ME (all Invitrogen)) at $1x10^6$ cells/ml +/- 100µg/ml LPS for 2, 4 and 6 days*. CD4+ T cells were enriched using MACS CD4+ T cell isolation kit (Miltenyi Biotec) to achieve >90% purity. CD4+ T cells were activated using either plate-bound anti-CD3 and anti-CD28 (bound overnight at 1µg/ml)* or murine CD3/CD28 T cell expander Dynabeads (Invitrogen).at 1:1 ratio to cells, which were maintained in culture at $1x10^6$/ml. For culure under Th0 or Th17 conditions, cells were isolated as above, but using a MACS naïve CD4+ T cell isolation kit (Miltenyi Biotec). Cells were then cultured in RPMI supplemented as above and with murine CD3/CD28 T cell expander Dynabeads (Invitrogen) at 3:1 ratio to cells for 7 days. For Th0 conditions, no other cytokines were added. For Th17 conditions cells were cultured as for Th0, supplemented with rhTGFβ1 ng/ml, rmIL-6 20 ng/ml rmIL-23 10 ng/ml, rmIL-1β 10 ng/ml, anti IL-410 µg/ml and anti IFNγ µg/ml (all cytokines were from Peprotech and all antibodies were from R&D). The cells were maintained at approximately 1 $x10^6$/ml by doubling the culture volume (and addition of further cytokines for Th17 conditions) on days 3 and 5 post isolation.

2.17.4 Assessment of cytokines in culture and proliferation

CD4+ T cells were maintained in culture at $1x10^6$/ml and IL-2*, IL-4*, IL-5*, IL-6, IFNγ* and IL-17A were assessed in cell culture supernatants using Quantikine ELISAs (R&D) at 48 hours except where otherwise specified. IL-17F was assessed using a Duoset ELISA kit (R&D) at 48 hours except where otherwise specified. Proliferation was assessed by tritiated thymidine incorporation at 48 hours*. *** The indicated experiments were performed by Matt Thomas**

2.17.5 Mouse Dermal Fibroblast Culture and IL-6 production.

Mouse dermal fibroblasts were cultured in CNT-05 media (Millipore). Cells were seeded at $3x10^3$/well in 96 well plates and cultured for 48hrs before the addition of

CD4+ T cell supernatant. Cells were cultured for a further 24hrs before harvest of supernatant and measurement of IL-6 by ELISA as above. For IL-17A neutralisation, a blocking antibody was used at 1µg/ml (R&D MAB421).

2.17.6 Flow cytometry

Cells were labeled in PBS (Invitrogen) supplemented with 0.5% BSA (Sigma) by adding the amount of flurophore-conjugated antibody recommended by the supplier. IL-17RA, IL-17RC and isotype control antibodies were from BD Pharmingen. Viable cells were gated based on forward and side scatter. For intracellular staining for IL-17, cells were restimulated for 6 hrs using CD3/CD28 in the presense of Golgistop (BD Biosciences) then fixed and stained in Cytofix/Cytoperm reagents (BD Biosciences) according to the manufacturer's instructions Anti-IL-17A and isotype control antibodies were from BD Biosciences. Flow cytometric analysis was performed using a FACSCanto II (BD Biosciences).

2.17.7 Cell stimulations and Akt ELISA

Cells were rested for 1hr in RPMI, then stimulated with IL-17A or IL-17F, cells were then lysed and phospho-AKT (S473) was measured by ELISA kit following the manufacturer's instructions (Invitrogen).

2.18 Statistics

All statistical tests were performed using Graphpad Prism 4 software. For the majority of comparisons, a Student's paired T Test was used and results were taken to be statistically significant at $p<0.05$. Where multiple observations were performed in the same experiment, a one way ANOVA with repeated measures was used where possible. Otherwise a Holmes correction was used.

Chapter 3: Results Section I

Characterisation of SHIP-1 activation in T cell lines and primary human T cells and its pro-survival role in cell lines

3.1 Background and objectives

Previous work has identified SHIP-1 as being present in primary T cells, but lost in some leukaemic T cell lines (244). Furthermore, SHIP-1 has been shown to be an important negative regulator of T cell signalling, for example in response to chemokines (294). It has also been shown to play an important role in protecting cells against death in response to oxidative stress (334). However, much of this work utilised cell lines. Therefore, the first aim of this section was to investigate SHIP-1 activation in primary human T lymphocytes and leukaemic T cell lines. The second aim was to characterise its protective role in T cell lines challenged with a range of pro-apoptotic stimuli.

3.2 Expression of SHIP-1 in primary human T cells and T cell lines

The first experiments were necessary to validate to the expression of SHIP-1 or a constitutively active SHIP-1 protein in cell lines and primary human cells. It has previously been reported that whilst primary T cells express SHIP-1, this expression is lost in some leukaemic cell lines such as Jurkats (244). However, to confirm this, activated primary human T cells, and the leukaemic cell lines CEMs, HUT78s and Jurkats were western blotted for SHIP-1. It was found that primary T cells and all of the cell lines apart from the Jurkats expressed SHIP-1 (Figure 3.1).

To investigate the effects of SHIP-1 expression, a constitutively active SHIP mutant, rCD2:SHIP was used. rCD2:SHIP is a chimeric protein, consisting of the extracellular and transmembrane domains of rat CD2 fused to the phosphatase domain of human SHIP-1. The protein is constitutively localised to the cell surface membrane and hence the SHIP-1 phosphatase domain is suitably situated to metabolise $PI(3,4,5)P_3$. This protein was expressed in Jurkats using a tet-off expression system as described previously (244). This experimental system allowed comparision of Jurkats which express no SHIP-1, with the rCD2:SHIP Jurkats which have a constitutively active SHIP-1 phosphatase domain. However, western blotting for the expression of rCD2 in transfected cells indicated that expression was “leaky”, i.e. that some rCD2:SHIP was expressed even in the presence of tetracycline (Figure 3.1). Therefore for further experiments with rCD2:SHIP Jurkats, WT Jurkats were used as controls (rather than rCD2:SHIP Jurkats in the presence of tetracycline).

3.3 Characterisation of SHIP-1 activity in human T cells

3.3.1 Phosphorylation of SHIP-1 in response to receptor stimulation

Upon activation of signalling cascades, SHIP-1 is recruited to the membrane and is then tyrosine phosphorylated upon Y^{1020}, which lies in the second of the NPXY motifs towards the C terminal of SHIP-1. A polyclonal antibody from Stem Cell Technologies recognises phosphorylation of this site, which may be taken as a marker of SHIP-1 activation as when phosphorylated, this motif is able to bind the phosphotyrosine binding (PTB) domains of Shc (254) and Dok2 (201). It was therefore investigated whether ligands for different receptors expressed on T cells and known to regulate PI3K, also regulated SHIP-1 phosphorylation, or whether SHIP-1 phosphorylation and PI3K activation were differentially regulated.

Phosphorylation of SHIP-1 in response to chemokines was observed in both primary T cells and CEMs. Phosphorylation of SHIP-1 on Y^{1020} was observed in response to stimulation of CD3 (part of the TCR complex), by the monoclonal antibody UCHT1 (10µg/ml) or CD28 (a costimulatory receptor), by the monoclonal antibody 9.3 (10µg/ml) as previously shown (335) (Figure 3.2). This phosphorylation was most consistently observed in response to CD3 stimulation, whilst the response to CD28 appeared transient. The chemokines CXCL10 (IP10), CXCL11 (ITAC), CCL22 (MDC), CCL17 (TARC) and CXCL12 (SDF) at 10 nM also induced phosphorylation of SHIP-1, although this was weaker than that induced by CD3 stimulation (Figure 3.2). It was also observed that phosphorylation of SHIP-1 did not correlate with phosphorylation of Akt. For example the phosphorylation of SHIP in primary T cells in response to CXCL10 is more sustained than that of Akt.

3.3.2 SHIP-1 is phosphorylated in response to oxidative stress

It has been demonstrated in Jurkats that reintroduction of SHIP-1 can protect against death caused by ROS generated by exposure of the cells to H_2O_2 (334). Therefore, it was appropriate to examine the ability of ROS to induce phosphorylation of SHIP-1 in primary human T cells. Application of H_2O_2 to activated primary human T cells or CEMs resulted in tyrosine phosphorylation of SHIP-1 (Figure 3.3). This was observed at concentrations as low as 3 µM, however at low concentrations of H_2O_2 the phosphorylation was sometimes weak and transient, whilst at higher concentrations of the level which results in substantial cell death (as determined by Annexin/PI staining, see below), phosphorylation was very strong and sustained.

A

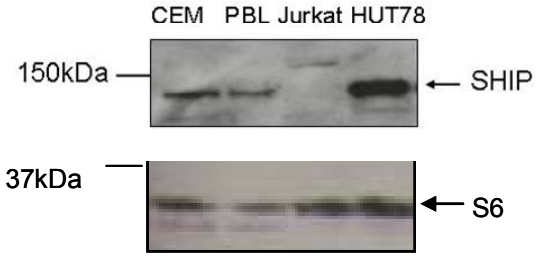

B

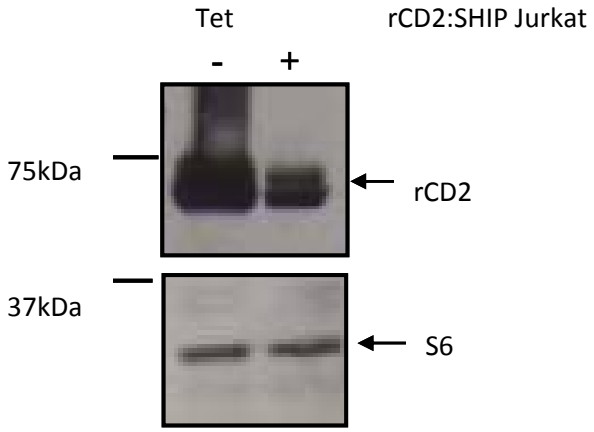

Figure 3.1 SHIP-1 and rCD2:SHIP expression. A. SHIP-1 is present in activated primary human T cells, and some cell lines. 1x 10^6 untreated cells were lysed and western blotted as described in the Methods for expression of SHIP-1 using an antibody that recognises the N terminal of the protein. B. rCD2:SHIP Jurkats express the rCD2:SHIP protein.1x 10^6 rCD2:SHIP Jurkats cultured in the presence or absence (for 48 hours) of tetracycline (2 µg/ml) were lysed and western blotted for expression of rat CD2. The results shown are representative of three separate experiments.

A. CEMs

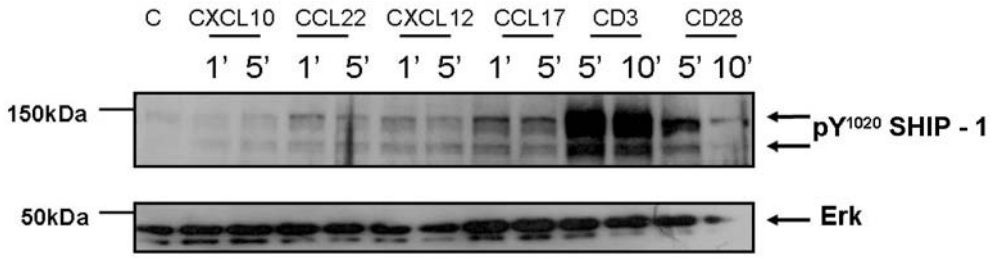

B. Activated primary human T cells

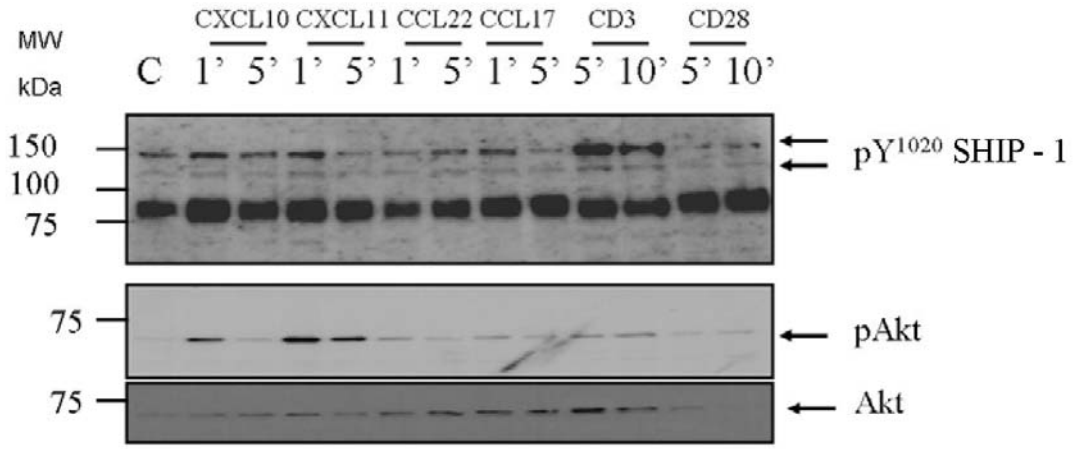

Figure 3.2 SHIP-1 is phosphorylated in response to CD3, CD28 and chemokine receptor stimulation A. 1x 10^6 CEMs were treated with 10 nM CXCL10, CCL22, CCL17, and CXCL12, or 10 µg/ml anti CD3 (UCHT1) or anti-CD28 (9.3) antibody for the indicated times, lysed and western blotted as described in Methods for phosphorylated SHIP-1 and pan-ERK to determine equal loading. B. Activated primary human T cells were treated with 10 nM chemokines or 10 µg/ml anti CD3 or anti-CD28 antibody for the indicated times lysed and western blotted as described in Methods for phosphorylated SHIP, phosphorylated S^{473} Akt and pan-Akt to determine equal loading. The results shown are representative of three separate experiments.

3.3.3 SHIP-1 is phosphorylated in response to TRAIL and TNFα

Given that H_2O_2 was a robust signal for SHIP-1 phosphorylation it was thought possible that a physiological stimulus known to generate ROS could also induce SHIP-1 phosphorylation. Therefore, it was decided to examine the phosphorylation of SHIP-1 in response to stimulation of death receptors, as these are known act partly through the generation of ROS (336, 337). However, whilst TRAIL induced a strong phosphorylation of SHIP-1 in activated primary human T cells, the phosphorylation that was induced by TNFα was weak and transient at best (Figure 3.3).

3.3.4 SHIP-1 is phosphorylated in response to ATP and bpVphen

Next it was investigated whether SHIP-1 phosphorylation is induced by stimulation purinergic receptors as their signalling pathways can also utilise ROS. Application of ATP at 10 μM, also induced SHIP-1 phosphorylation (Figure 3.3) in activated primary human T cells. The effects of bpVphen were also investigated, as this compound has been reported in the literature to inhibit PTEN (probably though oxidation of a cysteine residue in it catalytic site) and activate SHIP-1 to cause an increase in both $PI(3,4,5)P_3$ and $PI(3,4)P_2$ (232, 338, 339). In line with this, bpVphen was found to cause a strong phosphorylation of SHIP-1 and also to phosphoylate Akt (figure 3.3).

3.4 Phosphorylation of SHIP-1 correlates with its translocation to the membrane

As described above, SHIP-1 is reported to be phosphorylated upon its recruitment to the membrane. However, this phosphorylation is not essential for enzymatic activity *in vitro* (340), nor for its association with the Src kinase Lyn at the cell membrane, as inhibition of the kinase activity of Lyn using PP2 inhibits SHIP-1 phosphorylation but not its association with Lyn (341). It was therefore necessary to verify that phosphorylation of SHIP-1 may be taken as a marker for its recruitment to the cell membrane it T cells. To do this, CEMs were left untreated, or exposed to H_2O_2, then fixed, permeabilised and stained for SHIP and pY^{1020} SHIP-1 as described in Methods and visualised using a confocal microscope. pY^{1020} SHIP-1 was absent from unstimulated cells, but localised to the cell membrane upon H_2O_2 treatment (Figure 4). Staining with the SHIP-1 antibody was less successful but implied that SHIP-1 was distributed throughout the cytosol in unstimulated controls, and recruited to the cell membrane upon stimulation, with little remaining in the cytosol.

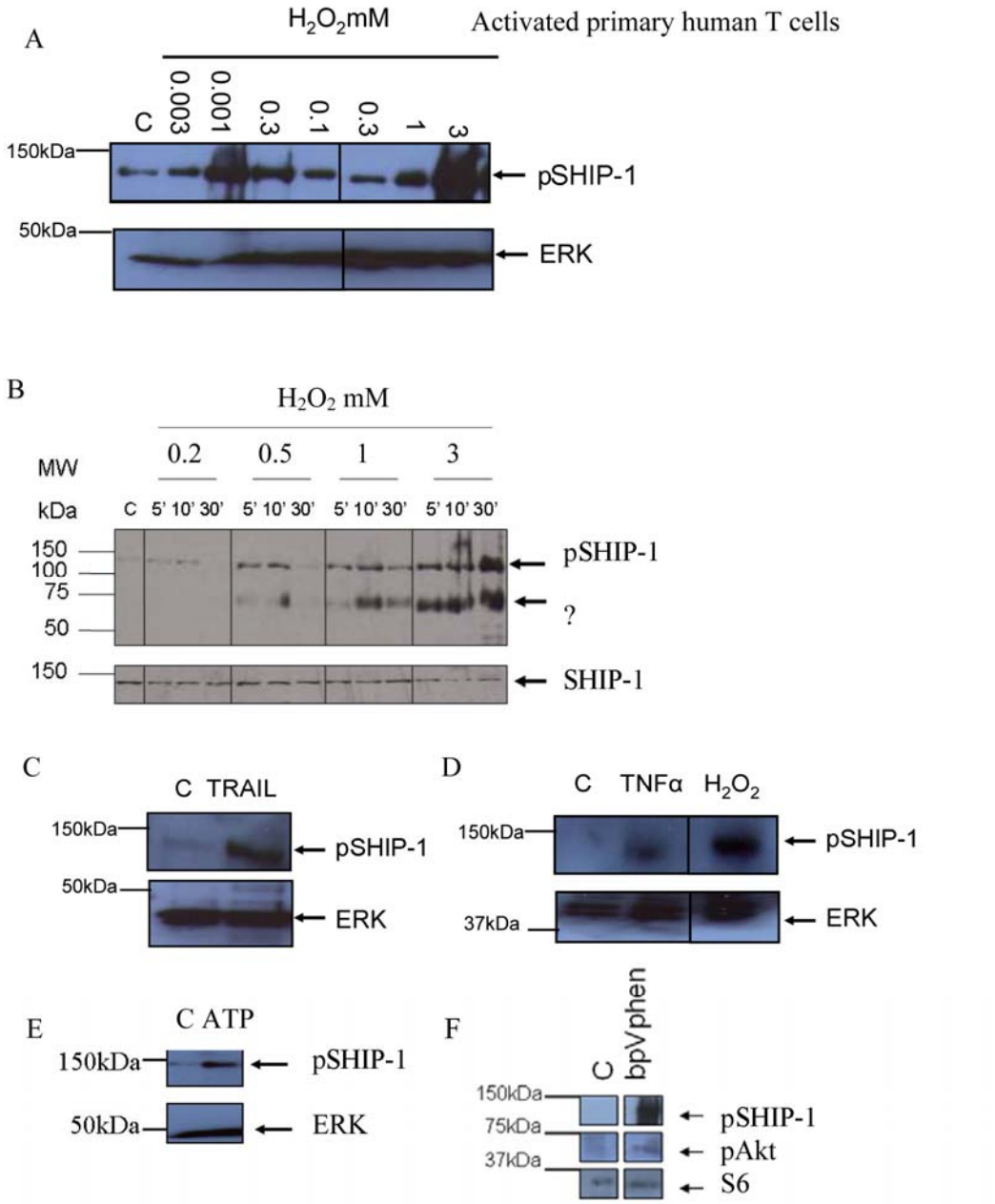

Figure 3.3 H_2O_2, TRAIL TNFα, ATP and bpVphen cause phosphorylation of SHIP-1 1x 106 Activated primary human T cells were exposed to various concentrations of H_2O_2 for 5 minutes (A) or the indicated times (B). Samples were western blotted for pSHIP (pY^{1020}) as described in the methods, then for ERK (A) or SHIP-1 (B) to ascertain equal loading. C. 1x 10^6 Activated primary human T cells were treated with 0.1µg/ml TRAIL for 1 minute. Samples were western blotted for pSHIP, then for ERK D. 1x 10^6 Activated primary human T cells were treated with 1ug/ml TNFα for 5 minutes (strongest phosphorylation seen from n=4 with 1mM H_2O_2 from same experiment for comparison). Samples were western blotted for pSHIP-1, then for ERK. 1x 10^6 activated primary human T cells were stimulated with 10µM ATP for 1 minute (E) or 30µM bpVphen for 30 seconds (F). Samples were western blotted for pY^{1020} SHIP-1 and pS^{473} Akt then for ERK (E) or S6 (F). The results shown are representative of three separate experiments.

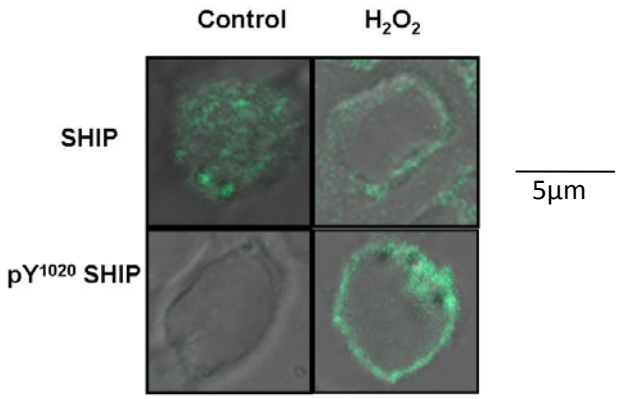

Figure 3.4 H_2O_2 causes phosphorylation and translocation of SHIP-1 2x 10^6 CEMs were left unstimulated (control) or stimulated with 1mM H_2O_2 for 5 minutes, after which cells were prepared for imaging with a confocal microscope as described in the methods. Cells were stained with either an antibody recognising the SHIP-1 N terminal or pY^{1020} SHIP-1 (green). Images shown are typical examples from the experiment, which was the most successful of three separate experiments (in terms of cell permeabilisation and antibody staining).

3.5 Phosphorylation of SHIP-1 is inhibited by the Src inhibitor PP2, but not by LY294002

SHIP-1 has been shown to be phosphorylated by Lyn, a member of the Src kinase family, for example in response to M-CSF in THP-1s and FcγRIIb stimulation in B lymphocytes (341). Therefore it was desirable to establish whether the same was true in T cells for the ligands investigated above.

Activated primary human T cells or CEMs were preincubated for 30 min with 10μM PP2, a non-selective Src kinase inhibitor. This inhibited phosphorylation in response to CD3, H_2O_2 and ATP even at high concentrations (e.g. 3mM ATP). It was also able to reduce the basal phosphorylation seen in activated primary human T cells, which appeared to vary between donors (Figure 3.5). In addition, to investigate whether SHIP-1 phosphorylation was PI3K dependent (for example, if $PI(3,4,5)P_3$ is required for the formation of the signalling complexes which recruit of SHIP-1 to the cell surface prior to its phosphorylation), activated primary human T cells or CEMs were preincubated for 30 min with 20μM LY294002, a PI3K inhibitor. This failed to inhibit tyrosine phosphorylation of SHIP-1 in response to H_2O_2, ATP, and CD3.

3.6 Experiments using Jurkats expressing CD2:SHIP

3.6.1 CD2:SHIP protects against H_2O_2 induced cell death

The generation of ROS is well known as an antimicrobial defence. However, ROS have also been reported as being important in a variety of signal transduction pathways, including TCR signalling (342) and death receptor signalling (343). It has also been shown that expression of SHIP-1 protected leukaemic T cells against ROS-induced cell death (263). To investigate this, the responses of the rCD2:SHIP Jurkat line to apoptotic stimuli were compared to those of wild type Jurkats. As described above, rCD2:SHIP Jurkats express a membrane localised SHIP-1 phosphatase domain, whilst wild type Jurkats entirely lack SHIP-1 expression. When measured with an MTT-based assay, the survival of (rCD2:SHIP Jurkats) following exposure to H_2O_2 was increased compared to that of the parental Jurkat cell line (Figure 3.6) (334). Because the MTT assay is redox based, there was concern that it would result in skewed results if ROS were still present. Therefore, cells were also assessed for annexin V binding at 6 hours after exposure to H_2O_2. This also

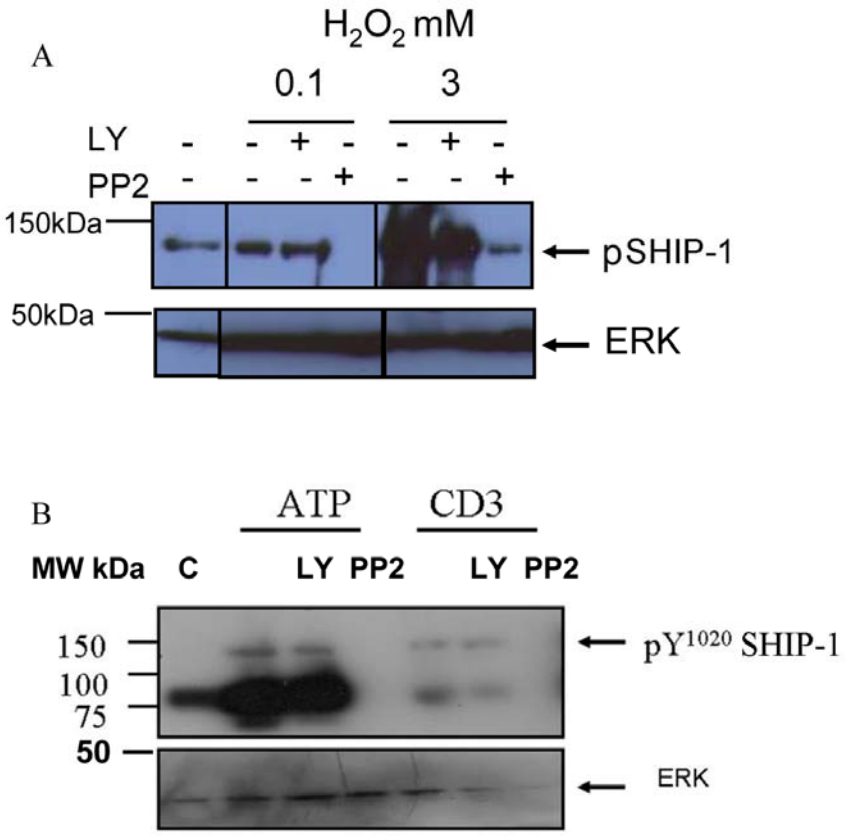

Figure 3.5 PP2 but not LY294002 inhibits SHIP-1 phosphorylation. 1x 10^6 activated primary human T cells were preincubated for 30 minutes in 10 μM PP2 or 20 μM LY294002 (LY) as indicated, then exposed to A. H_2O_2 for 1 minute or B. 3 mM ATP or 10 μg/ml anti-CD3 (UCHT1) for 5 minutes. Samples were western blotted for pSHIP-1 as described in the methods, then for ERK to ascertain equal loading. The results shown are representative of three separate experiments.

indicated that SHIP-1 significantly protected against H_2O_2 –induced cell death ($p<0.05$ ANOVA with repeated measures followed by Bonferroni post hoc analysis $p<0.01$ at all concentrations of H_2O_2).

3.6.2 CD2:SHIP protects against TRAIL-induced cell death

As described earlier, ROS are generated in many disease states and signalling pathways, however, there is no consensus on what concentration of H_2O_2 may correspond to physiological levels of ROS in healthy or diseased tissue. Therefore the ability of CD2:SHIP to protect against cell death in response to death receptor signalling was examined, as death receptors are known to rely upon generation of ROS and it has been reported that introduction of full length SHIP-1 into Jurkats could protect against FasL-induced cell death (264). The expression of TRAIL receptors is known to vary between Jurkat clones, however, in a trypan blue exclusion assay, TRAIL induced moderate levels of cell death in Jurkats. Furthermore, CD2:SHIP expression did protect against cell death in this instance (Figure 3.7 A, B). It was observed that with the trypan blue that after 24 hr there are higher basal levels of dead cells after 24 hr, probably because they are only in 0.1% FCS (higher levels of FCS are reported to interfere with death receptor signalling). However, the numbers of dead cells in the control samples were similar between Jurkats and rCD2:SHIP Jurkats.

3.6.3 CD2:SHIP fails to protect against TNFα-induced cell death

To further examine the protective role of SHIP-1 in death receptor signalling, the effects of TNFα were examined. In the first instance, TNFα induced cell death was examined by trypan blue exlusion at 6 and 24 hours (Figure 3.7 C, D). However there was no difference in cell survival between the Jurkat and rCD2:SHIP cell lines. In addition the number of cells was assessed using an MTT assay, with the SHIP core again conferring no benefit (Figure 3.7 E).

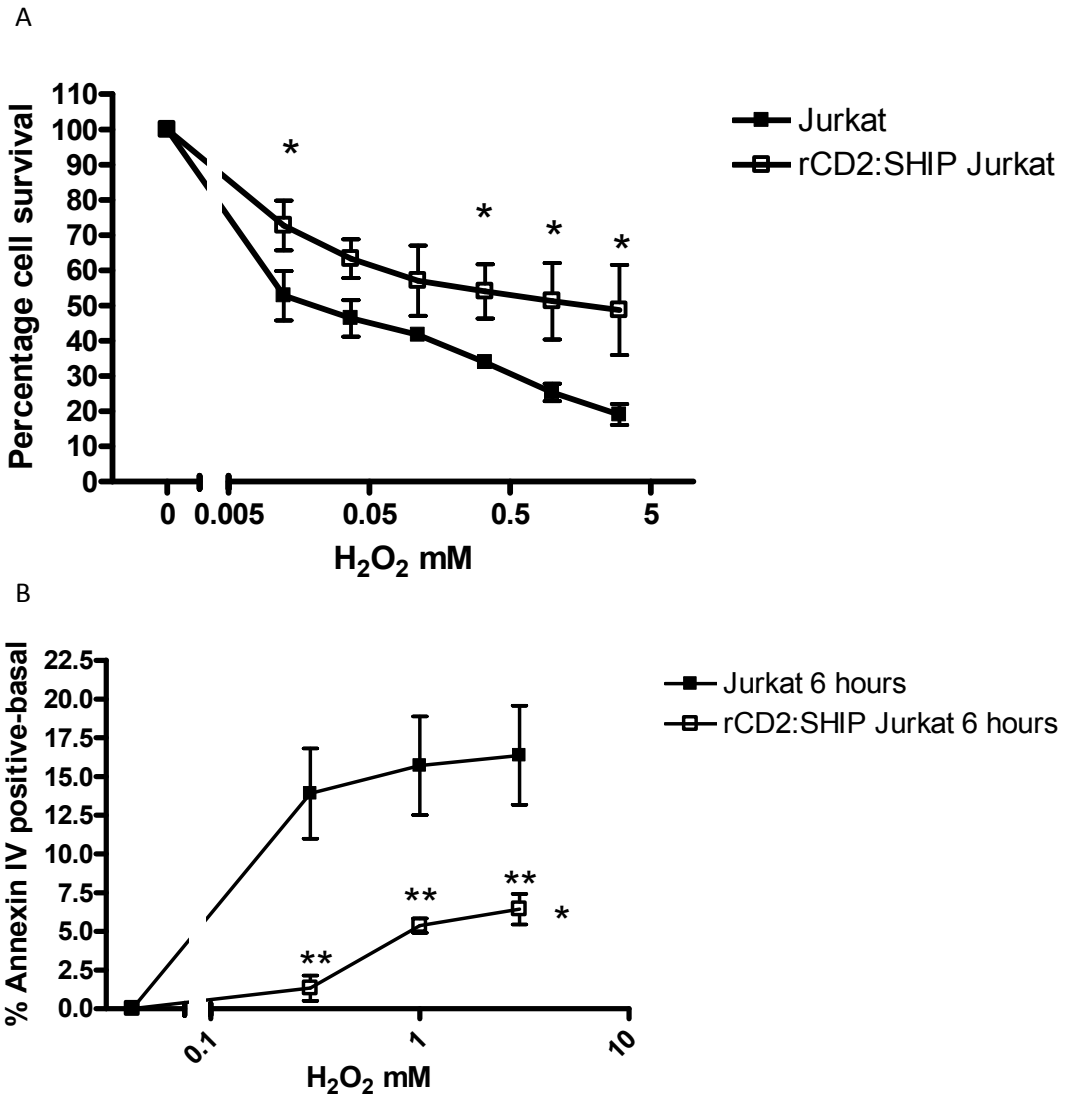

Figure 3.6 SHIP-1 protects against cell death in response to H_2O_2. Jurkats and rCD2:SHIP Jurkats were incubated with H_2O_2 at the indicated concentrations for 30 minutes, then washed into complete media. A. Cell metabolism (as a measure of cell number) was assessed with MTT after 24 hrs in a 96 well plate assay as described in the Methods. Cell survival was significantly enhanced by the presence of rCD2:SHIP. B. Cells treated as above were labelled with AnnexinIV-FITC antibody and $1x10^5$ cells per point were analysed by flow cytometry after 6 hrs (n=3 +/- SEM, $p<0.05$ 2 way ANOVA with repeated measures followed by Bonferroni post hoc test n=3).

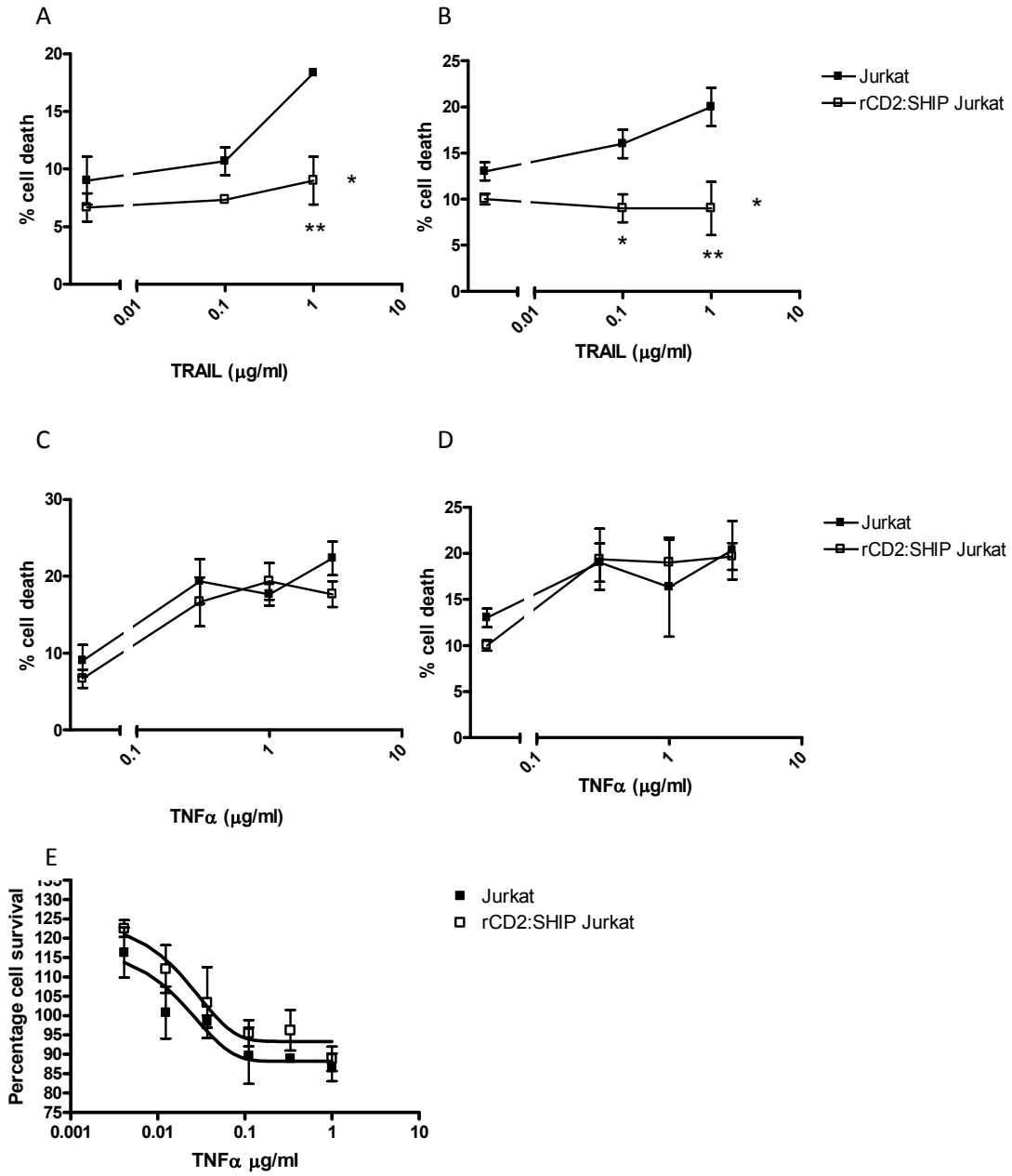

Figure 3.7 SHIP-1 protects against cell death in response to TRAIL but not TNFα. Jurkat and rCD2:SHIP Jurkats were incubated with 0.1μg/ml or 1μg/ml TRAIL for 6hr and 24 hr, before cell viability was assessed using trypan blue. A higher percentage of cells expressing rCD2:SHIP survived at both time points and both concentrations of TRAIL (*$p<0.05$ 2 way ANOVA with repeated measures followed by Bonferroni post hoc test n=3). Jurkat and rCD2:SHIP Jurkats were incubated with 0.3, 1 or 3μg/ml TNFα for C. 6hr and D. 24 hr, before cell viability was assessed using trypan blue. No difference was observed between percentage survival of the two cell types at either time point or concentrations of TNFα (2 way ANOVA with repeated measures n=3). E. Jurkat and rCD2:SHIP Jurkats were incubated with indicated concentrations of TNFα for 24hr, before cell viability was assessed using an MTT assay (typical results from n=3)

3.7 Summary

- SHIP-1 is expressed in primary human T cells, CEMs and HUT78s, but not Jurkats.
- SHIP-1 is activated in response to CD3 and CD28 receptor stimulation and in response to chemokines, ATP, TRAIL, bpVphen and H_2O_2.
- Phosphorylation of SHIP-1 correlated to its recruitment to the cell surface membrane.
- Phosphorylation can be inhibited by PP2 but not LY294002.
- Expression of a membrane localised SHIP-1 phosphatase domain protects against the death of Jurkats in response to ROS and TRAIL.

Chapter 4: Results Section II

The effect of lentiviral modulation of SHIP-1 expression in primary human T lymphocytes on viability and signalling.

4.1 Background and objectives

The first results section examined the role of SHIP-1 in leukaemic T cell lines and also investigated its activation in primary cells. However, one of the main aims of the thesis was to examine the function of SHIP-1 in primary T cells. Therefore the first aim of this section was to set up a lentiviral delivery system for use with primary human T lymphocytes in order to modulate expression of SHIP-1, either by silencing expression using shRNA, or by driving expression of the rCD2:SHIP protein used in the previous chapter. The second aim was to investigate the effect of these interventions on cell viability and signalling. Others have shown that the PI3K signalling pathway is a key modulator of actin polymerisation and of cell motility and chemotaxis (85, 344, 345), hence the final aim was to investigate the effects of SHIP-1 silencing on actin polymerisation.

4.2 Choice of delivery system

In the absence of commercially available compounds targeting SHIP-1, investigation of its actions in cells required a genetic approach. As reported elsewhere it is extremely difficult to introduce siRNA into primary T cells using either chemical transfection or electroporation (286, 346), without compromising viability. Furthermore rates of transfection are low, and the effect is transient. Previous experiments had been performed in the laboratory using Amaxa nucleofector technology, with disappointing results (286). Newer electroporation technology had since become available, and was investigated. As shown in Figure 4.1 electroporation of primary human T cells with a GFP expression plasmid resulted in low expression levels using an optimised protocol and an MP-100 Microporator. Microporation of freshly isolated CD4+ T cells gave a maximum of 10% of cells successfully expressing GFP and viable (death rates were between 30 and 95%). Microporation of day 10 Staphylococcal enterotoxin B (SEB) activated T cells was less successful and resulted in 80-98% cell death with a maximum of 3% of cells being viable and expressing GFP. Therefore it was decided to use a viral delivery system which can give higher rates of infection for introduction of shRNA and rCD2:SHIP (although the microporator was used to deliver tagged PH domains, see Chapter 5). Lentiviruses are particularly advantageous as they can infect non dividing cells (347, 348).

Condition	Voltage	Pulse width	Number of Pulses
1	0	0	0
2	2000	20	1
3	2050	20	1
4	2100	20	1
5	2150	20	1
6	2200	20	1
7	2250	20	1
8	2300	20	1
9	2350	20	1
10	2400	20	1
11	2450	15	1
12	2500	15	1
13	2000	15	2
14	2050	15	2
15	2100	15	2
16	2150	15	2
17	2200	15	2
18	2250	15	2

Figure 4.1 Electroporation allows delivery of DNA to primary T cells with low efficacy (Continues on next page)

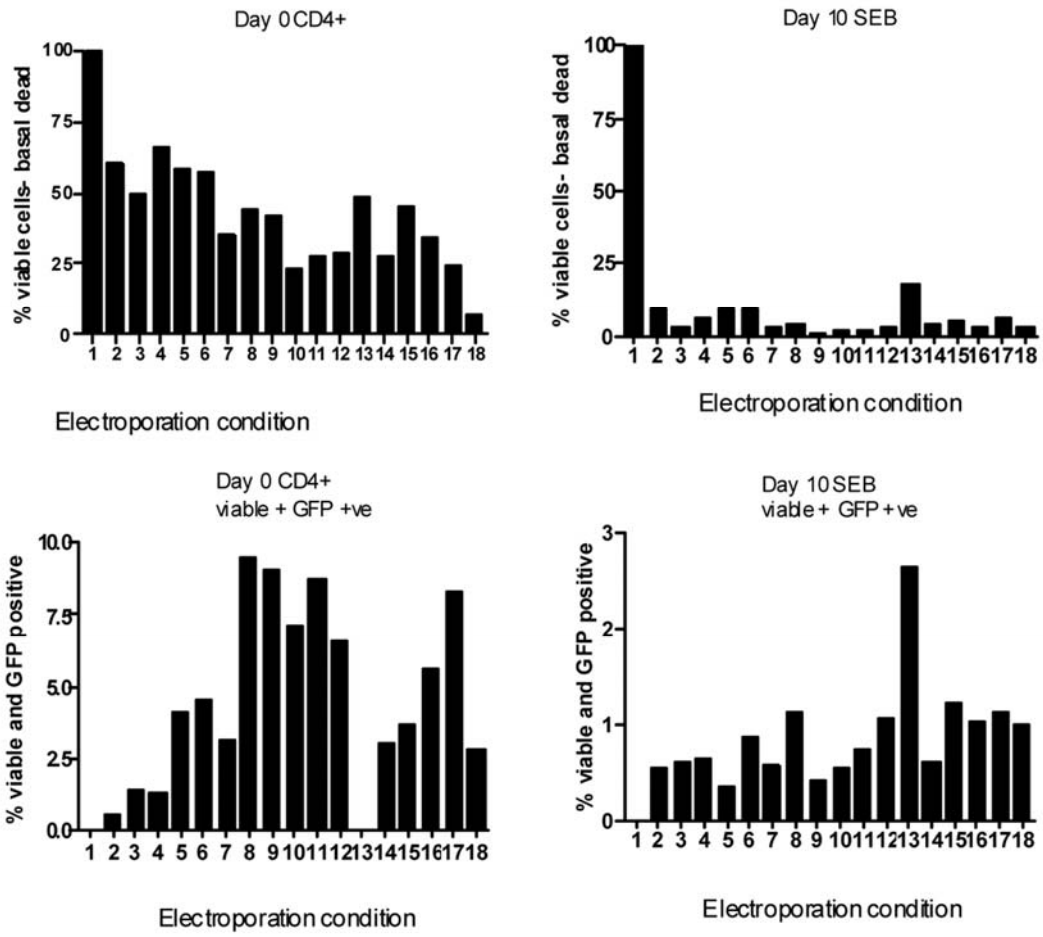

Figure 4.1 Electroporation allows delivery of DNA to primary T cells with low efficacy (cont'd) The Microporator MP-100 was used to electroporate cells. CD4+ were freshly isolated, whist PBMCs were cultured for 10 days in the presence of SEB and IL-2. Cells were washed into the supplied electroporation buffer at $2x10^7$ cells/ml in a volume of 10µL (i.e. $2x10^5$ cells/sample) and pulsed with 0.5 µg pCLPS GFP using the parameters described in the table. Cells were then cultured on CD3/CD28 beads and IL-2 (for CD4+) or with IL-2 (SEB activated T cells) for 48 hours. Cells were then washed into FACs buffer and GFP expression was assessed by flow cytometry of 1 $x10^5$ cells. FSC and SSC were used to identify viable cells.

4.2 Set up of Lentiviral delivery system

4.2.1 GFP encoding virus can infect Jurkat cells

Viral particles were assembled as described in the Materials and Methods. Briefly, packaging plasmids and an expression plasmid were chemically transfected into HEK293T cells and virus was manufactured by the cells and released into the supernatant. During optimisation, the pCLPS GFP expression vector was used, as expression of GFP could be easily monitored. To check that the chemical transfection of HEKS with the lentiviral expression and packaging plasmids was optimal, transfected cells were assessed for GFP expression by flow cytometry and found to be over 95% transfected (Figure 4.2A). Initially, the GFP lentivirus that was produced by transfected HEKS was used to infect Jurkat cells, as these are a rapidly proliferating cell line and therefore very easy to infect. As expected, over 95% infection levels could be achieved (Figure 4.2B).

4.2.2 Calculation of viral titre and demonstration of replication incompetence

Serial dilutions of the supernatant containing virus applied to HEKs were used to calculate viral titre, to be used to calculate the multiplicity of infection (MOI) values used below (Figure 4.3A). In the illustrated example ~ 20% of $4x10^5$ cells were infected by 3 ml of a 1:10 dilution meaning that each ml of undiluted supernatant contained approximately 2.7 $x10^5$ viral particles. In addition, as a safety precaution, supernatant from infected HEKs was applied to uninfected HEKs. This failed to result in new infection, indicating that the virus was replication incompetent (Figure 4.3B).

4.2.3 Primary human T cells can be infected with high efficacy using lentivirus

Having successfully established the lentiviral expression system in leukaemic cell lines, primary human T cells were then targeted. CD4+ T cells were isolated using a MACS untouched CD4+ or CD8+ isolation kits (which bind all other cells and retain them in the column and allow the desired cells to pass through), and activated for 24 hours using CD3/CD28 beads, then exposed to lentivirus for 24 hours. Initial rates of infection were fairly low (~13%) but spinoculation (centrifugation of the cells during infection) increased the rate of infection to ~30% (Figure 4.4A) and use of polybrene at 5 µg/ml further increased efficacy to ~ 45% (Figure 4.4B). Maximal efficacy was

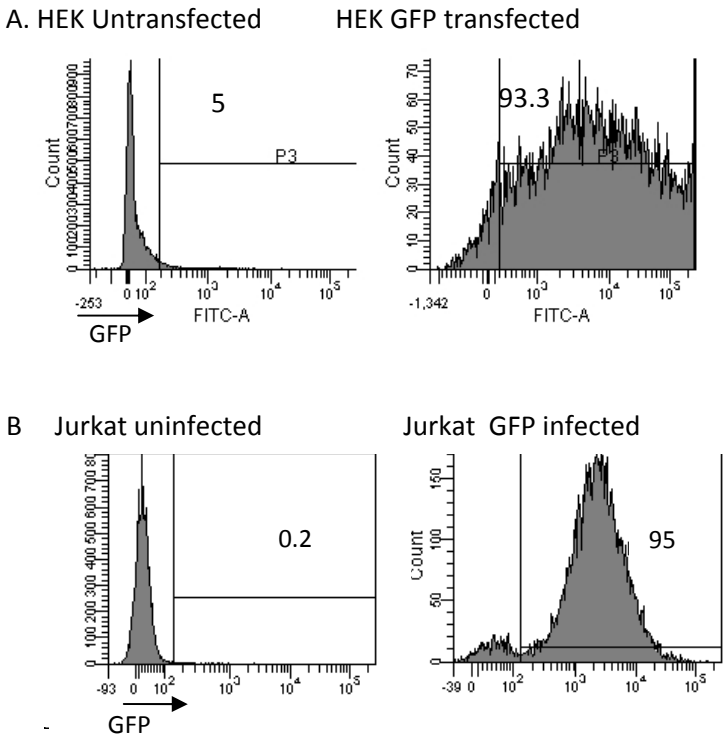

Figure 4.2 The Jurkat leukaemic cell line can be infected with high efficacy using lentivirus.

A. HEK293T cells were cultured to 60% confluency and transfected with viral plasmids as described in the Materials and Methods. After 48 hours cells were trypsinised and resuspended in FACs buffer and $1x10^5$ viable cells/sample were assessed by flow cytometry for GFP expression The percentage of cells that were gated as positive for GFP expression are indicated on each histogram B. Uninfected controls or Jurkats were infected with virus containing the pCLPS GFP as described in the Materials and Methods using 3 mls of supernatant from HEK293T cells to infect $1x10^6$ cells. $1x10^5$ viable cells/sample were assessed by flow cytometry for GFP expression three days post infection. Results are representative of three independent experiments.

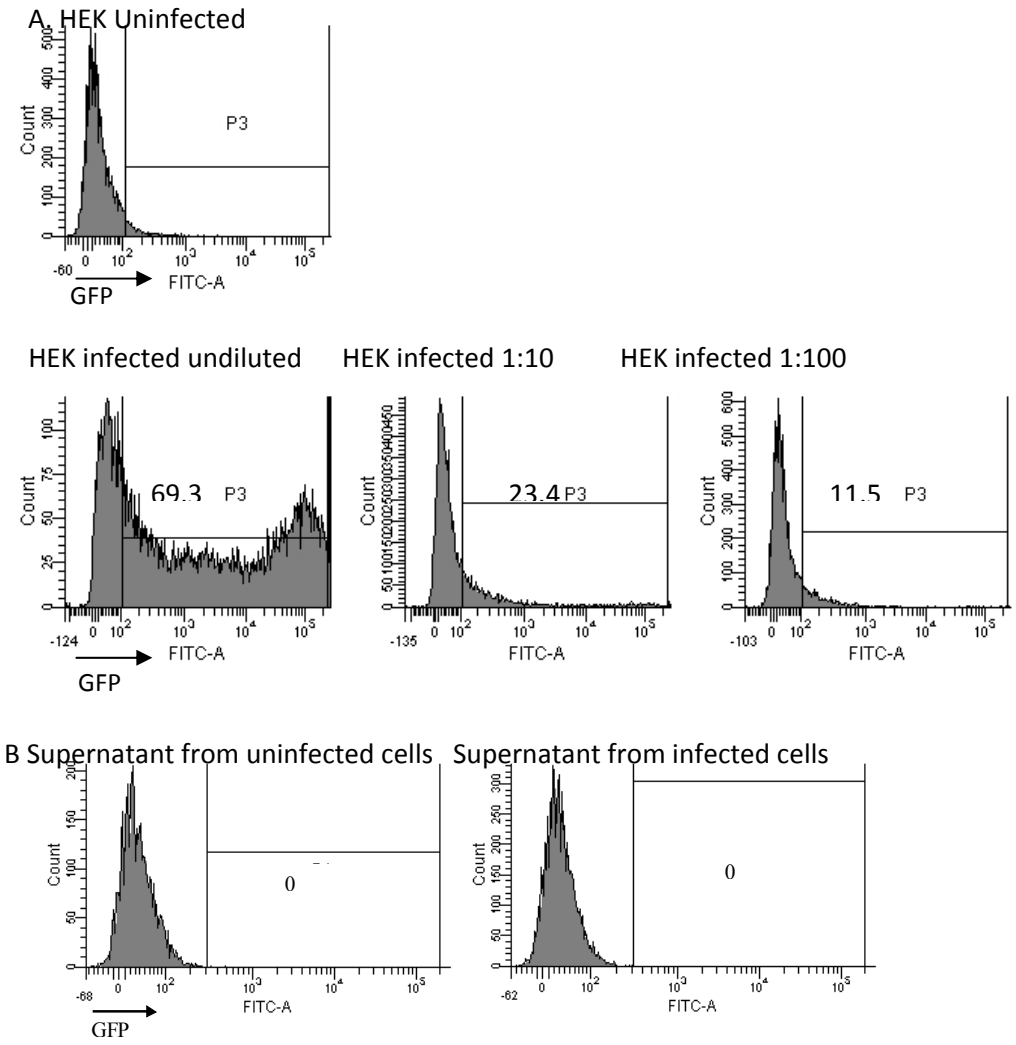

Figure 4.3 GFP can be effectively and safely expressed using lentivirus.

A. HEK293T cells were exposed to serial dilutions of media containing GFP virus, in order to calculate viral titre. Cells were plated at $2x10^5$/well in a 6 well plate and allowed to double over 24 hours to give $4x10^5$/well. Cells were exposed to 3ml of neat supernatant from virus-producing HEK-293T cells, or 1:10 or 1:100 dilutions. After 48 hours assessed by flow cytometry for GFP expression of $1x10^5$cells/point. B. Inability to replicate in HEK293T cells. GFP-encoding lentivirus was used to infect HEK293T cells. After a 48-hour incubation this supernatant was removed and used to culture uninfected HEK293T cells. After 48 hours this second set of cells was assessed by flow cytometry for GFP expression i) control HEKs ii) HEKs cultured with supernatant from infected HEKS. Results are representative of two independent experiments.

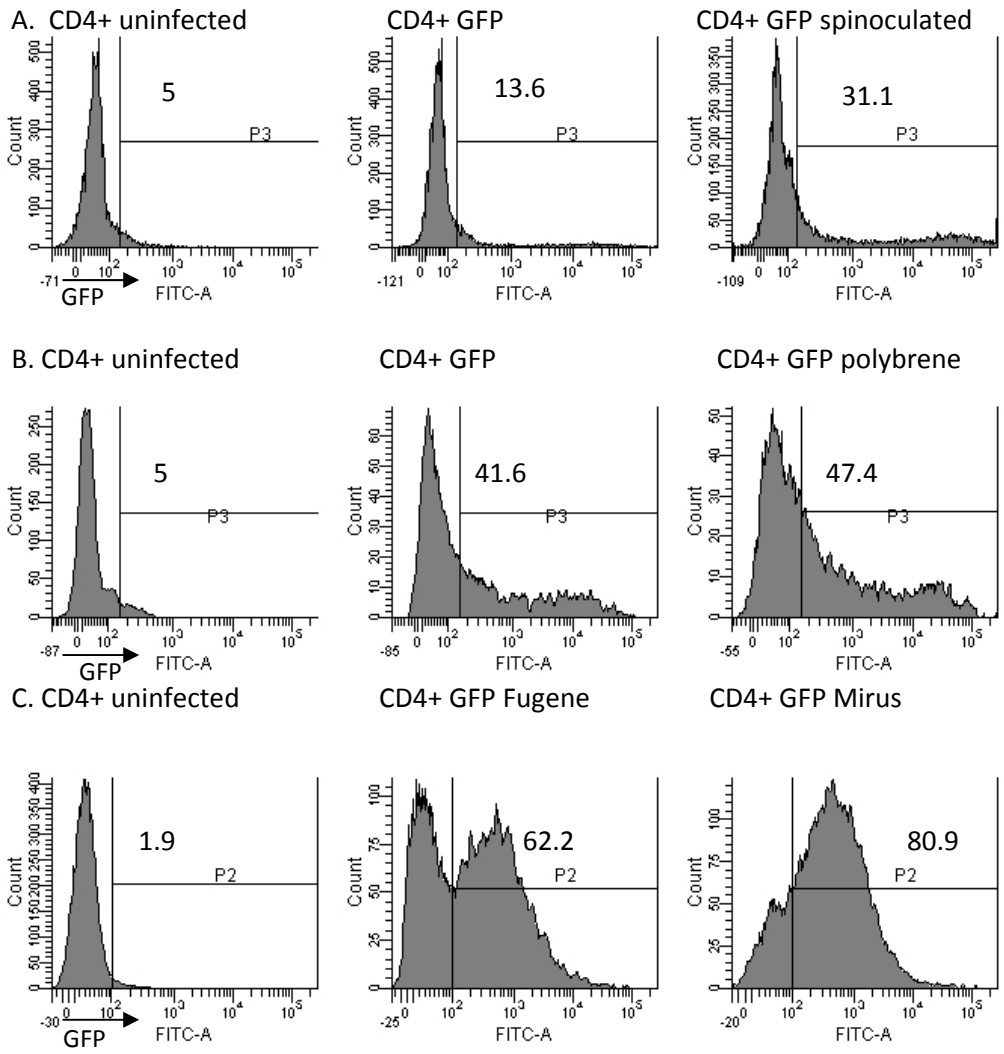

Figure 4.4 Optimal infection rates in primary human T cells require spinoculation and polybrene.
Primary human CD4+ were isolated and activated for 24 hours as described in the Materials and Methods. They were then infected at a MOI of 5 for 24 hours with lentivirus encoding GFP. Cells were then washed into complete media with IL-2 and cultured as normal. $1x10^5$ viable cells/sample were assessed by flow cytometry for GFP expression three days post infection. A. During infection, cells were cultured in an incubator for the full 24 hours or were spinoculated (centrifuged at 30°C, 300xg) for the first 90 minutes then cultured in an incubator for the remainder of the 24 hours. B. During infection, cells were spincoculated as above. In addition, infection was in the absence or presence of 5 µg/ml polybrene. C. CD4+ T cells were infected as above but at an MOI of 10 using virus prepared by transfecting HEK293 T with either Fugene 6 or Mirus transit LT1. All samples were analysed three days post infection for GFP expression using flow cytometry of $1x10^5$ viable cells/ point. Results are representative of two independent experiments.

achieved by improving production of the lentivirus by ensuring supercoiled DNA, optimal seeding densities of HEK293T cells and switching from Fugene to Mirus chemical transfectant (this increased the viral titre to approximately $1x10^6$/ml without need of ultracentrifugation) (Figure 4.4D). Three days and seven days post infection cells were assessed by flow cytometry and confocal microscopy respectively. CD4+ and CD8+ cells were found to have similar rates of infection (~80%) and similar levels of expression of GFP (Figure 4.5A). Confocal microscopy indicated that infected cells had a normal morphology and were otherwise unaffected by exposure to lentivirus (Figure 4.5B).

4.3 Expression of rCD2:SHIP reduces PI3K signalling and adversely affects viability

CD4+ T cells were infected with lentivirus encoding rCD2:SHIP (a constitutively active form of SHIP), expressed in the pCLPS plasmid. Rat CD2 was detected in infected cells by western blot and also by flow cytometry. Approximately 30-40% of cells were found to be infected three days post infection. Cells were sorted by expression of rCD2 using MACS columns to gain a population that was over 80% positive (Figure 4.6).

Uninfected cells and cells infected with a GFP-expressing virus appeared healthy whereas rCD2:SHIP infected cells were mostly dead six days post infection as confirmed by flow cytometry and confocal microscopy. Therefore the cells were examined three days after infection and were observed to have a higher percentage of apoptotic cells than control cells. The levels of pAKT, as an indicator of $PI(3,4,5)P_3$ levels (because sufficient numbers of cells for direct measurement of lipids were not obtained), were also assessed using cells at this timepoint (i.e., whilst there were still some viable cells). rCD2:SHIP CD4+ T cells three days postinfection had much lower basal phosphorylation of AKT and further phosphorylation was not induced in response to the chemokine CXCL11 (Figure 4.7).

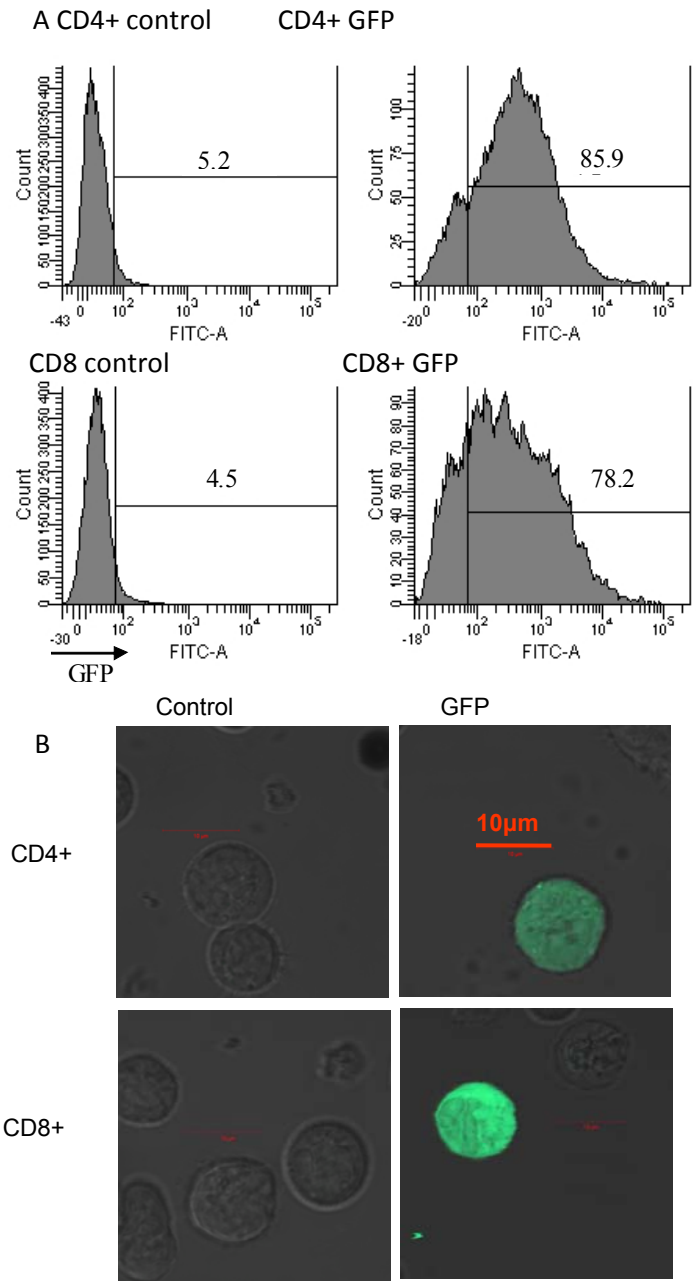

Figure 4.5 Primary human T cells can be infected with high efficacy using lentivirus

CD4+ and CD8+ cells were isolated from PBMCs from the same donor and cultured with anti-CD3/CD28 antibody coated beads (at a ration of 3 beads:1 cell) and IL-2 for 24 hours, after which they were exposed to GFP lentivirus as described in the methods. Cells were assessed for expression of GFP by A. flow cytometry after 3 days (live cells were washed into FACS buffer and $1x10^5$ viable cells were analysed immediately) and B. confocal microscopy after 6 days (live cells were washed into chemotaxis media at $1x10^5$/ml and 100µL samples aliquoted into coverslip-bottomed chambered slides and imaged on an LSM510 Meta confocal microscope). Results are representative of three independent experiments.

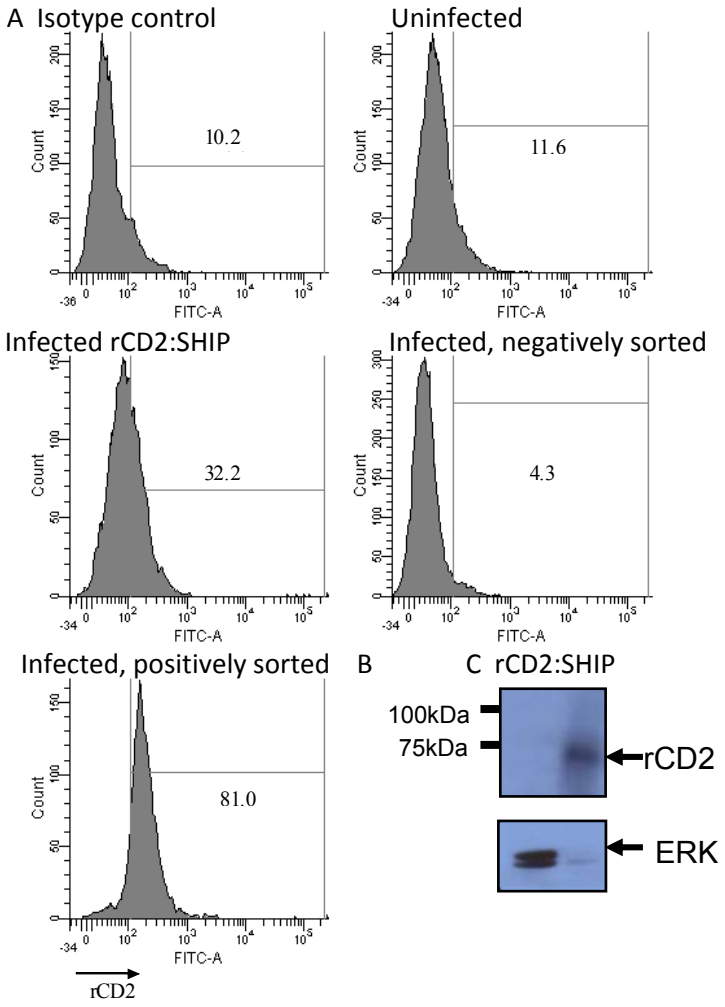

Figure 4.6 Expression of rCD2:SHIP by CD4+ and their selection by magnetic cell sorting

A. Cell populations were analysed for rCD2 expression by flow cytometry using FITC anti rCD2 and acquisition of $1x10^5$ viable cells. Sorting indicates the population that were sorted by MACS magnetic separation-negatively selected (uninfected) cells and positively selected (infected) cells. B. Western blot of uninfected and infected CD4+ cells for rCD2 expression and ERK (despite loading more protein into the uninfected lane, no rCD2 was detected).

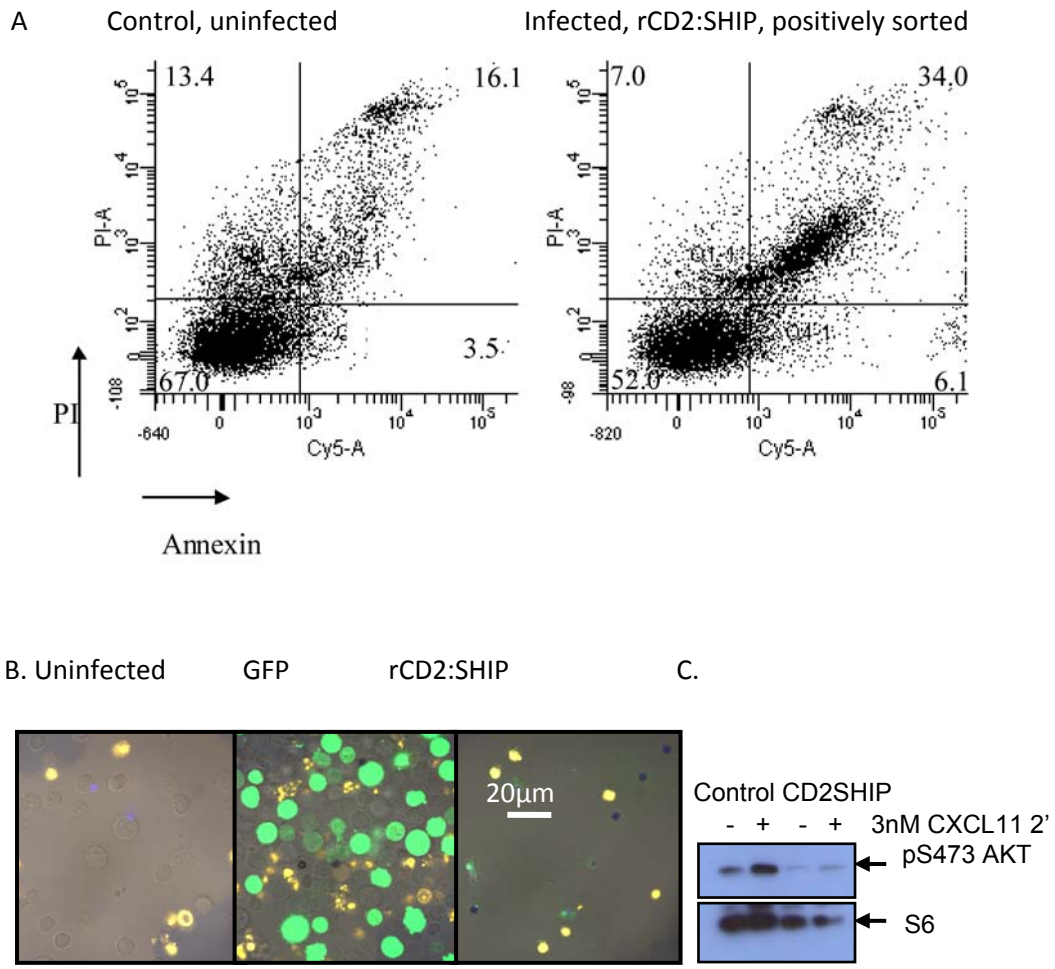

Figure 4.7 Expression of rCD2:SHIP reduces PI3K signalling and adversely affects viability

A. Control uninfected cells and cells infected with lentivirus encoding rCD2:SHIP were cultured for three days (i.e., four days post isolation) and infected cells were then magnetically sorted for expression of rCD2:SHIP. CD4+ T cells were stained for annexin IV and propidium iodide and their viability was assessed by flow cytometry of $1x10^5$ cells/sample. B. Control uninfected cells, and cells infected with lentivirus encoding GFP or rCD2SHIP were cultured for three days (i.e., four days post isolation) and rCD2:SHIP infected cells were then magnetically sorted for expression of rCD2:SHIP. Cells were cultured for a further three days then stained for annexin IV (yellow) to identify dead cells. Control and rCD2SHIP cells are also stained for rCD2 (green) as described in the Materials and Methods. Samples were aliquoted onto chambered coverslips and analysed on an LSM 510 Meta confocal microscope. C. Day four post isolation control and rCD2:SHIP cells prepared as in part A were stimulated with CXCL11. $1x10^6$ cells per sample were lysed and samples were diluted to equal concentrations of protein before being western blotted with the indicated antibodies as described in the Materials and Methods. S6 was blotted to indicate protein loading. Results are representative of three independent experiments.

4.4 Lentiviruses expressing shRNA can be used to silence SHIP-1 expression in primary human T cells

shRNAs against SHIP-1 encoded in a lentiviral expression plasmid were obtained from SIGMA, along with scrambled short hairpin control. These plasmids also encode a puromycin resistance element. CEM cells were infected with SHIP-1 shRNAs encoded by a variety of sequences as indicated in the Materials and Methods. All were found to reduce expression of SHIP-1 at the protein level. Upon infection of CD4+ T cells, infected cells were selected on the basis of puromycin resistance (using a concentration of 0.1 µg/ml, previously validated as described in the Materials and Methods). SHIP-1 shRNA (SHIP-1 shRNA 3) reduced SHIP-1 at the protein level whilst PTEN expression appeared to be upregulated (Figure 4.8).

4.5 Effect of silencing SHIP-1 in primary T cells

4.5.1 SHIP-1 silencing does not affect viability of T cells but reduces proliferation

Because of the key roles of PI3K signalling in cell growth and survival, it was thought prudent to check the viability of infected cells. CD4+ and CD8+ cells were infected with lentivirus encoding scrambled shRNA or SHIP-1 shRNA and selected on the basis of puromycin resistance and then their viability was assessed by PI and annexin staining seven days post isolation. Example plots of CD8+ and CD4+ T cells and bar graphs from pooled experimental data (Figure 4.9) demonstrate that SHIP-1 knockdown does not affect viability of T cells. The viability of the cells after 6 hours in 0.1% serum was also examined, as this was considered the maximum amount of time they would be in low serum or BSA during future experiments. Again loss of SHIP-1 did not increase the percentage of apoptotic cells.

The next experiment analysed the ability of SHIP-1 knockdown cells to proliferate in response to CD3/CD28 stimulation by labelling the cells with the fluorescent probe CFSE and using flow cytometry to track the dilution of the CFSE as the cells divide. Firstly cells were labelled with CFSE immediately upon isolation and then activated and infected with lentivirus encoding scrambled shRNA or SHIP-1 shRNA as described in the Materials and Methods. CFSE intensity was the examined seven days post-isolation. Figure 4.10A shows fewer peaks of CFSE when SHIP-1

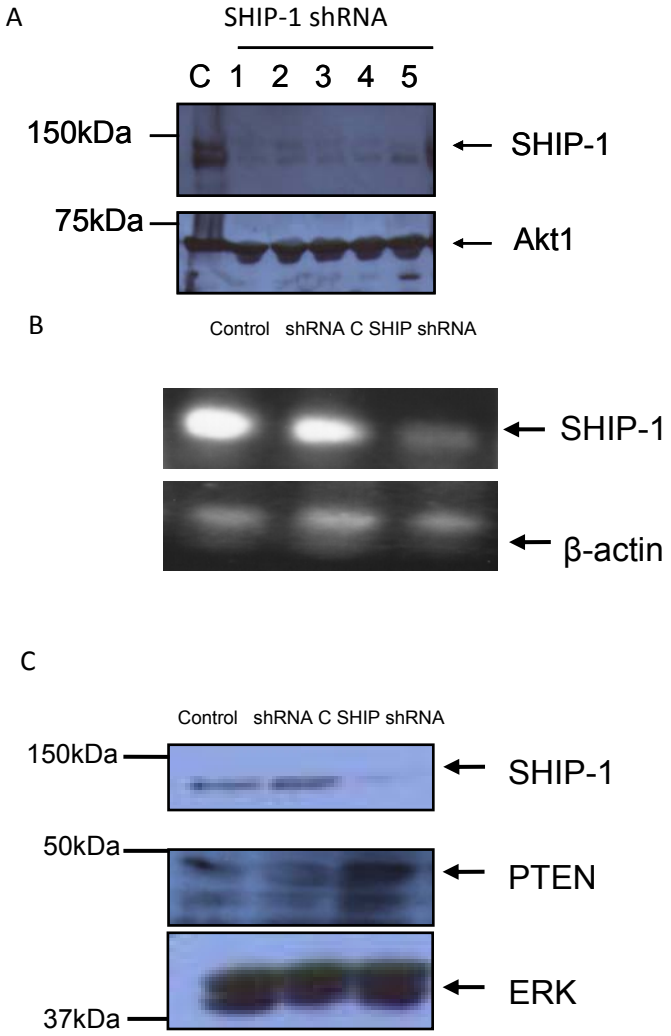

Figure 4.8 Lentiviruses expressing shRNA can be used to silence SHIP-1 expression in primary human T cells. A. Control CEM cells were left uninfected (C) or infected with lentiviruses encoding short hairpin RNA against SHIP-1. 1-5 represent different shRNA sequences as detailed in the Materials and Methods. After 3 days cells were selected with puromycin and after a further three days cells $1x10^6$ cells were lysed and samples were diluted to equal concentrations of protein before being immunoblotted with antibodies against SHIP-1 and Akt1. Next CD4+ T cells were left uninfected (Control), infected with a scrambled short hairpin lentivirus (shRNA C) or SHIP-1 shRNA. A. mRNA was isolated from at $5x10^6$ cells/point as described in the methods, Rt-PCR was used to obtain cDNA and semi-quantitative PCR used to determine expression of SHIP-1 and β-actin mRNA. B. $1x10^6$ cells were lysed and samples were diluted to equal concentrations of protein before being immunoblotted with antibodies against SHIP-1 and PTEN. Equal loading was verified by levels of ERK.

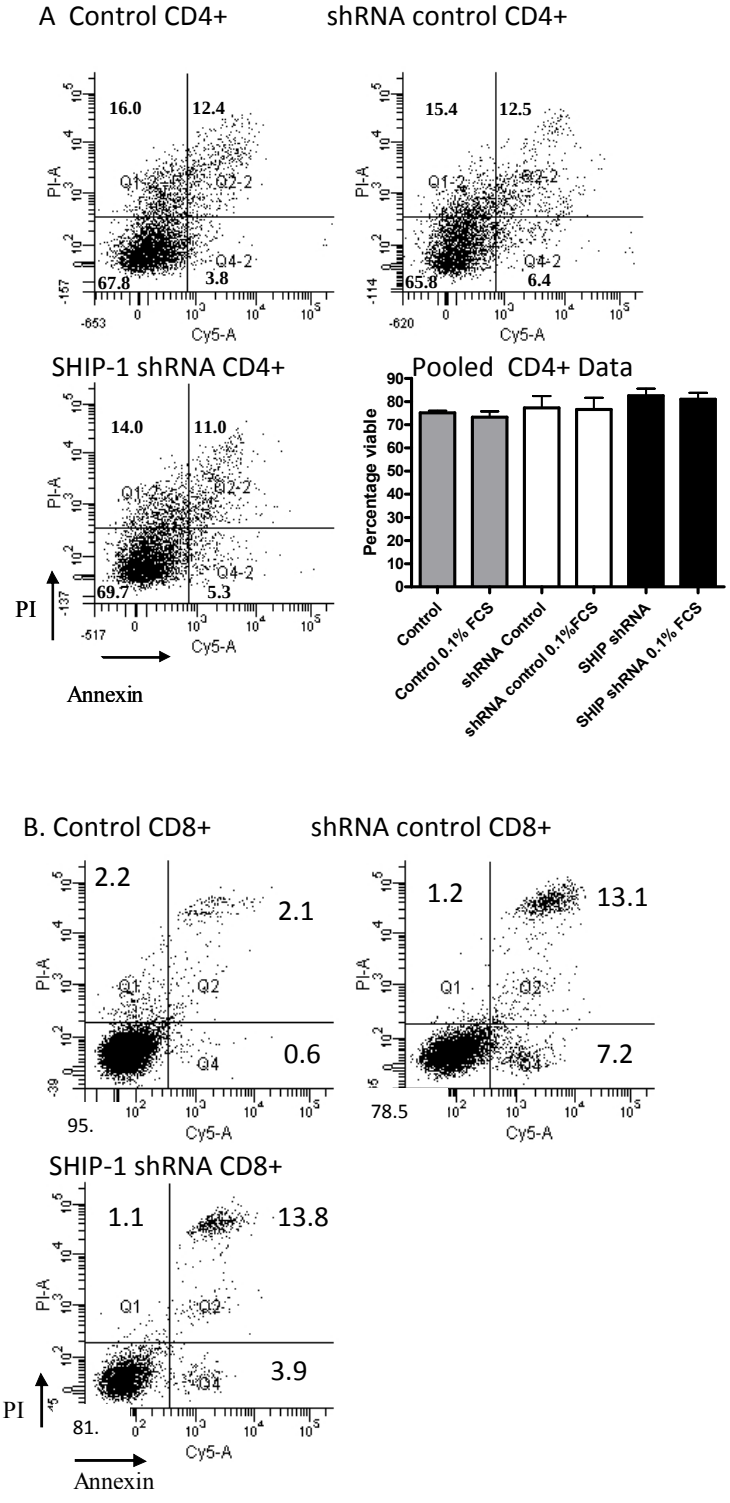

Figure 4.9 Silencing of SHIP-1 does not affect viability of T cells
CD4+ (A) or CD8+ (B) T cells were infected with lentivirus as indicated and cultured for a total of nine days before being stained with Annexin-Cy5 and propidium iodide as described in the Materials and Methods. Viability was assessed by flow cytometry of $1x10^5$ cells/sample. For the bar graph of pooled data for CD4+ T cells, cells were incubated in 10% FCS or 0.1% FCS for 6 hours before labelling (n=3 +/- SEM).

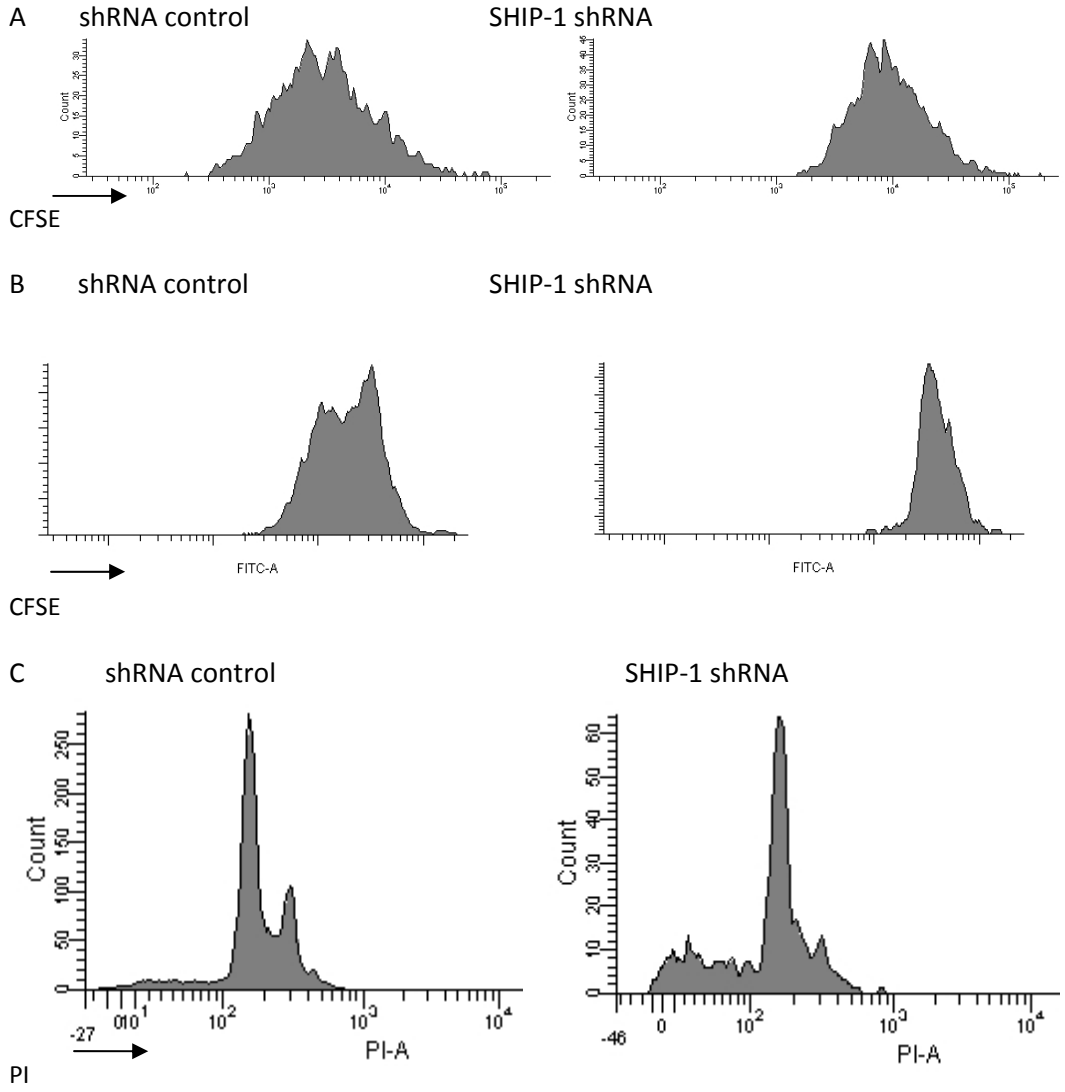

Figure 4.10 Silencing of SHIP-1 expression results in decreased proliferation.
A. Freshly isolated CD4+ T cells were loaded with CFSE and infected with lentivirus encoding shRNA as indicated. Proliferation was monitored by assessing CFSE intensity by flow cytometry on day 7 using $1x10^5$ viable cells per sample. B. Day 6 shRNA control or SHIP-1 shRNA infected CD4+ were rested overnight by removing them from CD3/CD28 beads, then loaded with CFSE on day 7 and restimulated with CD3/CD28 beads for 48hrs. CFSE content was then assessed by flow cytometry as above. C. shRNA control cells and SHIP-1 shRNA infected cells were fixed and permeabilised seven days post isolation and stained with propidium iodide as described in the methods. Propidium iodide concentration was then assessed by flow cytometry of $1x10^5$ cells/ sample. Histograms are from a single experiment representative of at least three independent experiments.

expression is silenced, and furthermore these peaks are of a higher intensity. This indicates that SHIP-1 silenced cells underwent fewer divisions i.e. that proliferation was reduced. Secondly cells were isolated, activated, infected and cultured as described in the methods for six days. They were then removed from the CD3/CD28 beads and rested in complete media overnight. On day seven they were loaded with CFSE and restimulated for 48 hours. Figure 4.10B shows that upon restimulation between days 7 and 9, a proportion of shRNA control cells undergo a division, in contrast, none of the SHIP-1 silenced cells has divided. Propidium iodide staining can be used on permeabilised cells to determine the stage of cell cycle. Cells in G_0 or G_1 have one set of chromosome pairs per cell, whilst during S phase DNA is being synthesised and cells contain an increased amount of DNA as the phase progresses and therefore stain more intensively with propidium iodide. During G_2 and M phase, two sets of chromosome pairs are present in each cell and so when these cells are stained with propidium iodide they fluoresce at twice the intensity when analysed by flow cytometry. Figure 4.10C demonstrates that unlike the shRNA control cells, SHIP-1 shRNA cells have undergone cell cycle arrest by day seven post isolation, with fewer of these cells having two copies of DNA.

4.5.2 Loss of SHIP-1 is not sufficient to sensitise T cells to TRAIL

It has been reported in the literature that primary T cells do not undergo apoptosis in response to TRAIL, although leukaemic cell lines are known to do so. As demonstrated in the previous results section that introduction of rCD2:SHIP could protect against cell death in response to TRAIL in Jurkats, it was possible that loss of SHIP-1 might sensitise primary cells to TRAIL. To investigate this, cells were exposed to TRAIL for 6 hours, at concentrations known to cause substantial apoptosis of Jurkats. However, this did not affect the viability of T cells, even when SHIP-1 expression was silenced (Figure 4.11).

4.6 PI3K signalling in the absence of stimulation is increased by silencing of SHIP-1

4.6.1 Basal PI(3,4,5)P_3 levels are increased by silencing of SHIP-1

Having verified loss of protein expression using SHIP-1 shRNA, the effects on PI3K signalling were investigated, beginning with its proximal target, PI(3,4,5)P_3 production. An anti-CD3 antibody, UCHT1, was used as a stimulus and 10µg/ml was confirmed as an optimum concentration by examining Akt phosphorylation in

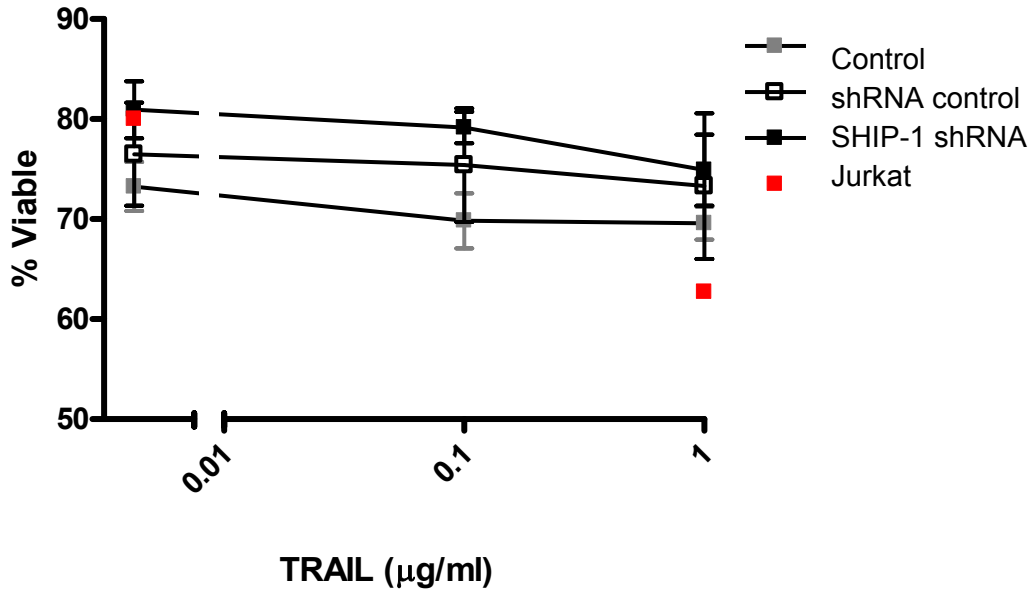

Figure 4.11 Silencing of SHIP-1 does not sensitise primary T cells to TRAIL
CD4+ cells were infected with lentivirus as indicated and cultured for a total of nine days. Cells were then incubated in 0.1% serum and the indicated concentrations of TRAIL for 6 hours before being stained with Annexin-Cy5 and propidium iodide. Viability was assessed by flow cytometry of $1x10^5$ total cells (n=3 +/- SEM)

response to a range of concentrations. The PI(3,4,5)P_3 ELISA successfully determined the amount of PI(3,4,5)P_3 (Figure 4.12). Levels in control cells were low but were increased upon stimulation with UCHT1. Pretreatment with the PI3K inhibitor LY294002 had no effect upon basal levels, but prevented an increase in response to UCHT1. The shRNA control had basal and stimulated levels of PI(3,4,5)P_3 very similar to control cells. SHIP-1 shRNA cells had an increase in levels of PI(3,4,5)P_3 under basal conditions and a further raise in PI(3,4,5)P_3 was observed upon treatment with UCHT1. No PI(3,4)P_2 (the product of SHIP-1 metabolism of PI(3,4,5)P_3) was detected in the mass blot in any of the control samples, probably because the lipid was not present in sufficient quantities. A spot was observed in the UCHT1 treated SHIP-1 shRNA sample, which would be unexpected as without SHIP-1 one would expect a decrease in PI(3,4)P_2 levels. However, a spot was also observed in the PI(3,4,5)P_3 control, indicating that the antibody was cross-reacting with PI(3,4,5)P_3, which, it was known from the PI(3,4,5)P_3 mass ELISA, was most abundant in the UCHTI stimulated SHIP-1 shRNA sample (this cross-reaction had also been reported on the manufacturer's website, and the mass blot has since been withdrawn from sale).

4.6.2 Basal phosphorylation of AKT and other PI3K-dependent proteins levels is increased by silencing of SHIP-1

Further downstream signalling events were then examined using an MSD mesoscale plate to examine phosphorylation of multiple proteins. Again, UCHT1 was used as a stimulus. The timecourse was verified by western blotting for pAkt in control cells. Cells infected with a virus expressing a scrambled short hairpin control showed no change in phosphorylation of AKT or its downstream targets p70S6K and GSK3β under basal or stimulated conditions compared to control cells (Figure 4.13). However, levels of basal phosphorylation were increased in SHIP-1 shRNA cells. (pooled data from three experiments). Both controls and SHIP-1 shRNA cells responded to stimulation by increased phosphorylation of the proteins, however the additional phosphorylation induced by UCHT1 was not greater in the SHIP-1 shRNA cells i.e. SHIP-1 controlled the basal levels of phosphorylation. Basal Akt phosphorylation was also observed to be increased by western blot (Figure 4.13). These results correlated well with the observed changes in PI(3,4,5)P_3 levels. A small increase was observed in the levels of ERK phosphorylation when SHIP-1 was silenced, when assessed by western blot either in unstimulated cells, or those exposed to anti-CD3 or CXCL11 (Figure 4.14).

4.6.3 Basal polymerisation of actin is increased by silencing of SHIP-1

Because PI3K signalling has been implicated in the control of actin polymerisation, and ultimately in cell motility, levels of polymerised actin were also assessed by staining with phalloidin. Control cells and shRNA control cells had very little polymerised actin under resting conditions, and this polymerised actin was localised to discreet areas of the cells. In contrast, SHIP-1 silenced cells displayed an increase in basal polymerisation of actin and the actin appeared to be distributed in a homogenous manner around the cell membrane when examined by confocal microscopy. However, all cells displayed an increase in actin polymerisation after exposure to CXCL11 (ITAC) (expression of CXCR3, the receptor for CXCL11 was unaffected by silencing of SHIP-1, see Figure 5.8). The increase in basal actin polymerisation was also verified by flow cytometry and SHIP-1 silenced cells were found to have approximately 75% more polymerised actin than control cells in unstimulated conditions (Figure 4.15).

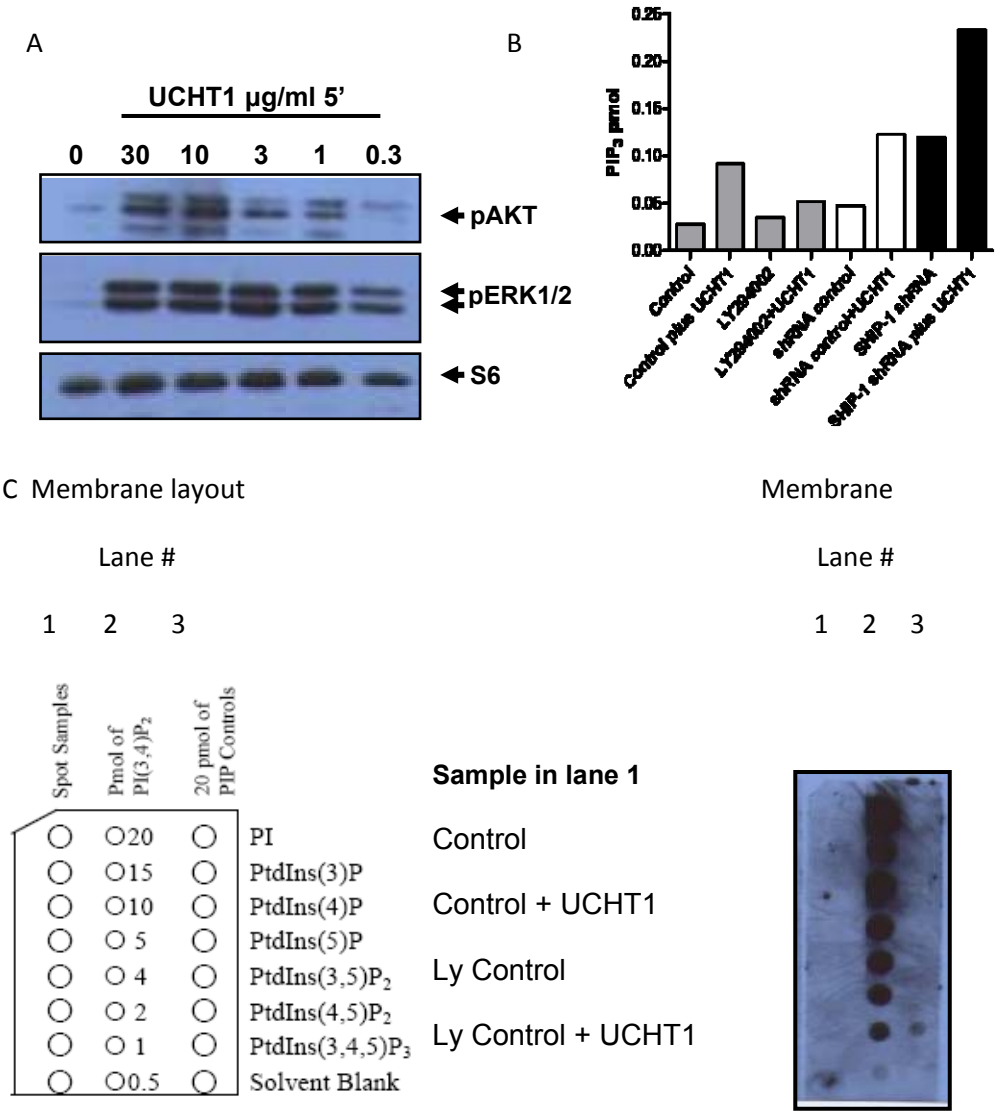

Figure 4.12 Measurement of PI(3,4,5)P_3 and PI(3,4)P_2 levels.
A. Assay was optimised by investigating the ability of varying concentrations of UCHT1 to induce phosphorylation of Akt and ERK in day 10 CD4+ T cells. 1x10^6 cells/point were treated as indicated with UCHT1 then lysed and western blotted for pS473 Akt pERK and S6 as described in the Materials and Methods. B. CD4+ Cells were infected with lentivirus as indicated and cultured for a total of ten days 2x10^6 cells per point were stimulated as indicated in the legend (LY294002 (Ly) 20µM 1 hr preincubation, UCHT1 10µg/ml 10 min,) in RPMI. Lipids were extracted following the manufacturer's protocol. Briefly, cells were collected in trichloroacetic acid (TCA), washed in TCA/EDTA, neutral lipids were extracted in methanol/chloroform, acidic lipids were extracted in methanol/chloroform/HCl. The phases were then split and the organic phase was dried under vacuum and resuspended in appropriate buffer for each assay. For measurement of PI(3,4,5)P_3 levels a mass ELISA (Eschelon biosciences K-3800) was used. C. Cell extracts prepared from cells treated as in part B were analysed for PI(3,4)P_2 levels using a mass blot (Eschelon biosciences-withdrawn). Data is from one experiment representative of two independent experiments.

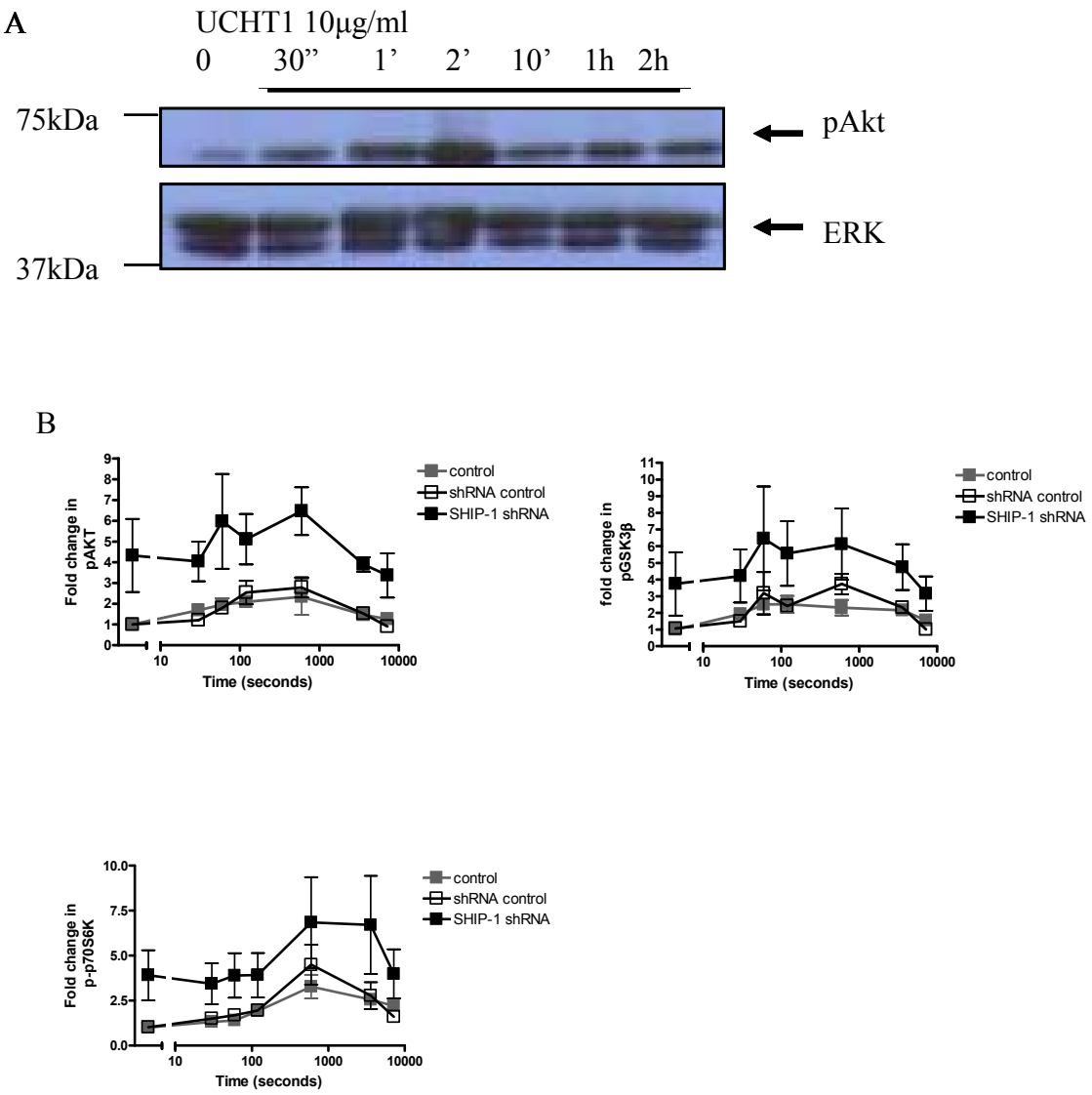

Figure 4.13 PI3K signalling in the absence of stimulation and in response to the CD3 stimulatory antibody UCHT1 is increased by SHIP-1 silencing

A. CD4+ Cells were cultured for a total of ten days. $1x10^6$ cells per point were stimulated as indicated in the legend with UCHT1 (10 µg/ml) then lysed and western blotted for pS473 Akt and ERK as described in the Materials and Methods. B. CD4+ Cells were infected with lentivirus as indicated and cultured for a total of ten days. Cells were stimulated with UCHT1 (10 µg/ml) as indicated at $4x10^5$ cells per point. Cells were lysed using the manufacturer's lysis buffer (MSD). Levels of phosphorylated proteins (pS^{473}AKT, pT^{421}/S^{424} p70S6K and pS^9 GSK3β) were assessed using an MSD mesoscale plate and normalised to levels of total protein in each sample, then as a fold change compared to levels in the unstimulated control (n=3 +/-SEM).

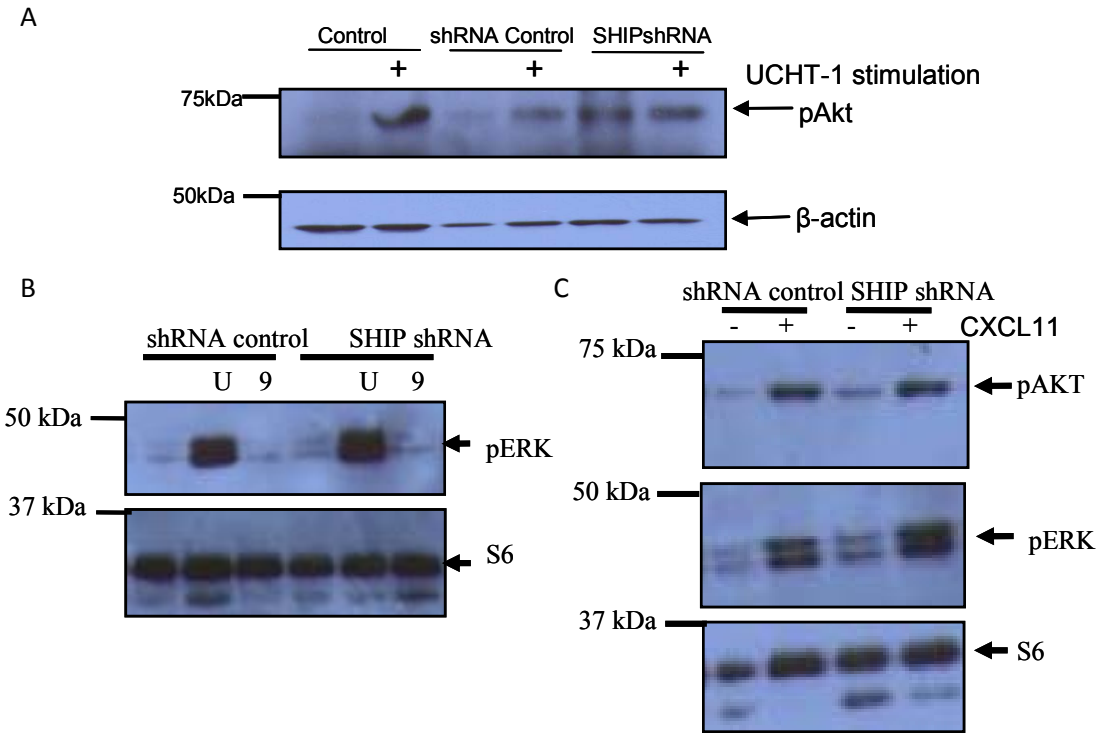

Figure 4.14 Phosphorylation of Akt and ERK in response to UCHT1 and CXCL11. CD4+ T Cells were infected with lentivirus as indicated and cultured for a total of 9-10 days. A. $1x10^6$ cells per point were stimulated as indicated with UCHT1 (10µg/ml) then lysed and western blotted for pS^{473} Akt and β actin as described in the Materials and Methods. B. $1x10^6$ cells per point were stimulated as indicated in the legend with UCHT1 (U) at 10µg/ml or 9.3 (9)(anti-CD28 antibody) at 10µg/ml for 5 minutes then lysed and western blotted for pERK and S6 as described in the Materials and Methods. C. $1x10^6$ cells per point were stimulated as indicated in the legend with CXCL11 for 2 minutes at 3nM, then lysed and western blotted for pS^{473} AKT, pERK and pan S6 as described in the Materials and Methods. Results are representative of at least two independent experiments.

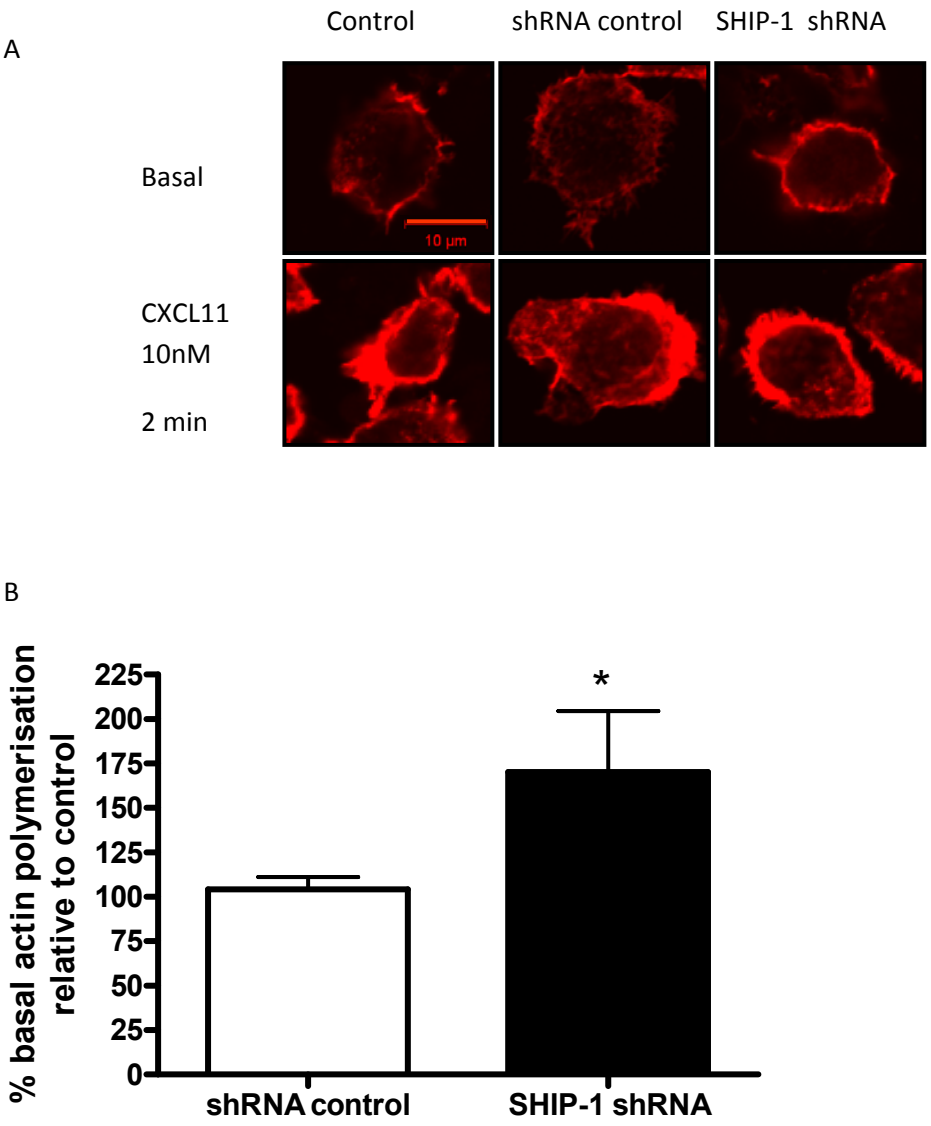

Figure 4.15 Actin polymerisation in resting cells is increased by silencing of SHIP-1 expression. CD4+ T cells were infected with lentivirus as indicated and cultured for a total of ten days. $1x10^6$ cells per point were stimulated with CXCL11 (10nM 2 minutes) as indicated, then fixed with BD cytofix/cytoperm and polymerised actin was stained with Phalloidin-TRITC (typical example representative of three independent experiments) B. Unstimulated cells were fixed and stained as above and analysed by flow cytometry at $1x10^5$ cells per point, pooled data n=5 mean +/- SEM * $P<0.05$ Student's paired T test.

4.7 Summary

- This section of the results demonstrated the successful set up of a lentiviral delivery system.
- Lentiviral- mediated introduction of an active form of SHIP-1 resulted in cell death.
- When the lentivirus was used to silence SHIP-1 expression, cells were viable (and remained insensitive to TRAIL), but had decreased proliferation.
- Silencing of SHIP-1 increased levels of $PI(3,4,5)P_3$ and increased levels of phosphorylation of proteins in the PI3K signalling pathway under resting conditions.
- Resting levels of actin polymerisation were also increased upon silencing of SHIP-1.

Chapter 5: Results Section III

The effect of silencing SHIP-1 expression on cell morphology, adhesion and motility

5.1 Background and objectives

It was seen in the previous section that loss of SHIP-1 led to an increase in basal PI3K signalling pathways in primary human CD4+ T cells and an increase in basal actin polymerisation. Hence the first aim of this section was to characterise any subsequent morphological changes, in SHIP-1 silenced cells. The second aim was to investigate the effect of silencing SHIP-1 expression on cell motility, which encompassed adhesion, basal motility and chemotaxis.

5.2 Cell morphology and expression of adhesion molecules, but not adhesion, are altered by SHIP-1 knockdown

5.2.1 Scanning electron microscopy reveals loss of microvilli upon silencing of SHIP-1

As well as the disordered actin polymerisation, when the SHIP-1 silenced cells were examined by confocal microscopy they also appeared smaller than their control counterparts. Therefore, SEM was undertaken to see if any further morphological changes were observed. It was seen that control cells had microvilli projections and upon treatment with 10nM CXCL11 (ITAC) (2 minutes) polarisation of the cells was observed, as they formed ruffles and lost microvilli expression. After a prolonged exposure to chemokine (1hr), cells no longer appeared motile but exhibited a rounded morphology (Figure 5.1) and interestingly they had not regained microvilli expression (n.b. some cells appeared resistant to exposure to chemokine, or were only affected transiently, as they were observed to have microvilli after 1 hour incubation in chemokine (Figure 5.2)).

Treatment with the PI3K inhibitor LY294002 (20μM), for 1 hour, did not affect expression of microvilli (Figure 5.1). Nor did the Src kinase inhibitor, PP2 (10 μM, 1 hour), (which can inhibit the phosphorylation of SHIP-1), alter expression of microvilli. In contrast, bpVphen, which activates SHIP-1 but inhibits PTEN, resulting in an increase in both $PI(3,4,5)P_3$ and $PI(3,4)P_2$ (338), at two different concentrations (3 and 30 μM, 1 hour) resulted in loss of the majority of microvilli from the cell surface. Treatment with LY294002 could not prevent microvilli loss in response to chemokine

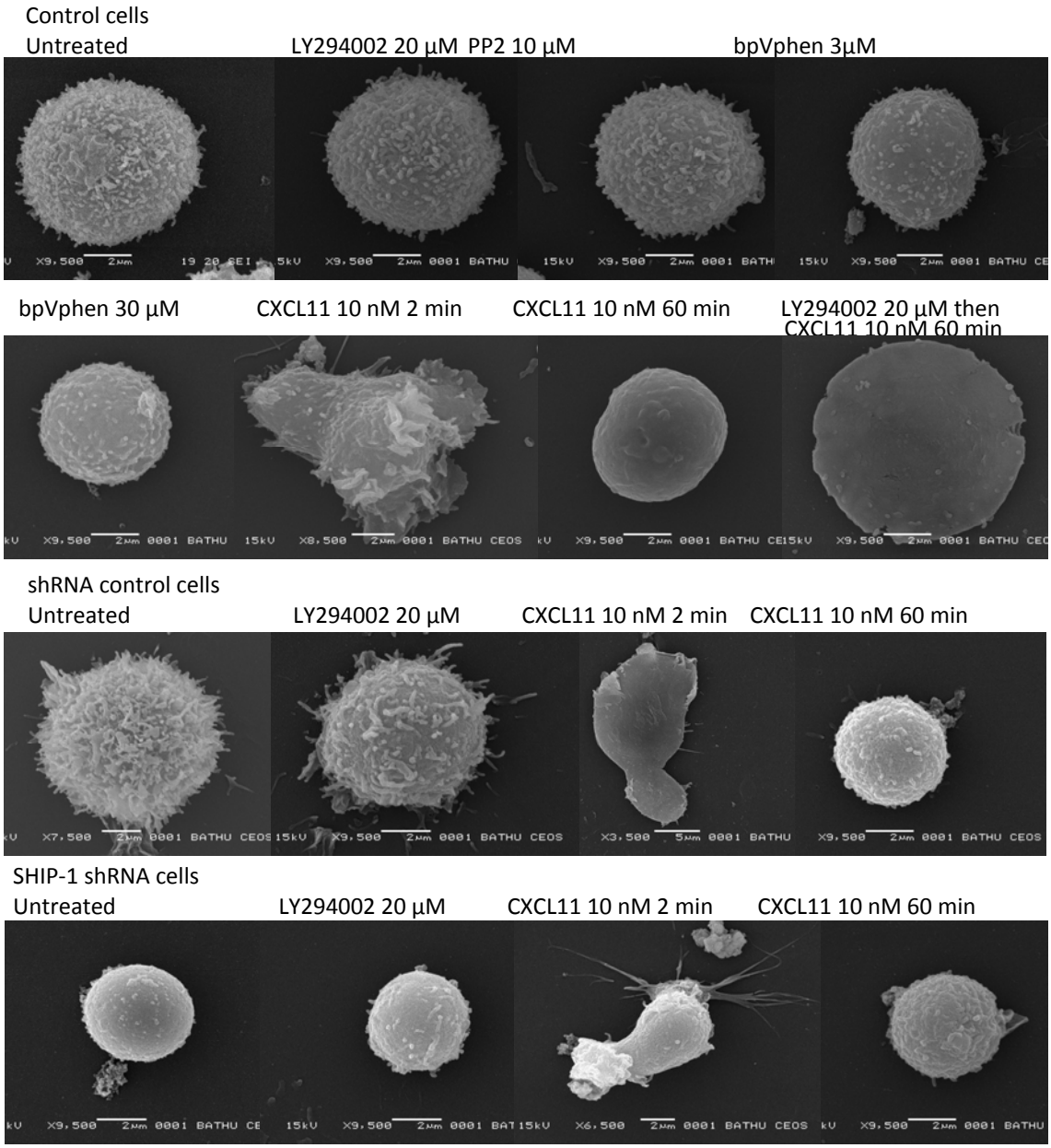

Figure 5.1 Cell morphology is altered by SHIP-1 silencing.

CD4+ T cells were infected with viruses encoding shRNA as previously and cultured for a total of nine days. The cells were washed into RPMI and incubated for 1 hour in inhibitors as indicated on thermanox coverslips in 24 well plates at $5x10^5$/ well. They were then stimulated with CXCL11 as indicated and then fixed and dehydrated and mounted for SEM as described in Materials and Methods. Images are taken from a single experiment, representative of three independent experiments. N.B. In some samples magnification has been adjusted to include whole cell in field of view, please refer to individual scale bars on images. White bar indicates 2µm in all pictures.

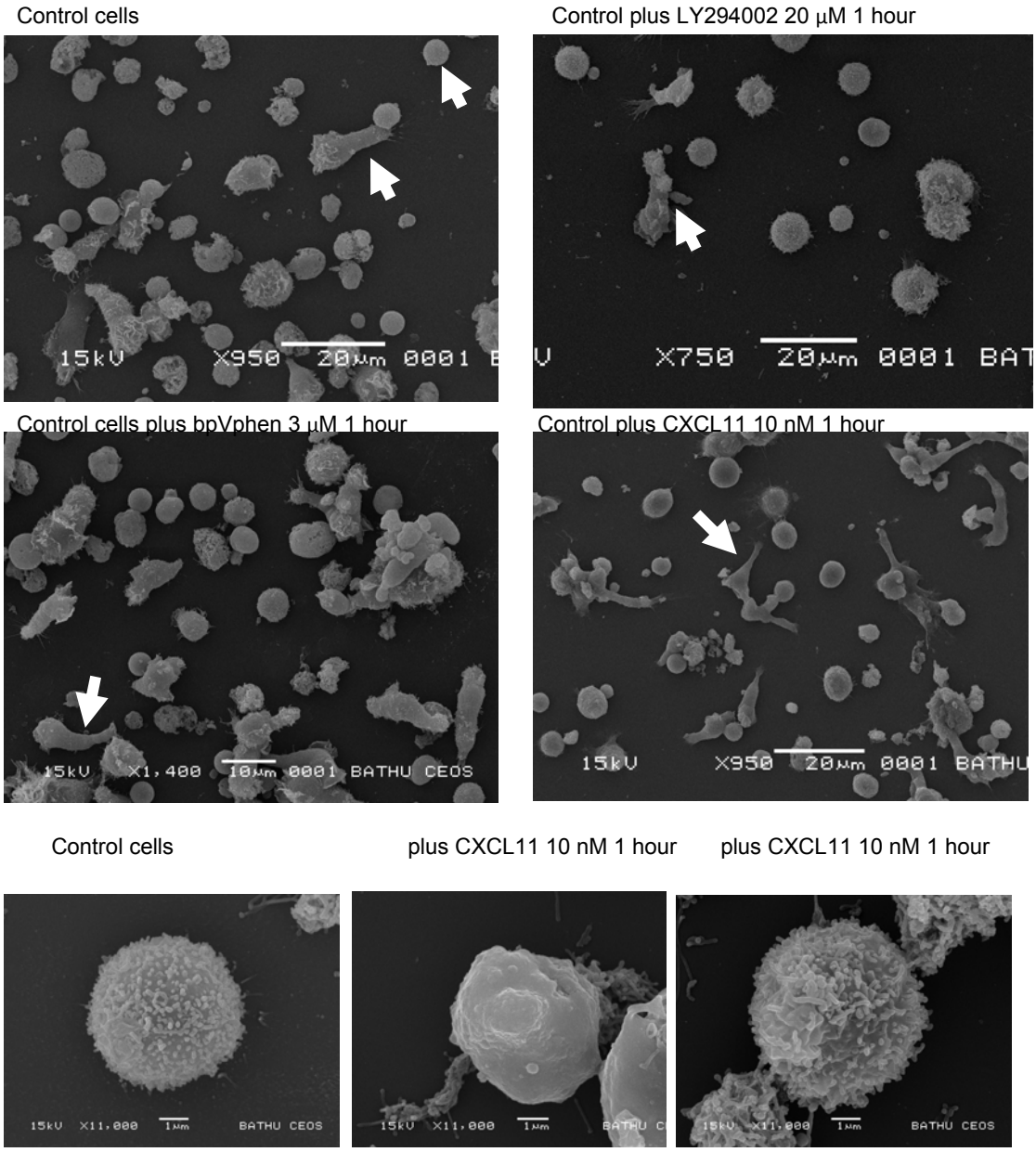

Figure 5.2 Additional SEM images of T cells indicating further points of interest
Overview of morphology: CD4+ Cells were cultured for 9 days. The cells were washed into RPMI and incubated for 1h in inhibitors as indicated on thermanox coverslips in 24 well plates at $5x10^5$/ well They were treated as indicated and then fixed and dehydrated and mounted for SEM as described in Materials and Methods. Images are taken from a single experiment, representative of three independent experiments.

(cells on this slide were damaged during preparation, the apparent increase in cells size is due to flattening after dehydration as indicated by cracks in the cell). shRNA control cells exhibited the same morphology as control cells, expressing microvilli in the absence of stimulation which were unaffected by exposure to LY294002. They polarised as previously described in response to CXCL11, and upon prolonged exposure they returned to a rounded morphology with near total loss of microvilli. SHIP-1 silenced cells lacked microvilli under resting conditions, being fairly spherical in appearance. Upon a short exposure to chemokine, they exhibited a normal ability to polarise, and again became rounded, without microvilli, upon long exposure to chemokine. Furthermore, LY294002 was unable to rescue the phenotype in resting SHIP-1 silenced cells (Figure 5.1).

Figure 5.2 indicates additional points about the morphology of the cells. The first image demonstrates that a range of morphologies are seen in control cells, with some lacking microvilli or appearing polarised. Even with LY294002 treatment (20μM 1 hour), some elongated cells can be observed. Polarised cells were also observed upon exposure to bpVphen (3μM 1 hour), despite loss of microvilli in non-polarised cells. Upon a prolonged exposure to chemokine (CXCL11 10nM 1 hour), some cells were still polarised whilst others exhibited a rounded morphology with loss of microvilli (these images are of cells found on the same slide). Furthermore, in every experiment, not all control cells lost microvilli upon prolonged exposure to chemokine. This may have been attributable to low expression of CXCR3.

5.2.2 Phosphorylation of ERM is decreased when expression of SHIP-1 is silenced

The next set of experiments examined the mechanism by which microvilli were lost when SHIP-1 expression was silenced. Microvilli are formed when ERM (Ezrin/Radixin/Moesin) proteins link the actin cytoskeleton to the surface membrane. It has been reported in the literature that microvilli are rapidly lost upon activation of the cell due to Rac1-mediated ERM dephosphorylation (349-351). When control cells were stained for phosphorylated ERM and examined by confocal microscopy, it was indeed found that pERM had a punctuate distribution that would correlate with its localisation to microvilli. LY294002 treatment (20μM, 1 hour) did not affect the localisation or abundance of pERM in control cells. SHIP-1 silenced cells had very

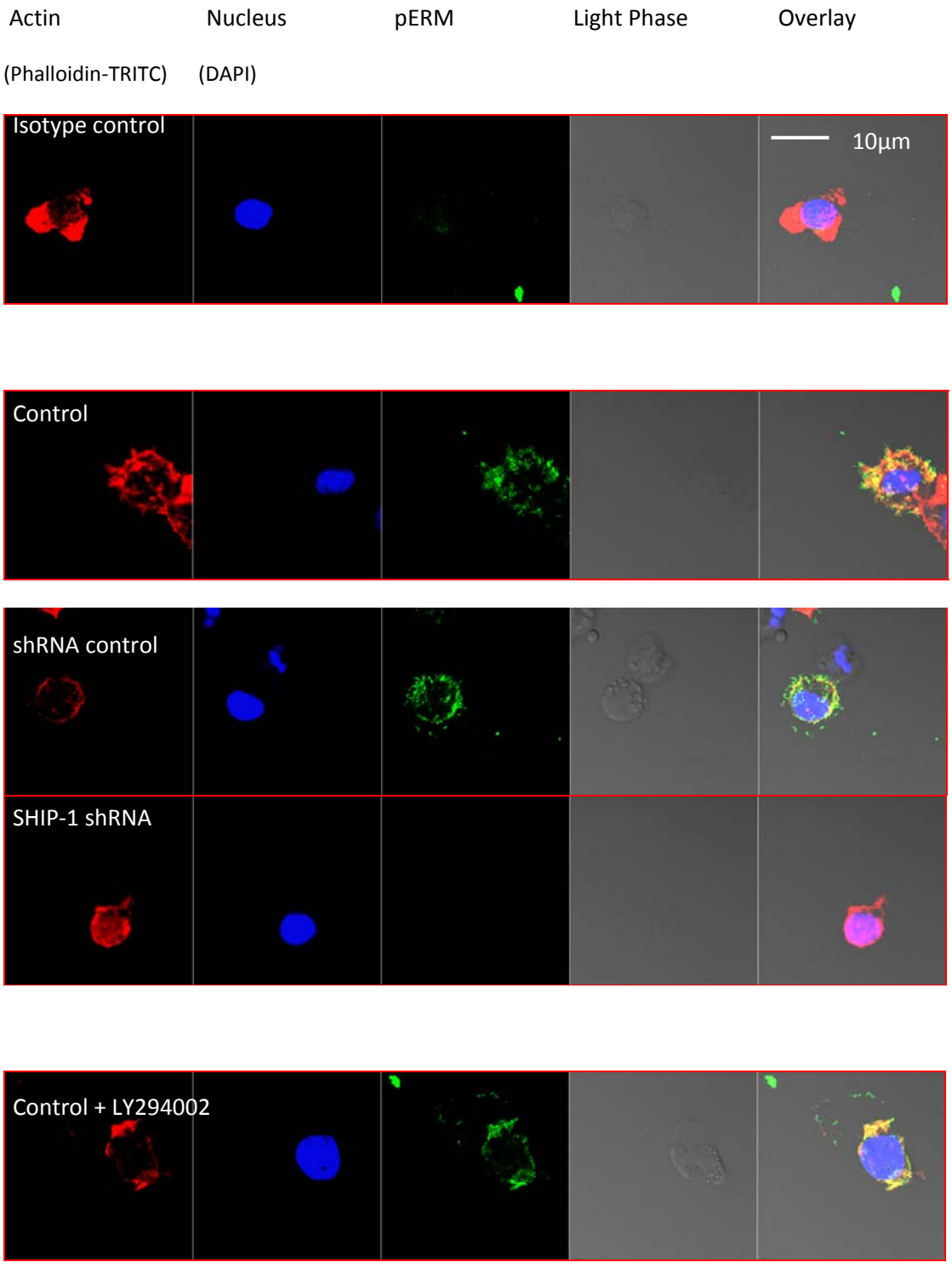

Figure 5.3 SHIP-1 silencing results in loss of ERM phosphorylation

(Figure continues on next page)

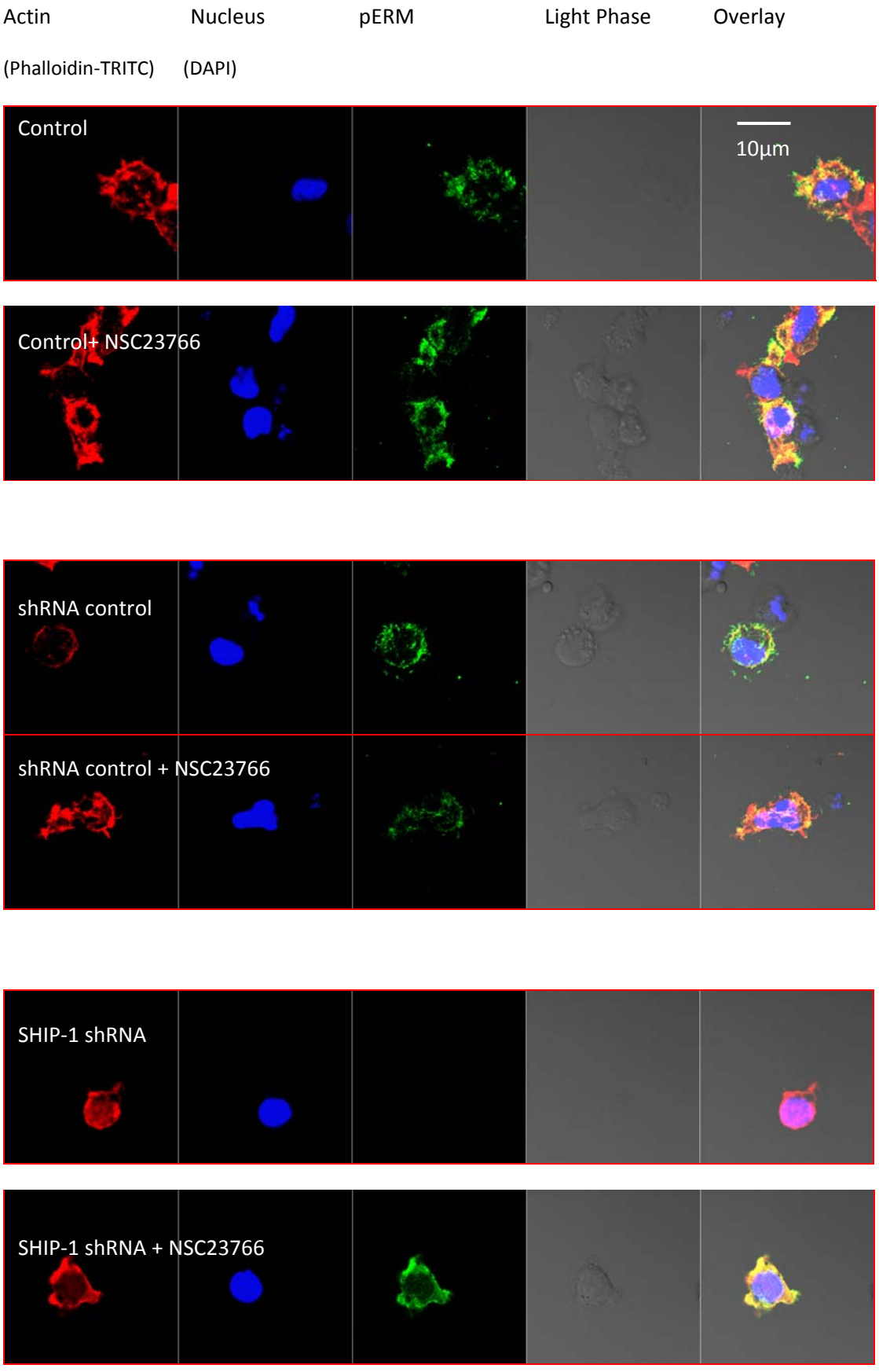

Figure 5.3 *(continued from previous page, see next page for legend)*

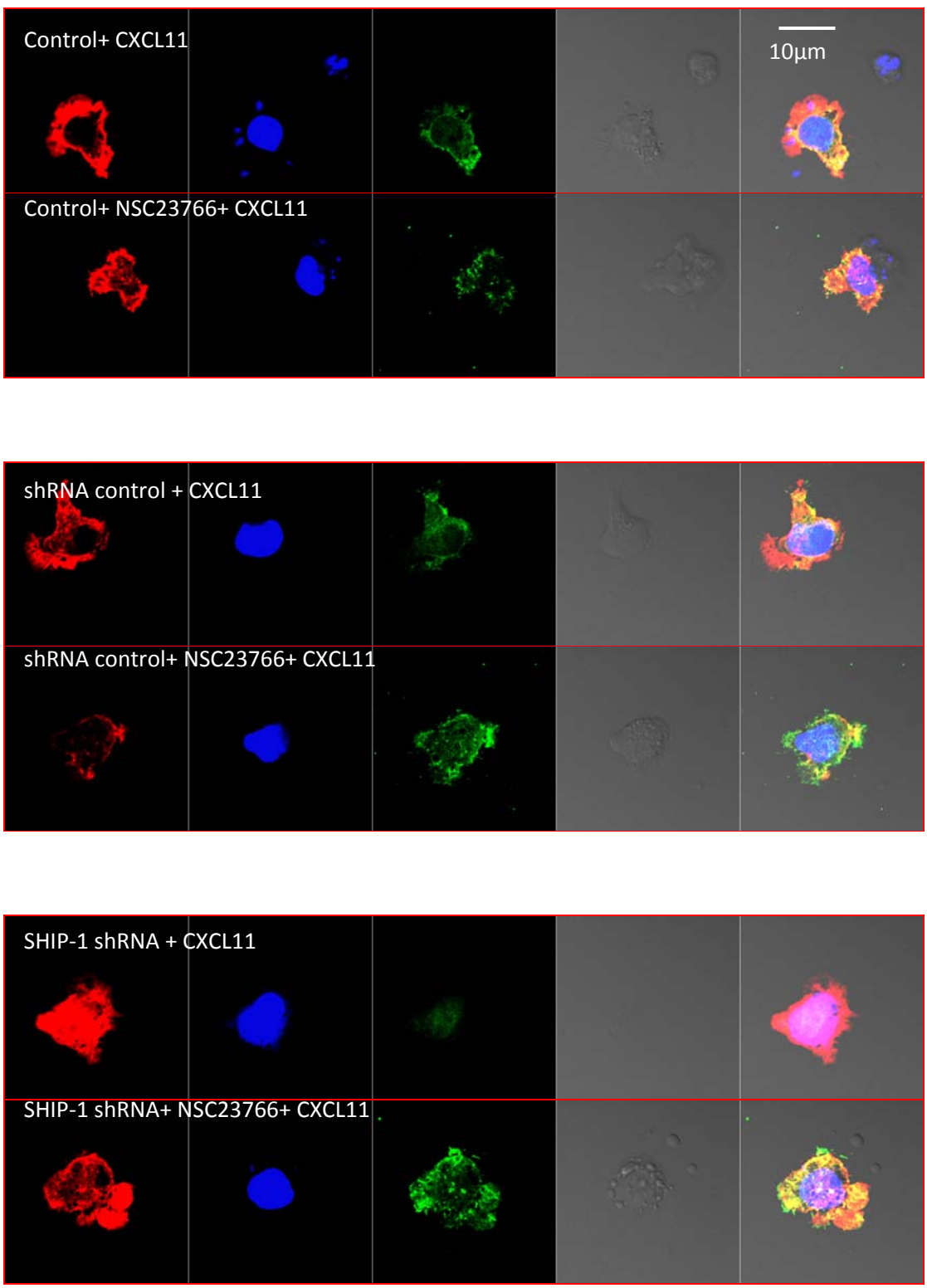

Figure 5.3 *(continued from previous page, see next page for legend)*

Figure 5.3 *(cont'd)* CD4+ T cells were cultured as described in Materials and Methods and infected with lentiviruses encoding shRNA as indicated. On day 9-10 $5x10^5$ cells/ point were rested in RPMI for 1hr with or without the Rac1 inhibitor NSC23766 100 μM (Calbiochem) and LY294002 20 μM. Cells were then stimulated with CXCL11 10nM for 10 minutes as indicated, the fixed with BD cytofix/cytoperm. Cells were stained overnight with pERM (pT^{567}Ezrin/ pT^{564}Radixin/ pT^{558}Moesin, Cell Signal Technology) or Rabbit IgG control in BD Perm/Wash at 4˚C, then washed twice and stained with Anti rabbit-FITC, Phalloidin-TRITC and DAPI for three hours at room temperature. Cells were further washed in Perm/Wash then in Milliq and mounted on coverslips and imaged on an LSM 510 Meta confocal microscope.

little pERM although one or two very small microvilli could be observed on some cells (Figure 5.3). As Rac1 has been shown to mediate ERM dephosphorylation, and SHIP-1 has been shown to act upstream of Rac, inhibiting Ras activation both through its catalytic and non catalytic functions (352-354), the effect of the Rac1 inhibitor NSC23766 (100μM, 1 hour) was also investigated. The inhibitor caused some aberrant morphology in control cells, which had generally lost their spherical appearance, although microvilli remained. When applied to SHIP-1 knockdown cells, the Rac1 inhibitor caused an increase in pERM, which did not appear localised to microvilli and it was not sufficient to completely restore the morphology of the cells to that of control cells. Phosphorylated ERM was largely lost from control cells upon exposure to CXCL11, as documented in the literature. Upon exposure to CXCL11, control cells retained more of their pERM, localised to microvilli, when treated with the Rac1 inhibitor. SHIP-1 silenced cells, pretreated with the Rac1 inhibitor also retained some phosphorylated ERM. When ERM phosphorylation was quantified by flow cytometry (Figure 5.4A), it was seen that whilst NSC23766 was sufficient to block ERM dephosphorylation in shRNA control cells treated with CXCL11, it did not fully restore ERM phosphorylation in SHIP-1 knockdown cells.

To ensure that the lack of phosphorylated ERM in the cells was not due to a lack of ERM proteins themselves, confocal microscopy and flow cytometry of ERM were undertaken. Images of individual cells indicated that ERM was present in both shRNA control cells and SHIP-1 shRNA cells (Figure 5.5 A). In the shRNA control cells the majority appeared localised in peaks on the cell surface membrane i.e. in microvilli. In contrast, upon silencing of SHIP-1, ERM was broadly distributed within the cell. Upon stimulation with CXCL11 (10 nM, 2 minutes), both shRNA control and SHIP-1 shRNA cells polarised, and ERM was localised to the cell membrane. ERM showed some evidence of being localised to the leading edge and uropod. Flow cytometry verified that there was no change in the levels of total ERM protein present in SHIP-1 silenced cells (Figure 5.5 B).

5.2.3 Expression of CD11a but not CD49d is reduced when SHIP-1 expression is silenced

Because many adhesion molecules are preferentially expressed upon the tips of microvilli, which are lost when SHIP-1 expression is silenced, the expression of two key

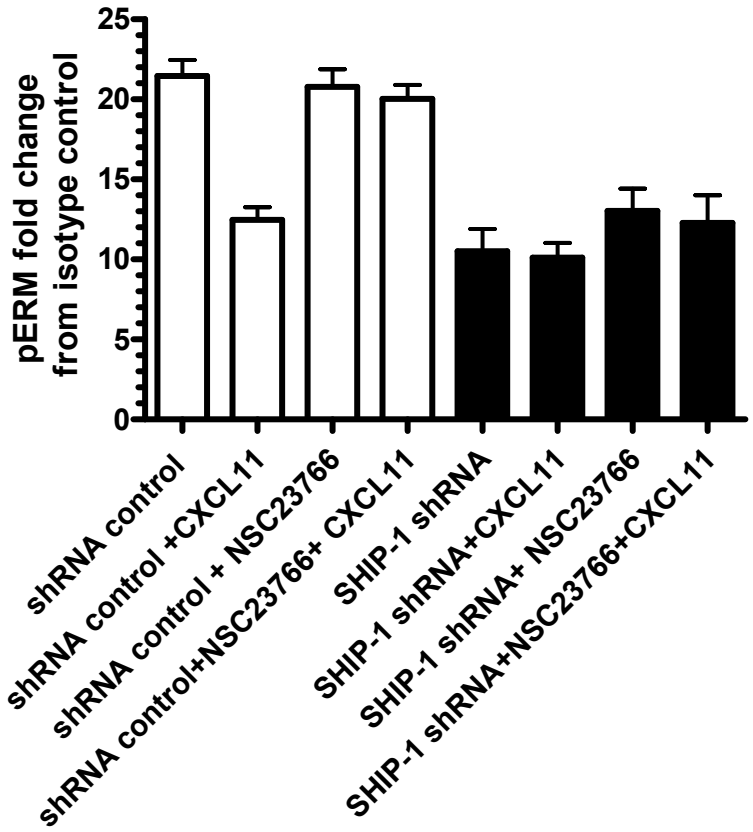

Figure 5.4 Quantification of ERM phosphorylation by flow cytometry reveals significant loss of phosphorylation upon silencing of SHIP-1.
CD4+ T cells were cultured as described in Materials and Methods and infected with lentiviruses encoding shRNA as indicated. On day 9-10 cells were treated as previously, with a 1 hour preincubation of the Rac inhibitor NSC23766 at 100μM for 1 hour, followed by a 2 minute application of 100nM CXCL11 for 2 minutes where indicated. Cells were fixed and stained for pERM and assessed by flow cytometry at $1x10^5$ cells/ point as described in the Materials and Methods. Results are from a single experiment.

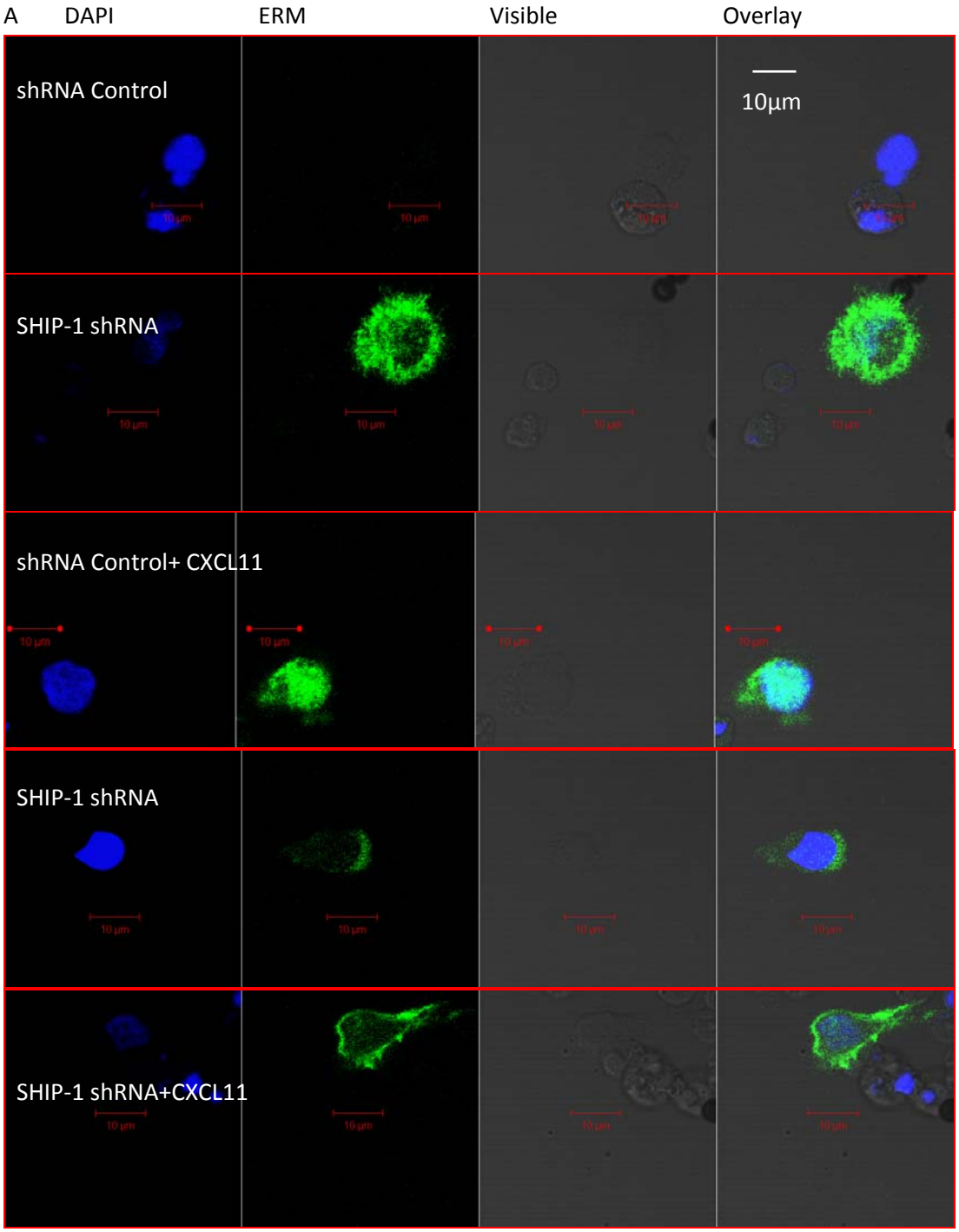

Figure 5.5 Levels of ERM protein are unaffected by silencing of SHIP-1 (figure continues on next page)

B

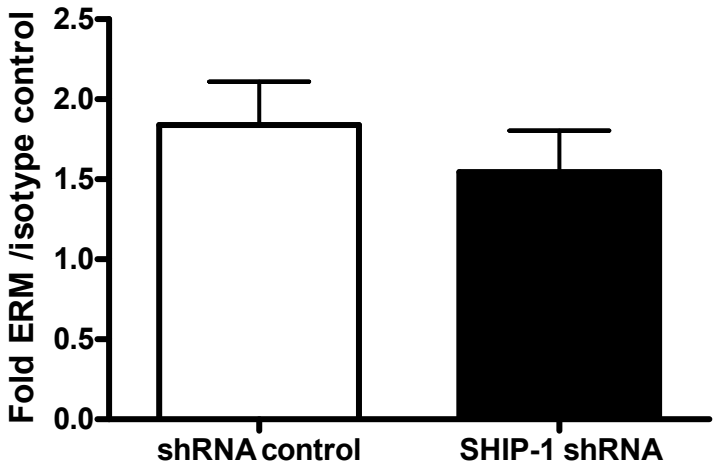

Figure 5.5 (cont'd) A. Confocal microscopy: CD4+ T cells were cultured for 10 days as described in the Materials and Methods.$1x10^6$ cells/point were left unstimulated or stimulated with CXCL11 10nM 2 minutes. Cells were fixed and stained with ERM antibody and DAPI and mounted on coverslips for confocal microscopy. B. CD4+ T cells were cultured as above, then fixed and stained for ERM. Cells were washed into FACS buffer and $1x10^5$ cells/sample were assessed by flow cytometry for the presence of ERM. Results are from a single experiment +/- SD.

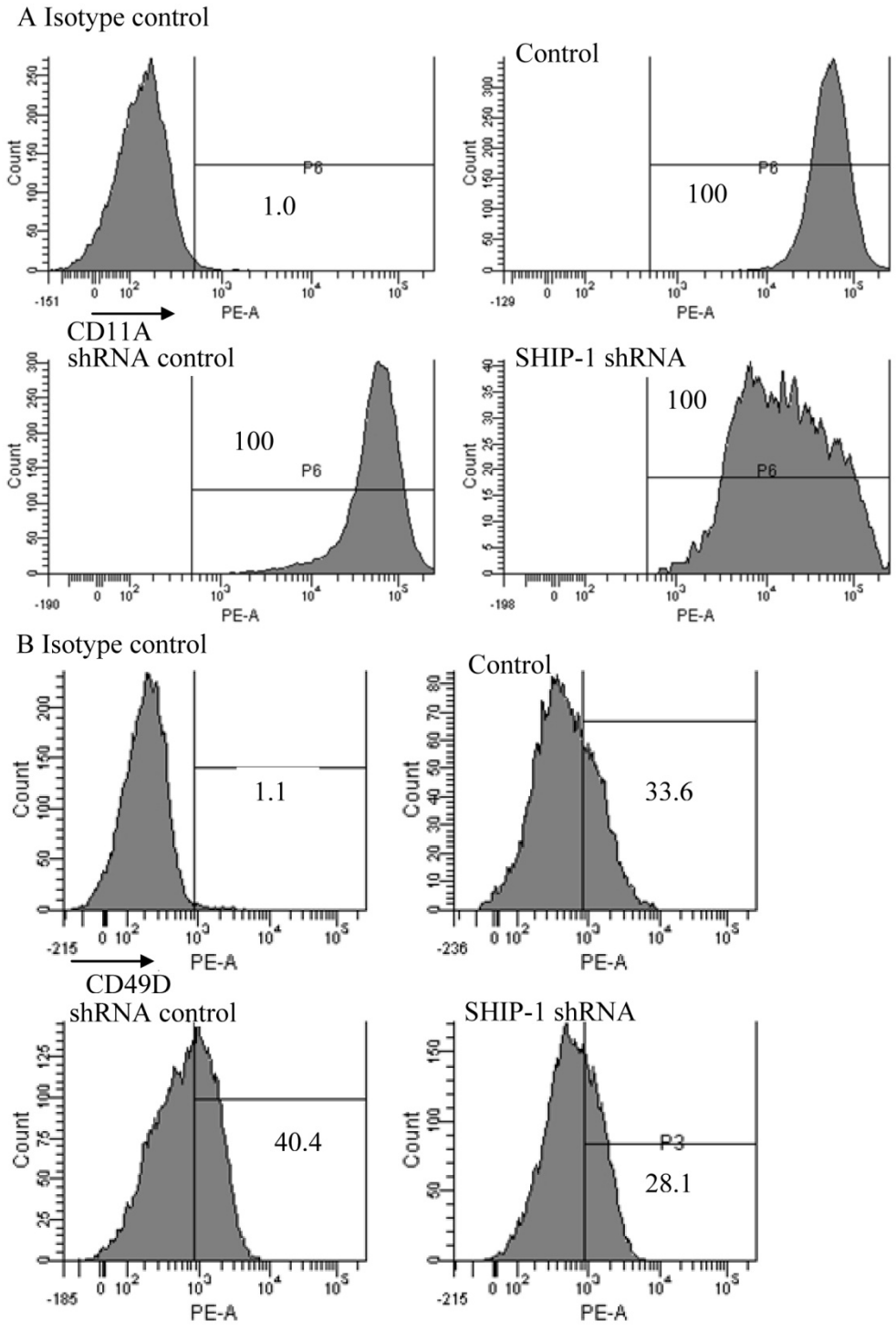

Figure 5.6 Expression of Adhesion molecules CD11a and CD49d.
(figure continues on next page)

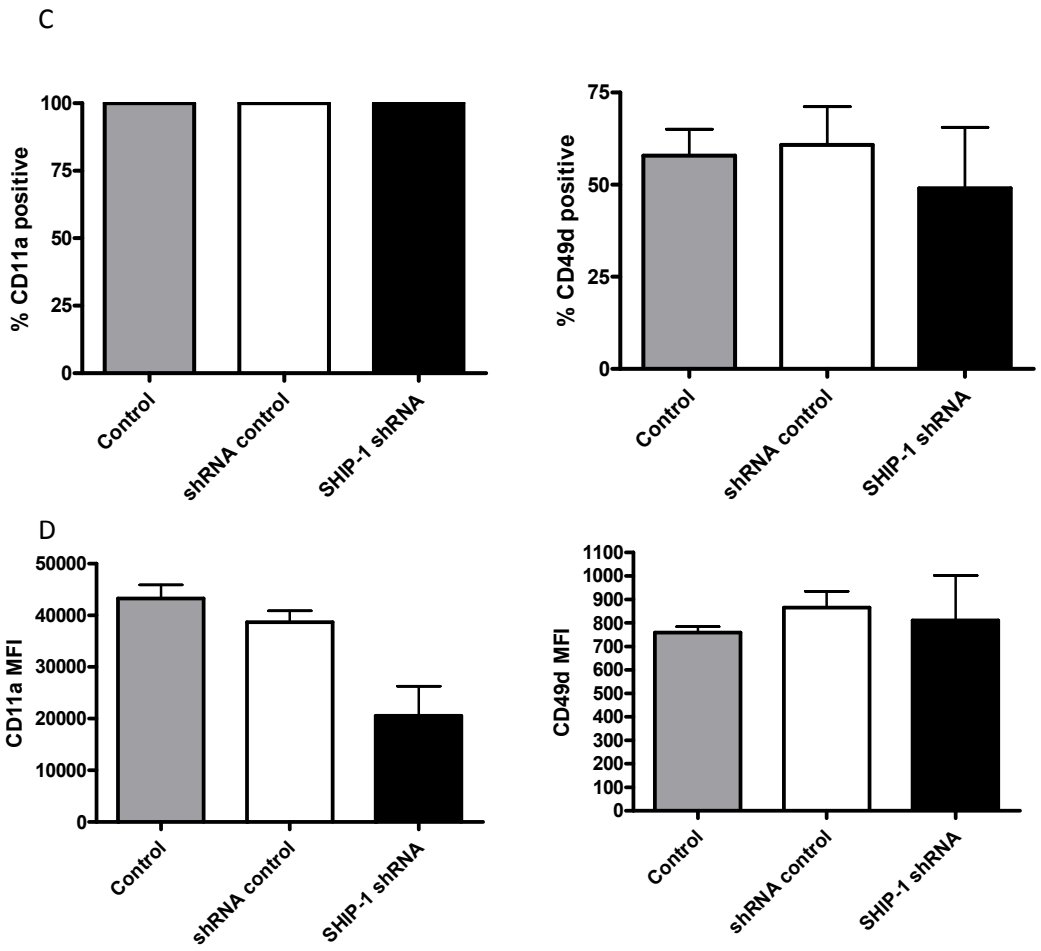

Figure 5.6 Expression of adhesion molecules CD11a and CD49d *(cont'd)* CD4+ T cells were cultured as described in Materials and Methods and infected with lentiviruses encoding shRNA as indicated. On day 9-10 cells were washed into serum free RPMI for 1 hour then stained for cell surface expression of CD11a and CD49d. Expression was analysed by flow cytometry of $1x10^5$ viable cells/ point. Histograms are representative of three independent experiments and bar graphs are pooled data from three independent experiments, error bars are SEM, *$p<0.05$ Student's paired T Test. MFI- mean fluorescence index

adhesion molecules was assessed. CD11a is also known as LFA-1A, which, along with CD18 forms LFA-1 (αLβ2) (355). All cells stained positive for this adhesion molecule (Figure 5.6). However, it was noted that SHIP-1 shRNA cells expressed CD11a at lower levels than control or shRNA control cells ($p<0.05$). CD49d (α4, which along with CD29/β1 forms VLA-4 (356)), was expressed on an equivalent percentage of cells and at an equivalent levels, regardless of SHIP-1 silencing.

5.2.4 Adhesion to fibronectin and ICAM is unaffected by silencing of SHIP-1

With the reduction of expression of CD11a in mind, the ability of the cells to adhere to fibronectin or ICAM coated plates was investigated and found to be unaffected by silencing of SHIP-1. Fibronectin (357) is a dimer that can be present in the plasma or as part of the extracellular matrix and can be adhered to by many different integrins including VLA-4(α4β1) (358), whilst ICAM1 (CD54) is present on leukocytes and the endothelium and is bound by LFA-1 (αLβ2) (359). In fact there was a non-significant trend towards increased adhesion in the SHIP-1 silenced cells. Similarly, when cells on a fibronectin coated plate were exposed to CXCL11 or UCHT1, there was an increase in adherence of all cells, including SHIP-1 silenced cells (Figure 5.7).

5.3 Basal motility but not chemotaxis, is reduced by silencing of SHIP-1

Due to the observed morphological changes in SHIP-1 silenced cells, coupled with evidence from SHIP-$1^{-/-}$ neutrophils (which have a reduced basal motility), and SHIP-$1^{-/-}$ murine T cells (which have a normal basal motility but increased chemotaxis towards CXCL12) (293, 360), it was thought likely that the SHIP-1 silenced T cells might exhibit altered motility. Therefore their basal motility and their ability to chemotax to the chemokine CXCL11 (ITAC) was assessed.

5.3.1 CXCR3 expression is unaffected by silencing of SHIP-1

First, the expression of CXCR3, the receptor for CXCL11, was assessed by flow cytometry and it was found that expression was unaltered by either shRNA control or SHIP-1 silencing in the case of CD4+ T cells. However in CD8+ T cells CXCR3 expression showed evidence of being reduced by silencing of SHIP-1 (Figure 5.8). Therefore, further efforts proceeded using CD4+ T cells.

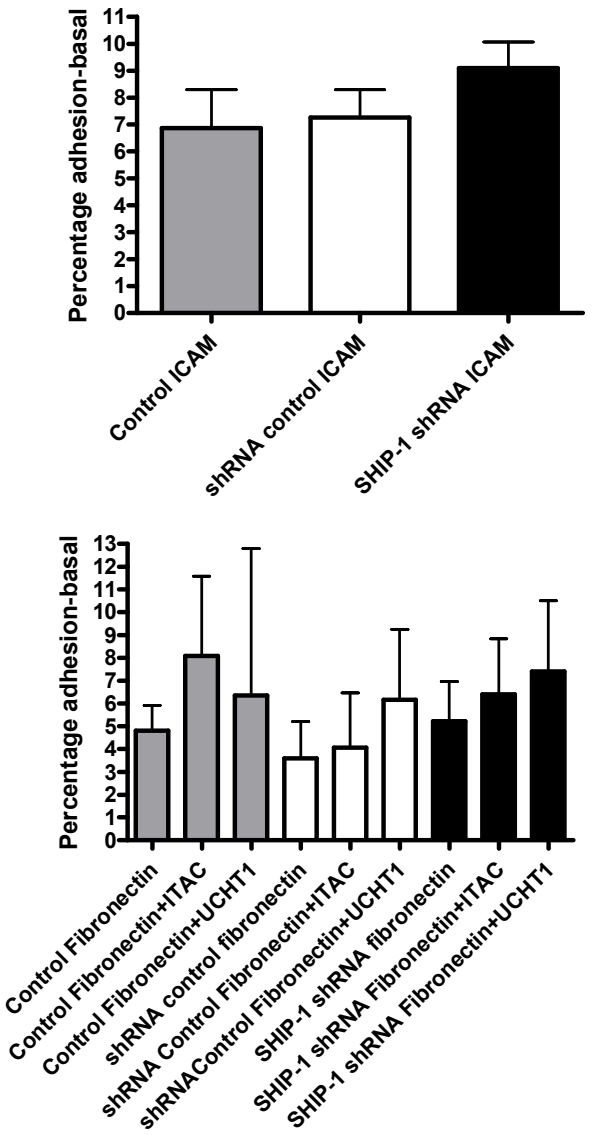

Figure 5.7 Adhesion of cells is not adversely affected by silencing of SHIP-1
CD4+ T cells were cultured as described in Materials and Methods and infected with lentiviruses encoding shRNA as indicated. On day 9-10 cells were labelled with CFSE and their ability of cells to adhere to ICAM or fibronectin coated 96-well plates was assessed by analysis on a plate reader as described in the Materials and Methods. CXCL11 at 10nM or UCHT1 at 10µg/ml was applied for 15 minutes as indicated (n=3 +/- SEM).

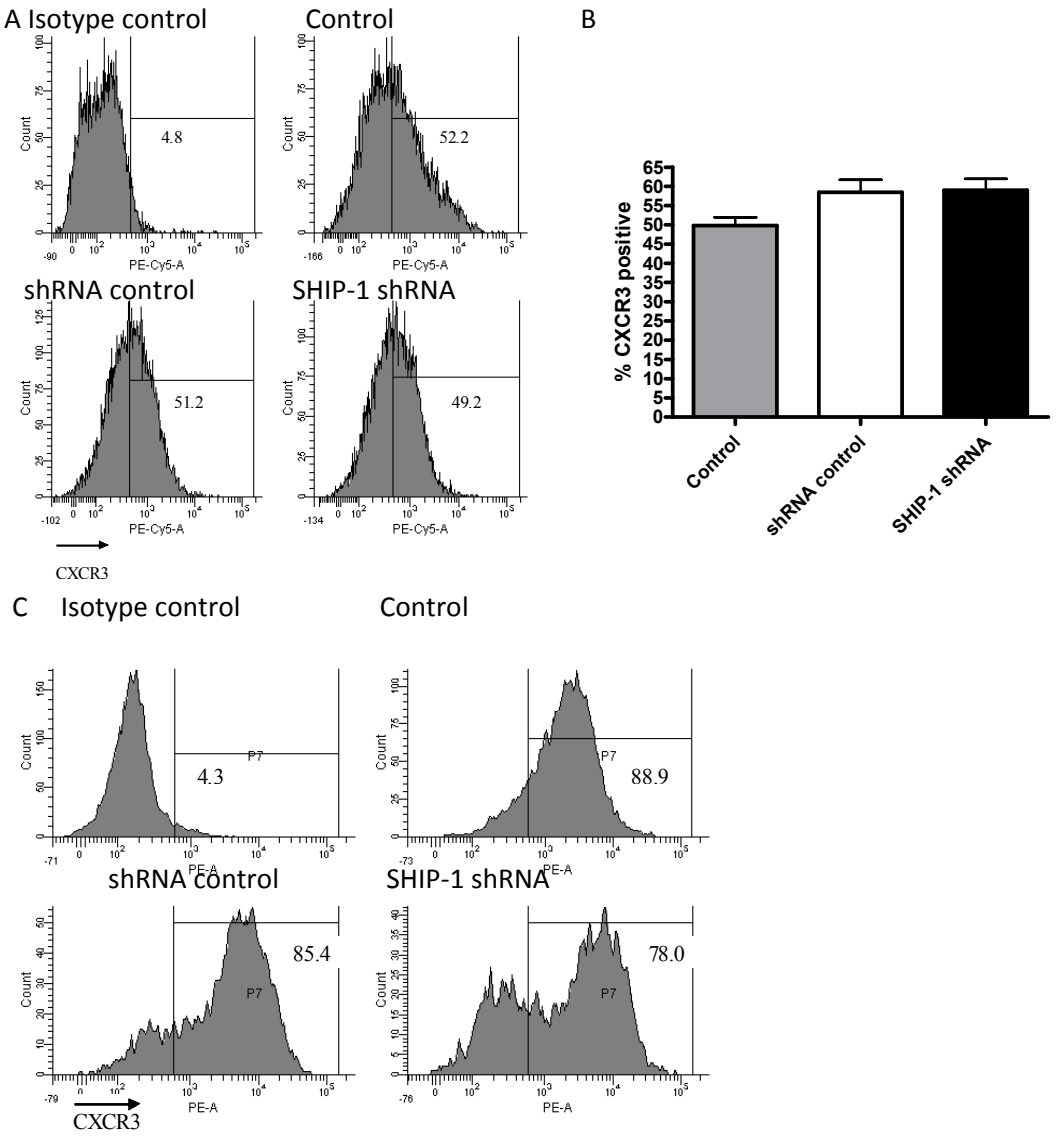

Figure 5.8 Expression of CXCR3 is unaffected by SHIP-1 silencing in CD4+ T cells, but is reduced in CD8+ T cells.
CD4+ or CD8+ T cells were cultured as described in Materials and Methods and infected with lentiviruses encoding shRNA as indicated. On day 9-10 cells were then examined by flow cytometry at $1x10^5$ viable cells/ point to determine the cell surface expression of CXCR3, the receptor for CXCL11. A. Typical flow cytometry plots for CD4+ T cells. B. CD4+ T cells: bar graph is pooled data from three independent experiments, error bars are SEM. C. Typical flow cytometry plots for CD8+ T cells.

5.3.2 Basal motility in a neuroprobe chamber is reduced by silencing of SHIP-1

The first assay to assess basal motility and chemotaxis utilised a Neuroprobe chemotaxis chamber. In this assay varying concentrations of chemokine were placed in the bottom wells of a 96 well plate, and a filter with 5μm pores was placed on top. CD4+ T cells in suspension were pipetted onto the filter and allowed to migrate through the pores to the chemokine. The number of cells which migrated in a Neuroprobe chemotaxis plate in the absence of chemokine was significantly reduced by silencing of SHIP-1 ($p<0.05$). This reduction in basal motility reduced the number of cells that chemotaxed to CXCL11 at all concentrations (0.3-30 nM), although the chemotactic index (the number of cells that migrated to chemokine divided by the number that migrated basally) was unaffected (Figure 5.9).

5.3.3 Basal motility on a fibronectin coated slide is reduced by silencing of SHIP-1

Reduced motility can be due to a number of factors. For example the cells may be immobile, or they may fail to commit to migrating in a particular direction, effectively moving in circles, or they may form pseudopods but fail to commit to the most promising one (287, 288). Therefore in order to investigate the findings from the Neuroprobe assay in more detail, an Ibidi chemotaxis slide was used, on which the cells could be recorded and their individual paths tracked and analysed as discussed in Materials and Methods. It was found that the basal motility of the cells was also reduced on a fibronectin coated Ibidi chemotaxis slide, with a reduction in accumulated distance travelled (total path length), Euclidean distance travelled (straight line distance from start to end point), and average velocity in the absence of chemokine. However, only a difference in Euclidean distance travelled was observed during chemotaxis towards CXCL11 (100 nM) (Figure 5.10, Figure 5.11). When the data were expressed as a chemotatic index the findings mirrored those using the Neuroprobe chemotaxis assay, with the Euclidean Index being unaffected by silencing of SHIP-1 (Figure 5.11). However, the indices for the accumulated distance and velocity were increased by silencing of SHIP-1. A higher concentration of chemokine was used in this experiment compared to the previous experiment as the final concentration reaching the cells is less than a third of that used.

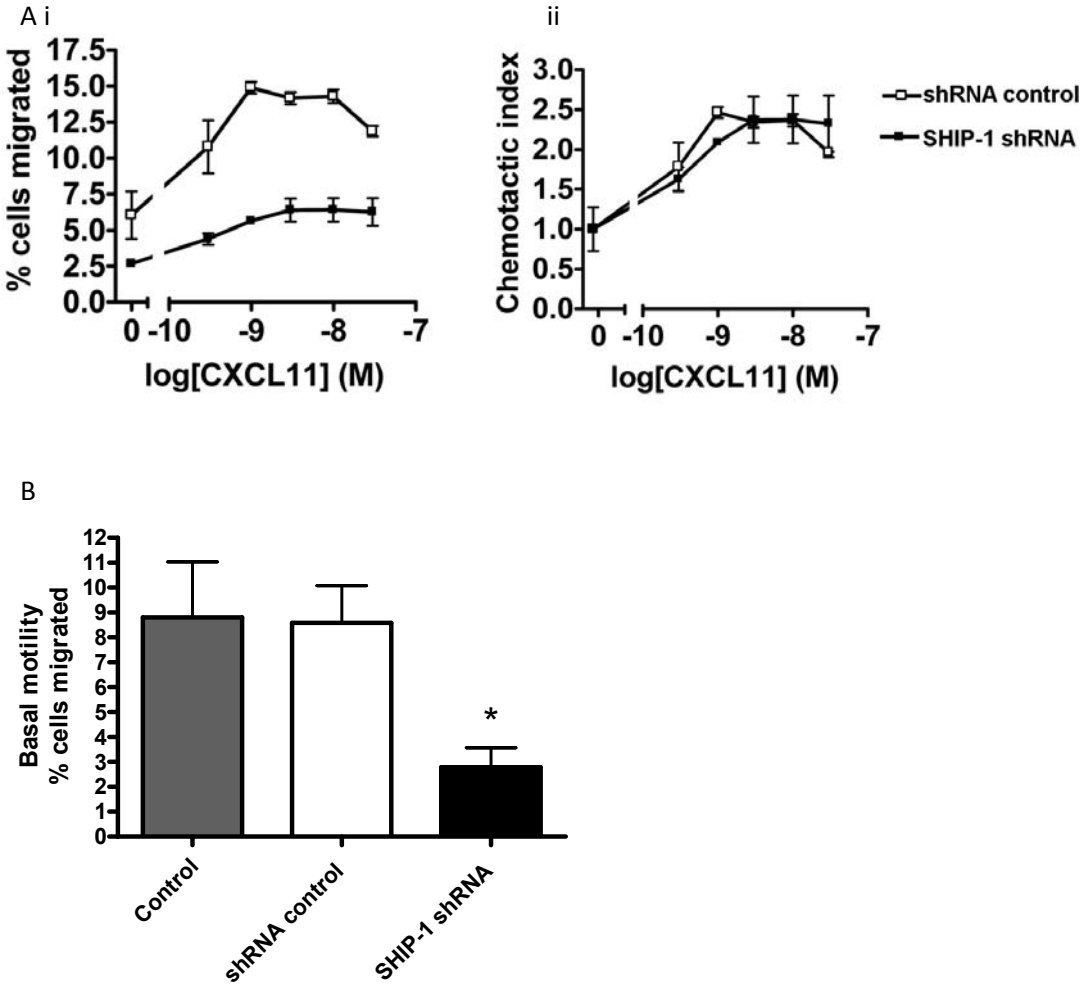

Figure 5.9 Basal motility is reduced by silencing of SHIP-1 expression but chemotaxis is unaffected.

CD4+ T cells were cultured as described in Materials and Methods and infected with lentiviruses encoding shRNA as indicated. On day nine the chemotactic ability of the cells was assessed in a neuroprobe chemotaxis chamber for 3 hours at 37˚C as described in the Materials and Methods A. Results from a single experiment typical of three independent experiments. i. Percentage cells migrated ii. Chemotactic index normalised to basal level for each shRNA. B. Pooled data from four independent experiments +/- SEM *p<0.05 Student's T Test.

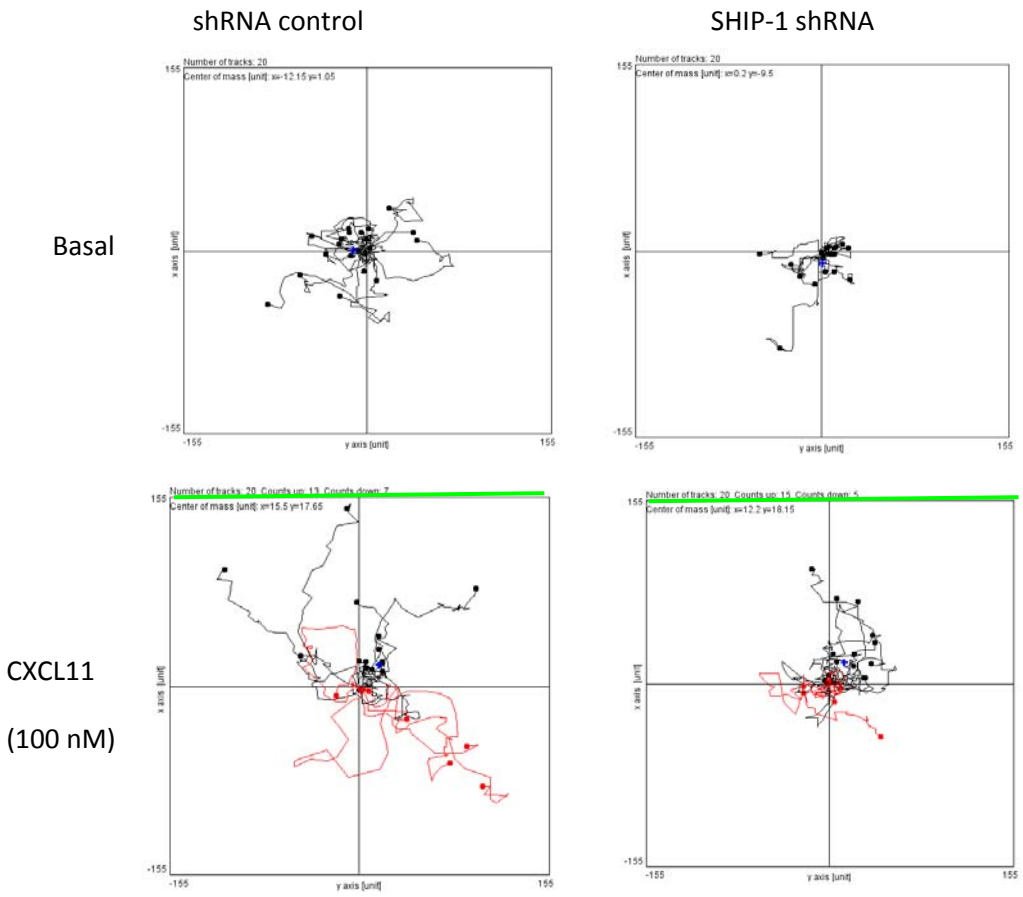

Figure 5.10 Chemotaxis on fibronectin coated surface is reduced by SHIP-1 silencing CD4+ T cells were cultured as described in Materials and Methods and infected with lentiviruses encoding shRNA as indicated. The chemotactic ability of the cells was assessed after nine days of culture using a fibronectin coated Ibidi chemotaxis slide for 15 minutes at 37˚C as described in the Materials and Methods. 20 individual cell tracks were analysed from a single experiment typical of three independent experiments, using imageJ. Where CXCL11 was used, the source is indicated by a green bar and black tracks are from cells that have migrated towards it, red tracks indicate cells that have migrated away.

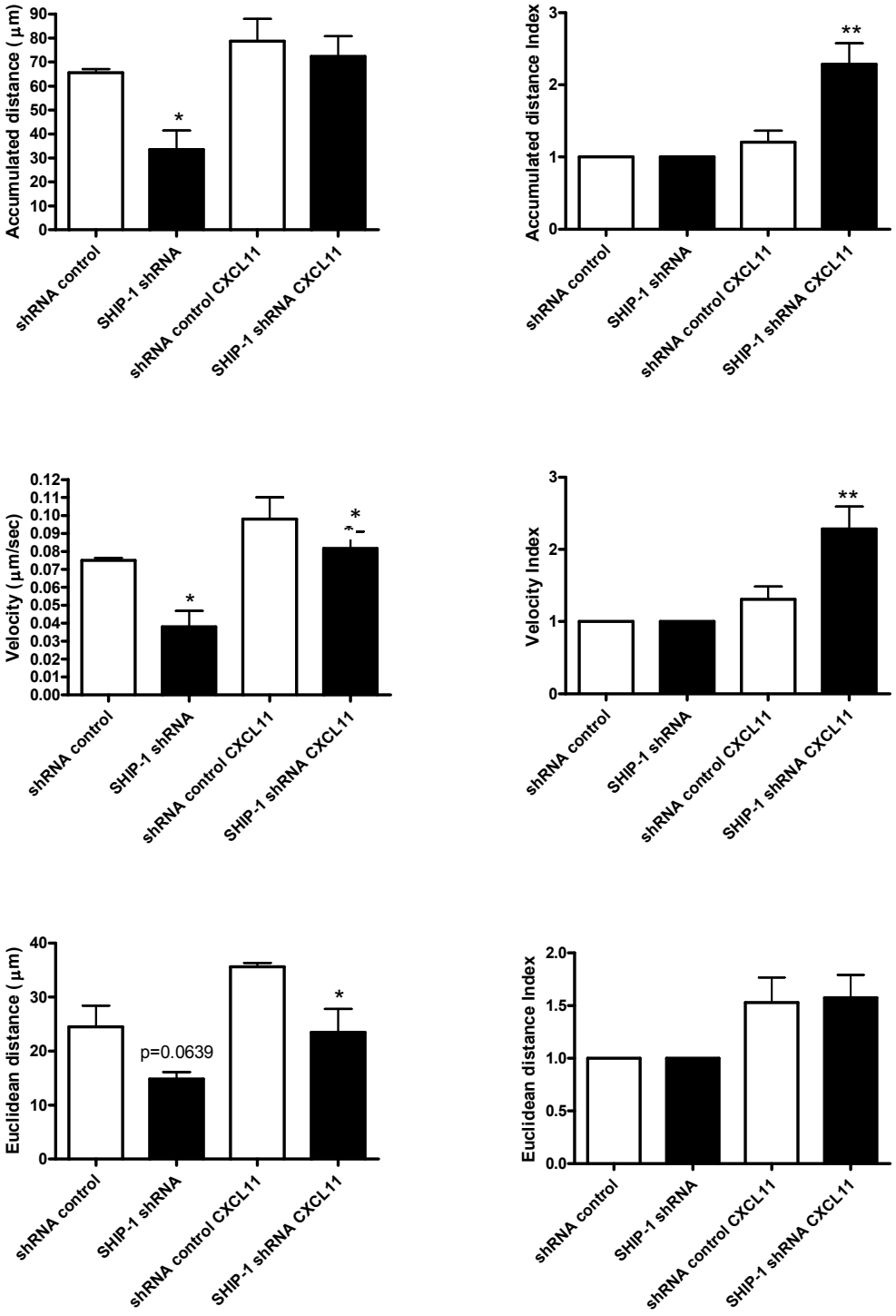

Figure 5.11 Chemotaxis on fibronectin coated surface is reduced by SHIP-1 silencing II CD4+ T cells were cultured as described in Materials and Methods and infected with lentiviruses encoding shRNA as indicated. The chemotactic ability of the cells was assessed after nine days of culture using a fibronectin coated Ibidi chemotaxis slide for 15 minutes at 37˚C as described in the Materials and Methods. Data was analysed using ImageJ and is pooled from three independent experiments. *p<0.05 **p<0.01

5.4 Summary

- CD4+ T cells in which SHIP-1 has been silenced have an aberrant morphology with a loss of microvilli which could not be restored by PI3K inhibition
- SHIP-1 silenced cells also lack phosphorylated ERM
- ERM phosphorylation could be partially restored in SHIP-1 silenced cells using a Rac1 inhibitor (Figure 5.12)
- Expression of CD11a, but not CD49d, was slightly reduced by silencing of SHIP
- The ability to adhere to ICAM or fibronectin was not affected by silencing of SHIP
- CXCR3 expression was unaffected in CD4+ T cells but was reduced in CD8+ T cells when SHIP-1 expression was silenced
- In two different assays, basal motility of CD4+ T cells was reduced, but chemotaxis was unaffected when expression of SHIP-1 was silenced.

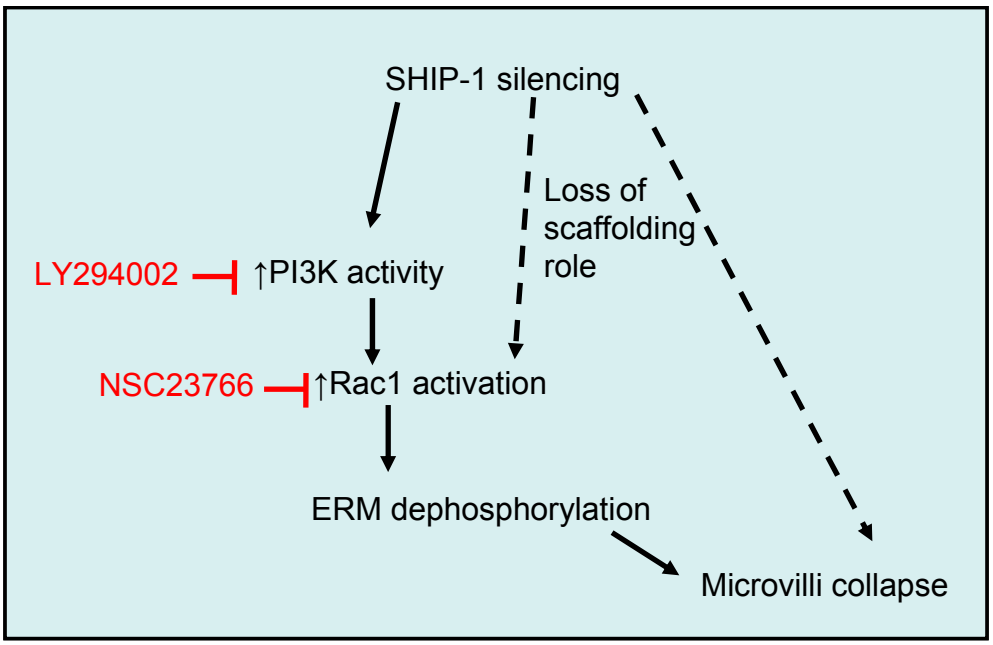

Figure 5.12: Summary of effects of SHIP-1 silencing on microvilli loss

Silencing of SHIP-1 leads to increased PI3K signalling which in turn can lead to increased Rac1 activation and ERM dephosphorylation, culminating in microvilli collapse. However the microvilli loss is insensitive to PI3K inhibition and is only partially ameliorated by Rac1 inhibition. This suggests that SHIP-1 negatively regulates microvilli collapse through its scaffolding functions, independently of its phosphatase activity. This theory will be examined fully in the Discussion.

Chapter 6: Results Section IV

Localisation of PH domain probes and phosphorylated SHIP-1 during chemotaxis

6.1 Background and objectives

It has been previously reported that PI3K signalling localises to the leading edge of the cell and that lipid phosphatases are required to maintain this polarisation and to aid prioritisation of chemotactic cues by aiding commitment to the most promising emerging pseudopod (287). The TAPP PH domain has specificity for $PI(3,4)P_2$ whilst the Akt PH domain can be recruited to both $PI(3,4)P_2$ and $PI(3,4,5)P_3$. It has previously been demonstrated that when either domain is conjugated to a fluorescent reporter, their localisation can be tracked (293). In cell lines they have been shown to be recruited to the cell membrane upon receptor stimulation. Furthermore the Akt PH domain has been shown to localise to the leading edge of chemotaxing neutrophils.

The results in the previous chapter demonstrated that loss of SHIP-1 results in a decreased basal motility of primary human T cells. Therefore the aim of this chapter was to investigate the role of SHIP-1 in primary T cell chemotaxis in more detail by examining the localisation of fluorescently-tagged PH domains and phosphorylated SHIP-1 in T cells during chemotaxis.

6.2 Localisation of TAPP PH domain probes

6.2.1 TAPP PH weakly localises to pseudopods in motile primary T cells

To investigate the localisation of $PI(3,4)P_2$ in primary human CD4+ T cells, the GFP TAPP PH reporter was electroporated into cells. The TAPP PH domain is specific for $PI(3,4)P_2$ and therefore its localisation can be taken as a marker of SHIP-1 activity (251, 361). Transfection rates were modest (Section 4.2), and expression was weaker than with lentivirus (see Chapter 4), but cells appeared viable and healthy. However, only weak localisation of the probe to the leading edge was seen when the cells were basally motile on a fibronectin coated slide (Figure 6.1), or chemotaxing towards CXCL11 (Figure 6.2). The probe appeared to be located in pseudopods and at the leading edge but did not appear to have definitive membrane localisation. Similarly, a range of other stimuli including bpVphen and CD3/CD28 beads failed to induce definitive membrane localisation of the probe (Figure 6.3), despite the fact that both of these conditions were demonstrated in Chapter 3 to induce phosphorylation of SHIP-1. To test for defects in the probe an RFP-TAPP PH probe was also used. This probe was very weakly expressed and demonstrated a largely uniform cellular distribution, both in resting cells and upon stimulation with H_2O_2 (Figure 6.4).

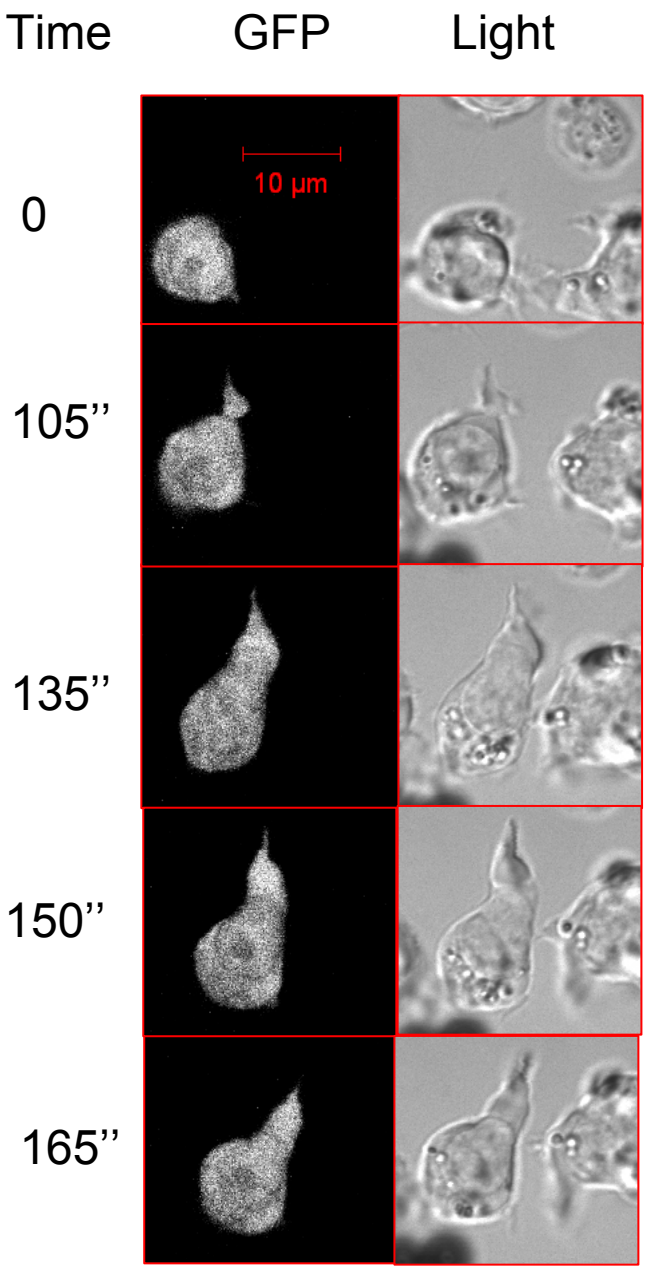

Figure 6.1 TAPP PH-GFP localisation in T cells during basal motility on fibronectin-coated slide
CD4+ T cells were electroporated with TAPP-PH-GFP as described in Materials and Methods and on day 2 post isolation were resuspended in chemotaxis media and placed in a fibronectin coated Ibidi chemotaxis slide. Cells were allowed to settle for 15 minutes, after which motile cells were recorded using video microscopy on an LSM510 Meta confocal microscope at 37°C. Images are of a single cell representative of cells recorded in two independent experiments.

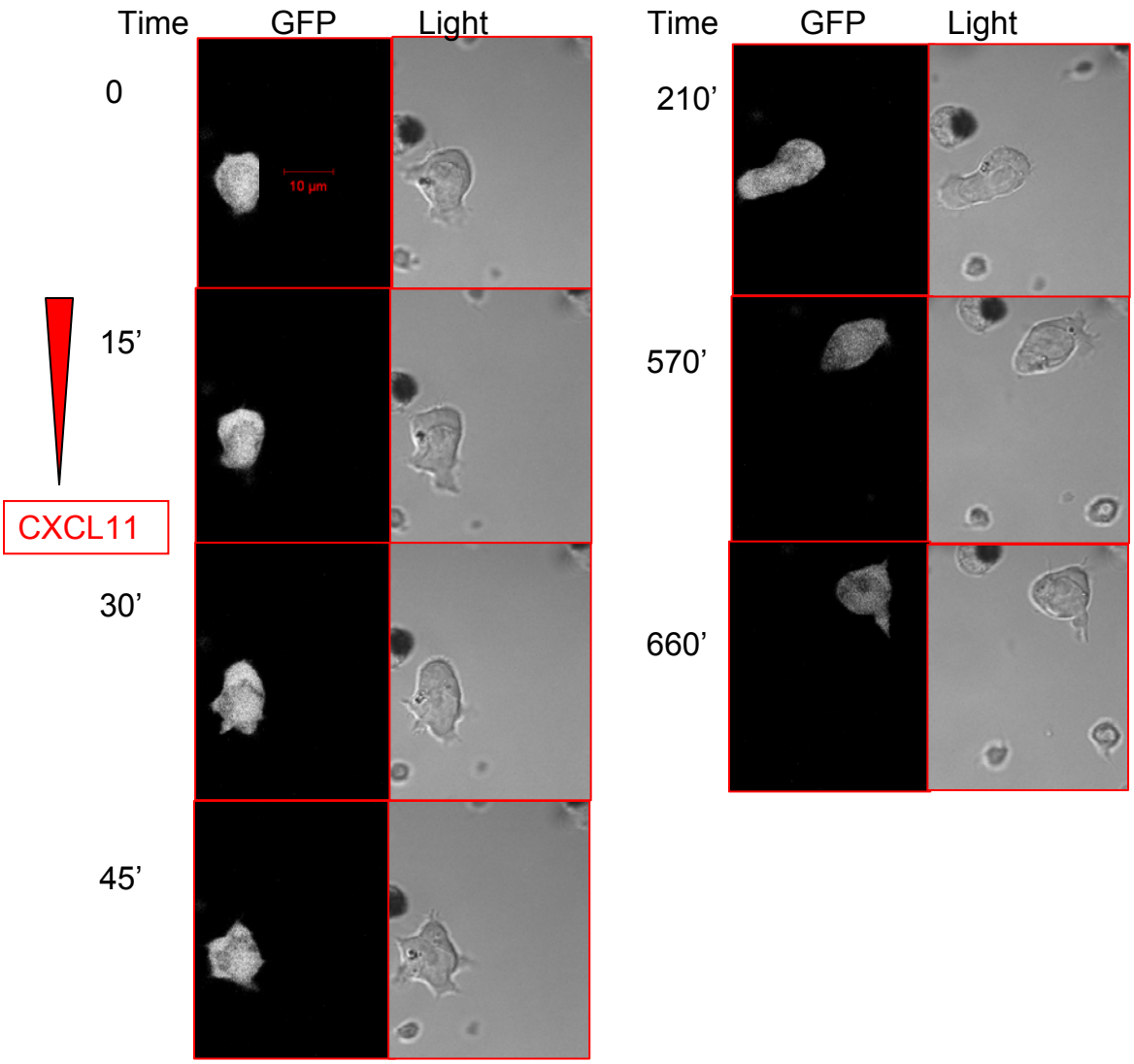

Figure 6.2 TAPP PH-GFP localisation in T cells during chemotaxis to CXCL11

CD4+ T cells were electroporated with TAPP-PH-GFP as described in Materials and Methods and on day 2 post isolation were resuspended in chemotaxis media and placed in a fibronectin coated Ibidi chemotaxis slide loaded with 100 nM CXCL11 in the top chamber as described in Materials and Methods. Cells were allowed to settle for 15 minutes, after which motile cells were recorded using video microscopy on an LSM510 Meta confocal microscope at 37°C. Images are of a single cell representative of cells recorded in two independent experiments.

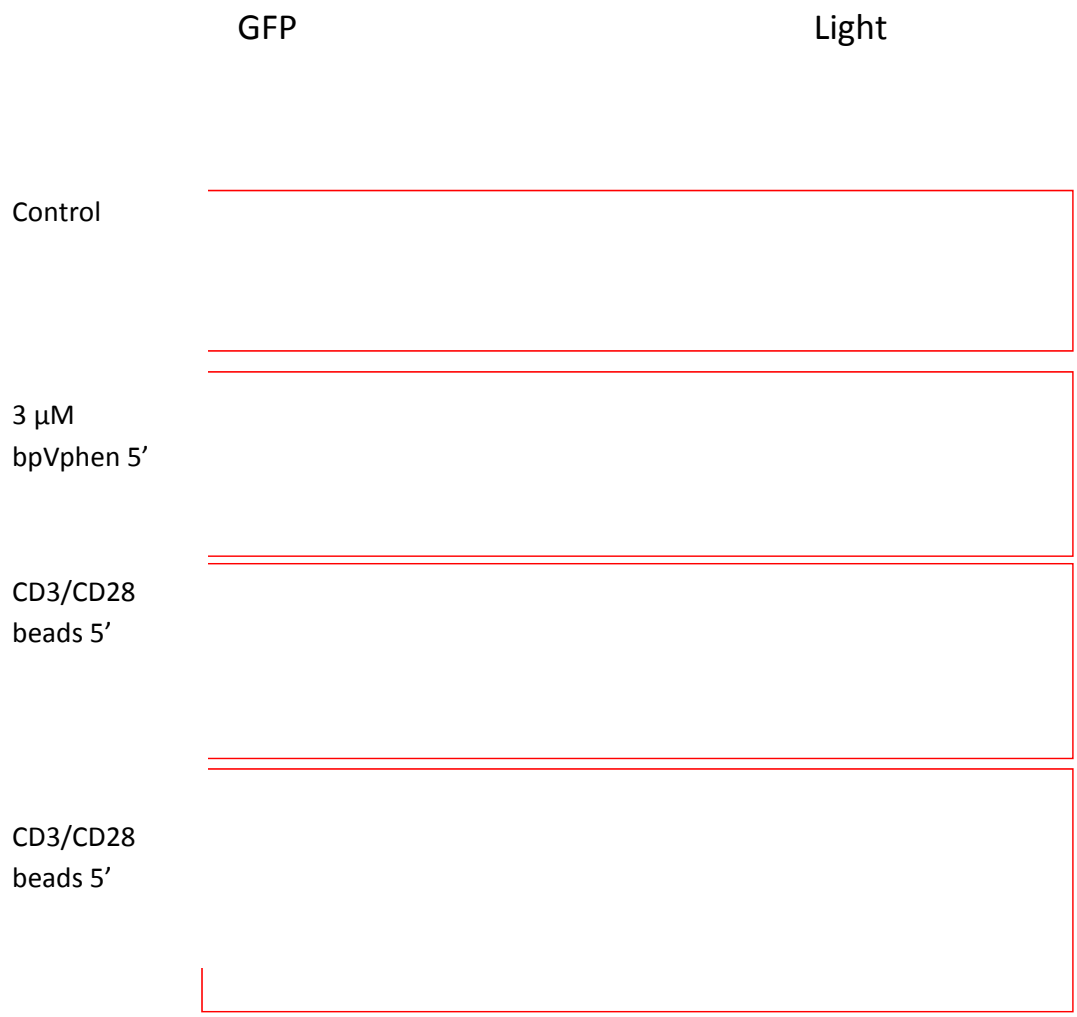

Figure 6.3 TAPP PH-GFP localisation in T cells
CD4+ T cells were electroporated with TAPP-PH-GFP as described in Materials and Methods and on day 2 post isolation were resuspended in chemotaxis media and placed in a chambered coverslip and allowed to settle for 15 minutes before stimulation was applied as indicated. Cells were recorded using video microscopy on an LSM510 Meta confocal microscope at 37°C. Images are representative of cells recorded in two independent experiments.

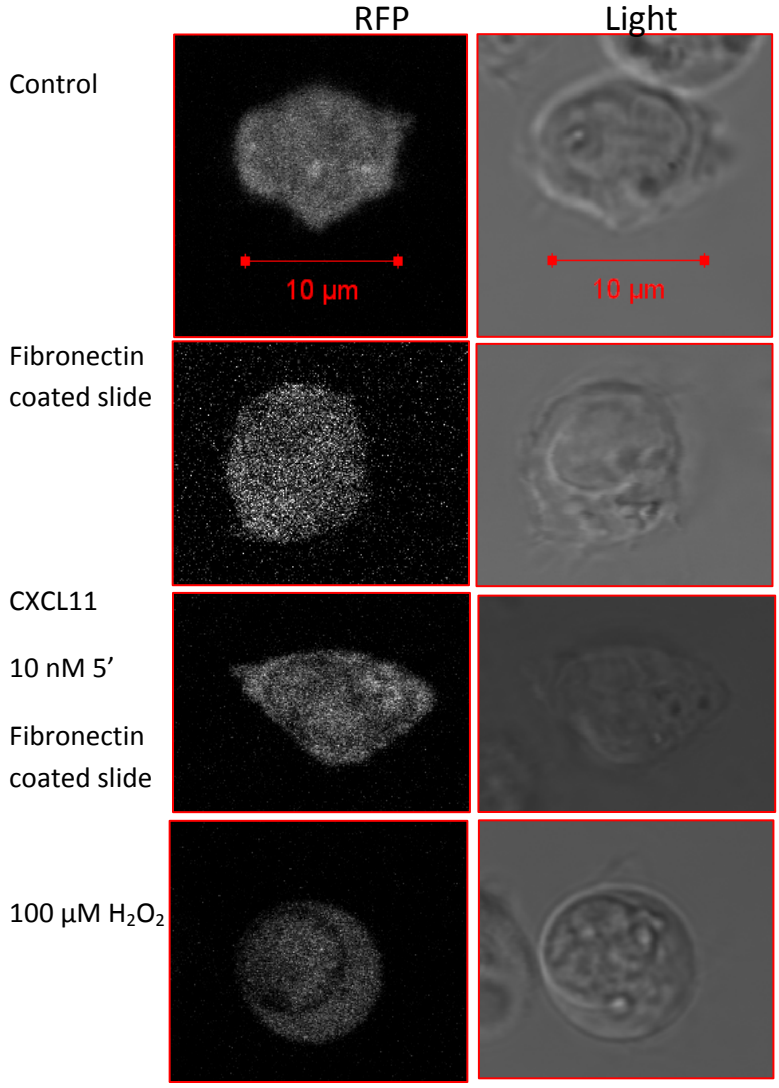

Figure 6.4 TAPP PH-RFP localisation in T cells
CD4+ T cells were electroporated with TAPP-PH-RFP as described in Materials and Methods and on day 2 post isolation were resuspended in chemotaxis media and placed in a chambered coverslip and allowed to settle for 15 minutes before stimulation was applied as indicated. Cells were recorded using video microscopy on an LSM510 Meta confocal microscope at 37°C. Images are representative of cells recorded in two independent experiments.

There was a barely discernable localisation of the probe to pseudopods in the presence of 10nM CXCL11 (Figure 6.4).

6.2.2 Mutant TAPP PH is diffusely distributed in primary human T cells

In the next set of experiments a mutant TAPP PH probe was used, which due to a R212L mutation, is unable to bind $PI(3,4)P_2$ (244). This was clearly excluded from the nucleus, unlike the wildtype probe, but did not localise to the membrane upon stimulation with H_2O_2, CD3/CD28 beads or CXCL11 (10nM). Treatment with LY294002 (20μM) for 1 hour did not alter distribution, with the probe remaining excluded from the nucleus (Figure 6.5).

6.2.3 Akt PH localises to the membrane in primary T cells

Next, cells were transfected with a GFP tagged Akt-PH protein. The PH domain of Akt is reported to have affinity for both $PI(3,4,5)P_3$ and $PI(3,4)P_2$ (362) and it's localisation is therefore indicative of PI3K irrespective of SHIP-1 activity. This was diffuse in resting cells but localised to the membrane in cells adhered to fibronectin, motile cells stimulated with 10nM CXCL11, or those stimulated with CD3/CD28 beads (Figure 6.6) indicating the activity of PI3K at the cell membrane under these conditions. In contrast a mutant Akt PH (R25C) domain remained diffuse upon stimulation (Figure 6.7).

6.3 Phosphorylated SHIP-1 is diffusely distributed in motile T cells

As the experiments with TAPP PH domain probes had failed to show strong enrichment of the probe to the cell surface membrane, it was next investigated whether phosphorylated SHIP-1 could be identified at the membrane in motile cells. Control CD4+ T cells were left unstimulated or stimulated with CXCL11 (10nM, 2 minutes), fixed, stained for pY^{1020}SHIP-1 and DAPI and visualised by confocal microscopy. Similar to the results seen with CEMs in the first results section, in unstimulated cells there was very little phosphorylated SHIP-1 present. Upon chemokine stimulation the cells polarised and there was an increase in the amount of phosphorylated SHIP-1. However, it showed a similar distribution to the TAPP PH domain probes, i.e. it did not strongly localise to the cell surface membrane, although some weak localisation to emerging pseudopods could be seen (Figure 6.8).

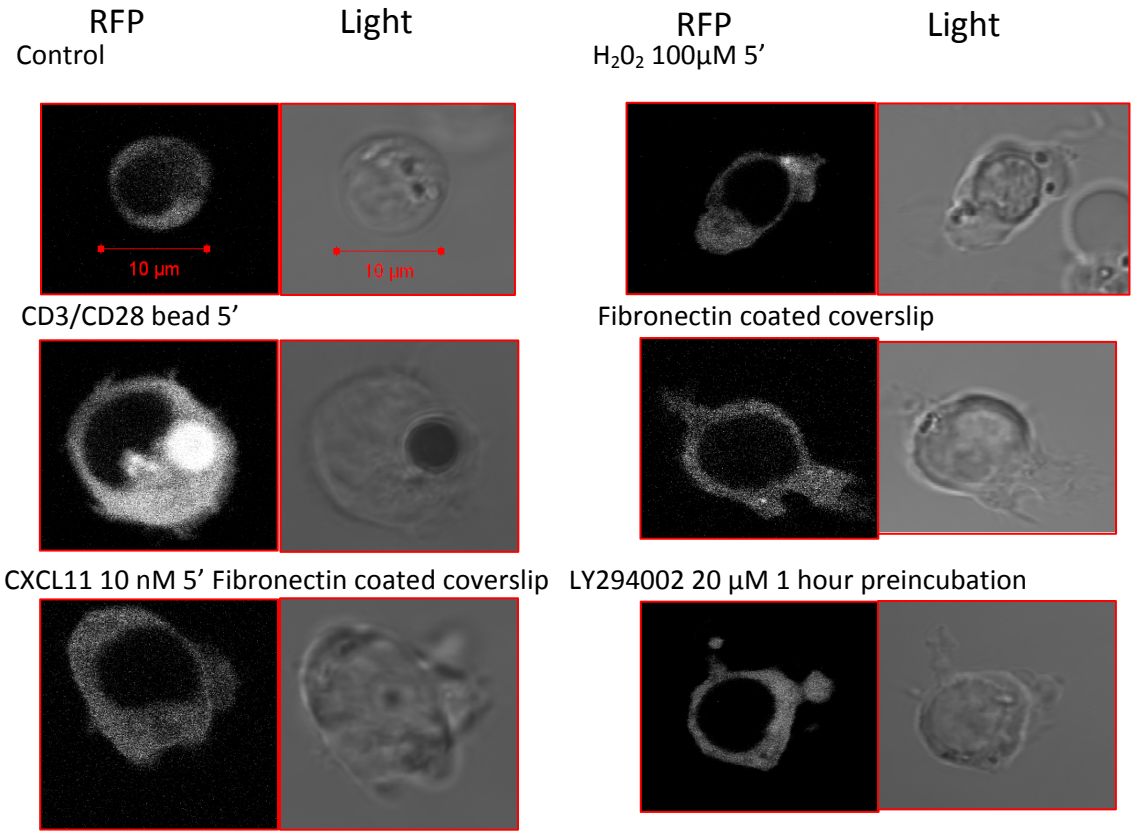

Figure 6.5 Mutant TAPP PH-RFP localisation in T cells
CD4+ T cells were electroporated with TAPP-PH^{R212L}-RFP as described in Materials and Methods and on day 2 post isolation were resuspended in chemotaxis media and placed in a chambered coverslip and allowed to settle for 15 minutes before stimulation was applied as indicated. Cells were recorded using video microscopy on an LSM510 Meta confocal microscope at 37°C Images are representative of cells recorded in two independent experiments.

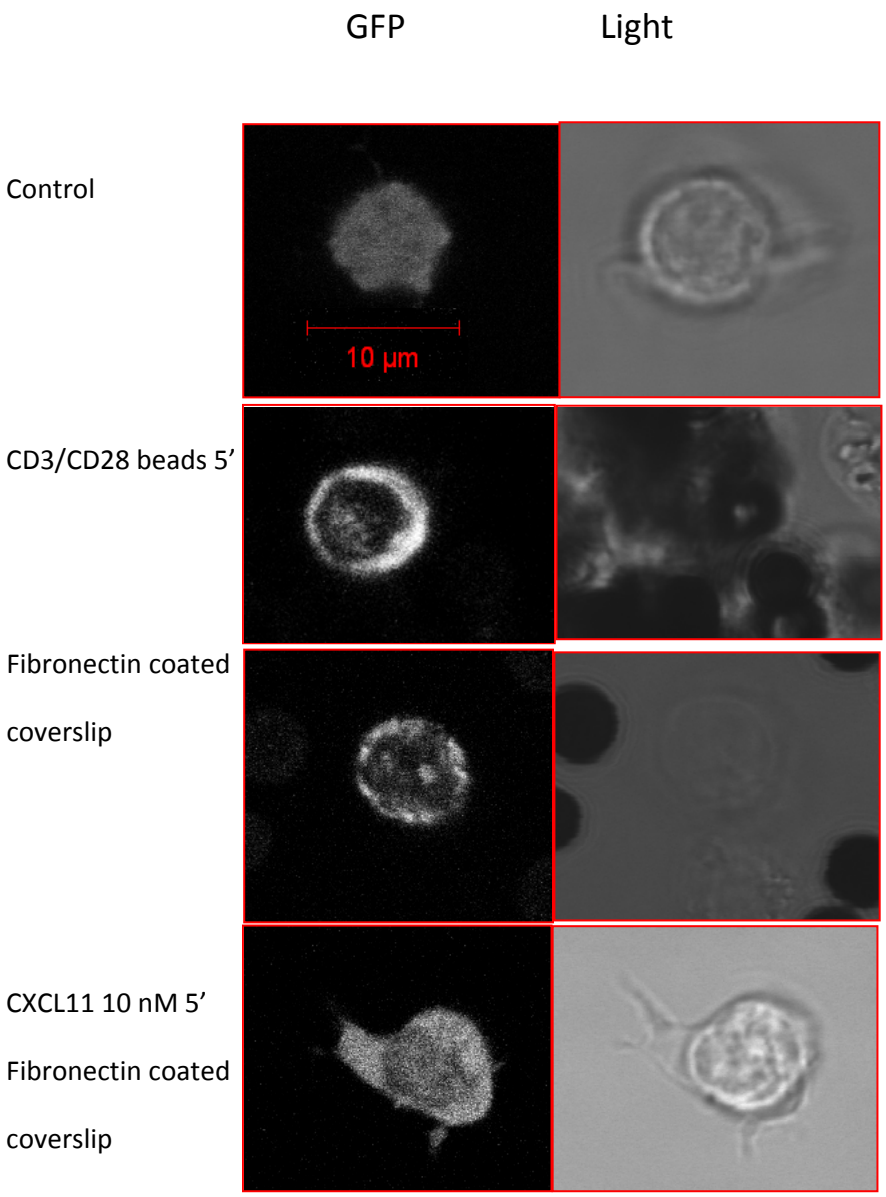

Figure 6.6 GFP Akt PH domain localises to membrane upon stimulation of CD4+ T cells.
CD4+ T cells were electroporated with Akt-PH-GFP as described in Materials and Methods and on day 2 post isolation were resuspended in chemotaxis media and placed in a chambered coverslip and allowed to settle for 15 minutes before stimulation was applied as indicated A. At rest in chambered coverslip B. CD3/CD28 bead 5 minutes C. On fibronectin coated coverslip D. 10nM CXCL11 on fibronectin coated coverslip 5 minutes. Cells were recorded using video microscopy on an LSM510 Meta confocal microscope at 37°C. Images are representative of cells recorded in two independent experiments.

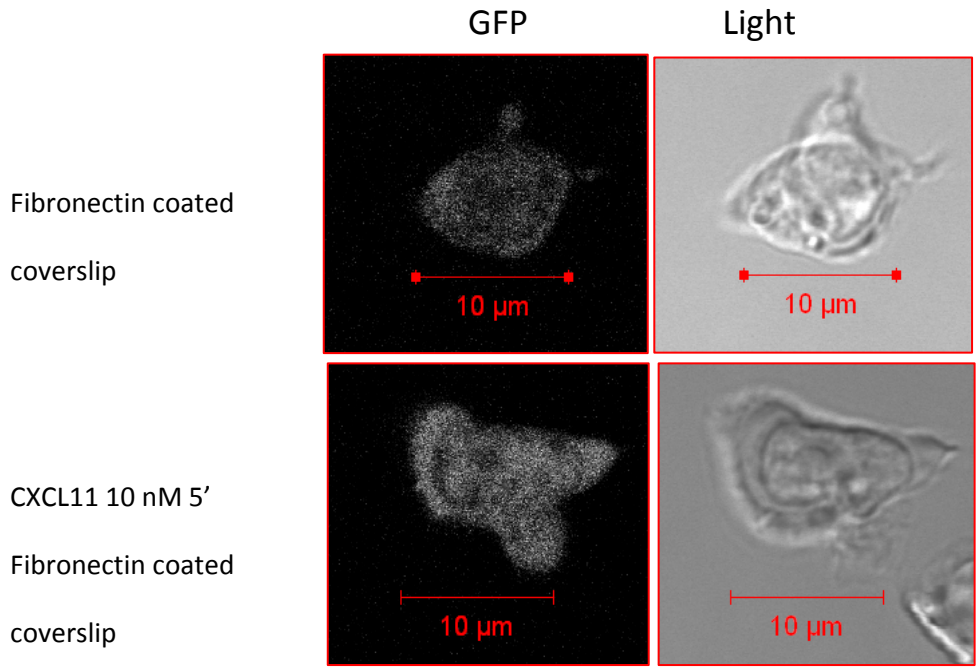

Figure 6.7: Mutant GFP Akt-PH domain remains diffuse
CD4+ T cells were electroporated with Akt-PH^{R25C}-GFP as described in Materials and Methods and on day 2 post isolation were resuspended in chemotaxis media and placed in a chambered coverslip and allowed to settle for 15 minutes before stimulation was applied as indicated. Cells were recorded using video microscopy on an LSM510 Meta confocal microscope at 37°C. Images are representative of cells recorded in two independent experiments.

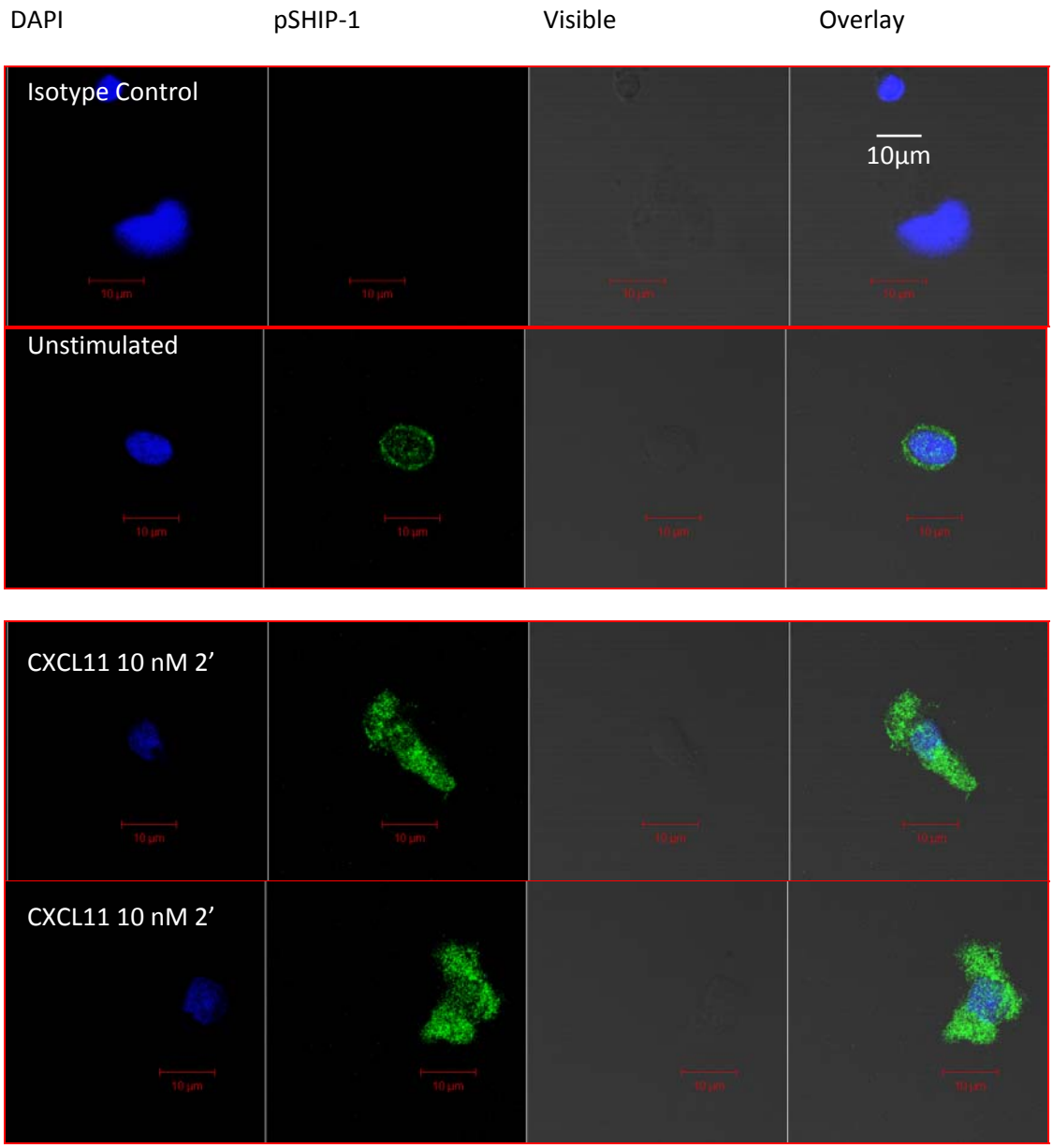

Figure 6.8 Phosphorylated SHIP-1 is present in motile cells but is broadly distributed

CD4+ T cells were isolated and cultured as described in the Materials and Methods. On day 10 post isolation $1x10^6$ cells/ point were left unstimulated or stimulated with CXCL11 for 2 minutes. Cells were then fixed and stained for pY^{1020} SHIP-1 and DAPI and mounted on coverslips and imaged by confocal microscopy as described in the Methods. Results are from a single experiment.

6.4 Summary

- The TAPP PH domain was weakly recruited to the leading edge and emerging pseudopods on motile CD4+ T cells
- A mutant TAPP PH domain failed to localise to specific areas of the cells, but was excluded from the nucleus
- The Akt PH domain was weakly recruited to the leading edge of motile CD4+ T cells and was also recruited to the membrane upon stimulation
- A mutant Akt PH domain failed to localise to specific areas of the cells
- Phosphorylated SHIP-1 is diffusely distributed in the motile cell

Chapter 7: Results section V

The effect of silencing SHIP-1 on T cell functions

7.1 Background and Objectives

Knockout of SHIP-1 in mice leads to changes in T cell development and function. In the whole animal knockout there is an increase in Tregs (185) and the cells are biased towards a Th2 phenotype that drives lung inflammation (184). *In vitro*, T cells from these animals are prone towards skewing towards Tregs at the expense of Th17 development (186). In contrast, when SHIP-1 is deleted only from T cells, a change in the levels of Tregs or Th17 was not observed. However, cells were more susceptible to skewing of Th1 at the expense of Th2 (183). In addition, the CD8+ T cells from these animals had an increased cytotoxic capacity (183).

Given the contradictions between these two models, it is not clear what the role of SHIP-1 might be in mature human T cells. Therefore, the aims of this results section were to investigate the ability of T cells to skew to Th1, Th2, Th17 and Treg phenotypes and also to investigate the cytotoxic actions of CD8+ T cells when SHIP-1 expression is silenced.

7.2 Ability to skew to Th1, Th2, Th17 and Treg phenotypes is altered by SHIP-1 silencing

7.2.1 Skewing requires isolation of naïve CD4+ T cells

Previous experiments had been performed using pan CD4+ T cell isolation. Upon flow cytometry of these freshly isolated cells, a subpopulation was found to express CD25, a marker for Tregs and activated cells (37) (Figure 7.1 A,B). In addition, it would be expected that some Th1, Th2 and Th17 would also be found in the pan CD4+ T cell population. Therefore, in order to start out with unbiased population, a naïve CD4+ T cell isolation kit was used to isolate cells for the following experiments. Naïve CD4+ T cells were found to be infected with lentivirus encoding for GFP at equal or greater percentage than pan CD4+ T cells, when infected cells were analysed for GFP expression by flow cytometry (Figure 7.1)

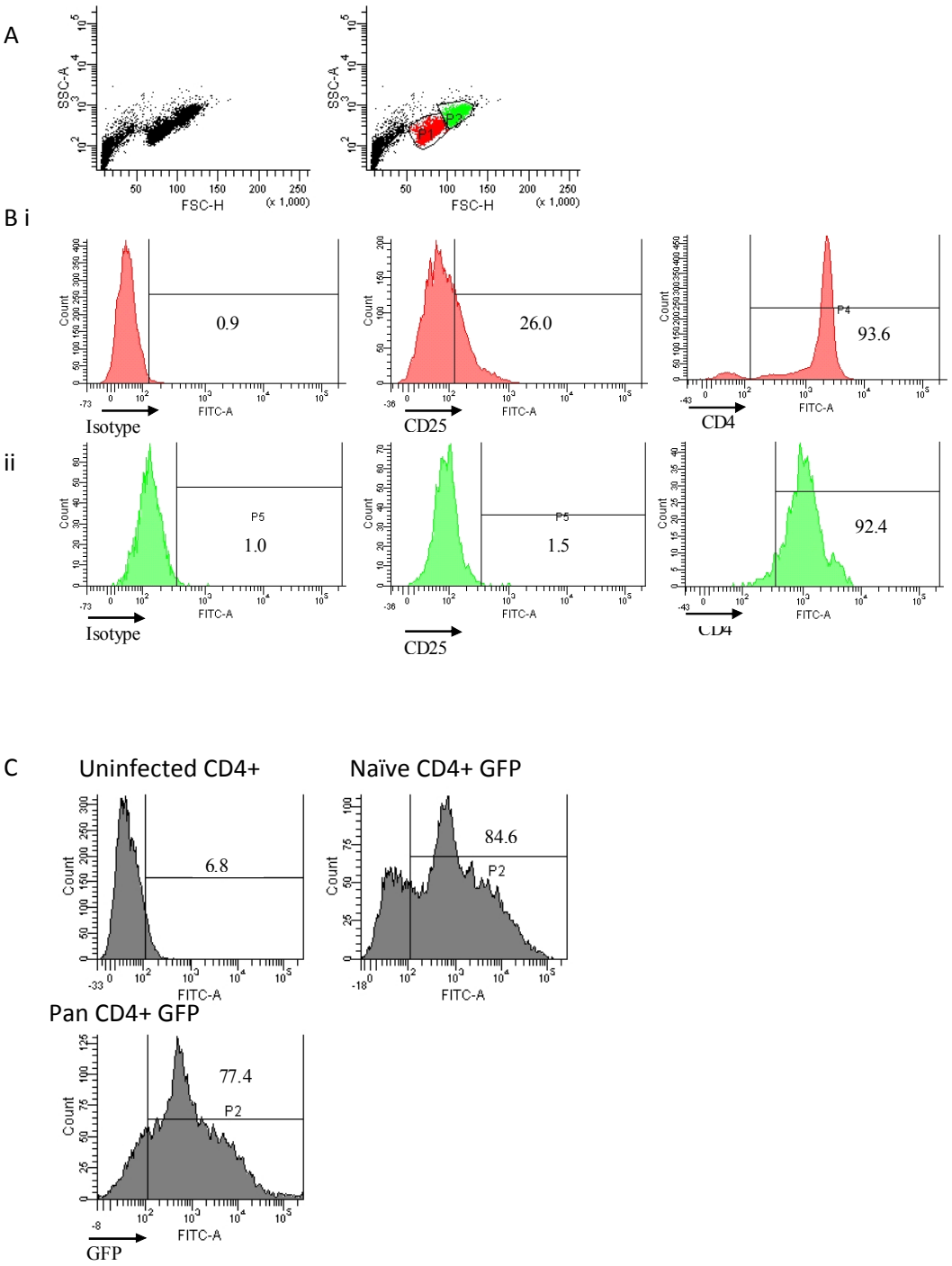

Figure 7.1 Expression of CD25 by freshly isolated pan CD4+ and infection of naïve CD4+ with GFP. Pan human CD4+ T cells were isolated by magnetic separation as described in Materials and Methods. A. Two distinct populations were gated by flow cytometry based on FSC (cell size) and SSC (granularity). B. The populations identified in part A were stained for either CD4 or CD25 expression as described in the Materials and Methods i. P1 (red) ii P3 (green). 1 x 10^5 viable cells were acquired for each point. C. Naïve or pan CD4+ T Cells were isolated by magnetic separation and infected with GFP encoding lentivirus after 24 hours of activation. Three days post infection GFP expression was assessed by flow cytometry of 1 x 10^5 viable cells.

7.2.3 Th1 skewing is unaffected by silencing of SHIP-1

Using a combination of cytokines and neutralising antibodies as described in the Materials and Methods, shRNA control cells were successfully polarised under Th1 conditions to release the signature Th1 cytokine IFNγ, but SHIP-1 silenced cells failed to release increased IFNγ. However, this result was not statistically significant, due to the variation in amount of IFNγ released by shRNA control cells between different donors (Figure 7.2). Moreover, intracellular staining for IFNγ showed that an equivalent percentage cells still stained positive for IFNγ under Th1 conditions when SHIP-1 expression was silenced (Figure 7.3).

Levels of other secreted Th1 cytokines were also measured. IL-12p70, which was increased in Th1 conditions by both shRNA control and SHIP-1 silenced cells, with silencing of SHIP-1 have no effect on its production. The production of IL-1β was increased under skewing Th1 conditions by both shRNA control cells and SHIP-1 silenced cells, however there was a non-significant trend under Th0, Th1 and Th2 conditions for less IL-1β to be produced by SHIP-1 silenced cells. IL-8 (CXCL8) and TNFα may both be considered as Th1 cytokines (363) and followed the same trends as IFNγ with shRNA control cells successfully polarised under Th1 conditions to produce increased levels of IL-8 and TNFα, but SHIP-1 silenced cells failed to increase production of these cytokine under Th1 conditions (although this was statistically non-significant). IL-2 has been characterised as a Th1 cytokine (8) but is also key for proliferation of all T cells and for the development and maintenance of Tregs (364). IL-2 production was higher under Th0 and Th1 conditions than it was under Th2 conditions, however levels varied considerably between donors and no firm conclusions could be drawn about the effect of SHIP-1 silencing on IL-2 production.

7.2.4 Th2 skewing is altered by silencing of SHIP-1

The levels of four secreted Th2 cytokines were analysed, including the signature cytokine IL-4. Using a combination of cytokines and neutralising antibodies as described in the Materials and Methods, shRNA control T cells were successfully polarised under Th2 conditions to release the signature Th2 cytokine IL-4. Levels of secreted IL-4 were increased approximately four fold by Th2-skewed shRNA control cells vs Th0 shRNA control cells (Figure 7.4). Silencing of SHIP-1 expression resulted in a dramatic increase in levels of secreted IL-4 production under Th2 conditions (a further five-fold

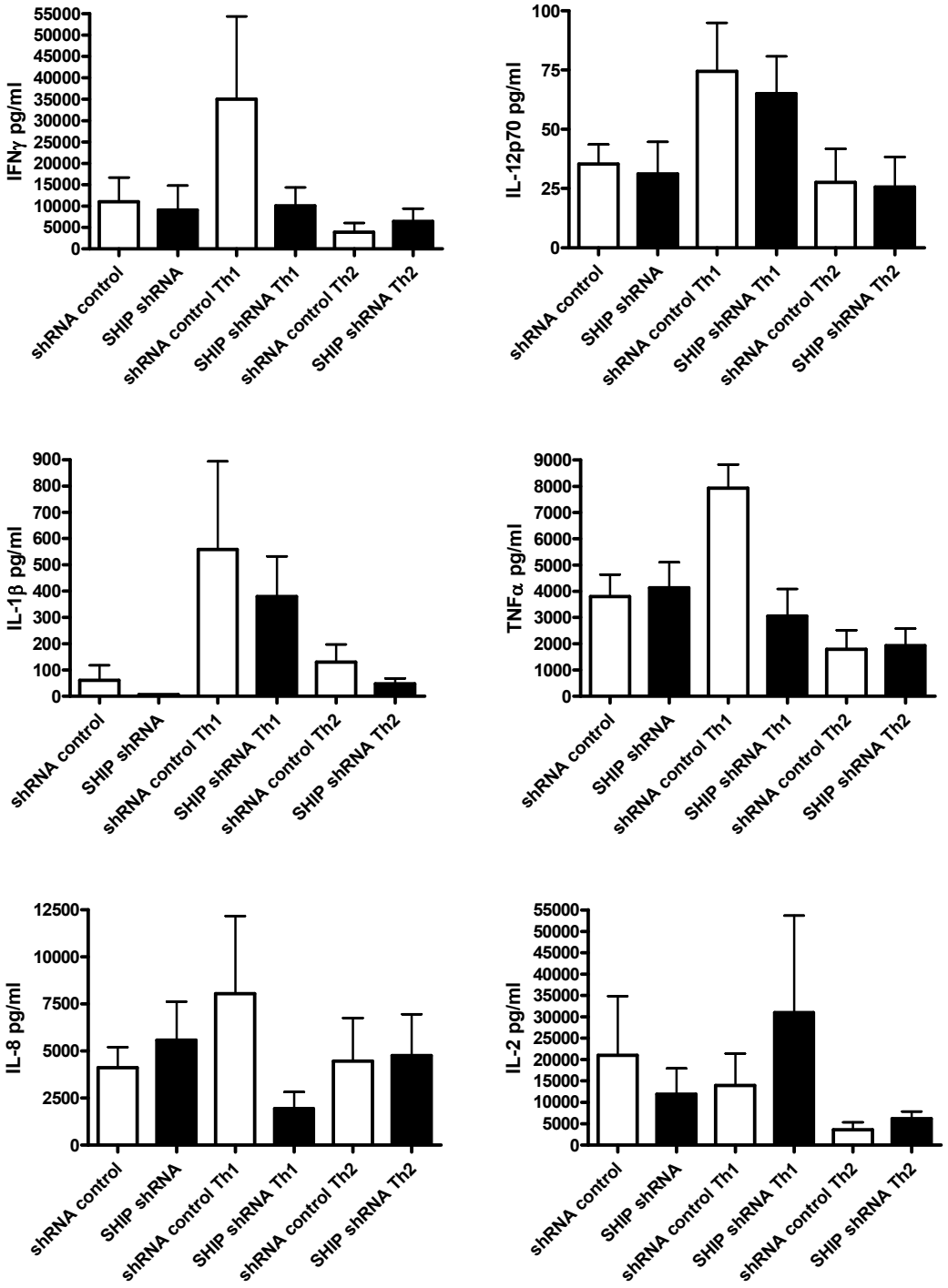

Figure 7.2 Expression of Th1 cytokines is altered by silencing of SHIP-1
Naïve CD4+ T cells were infected with shRNA encoding lentiviruses and cultured in Th0, Th1 or Th2 conditions as described in Materials and Methods for 8 days. Cells were then washed three times and resuspended in complete media with CD3/CD28 beads in a 1:1 ratio for 16 hrs at 1x 10^6/ml after which supernatant was collected and cytokines were analysed using a mesoscale 10 plex plate following the manufacturer's instructions. Data is pooled from at least 4 independent experiments. Error bars are SEM. For clarity, only shRNA and SHIP-1 shRNA results are shown.

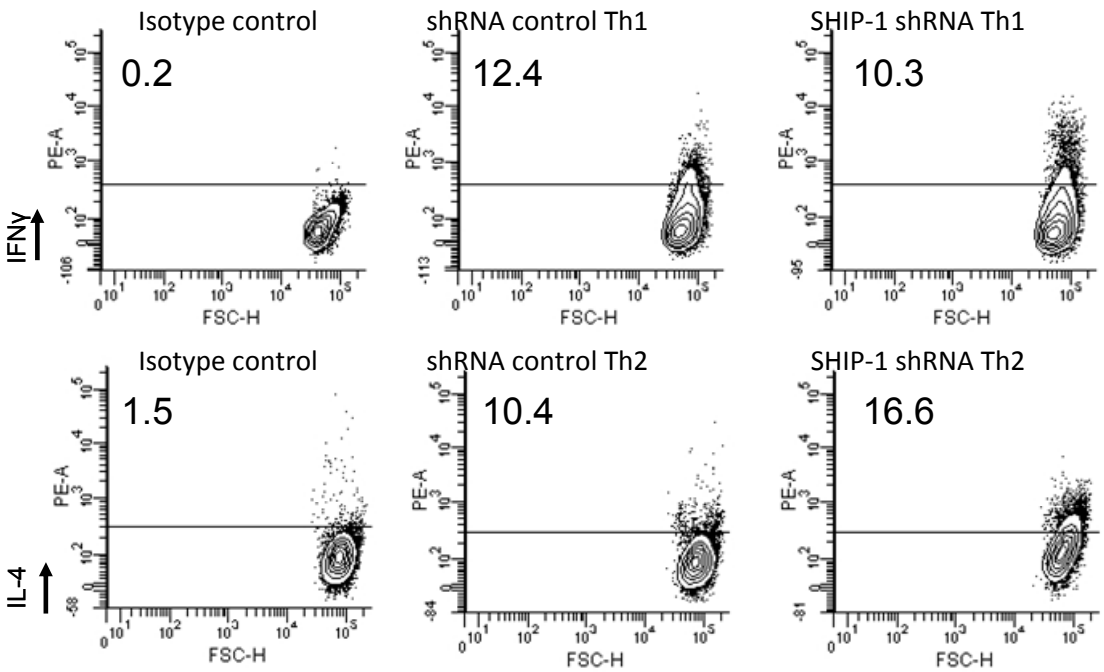

Figure 7.3 Staining of IFNγ and IL-4 in T cells shows increased skewing to Th2 upon silencing of SHIP-1

Naive CD4+ T cells were infected with shRNA encoding lentiviruses and cultured under Th1 or Th2 conditions as described in Materials and Methods for 9 days. Cells were then washed into complete media and incubated on CD3/CD28 beads for 6 hrs in the presence of Golgistop. Cells were then fixed and stained for the appropriate cytokine and expression assessed by flow cytometry of $1x10^5$ cells/ point. Plots are representative of three separate experiments.

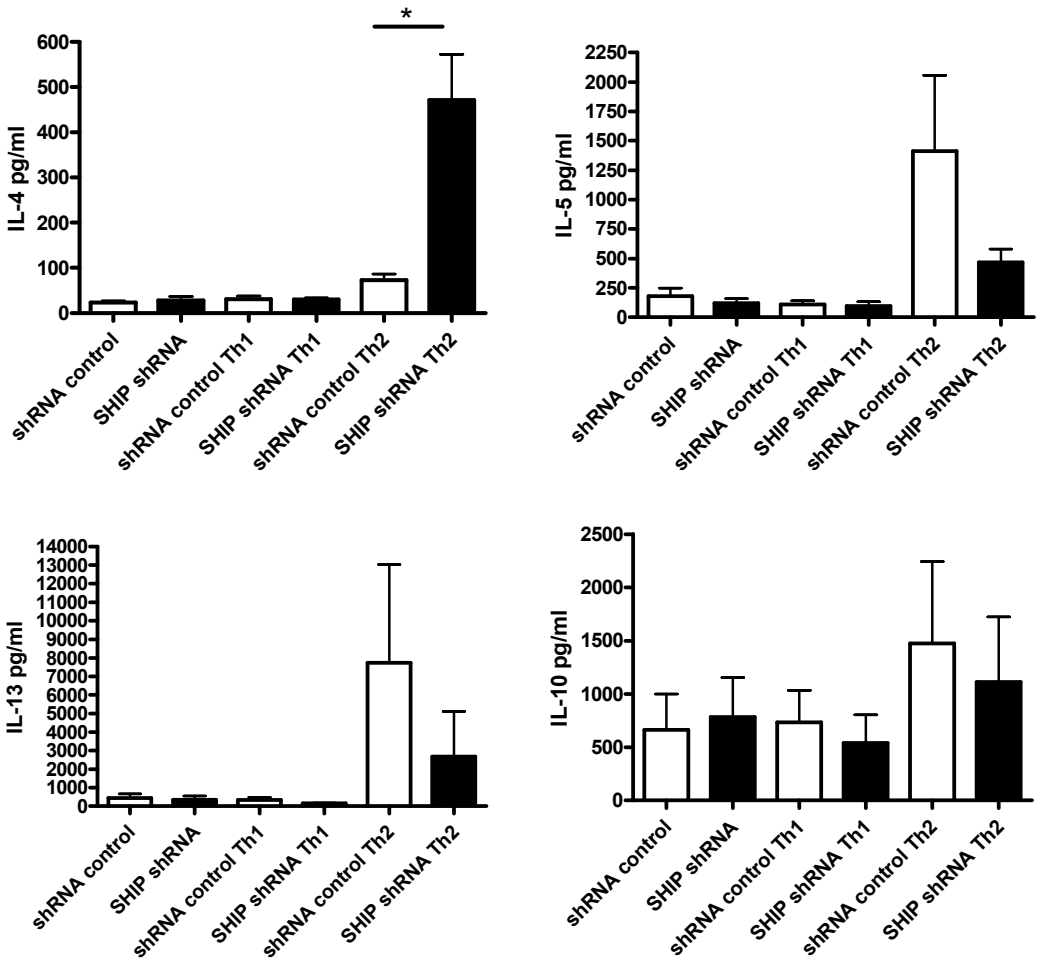

Figure 7.4 Expression of Th2 cytokines is altered by silencing of SHIP-1
Naïve CD4+ T cells were infected with shRNA encoding lentiviruses and cultured in Th0, Th1 or Th2 conditions as described in Materials and Methods for 8 days. Cells were then washed three times and resuspended in complete media with CD3/CD28 beads in a 1:1 ratio for 16 hrs at 1x 10^6/ml after which supernatant was collected and cytokines were analysed using a mesoscale 10 plex plate following the manufacturer's instructions. Data is pooled from at least 4 independent experiments. Error bars are SEM. For clarity, only shRNA and SHIP-1 shRNA results are shown.* $p<0.05$ Student's paired T Test with Holmes correction.

increase $p<0.05$. Upon use of a Holmes correction to take into account the three paired T-tests performed the probabilities of the observed difference in IL-4 production remained less than 0.05). Upon intracellular staining for IL-4 there was an increase in the percentage of SHIP-1 silenced cells staining IL-4 positive under Th2 conditions (15% vs. 9% of shRNA control cells under Th2 conditions) (Figure 7.3). In contrast, whilst there was a large increase in production of both IL-5 and IL-13 by shRNA control cells under Th2 conditions (5 and 15 fold respectively vs. production under Th0 conditions), SHIP-1 silenced cells failed increase production by the same amount (3 and 5 fold respectively vs. Th0 conditions p= n.s.). IL-10 is produced by Th2s and suppresses the production of Th1 cytokines, however it is also produced by some Tregs (365). Levels of secreted IL-10 were not affected by silencing of SHIP-1.

7.2.5 Th17 skewing is facilitated by silencing of SHIP-1

Naïve CD4+ were isolated from PBMCs and cultured under Th0 or Th17 conditions or Th17 conditions with the addition of IL-23 as described in the Materials and Methods. Levels of secreted IL-17 were assessed by dot blot. Some IL-17 was present in the supernatant from Th0 cells, possibly indicating the presence of Th17 cells which had been generated by the donor, or that had spontaneously skewed. Culture of cells under Th17 skewing conditions caused an increase in production of IL-17A but culturing with IL-23 did not cause a further increase in production (Figure 7.5). However, for the following experiments IL-23 was include in the skewing media as there was some evidence in the literature that it might aid the maintenance of a Th17 phenotype (32). In the next experiment, control, shRNA control or SHIP-1 silenced cells were cultured under Th0 or Th17 conditions and levels of secreted IL-17 were assessed by dot blot. Exposure to control shRNA further increased IL-17A production under Th17 skewing conditions, possibly due to additional cytokines derived from the HEK supernatant. A further increase in production was caused by silencing of SHIP-1 expression (Figure 7.6). When these results were quantified by ELISA, the same results were seen, although they did not achieve statistical significance. Concomitant with this an increase in IL-17A positive cells was detected when SHIP-1 expression was silenced under Th17 conditions (shRNA control cells 22% positive, SHIP-1 silenced cell 34% positive for IL-17A).

7.2.6 STAT3 phosphorylation is not affected by silencing of SHIP-1

STAT3 is a key transcription factor, required for the generation of Th17s and the production of IL-17, and requires phosphorylation in order to be active (366). IL-6 signalling can lead to phosphorylation of STAT3, in naïve T cells and sometimes in

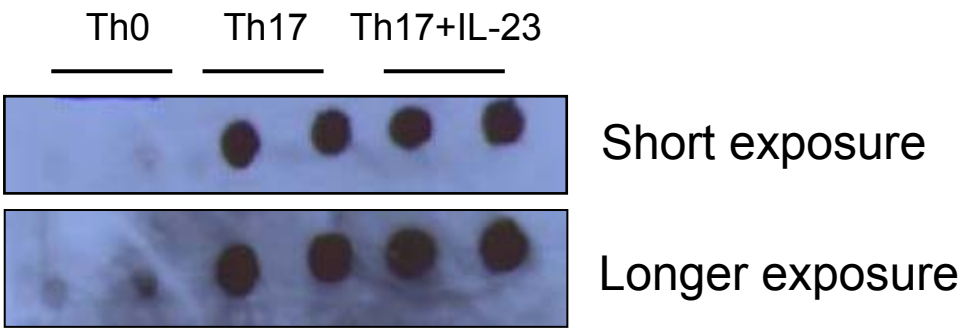

Figure 7.5 IL-17 expressing cells can be generated from naïve human CD4+ T cells

Primary human T cells were skewed *in vitro* to produce IL-17. Naïve CD4+ T cells were isolated from PBMCs as described in the Methods and cultured with CD3/C28 beads under Th0 conditions (IL-2), Th17 conditions (IL-1β, IL-6, anti IFNγ, anti-IL-4) or in Th17 conditions plus IL-23, for five days. Then the culture volume was doubled and cells were cultured for a further nine days in the presence of IL-2. After this time cells were counted and each culture was determined to have equal numbers of cells at 1x 10^6/ml. 5 µL of supernatant was spotted onto nitrocellulose membrane and blotted for IL-17.

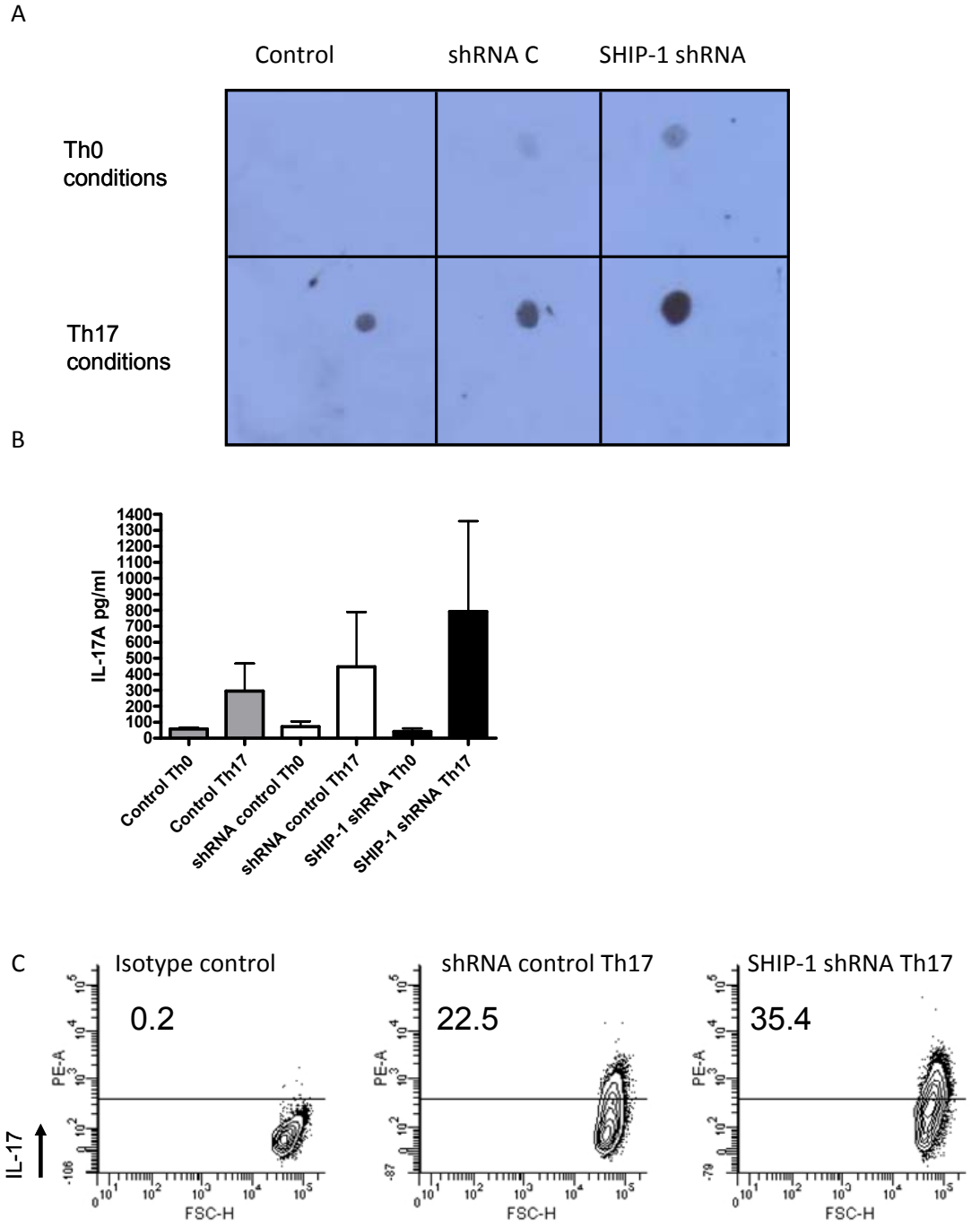

Figure 7.6 Th17 skewing is increased by silencing of SHIP-1
Naive CD4+ lymphocytes were infected with lentivirus to deliver shRNA and cultured under appropriate skewing conditions as described in Materials and Methods for 8 days. Cells were then washed three times and resuspended in complete RPMI with CD3/CD28 beads (1:1 ratio bead:cell) for 16 hrs at 1x 10^6/ml. Following this supernatant was collected and levels of IL-17A were assessed by dot blot or ELISA, following the manufacturer's protocol. A. Dot blot is representative of three independent experiments B. ELISA data is pooled from three independent experiments, error bars are SEM. C. For intracellular staining, cells were restimulated as above, but for 6 hours only, in the presence of Golgistop. Cells were then fixed and stained with anti-IL-17A and analysed using flow cytometry of 1x 10^5 cells/ point, plots are representative of three independent experiments.

activated T cells (366). Control, shRNA control or SHIP-1 silenced CD4+ T cells were cultured under Th0 or Th17 conditions and then STAT3 phosphorylation was assessed in fixed cells by flow cytometry. STAT3 phosphorylation was low in all Th0 cells (Figure 7.7). However, an increase was observed in cells exposed to control shRNA compared to uninfected cells. No further increase was detected when SHIP-1 expression was silenced. Furthermore, application of IL-6 did not affect levels of STAT3 phosphorylation in either control shRNA control or SHIP-1 silenced cells as assessed by flow cytometry.

7.2.7 Silencing of SHIP-1 leads to an increase in the percentage of Tregs

Naïve CD4+ T cells were isolate from PBMCs, infected with shRNA control or SHIP-1 shRNA encoding lentiviruses and cultured under Th0 conditions as described in the Materials and Methods. After nine days cells were assessed for surface expression of CD25, a marker of Tregs and activated T cells (37), by flow cytometry. Expression of CD25 was detected upon approximately 60% of control cells, compared to ~75% of shRNA control cells (Figure 7.8). Approximately 80% SHIP-1 shRNA treated cells were positive for CD25 but this increase was not statistically significant compared to shRNA controls. However, SHIP-1 shRNA cells had expressed higher levels of CD25 per cell ($p<0.05$), as indicated by the increase in mean fluorescence and demonstrated in the histograms.

Further to this, triple staining for CD4, CD25 and foxp3 (the key transcription factor for Treg development (367)) was used to identify Treg populations. In line with previous results (185, 186), it was seen that there was an increase in $CD25^{high}$ $foxp3^{+}$ cells upon infection with SHIP-1 shRNA from approximately 5% of control and shRNA control cells to 15% of SHIP-1 silenced cells ($p<0.05$). Infection with control shRNA did not affect the percentage of cells that were foxp3 positive compared to uninfected controls.

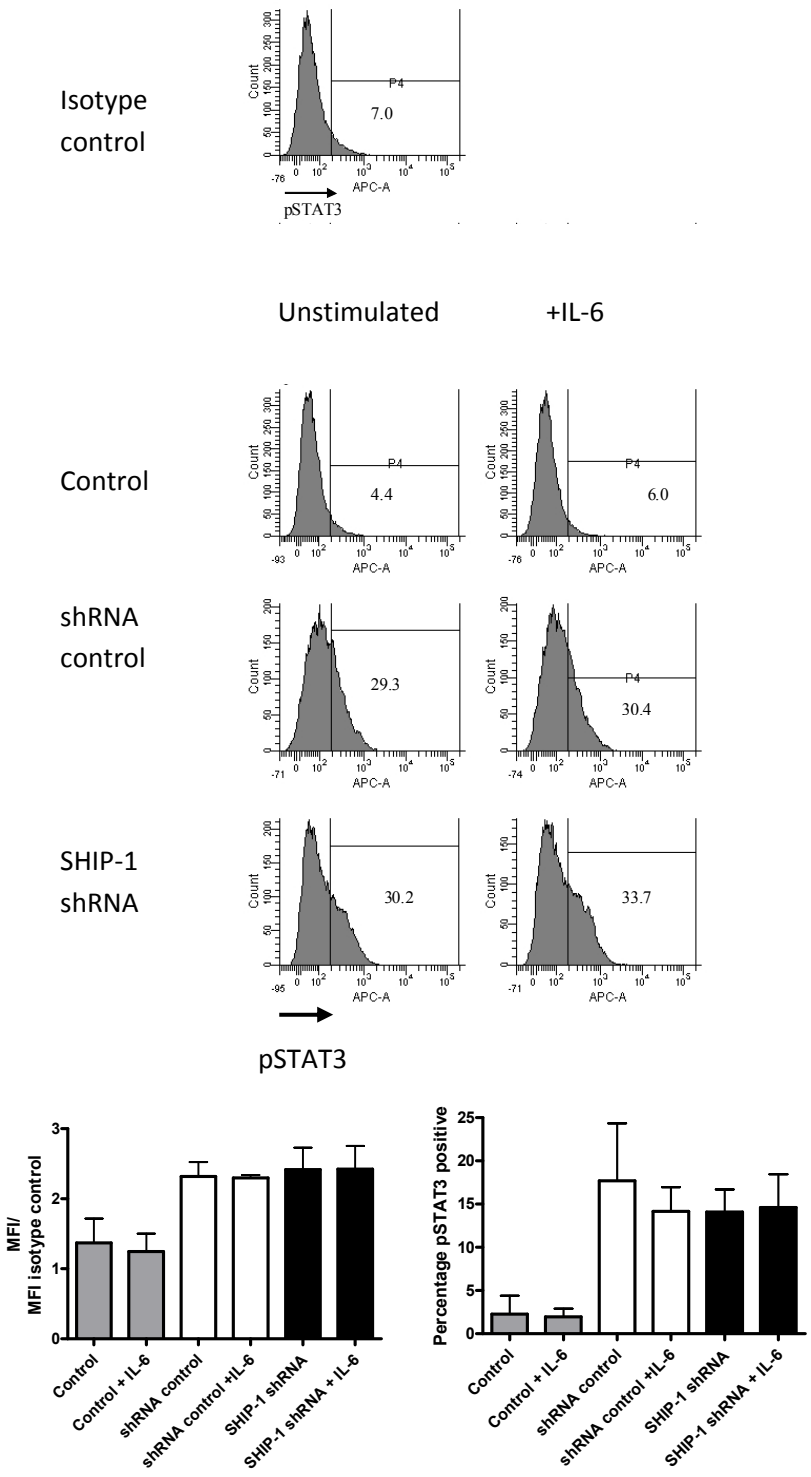

Figure 7.7 STAT3 phosphorylation is not increased by silencing of SHIP-1. Naive CD4+ lymphocytes were infected with lentivirus to deliver shRNA as indicated and cultured as described in Materials and Methods for 8 days under Th0 conditions. Cells were then removed from CD3/CD28 beads, rested for 1 hr and stimulated with IL-6 (100ng/ml 1 min) as indicated, then fixed and stained for STAT3 phosphorylation, which was assessed by flow cytometry of $1x10^5$ cells/ point. Representative histograms are shown, along with pooled data from three independent experiments, error bars are SEM

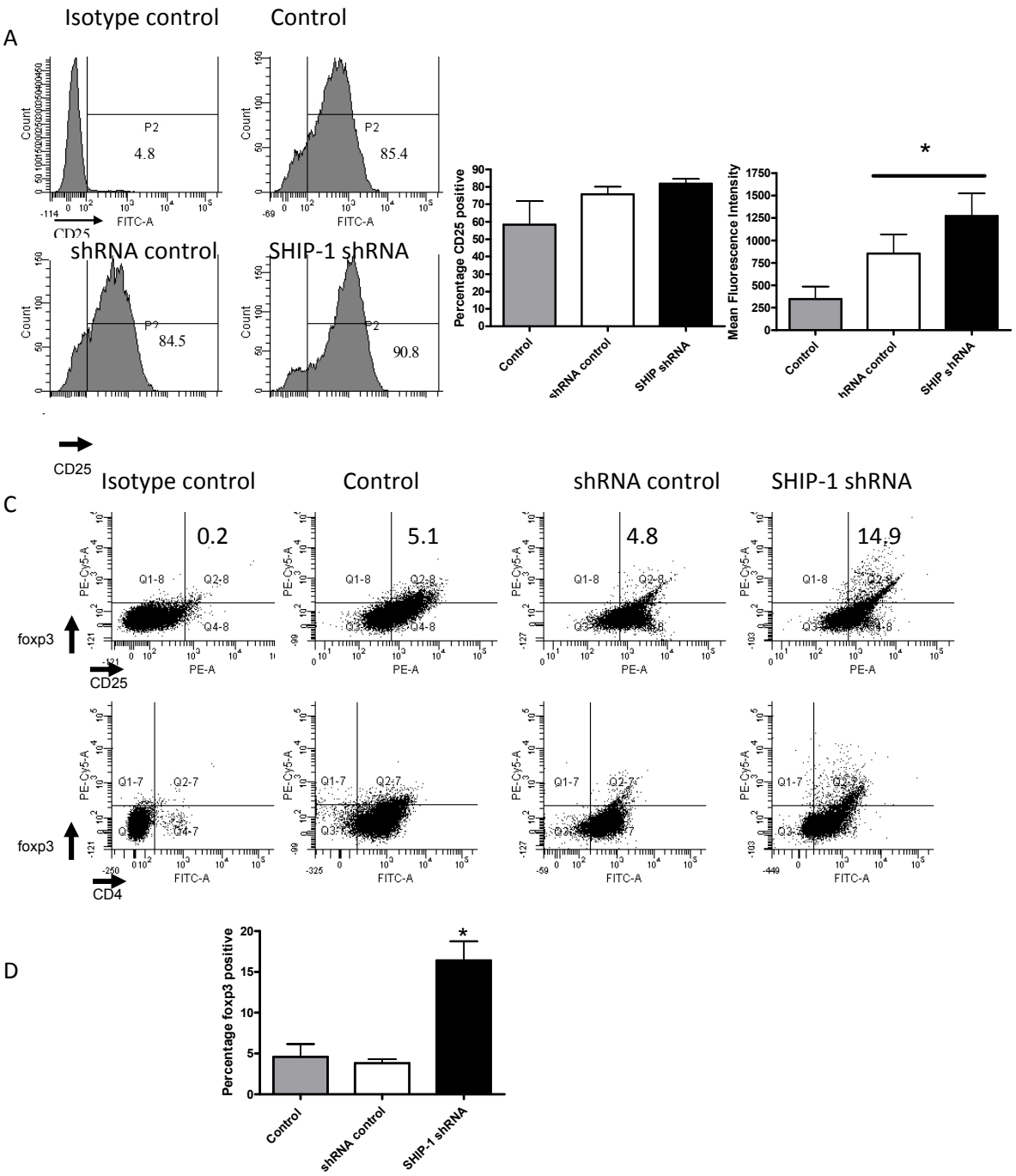

Figure 7.8 CD25 and foxp3 expression are increased when SHIP-1 expression is silenced Naive CD4+ T lymphocytes were infected with lentivirus to deliver shRNA as indicated and cultured under appropriate Th0 conditions as described in Materials and Methods for 9-10 days. A. Cells were then washed and stained for extracellular expression of CD25 and assessed by flow cytometry of $1x10^5$ cells/ sample Histograms are representative of three independent experiments B. Bar graphs are pooled data from three independent experiments, completed as in part A, error bars are SEM. * $p<0.05$, Student's paired T Test. C. Cells were cultured for 9-10 days as described in Materials and Methods and infected with lentivirus as indicated. Cells were then washed and stained for extra cellular expression of CD25 and CD4 then permeabilised and stained for foxp3 and assessed by flow cytometry of $1x10^5$ cells/ sample Histograms are representative of three independent experiments D. Bar graphs are pooled data from three independent experiments performed as in part C, error bars are SEM. * $p<0.05$, Student's paired T Test.

7.3 CD8+ T cell cytotoxicity is not potentiated by silencing of SHIP-1

7.3.1 Establishment of a model system to evaluate human CD8+ T cell cytotoxicity

It had been reported in the literature that loss of SHIP-1 caused murine CD8+ T cells to have an increase in their cytotoxicity (181). Using murine T cells it is standard practice to investigate cytotoxicity using transgenic T cells that are specific for OVA and to target their killing towards OVA expressing cells. Clearly this was not possible using human T cells. Therefore a modified protocol was devised based upon protocols from Grant *et al.* and Sloan *et al.* (368, 369). In this experiment A20 murine B cell lymphoma cells were labelled with CFSE to enable them to be distinguished from T cells using flow cytometry. UCHT1 (an antibody which is raised in mice) was used to stimulate the TCR on the CD8+ T cells and the invariant chain of the antibody was bound by Fc receptor on the A20 cells in order to direct the killing of the CD8+ towards the target cells (as illustrated in the Materials and Methods). Cells were incubated for three hours and then stained with cy-5 conjugated annexin V and assessed by flow cytometry. It can be seen that target cells on their own have a proportion that are apoptotic. Upon coculture for three hours with either UCHT1 or CD8+ T cells, the percentage of viable cells is not affected. However upon addition of both UCHT1 and CD8+ T cells to the target cells, the percentage staining positive for annexin is increased (from 31% to 83% at effector to target 5:1 ratio) (Figure 7.9 A). A lower ratio of effector:target 1:2 was used for subsequent experiments in order that an increase in efficiency of killing could be detected. Cytotoxicity was not affected by pretreatment (followed by washing before addition to the assay) of effector cells with wortmannin in line with other reports that PI3K is not required for cytotoxicity of CD8+ T cells (370) (wortmannin was used as it is irreversible and would therefore be expected to still inhibit PI3K activity during the cytotoxicity assay, although it had been washed from the media) (Figure 7.9 B). In addition preincubation with the PI3K inhibitors LY294002 and ZSTK474 did not affect cytotoxicity.

7.3.2 Silencing of SHIP-1 does not increase CD8+ T cell cytotoxicity

The assay was then repeated using shRNA control CD8+ T cells and SHIP-1 silenced CD8+ T cells at a 1:2 effector to target ratio. It was found that upon addition of UCHT1, SHIP-1 shRNA CD8+ T cells did not kill a higher percentage of A20 cells than the shRNA control cells, and in fact the percentage of target cells killed by the CD8+ T cells dropped from 24 to 9% upon silencing of SHIP-1. It was also noted that this assay resulted in a higher percentage of the SHIP-1 shRNA CD8+ staining positive for annexin (Figure 7.9 C). 24% of the SHIP-1 silenced cells became annexin positive in the presence of A20 plus UCHT1, compared to 10% of shRNA controls.

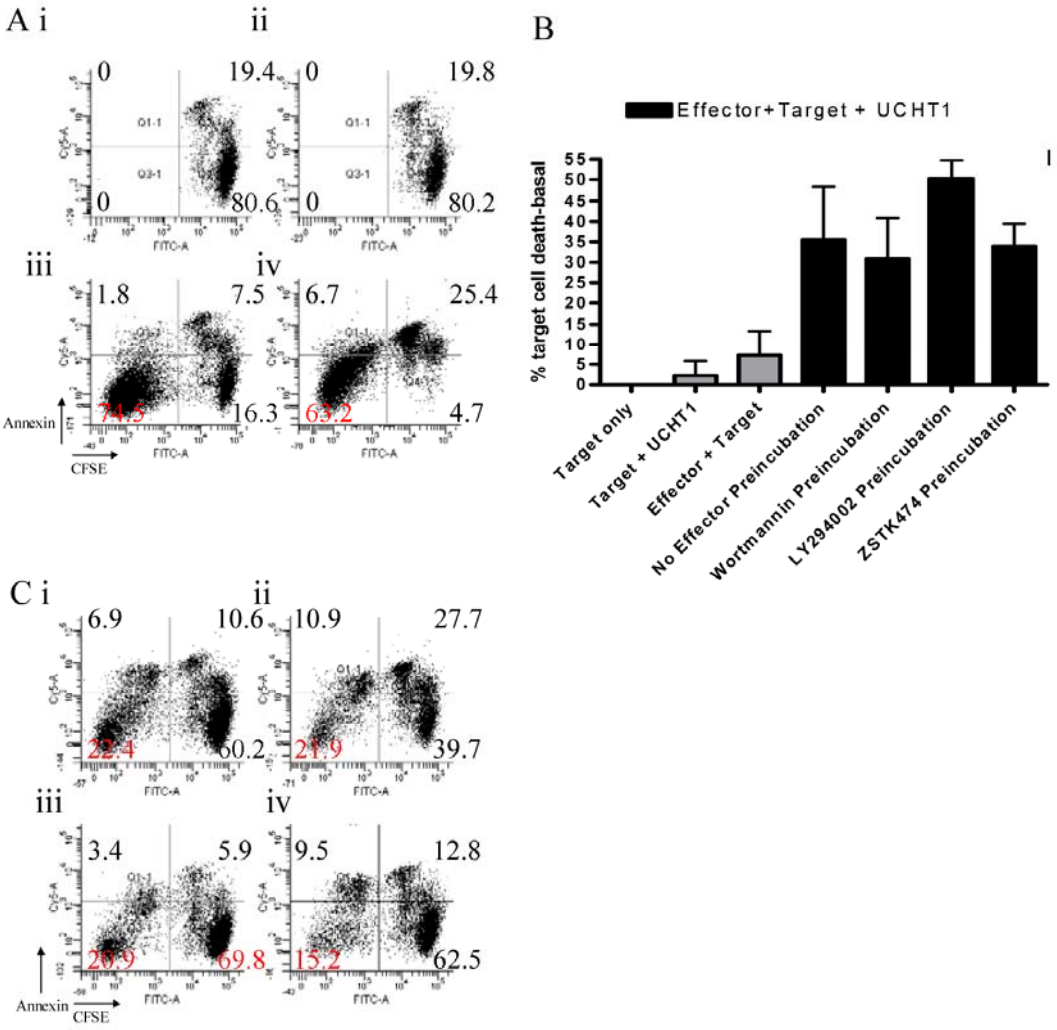

Figure 7.9 Cytotoxicity of CD8+ T cells is not increased by SHIP-1 silencing
CD8+ lymphocytes were infected with lentivirus to deliver shRNA as indicated and cultured as described in Materials and Methods for 9-10 days. Cells were then set up in a cytotoxicity assay as described in the Materials and Methods. A20 cells were labelled with CFSE to distinguish them by flow cytometry. A20 and CD8+ T cells were cultured together as indicated with or without UCHT1. Cells were then washed into annexin staining buffer, labelled with cy-5 conjugated annexin and $1x10^5$ total cells acquired per point by flow cytometry A.UCHT1 directs CD8+ T cells to kill target A20 cells i. CFSE labelled target cells ii CFSE labelled target cells plus UCHT1 iii Effector CD8+ plus CFSE labelled target cells (5:1 ratio). iv. Effector CD8+ plus CFSE labelled target cells plus UCHT1 (4:1 ratio). B. PI3K inhibitors do not affect CD8+ cytotoxicity. Cells were prepared as above, except CD8+ T cells were preincubated with PI3K inhibitors (wortmannin 100nM, LY294002 20μM, ZSTK474 1μM) for 1 hour before being cocultured with A20 cells at E:T ratio of 1:2. n=3 +/- SEM. C. Cytotoxicity of CD8+ T cells is not increase by SHIP-1 silencing i. shRNA control effector cells plus CFSE labelled target cells (1:2 ratio) ii. shRNA control effector cells plus CFSE labelled target cells plus UCHT1 (1:2 ratio) iii. SHIP-1 shRNA effector cells plus CFSE labelled target cells(1:2 ratio) iv. SHIP-1 shRNA effector cells plus CFSE labelled target cells plus UCHT1(1:2 ratio). Results are from a single experiment.

7.4 Summary

- Th1 skewing and Th1 cytokine production were unaffected by silencing of SHIP-1
- IL-4 production under Th2 conditions was increased but that of IL-5 and IL-13 was decreased upon silencing of SHIP-1
- The percentage of cells staining positive for IL-4 increased upon silencing of SHIP-1
- The proportion of naïve cells differentiating into Tregs under Th0 conditions increased upon silencing of SHIP-1
- Th17 skewing and IL-17 A production was increased upon silencing of SHIP-1
- CD8+ cytotoxicity was reduced when SHIP-1 expression was silenced, and the cells had an increased tendency to die during cytotoxic targeting of A20 cells

Chapter 8: Results section VI

The role of PI3Kγ in murine IL-17 production

8.1 Background and Objectives

IL-17A and IL-17F are produced by CD4 + T cells (Th17 cells), γδ T cells (371), CD8+ T cells (57, 372), natural killer T cells, macrophages and neutrophils (31, 371). IL-17 is produced in response to IL-23 by γδ, CD4+ and CD8+ T cells (373, 374) and can also be produced in an innate immune response, for example in response to complement C5a signalling (375), or toll-like receptor engagement (374).

IL-17A drives a tissue based immune response to combat extracellular pathogens such as bacteria and fungi via the production of IL-6, IL-8, GM-CSF, MMPs and chemokines including CXCL1 and CXCL10 (31) to orchestrate the recruitment of macrophages and neutrophils to tissues (33). IL-17F has about 50% homology to IL-17A with similar functions (31, 36, 39). IL-17A and IL-17F have been implicated in airway inflammation (36, 40, 41) as well as diseases including multiple sclerosis, psoriasis, inflammatory bowel disease (IBD), rheumatoid arthritis and systemic lupus erythromatosis (SLE) (36, 42). It has been suggested that IL-17A and IL-17F may have different functions *in vivo,* for example IL-17A may play a larger role in arthritis and EAE models, whilst IL-17F may be more important in IBD (376, 377). IL-17 receptors have been shown to play critical roles in autoimmune diseases, for example, IL-17RA$^{-/-}$ deletion in mice prevented progression to chronic destructive synovitis in a model of arthritis (378). Furthermore, IL-17A and IL-17F are thought to have both pro- and anti- tumour functions, with IL-17F in particular exacerbating tumour growth by facilitating angiogenesis (43).

For these reasons there is great interest in targeting the IL-17 pathway in disease (376). A range of therapeutic strategies are being developed to target the Th17 signalling axis (376). An anti IL-17-mAb, AIN457, is the most clinically advanced of several IL-17 neutralising antibodies (376) and is currently in clinical trials for use in Crohn's disease and psoriasis.

PI3Kγ is predominantly expressed in haematopoetic cells as described in the Introduction. PI3Kγ aides chemotaxis of leukocytes including neutrophils and eosinophils, and a lack of PI3Kγ prevents hyperresponsiveness, inflammation and

remodelling of the airways in an OVA based model of asthma (175). There are some defects in thymocyte development in PI3Kγ null mice (168, 174-176). Both *in vitro* and *in vivo* activation of T cells are normal, although PI3Kγ$^{-/-}$ effector CD4+ T cells fail to migrate to sites of peripheral inflammation, and *in vitro* they fail to migrate to CCL22 (177). Furthermore, loss of PI3Kγ reduces the severity of autoimmune diseases such as CIA and SLE (127).

The class 1B catalytic isoform p110γ pairs with either of the regulatory subunits p84/p87 or p101 and is activated by G-protein βγ subunits and signals downstream of GPCRs (131, 132). However, PI3Kγ can also be directly activated by Ras (379), and is bound by Ras on both its Ras binding domains and by an association of Ras with the catalytic domain of PI3Kγ (380). All isoforms of GTP- Ras can activate PI3Kγ (381).

It has been previously reported that loss of PI3Kδ kinase activity, or dual loss of PI3Kγ and PI3Kδ kinase activity can affect production of Th1 and Th2 cytokines (168, 180), however, no investigation into the role of PI3K isoforms in the production of IL-17 had been performed. Therefore the aim of this results section was to profile the effect of loss of PI3Kγ on IL-17 production and to gain an understanding of the role of PI3Kγ in IL-17 receptor signalling.

8.2 Lack of PI3Kγ causes an increase in IL-17A production

This work started from experiments performed by Matt Thomas at Novartis, which are shown in Figure 8.1:

"BALB/c mice were exposed to LPS, and BAL levels of cytokine were measured over 48hr. An increase in IL-17A production was observed in PI3Kγ$^{-/-}$animals after 24hrs, rising to 6-fold higher levels by 48hrs (Figure 8.1 A). Levels of IL-1β and TNFα did not differ significantly between wild-type (WT) and knockout animals (data not shown). Splenocyte cultures stimulated with LPS in vitro also resulted in a significant enhancement in IL-17A production in cells lacking PI3Kγ (Figure 8.1 B). Similarly T cells from PI3Kγ kinase dead knock-in animals, or PI3Kγ knockouts of a different background strain (129sv) also displayed increased levels of IL-17A production (Figure 8.1 C). More detailed analysis of wild-type and PI3Kγ$^{-/-}$ CD4+ T cells

stimulated with anti-CD3 and anti-CD28 demonstrated a near identical degree of proliferation and comparable production of IL-2, IL-4, IL-5, IL-6 and IFNγ, despite a 30-fold increase in IL-17A levels (Figure 8.1D)."

8.3 IL-17A produced by PI3Kγ T cells is functional

It was thought that the IL-17 produced by PI3Kγ$^{-/-}$ CD4+ T cells might not be functional and hence might fail to activate a negative feedback pathway. The assay to determine functionality used wild-type mouse dermal fibroblasts (MDF) which produce IL-6 in a concentration-dependent manner in response to IL-17A. They also produce IL-6 in response to IL-17F but the concentrations of IL-17F required are ~2 logs higher (Figure 8.2 A, B).

Wild-type and PI3Kγ$^{-/-}$ CD4+ T cells were stimulated with CD3/CD28 T cell expander Dynabeads overnight to generate IL-17^{lo} wild-type and IL-17^{hi} PI3Kγ$^{-/-}$ supernatants. When supernatants were applied to the MDF, they produced IL-6 in accordance with the increased IL-17A content - with more IL-6 production being induced by PI3Kγ$^{-/-}$ supernatant ($p<0.01$). To confirm that IL-6 production was induced by IL-17A rather than any other component of the supernatant, a neutralising/blocking antibody was added, at a concentration sufficient to block 10ng/ml IL-17A (Figure 8.2 C), which inhibited IL-6 production in both supplemented cultures. The non-significant increase in IL-6 production by PI3Kγ$^{-/-}$ CD4+ supernatant-treated MDF cultures vs wild type derived supernatant effects in the presence of anti-IL-17A Ab may be attributable to higher levels of IL-17F in the PI3Kγ$^{-/-}$ CD4+ supernatants (see below). The significant ($p<0.05$), Student's paired T Test) IL-17A-dependent IL-6 production by the MDF in response to PI3Kγ$^{-/-}$ CD4+ T cell supernatant indicated that the IL-17A was functional (Figure 8.2 D).

8.4 Kinetics of IL-17A and IL-17F production

It was thought that the increase in IL-17A production by PI3Kγ$^{-/-}$ cells might be due to differing kinetics of production, with a peak in WT production occurring earlier or later than the timepoints used in previous experiments. In order to dissect the kinetics of production, IL-17A was measured at 1, 4, 24, 48 and 72h in cultures of CD4+ T cells (Figure 8.3 A). The kinetics of production of IL-17A by PI3Kγ$^{-/-}$ cells mirrored that of WT cells, with the amount secreted increased at all timepoints. As IL-17F has been

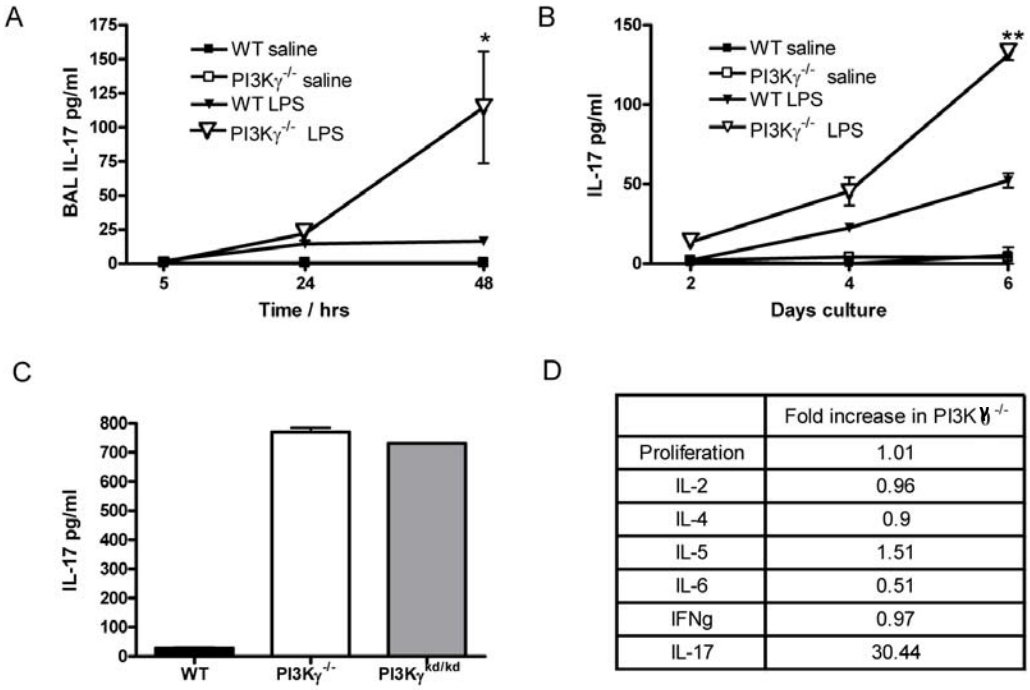

	Fold increase in PI3Kγ-/-
Proliferation	1.01
IL-2	0.96
IL-4	0.9
IL-5	1.51
IL-6	0.51
IFNg	0.97
IL-17	30.44

Figure 8.1. Lack of PI3Kγ leads to enhanced IL-17 production *in vivo* and *in vitro* in response to LPS or CD3/CD28 stimulation. A. Increased IL-17A detected in the BAL fluid of PI3Kγ$^{-/-}$ mice stimulated intranasally with LPS. B. Enhanced IL-17 release from PI3Kγ$^{-/-}$ over WT splenocytes cultured over time, stimulated with saline or LPS. C. Comparison of WT, PI3Kγ$^{-/-}$ and PI3Kγ kinase dead CD4^{+} T cells stimulated with plate bound anti-CD3 and anti CD28. Mean of n=3, +/- SD. D. Fold-differences in proliferation and cytokine release in PI3Kγ$^{-/-}$ and WT CD4^{+} T cells stimulated with plate bound anti-CD3 and anti CD28, n=1. ***These experiments were performed by Matt Thomas***

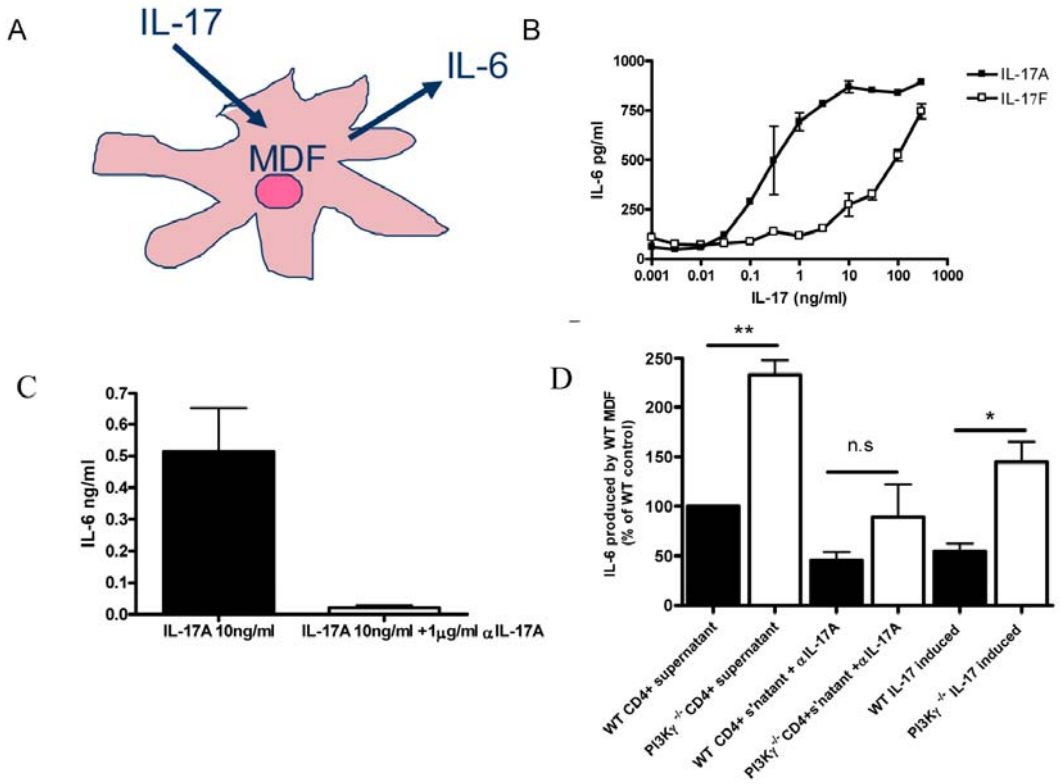

Figure 8.2. The functionality of IL-17 generated by PI3Kγ$^{-/-}$ T cells.

A. Schematic of the IL-17 production assay. IL-17 in the culture media induces production of IL-6 by mouse dermal fibroblasts B. Concentration dependent responses to IL-17A and IL-17F in the MDF assay. IL-17A and IL-17F at the indicated concentrations were added to MDFs and 24 hours later, IL-6 in the supernatant was assessed by ELISA. Data representative of three independent experiments, error bars are SD. C. Validation of an IL-17A blocking/neutralising antibody. 10ng/ml IL-17A was added to MDF cultures in the absence or presence of 1μg/ml anti-IL-17A and the IL-6 in the culture supernatant was assessed by ELISA. Data representative of three independent experiments, error bars are SD. D. Supernatant from WT or PI3Kγ$^{-/-}$ BALB/c CD4^{+} T cells, cultured as described in the Materials and Methods, was removed at 48hr and incubated on a WT mouse dermal fibroblast cell line for 24 hr. The IL-6 produced by the MDF in response to the CD4^{+} T cell supernatant was assessed by ELISA. and is shown in the first two bars. The component of IL-6 production that could not be neutralised by addition of an anti-IL-17A antibody to the MDF culture when the CD4^{+} supernatant was added is shown in bars three and four. The remainder of the IL-6 production was deemed to be dependent upon IL-17A from the CD4^{+} culture supernatants and is shown in columns five and six. Data from three independent experiments, +/- SEM.

demonstrated to have a more important role in suppressing IL-17A production (382) it was postulated that a lack of IL-17F might be driving the increase in IL-17A. However levels of IL-17F in the supernatant of PI3Kγ$^{-/-}$ cells were also increased at all time-points (Figure 8.3 B) ruling out the possibility of lack of IL-17F-driven suppression of IL-17A production. To determine whether the increased IL-17 observed in animals / cell cultures lacking PI3Kγ was due to expansion of a Th17-like population, cells activated for 48hr were cultured for 4 hours in the presence of Golgistop and then stained for IL-17A. No increase in the percentage of IL-17+ve cells in the PI3Kγ$^{-/-}$ cultures was observed (Figure 8.3C). Instead an increase in the mean fluorescence of the cells was observed, similar to data published by Nagata *et al.* (382). Taken together these data indicated that PI3Kγ$^{-/-}$ T cells are not more susceptible to skewing to Th17 *in vivo* or *in vitro* but instead individual cells each produce more IL-17 than their WT counterparts, and this increase is consistently sustained over time.

8.5 Expression of IL-17RA and IL-17RC by PI3Kγ-/- CD4+

To determine whether the aberrant IL-17 levels produced by T cells lacking PI3Kγ were due to altered IL-17 receptor levels, expression patterns were investigated. Freshly isolated PI3Kγ$^{-/-}$ CD4+ expressed a significantly higher level ($p<0.05$) of IL-17RA than their WT counterparts. IL-17RC surface expression was very low on freshly isolated cells with no significant difference between WT and PI3Kγ$^{-/-}$ cells (Figure 8.3 Di). Typical flow cytometry plots are shown in Figure 8.3 Dii, indicating that there are not distinct IL-17RA or IL-17RC positive populations, but rather that the mean level of expression of IL-17RA on individual cells is increased by loss of PI3Kγ.

8.6 Involvement of PI3Kγ in IL-17 production by naïve cells and upon skewing

To further investigate whether there was a change in the expansion of Th17 cells in the PI3Kγ$^{-/-}$ cultures, and also whether there was still some regulation of IL-17 production, cells were cultured under Th17 skewing conditions. To do this, naïve CD4+ T cells were used. Therefore in the first experiment, naïve CD4+ were isolated from the spleen and cultured as previously. IL-17A and IL-17F in the supernatant were measured after 48hr (Figure 8.4 A) as had been done previously using pan CD4+ T cells. Significantly more IL-17A was generated by PI3Kγ$^{-/-}$ cells than WT cells, with a trend towards more IL-17F production, although levels were lower than in experiments with pan CD4+. Again this reiterated the finding that increased IL-17 production was not due to the presence of increased numbers of *in vivo* generated Th17s.

Next naïve cells were cultured for seven days under Th0 or Th17 conditions and the levels of IL-17 in the supernatant were quantified. Under both Th0 and Th17 conditions the PI3Kγ$^{-/-}$ cells produced more IL-17A and IL-17F than their equivalent WT counterparts (Figure 8.4 B). However, there was no increase in the percentage of cells staining positive for either the characteristic Th17 chemokine receptor CCR6 (Figure 8.4 C) or IL-17A (Figure 8.4 D). Finally, the expression of IL-17 receptors was characterised in both Th0 and Th17. It was observed that expression of IL-17RA was not altered by skewing to Th17, however, under Th0 conditions (but not Th17 conditions) there was a marked upregulation of IL-17RA in PI3Kγ$^{-/-}$ cells (Figure 8.4 E). The same trends were observed with IL-17RC, although expression levels were more varied and the trend did not reach significance.

8.7 Involvement of PI3Kγ in IL-17 signalling

The altered levels of IL-17 receptors suggested a failure of a negative feedback loop upon IL-17 production in PI3Kγ$^{-/-}$ CD4+ T cells (383). To investigate this, freshly isolated WT and PI3Kγ$^{-/-}$ CD4+ T cells were stimulated with a range of concentrations of IL-17A and IL-17F, and Akt phosphorylation was measured by ELISA. Phosphorylation of Akt was observed in response to 30ng/ml IL-17A in WT cells only (Figure 8.5 A), despite increased IL-17RA expression in PI3Kγ$^{-/-}$ cells. No phosphorylation of Akt was observed either in WT or PI3Kγ$^{-/-}$ cells in response to IL-17F up to 100 ng/ml (Figure 8.5 B).

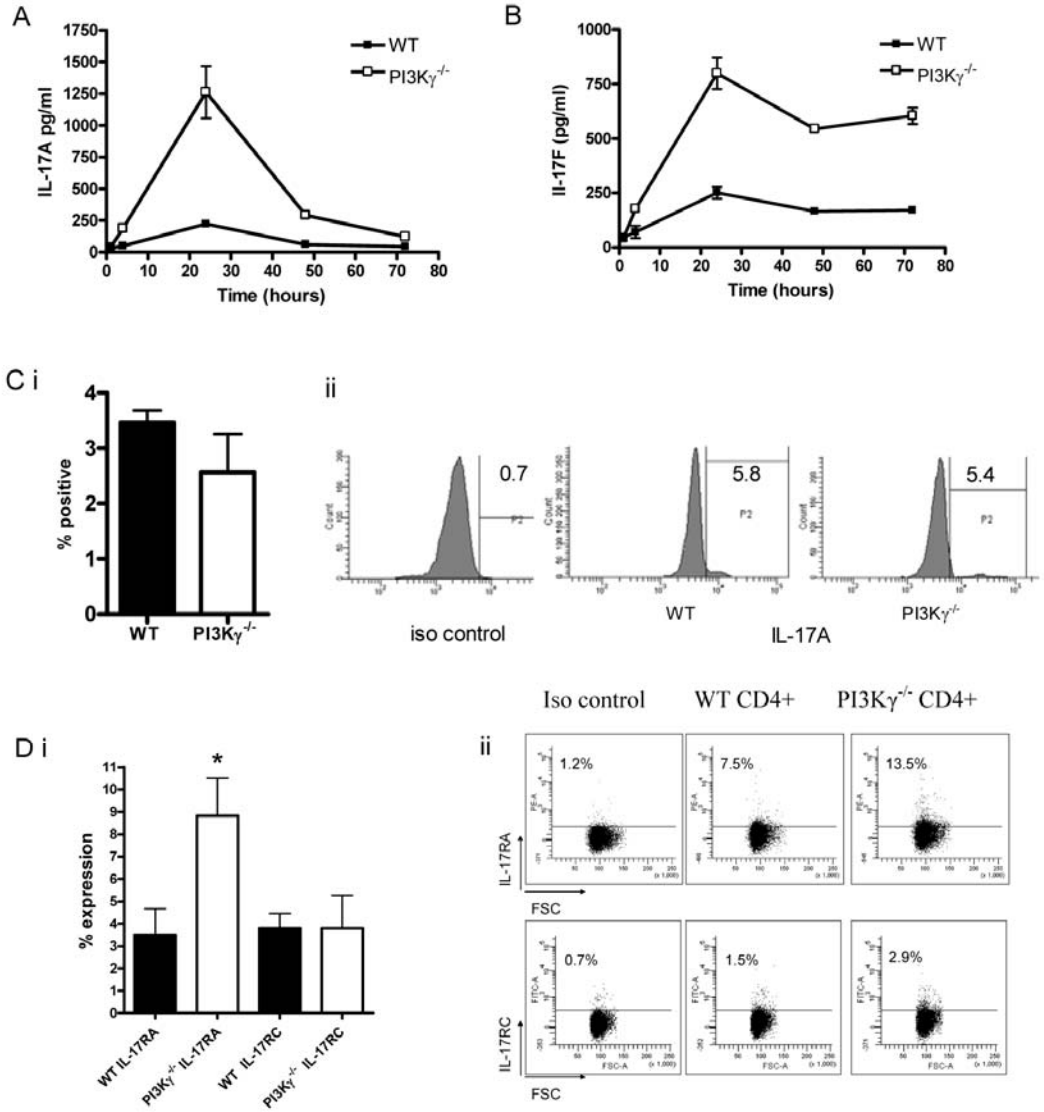

Figure 8.3. Characterisation of IL-17 production by CD4$^+$ T cells. More IL-17A and IL-17F are produced by CD4$^+$ T cells with genetic loss of PI3Kγ. ELISA detection of A. IL-17A and B. IL-17F from supernatants of WT or PI3Kγ$^{-/-}$ BALB/c CD4$^+$ T cell cultures, maintained as described in Materials and Methods, at 1, 4, 24, 48 and 72hr timepoints. Data are from one experiment representative of three independent experiments. Error bars are SD. C. CD4$^+$ cells were cultured for 48hr on CD3/CD28 beads as described in Materials and Methods. For the final six hours cells were restimulated on CD3/CD28 beads in the presence of golgistop, then fixed and stained for IL-17 or isotype control. i. Bar graph is pooled data from three independent experiments, error bars are SEM. ii Flow cytometry plots are from a single experiment, representative of three independent experiments. D. Expression of the IL-17RA and IL-17RC on the surface of CD4$^+$ freshly isolated from WT or PI3Kγ$^{-/-}$ BALB/c mice were assessed by flow cytometry. i. Bar graph is pooled data from three independent experiments, error bars are SEM. ii. Plots are from a single experiments representative of three independent experiments.

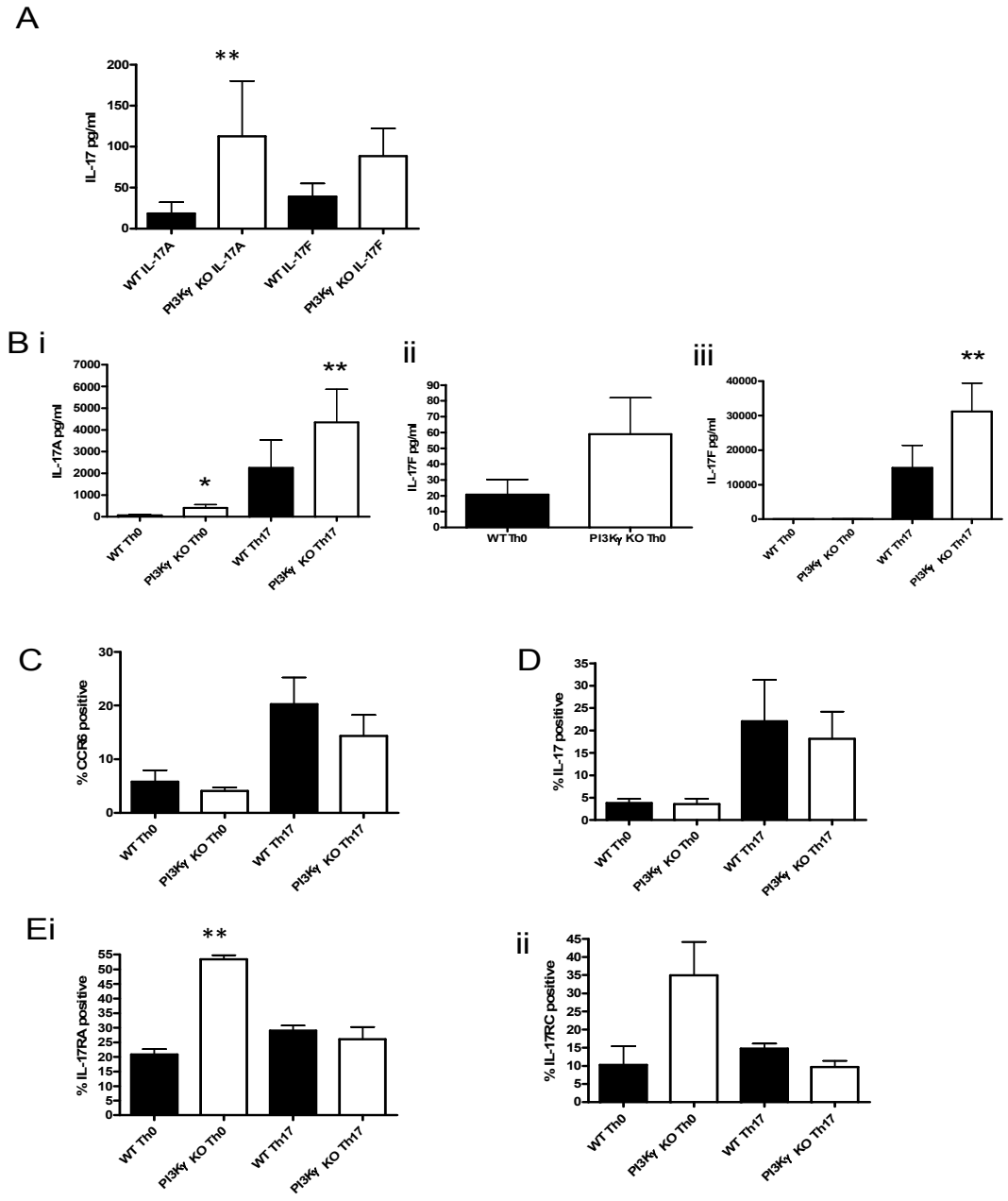

Figure 8.4 PI3Kγ$^{-/-}$ T cells skewed to Th17 still produce more IL-17A and IL-17F than their WT Th17 skewed counterparts. A. Naïve CD4+ were isolated from WT or PI3Kγ-/- BALB/c mice and cultured for 48 hours on CD3/CD28 beads and the concentrations of IL-17A and IL-17F in their supernatants were assessed by ELISA. B. Naïve cells were culutred under Th0 or Th17 conditions for six days, then restimulated for 16 hours and the IL-17A (Bi) and IL-17 F (Bi and ii) were assessed by ELISA. C. The expression of CCR6 on day 7 Th0 and Th17 skewed cells was assessed using flow cytometry. D. Day 7 cells were restimulated on CD3/CD28 beads for 6 hours in the presense of golgistop, then fixed and stained for IL-17A which was assessed by flow cytometry. E. Expression of i. IL-17 RA and ii. IL-17RC was assessed by flow cytometry on the surface of day 7 Th0 and Th17 skewed cells. Averaged data are from at least three independent experiments, error bars are SEM.

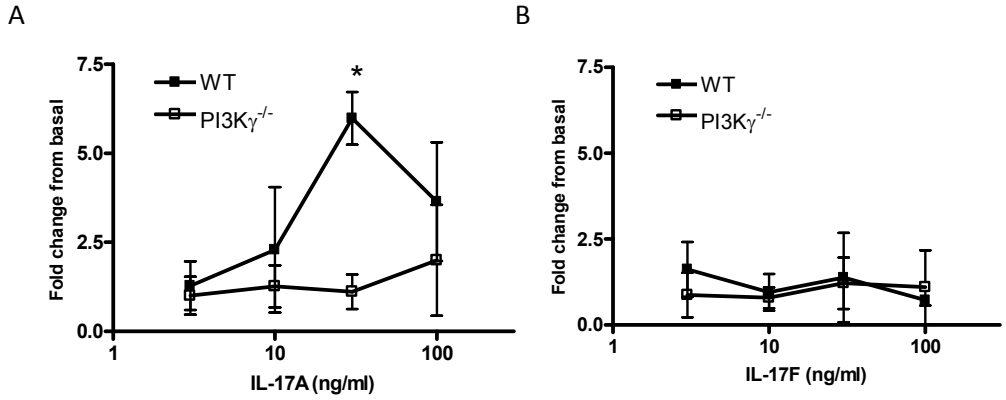

Figure 8.5 Intracellular Signalling by CD4$^+$ T cells in response to IL-17.

PI3K signalling in response to IL-17. Phosphorylation of AKT was quantified by ELISA and normalised to unstimulated WT or PI3Kγ$^{-/-}$ CD4$^+$ cells in response to A. IL-17A or B. IL-17F applied for 5 minutes at the indicated concentrations. Averaged data are from at least three independent experiments, error bars are SEM

8.8 Summary

Previous work has shown that murine T cells produce an increased amount of IL-17A in response to a variety of stimuli both *in vitro* and *in vivo* when PI3Kγ was knocked out, or a catalytically inactive mutant was knocked in. In this chapter it was demonstrated that

- Both IL-17A and IL-17F production are increased upon knockout of PI3Kγ
- There is aberrant expression of the IL-17RA and IL-17RC receptors
- The IL-17A produced by PI3Kγ$^{-/-}$ T cells is functional
- The increase in IL-17 production is not due to an expansion in the Th17 population
- Upon culture in Th17 conditions, the increase in Th17 cells is equivalent in WT and PI3Kγ$^{-/-}$ cells, however, the PI3Kγ$^{-/-}$ cells still produce more IL-17A and IL-17F
- IL-17A but not IL-17F signals through PI3Kγ in murine T cells

These results are summarised in Figure 8.6

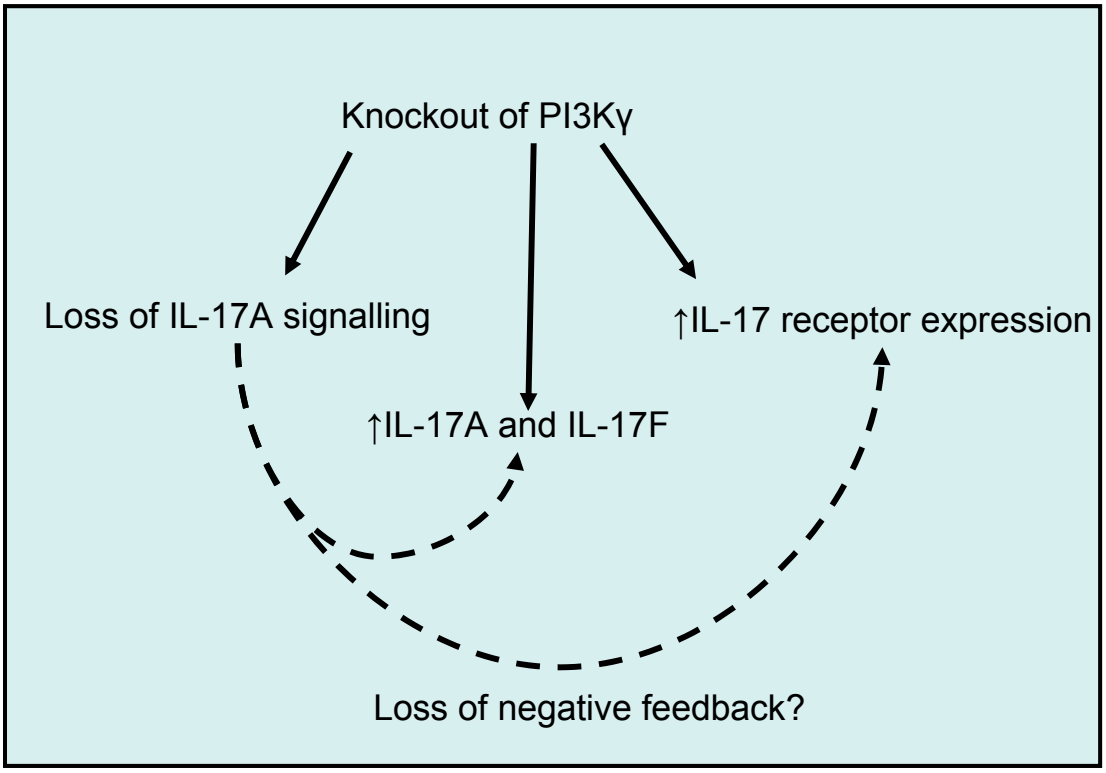

Figure 8.6 Summary of the effects of PI3Kγ knockout on IL-17 signalling and production

In murine T cells, loss of PI3Kγ led to a loss of IL-17A induced signalling through Akt and also to an increase in the expression of IL-17 receptors and increased production of IL-17A and IL-17F. It is possible that the IL-17A signalling through PI3Kγ is required to negatively regulate both receptor expression and IL-17 production. This hypothesis will be examined in the Discussion.

Chapter 9: Discussion

9.1 Overview

In this thesis the role of SHIP-1 in T lymphocyte function has been extensively investigated. It was shown that SHIP-1 was activated in response to a variety of stimuli in primary human T cells. Furthermore, expression of rCD2:SHIP protected Jurkats against apoptosis in response to H_20_2 and TRAIL. Next a lentiviral delivery system was successfully established so that SHIP-1 expression could be modulated in primary human cells. Expression of rCD2:SHIP in these cells led to their death, however, cells in which SHIP-1 expression had been silenced were still viable, although they failed to proliferate. SHIP-1 silenced cells displayed an increase in basal PI3K activity and actin polymerisation. They also had a loss of microvilli expression and a decrease in basal motility. However, they were still able to migrate towards chemokines. Experiments using fluorescent PH domain reporters and staining for phosphorylated SHIP-1 also revealed only a weak localisation of both to the leading edge of polymerised cells. The final section examined the role of SHIP-1 in T cell functions. Silencing of SHIP-1 led to a reduction in Th1 cytokine production under Th1 skewing conditions. Under Th2 skewing conditions, silencing of SHIP-1 resulted in an increase in production of IL-4. Notably under Th0 conditions there was an increase in the percentage of Tregs. Finally CD8+ T cells had a tendency towards a decrease in cytotoxic function upon silencing of SHIP-1. These findings will now be discussed in more detail.

9.2 Expression of SHIP-1

Expression of SHIP-1 in primary T cell and T cell lines was in agreement with that previously reported in the literature (244). Expression of rCD2:SHIP-1 was also verified in stably transfected cell lines, however, the expression was deemed too leaky to use the “off” Jurkats as negative controls for future experiments. Since the generation of this cell line, more easily controlled promoter systems have been developed, which would be alternative options for future experiments (384, 385).

9.3 SHIP-1 is phosphorylated in response to a variety of stimuli

The first section of the results indicates that SHIP-1 is phosphorylated in response to a variety of stimuli. Confocal imaging of SHIP-1 verified that phosphorylation of SHIP-1 on Y^{1020} may be taken as a marker for its recruitment to the cell membrane it T cells. Staining with the pan SHIP-1 antibody was less successful but implied that

SHIP-1 was distributed throughout the cytosol in controls, and recruited to the cell membrane upon stimulation in line with the report of others (386).

As the phosphorylation of SHIP-1 on Y^{1020} can be taken as a marker of its recruitment to the cell membrane and hence its activity, it is clear that SHIP-1 will play a variety of roles in PI3K mediated signalling events. However, western blotting for phosphorylated Akt and phosphorylated SHIP-1 in response to a variety of stimuli such as chemokines and anti-CD3 indicated that SHIP-1 is differentially activated compared to Akt. These findings support the idea that other negative regulators of PI3K signalling such as PTEN and Phlpp may contribute to differential activation of AKT (387) and that SHIP-1 modulation of PI3K signalling directs the pathway towards different outcomes. However, in some cases, a lack of Akt response may indicate that timepoints or concentrations of chemokine were not optimal. Previously it has been reported that in B cells, SHIP-1 is not phosphorylated in response to CXCL12 stimulation (294). However, the situation may be different in T cells, or the phospho-specific antibody may be more sensitive than immunoprecipitation of SHIP-1 followed by probing with 4G10 (an antibody that recognises phosphotyrosine residues). The strong phosphorylation of SHIP-1 observed in response to H_2O_2 may be partly due to inactivation of the (as yet unidentified) phosphatase responsible for the dephosphorylation of SHIP-1 by oxidizing conditions (388). Others have also reported that hydrogen peroxide stimulates the PI3K-dependent recruitment of $PI(3,4)P_2$ binding proteins (389). It was somewhat surprising that SHIP-1 was not strongly phosphorylated in response to CD28 stimulation, as it has been previously reported to act downstream of this receptor, and PI3K is strongly activated by CD28 signalling (335).

The PI3K inhibitor LY294002 did not affect phosphorylation of SHIP-1 in response to stimuli, suggesting that phosphorylation is PI3K-independent as has been reported for IgE stimulated SHIP-1 phosphorylation in basophils (390). However, the Src kinase inhibitor PP2 was successful in reducing both basal and induced levels of SHIP-1 phosphorylation in response to H_2O_2, consistent with reports that the Src kinase Lyn is responsible for phosphorylation of SHIP-1 (255, 341). However, this phosphorylation is not essential for SHIP-1's enzymatic activity *in vitro* nor for its association with the Src kinase Lyn at the cell membrane as inhibition of the kinase activity of Lyn using PP2 inhibits SHIP-1 phosphorylation but not its association with

Lyn (340). bpVphen was found to induce phosphorylation of both Akt and SHIP-1, which was indicative of its actions in raising levels of both $PI(3,4,5)P_3$ and $PI(3,4)P_2$ (388). This was important to validate for later work investigating the actions of bpVphen on cell morphology. The identity of the band recognised by the pY^{1020} SHIP-1 antibody at approximately 75kDa remains unknown. Variants of SHIP-1 with molecular weights this low have not been reported in the literature. It is possible that the antibody cross reacts with another protein with a NPXY motif. Alternatively, this band may be due to proteolytic cleavage of SHIP-1 after cell lysis (391).

9.4 The role of SHIP-1 in apoptosis

The investigation into the role of SHIP-1 in ROS and death receptor signalling yielded some interesting results. The finding that CD2:SHIP protected against cell death was in line with Gloire *et al.* (263), who found that expression of SHIP-1 protected leukaemic T cells against ROS-induced cell death. It has been reported in the literature that inhibition of Akt sensitises cancer cell lines to TRAIL induced apoptosis by increasing TRAIL-mediated cleavage of Bid. It also sensitised cells to Fas mediated apoptosis (392). It has also been reported that reintroduction of SHIP-1 into Jurkats sensitises them to Fas mediated apoptosis (264). In addition, it has been shown that introduction of constitutively active Akt or loss of SHIP-1 causes an increase in Fas expression and cell death in *Francisella tularensis*-infected macrophages (393).

SHIP-1 is reported to be recruited to a YxxL motif on death receptors including TNF, TRAIL and Fas receptors and thus negatively regulate cell death (394). It may be that the lack of SH2 domain in the rCD2:SHIP construct, which would prevent its recruitment to the TNF receptor, was responsible for its inefficacy. It is not clear why SHIP-1 protects against death induced by TRAIL but not by TNFα. The presence of CD2:SHIP may alter the expression of TRAIL or TNF receptors, although this could be quantitated by western blotting or flow cytometry with the appropriate antibodies. Kim *et al.* reported that SHIP-1 null HPCs are still sensitive to the suppressive effects of TNFα in a colony forming assay (360), i.e. that SHIP-1 probably does not regulate TNFα signalling. Some limitations of the CD2:SHIP molecule must be born in mind. Firstly it does not have the ability to cluster in the vicinity of its substrate and secondly it lacks the binding domains that allow SHIP-1 to perform a scaffolding

function for the recruitment of other molecules. However, a comparison of this approach with reintroduction of full length SHIP-1 would clarify these issues (334).

9.5 Safety and efficacy of lentivirus

As reported elsewhere it is extremely difficult to introduce siRNA into primary T cells using either chemical transfection or electroporation (286, 346), without compromising viability. Furthermore rates of transfection are low, and the effect is transient. These findings were repeated using one of the most up to date electroporation systems available, the Microporator MP-100. This resulted in a maximum of 8% of cells that were viable and transfected with a GFP expression plasmid, making it unsuitable for many experiments. This percentage was achieved in freshly isolated CD4+ T cells. When PBMCs were activated for 10 days in the presence of SEB before electroporation, less than 3% of cells were transfected and viable. This was despite the manufacturer's report that 30% of PBMCs could be transfected. Therefore it is preferable to use a viral delivery system which can give higher rates of infection and also utilise shRNA. Adenoviruses and adenovirus associated viruses can deliver transient shRNA, but are not efficient at infecting primary T cells (395), whilst mouse stem cell virus (MSCV) and the Moloney murine leukaemia virus (MoMLV) or lentivirus (e.g. HIV, FIV or EIAV) can integrate into the host cell DNA. Lentiviruses are particularly advantageous as they can infect non dividing cells (347, 348). A variety of plasmids for lentiviral delivery of shRNA are now commercially available (347). In addition, the lentiviral plasmid can also be used to introduce DNA coding for full length proteins.

With this in mind, it was satisfying to note that the Jurkat cell line could be infected with high efficacy and that the cells appeared normal, with strong expression of GFP. Furthermore, supernatant from infected cells was unable to infect other cells, indicating that the four plasmid expression system had worked effectively and made replication incompetent viral particles (328). Similarly, primary human T cells could also be infected at a very high percentage (over 85%), without any effect on viability, in line with reports in the literature (396). Spinoculation and use of polybrene enhanced infection rates. Spinoculation sediments the virus onto the cell (397) whilst polybrene is a polycation that is thought to increase viral infection by aiding the interaction of the negatively charged membrane of the virus and the target cell (327).

9.6 Overexpression of constitutively active SHIP-1 in primary cells leads to death

It was hoped that silencing of SHIP-1 expression in primary cells would be complemented by a model of SHIP-1 activation in these cells. This would utilise the rCD2:SHIP chimeric protein, used successfully in the first results chapter and by others (244, 256, 294). To this end, the DNA was cloned into the lentiviral expression vector pCLPS, which was used previously to express GFP when validating the lentiviral delivery system. This was used to infect primary cells and the rat CD2 protein was detected by flow cytometry and by western blotting (at the correct molecular weight to be part of the chimeric protein). Furthermore, the infected cells could be enriched using MACs columns. However it was observed using flow cytometry that three days after infection, only 30% of the population was positive for rCD2, whereas infection rates of over 80% had been achieved with the same vector encoding GFP. Furthermore, it was noted on the FSC/SSC dot plots, that there was an increased amount of debris and that therefore the infected cells were most likely dying. To ascertain this, day three post infection the cells were stained with annexin and propidium iodide and assessed by flow cytometry. They were found to have an increase in the percentage of apoptotic cells (and presumably by this stage a substantial proportion had already undergone apoptosis or necrosis, to judge from the amount of debris). This finding was confirmed by confocal microscopy, in which rCD2:SHIP cell cultures had a lot of debris and cells that were staining positive for propidium iodide. Western blotting confirmed that levels of basal or CXCL11 induced Akt phosphorylation were reduced by expression of rCD2:SHIP (although equal loading was difficult as protein quantification by Bradford assay was confounded by dead cells). These observations were unsurprising, given the key role of the PI3K pathway in cell growth and survival (290, 295, 398-400). Furthermore overexpression of inositol polyphosphate 5-phosphatase type IV (5ptase IV), which metabolises $PI(4,5)P_2$ and $PI(3,4,5)P_3$, suppressed cell growth, increased basal cell death by apoptosis and also sensitised cells to Fas mediated apoptosis (401).

In general, interest in the PI3K pathway has focussed on its role in cancer and inflammation. Particularly in cancer it has been noted that a high proportion of both solid tumours and leukaemias exhibit mutations in the PI3K pathway (or upstream activators such as growth factor receptors). This can be at the level of activating mutations in the PI3K itself, (most commonly in PI3Kα), or in Akt, or a loss of a

negative regulator. In solid tumours this is PTEN, but SHIP-1 is lost in leukaemias or has inactivating mutations. Therefore a core principal of cancer research has been to develop PI3K and Akt inhibitors, some of which are showing early success in clinical trials. However, there is conflicting information as to whether inhibiting the PI3K pathway induces growth arrest or can actually initiate apoptosis or necrosis. Until recently, evidence had pointed towards the growth arrest, at least when PI3K inhibitors were given as a monotherapy (a situation that would be unlikely to be the case in the clinic (295, 402, 403)). However, recent research has pointed towards the the initiation of apoptosis by PI3K inhibitors (299). It is somewhat hard to envisage how a PI3K inhibitor, even if it were selective for the alpha isoform, could selective induce cell death or even growth inhibition in cancerous cells, without impacting upon normal cells, particularly upon insulin signalling. However, a theory of oncogene addiction has been proposed, in which cancerous cells become uniquely dependent upon the mutated pathway for growth and survival and are therefore much more susceptible to inhibition of this pathway than are wild type cells.

This theory does not appear to hold water with the results described here, when inhibition of PI3K signalling by diversion of the $PI(3,4,5)P_3$ product to $PI(3,4)P_2$ rapidly induced death of cells. The fact that this was not seen in the Jurkats may be attributable to the relative strengths of the promoters used to drive the transcription of rCD2:SHIP and therefore the relative abundance of the protein in the cells. It is to be expected that small molecule inhibitors may not, over a sustained period, be at high enough intracellular concentrations to cause complete inhibition of signalling mechanisms. SHIP-1 has also been shown to regulate Akt localisation at the cell membrane as well (404). This was confirmed in primary cells by decreased basal and stimulated Akt phosphorylation upon introduction of rCD2:SHIP. Nevertheless, some weak Akt phosphorylation can be seen in the infected cells and therefore, inhibition of PI3K signalling pathways may have serious consequences in primary cells.

An alternative explanation is that the $PI(3,4)P_2$ product may activate signalling pathways contribute to cell death or interfere with survival. Relatively little is known about the specific $PI(3,4)P_2$ binding proteins (405, 406), although TAPP2 has been demonstrated to interact with the cytoskeletal proteins utrophin and syntrophin and to facilitate adhesion to fibronectin and laminin. However, TAPP2 is an unlikely culprit

for cell death as TAPP2 expression was upregulated in aggressive B cell leukaemias with increased adhesion probably contributing to disease progression (407).

As well as the rCD2:SHIP construct, others have used retrovirus to reintroduce full length SHIP-1 into Jurkats and found similar effects i.e. a decrease in $PI(3,4,5)P_3$ and pAkt levels. However, although there was reduced proliferation, due to slow transit through G1, there was not complete cell cycle arrest or apoptosis. The decreased proliferation was due to decreased phosphorylation of Rb and increased stability of $p27^{Kip1}$, two regulators of cell cycle at the G1 stage (408). Alternative experimental strategies would be to overexpress full length SHIP-1, to clone the rCD2:SHIP into a lentiviral vector with a weaker promoter, or a lentiviral inducible promoter system (409-411) or to use a small molecule pharmacological approach. The latter option has been explored by other (319, 320, 323). SHIP-1 is reported to be an allosterically modulated enzyme (although others have questioned this (257)) and the compound reported in the literature facilitates its activation by binding to the allosteric binding site (319, 320). This compound has been reported to be anti-proliferative and cytotoxic against human multiple myeloma cells (323). As mentioned above (408), in Jurkats overexpression of WT SHIP-1 has been shown to have no effect on proliferation. In erythroid cells, overexpression of catalytically inactive SHIP-1 decreases proliferation. However, overexpression of either WT SHIP-1 or a catalytically inactive mutant causes an increase in apoptosis, highlighting the important difference between the scaffold and catalytic functions of SHIP-1 and that $PI(3,4)P_2$ can be crucial for proliferation (332). Since the increased apoptosis of SHIP-1 overexpressing cells was not caused by the 5-phosphatase activity of SHIP-1, other regulatory domains appear to be involved in this process, like the noncatalytic C-terminal proline-rich region or the N-terminal SH2 domain which were found to be essential for the inhibitory signalling of B cells and the increased apoptosis observed in DA-ER cells (a murine myeloid cell line), respectively (412, 413). Furthermore, different non-catalytic domains can have important functions, for example the proline rich domain is required for inhibitory signalling in B cells and the SH2 domain is required for some proapototic functions of SHIP-1 (412).

Overexpression of full length SHIP-1 would have several advantages over rCD2:SHIP, which is somewhat flawed as although it has constitutive membrane localisation it does not necessarily colocalise with PI3K- containing signalling

complexes generating its substrate (which may be in discreet areas of the cell). Moreover rCD2:SHIP lacks the other binding domains of SHIP-1 that constitute its adapter function (258). Whichever explanation for the death of rCD2:SHIP expressing T cells is correct, the fact remained that by 7 days post infection, no intact cells remained, and the rapid cell death made it impossible to gather further data from these cells, and therefore further research concentrated on silencing of SHIP-1 expression.

9.7 Lentiviruses expressing shRNA can be used to silence SHIP-1 expression in primary human T cells

Initial experiments used CEMs to evaluate the ability of five different shRNAs to reduce expression of SHIP-1, and all five proved successful. The remainder of the experiments were conducted using primary human T cells. Use of the lentiviral system allowed the introduction of shRNA and RNA coding for proteins, without adversely affecting the viability of the cells. Infection rates of over 85% could be achieved, and furthermore, in the case of shRNA-encoding plasmids, the uninfected population could be killed using puromycin. The only parameters that were altered between control and shRNA control-infected cells appeared to be the percentage expressing CD25 and ability to skew to Th17 (see later). Assessment of SHIP-1 silencing at both the mRNA and protein level gave confidence in the methodology. Lentiviral delivery systems are now the preferred method for silencing of protein expression in many primary cells, and even in cell lines, as they give sustained silencing over indefinite numbers of cell divisions, and the virus itself does not damage the cell. This is in contrast to other methods such as chemical transfection, electroporation or adenoviral infection, all of which variously damage the cell or induce an immune response.

9.8 SHIP-1 silencing does not affect viability of T cells but reduces proliferation

Viability of the primary cells was assessed using annexin and propidium iodide staining. This was performed on day nine post isolation, at which point, all uninfected cells had been killed on the basis of puromycin selectivity, and it was hoped that these dead cells would have degraded enough so as not to impinge upon the assay result. Furthermore, it gave time not only for SHIP-1 shRNA to be expressed by the cell, but also for existing SHIP-1 protein to be degraded. It was found that for both CD4+ and CD8+ T cells, viability was not adversely affected by silencing of SHIP-1

expression. The caveat of this is that some cells may have died very early on at the point at which SHIP-1 protein levels began to fall.

Additionally, the viability of the cells after 6 hours in 0.1% serum was assessed, and found to be unaffected by SHIP-1 silencing. This gave confidence that experiments that required long periods in low serum or BSA (such as a neuroprobe chemotaxis assay) would not cause apoptosis in SHIP-1 silenced cells and thus compromise the results. In general, loss of SHIP-1 has not been reported to reduce viability (183), but instead has been implicated in the progression of several leukaemias (269-271).

A final experiment examined the effect of exposure to TRAIL. It has been reported that primary T cells are insensitive to TRAIL and do not undergo apoptosis in response to it, possibly because they have low levels of TRAIL receptors and high levels of the antiapoptotic proteins TRAIL-R4 and c-FLIP (414) . Certain T cell lines such as CEMs also have low levels of TRAIL receptors and are reported to be resistant to TRAIL-induced cell death, whereas Jurkats are sensitive to this agent (415). Results in the previous chapter indicated that introduction of rCD2:SHIP to Jurkats protected them against TRAIL-induced death. Therefore it was logical that loss of SHIP-1 might be sufficient to confer sensitivity to primary T cells. However, it was found that silencing of SHIP-1 expression did not allow TRAIL to induce apoptosis of the primary cells. This may suggest that rCD2:SHIP has substantially different qualities to endogenous SHIP-1 (see later). It may also be that the multiple other abnormalities in Jurkats (such as a loss of PTEN) (244), mean that they respond differently to the presence or absence of SHIP-1 than do primary T cells.

Reduced numbers of SHIP-1 silenced cells were recovered following selection, despite the fact that they had not been observed to undergo excessive apoptosis. Therefore cells were labelled with CFSE to observe their proliferation. Two different protocols were used. Firstly, cells were labelled immediately post isolation, before infection with lentivirus. This had the advantage of the cells being relatively uniform in size, and guaranteed that the shRNA cells and SHIP-1 shRNA cells would have started out with identical amounts of CFSE, as they were labelled as one population and then subsequently infected with different lentiviruses. In addition, although CFSE

is generally regarded as non-toxic at low concentrations and is generally suitable for labelling lymphocytes, it can be toxic to activated T cells and if cells are labelled with too much CFSE they exhibit reduced proliferation (416).

In this assay, proliferation was observed to be reduced in SHIP-1 silenced cells compared to shRNA control cells. The SHIP-1 shRNA cells were still observed to have undergone some divisions in this assay. However, this could have been during the initial activation before exposure to lentivirus, or after infection when shRNA was present in the cell and inhibiting new production of SHIP-1 but SHIP-1 protein synthesised prior to infection was still present. Therefore a further assay was done to establish whether once a maximum amount of SHIP-1 protein had been lost, whether the cells would undergo proliferation. With the caveats mentioned above, the assay was optimised using lower concentrations of CFSE and loading in the presence of FCS. In addition, flow cytometry was used on a sample from each population immediately following CFSE loading, to verify equal staining. In this instance, no proliferation of SHIP-1 shRNA cells was observed, whereas a proportion of shRNA control cells underwent a division over the course of 48 hours. This low level of proliferation in the control cells is probably attributable to reduced proliferation seen after reactivation of previously activated cells, but a component may also be due to the anti-proliferative effect of CFSE, despite every effort being taken to optimise the protocol.

The next experiment examined in further detail the lack of proliferation observed in SHIP-1 shRNA cells. Propidium iodide was used to stain fixed cells in order that their DNA content could be quantified by flow cytometry. It was found that by day 7, SHIP-1 shRNA cells had undergone cell cycle arrest in G0 and/or G1, whereas shRNA control cells were found to be in S, G2 and M phases as well as G0/G1. These findings were somewhat unexpected for a number of reasons. Firstly, activating mutations of PI3Ks, or upstream components, are frequently detected in cancers, and PI3K inhibitors can reduce proliferation of primary cells and cancer cell lines, as well as showing some early success in the treatment of solid tumours and leukaemias. Secondly, PTEN is a well known tumour suppressor (417). Thirdly, some (269-272) studies have identified SHIP-1 as being lost in a proportion of leukaemias (and indeed, gene transfer of SHIP-1 into AML cells from patients, blocked their proliferation (418)), suggesting that it may also be a negative regulator of cell cycle

progression. However, others have queried whether lack of detectable SHIP-1 expression is due to lysates being prepared using an NP-40 based lysis buffer, without adequate PMSF, which can allow proteolytic cleavage of SHIP-1. When an SDS based lysis buffer has been used instead, SHIP-1 is frequently detected (391, 419). Furthermore, reports of the T cell specific SHIP-1 knockout mice indicated that loss of SHIP-1 did not affect proliferation of these T cells, either *in vitro* or *in vivo* (183).

Interestingly, loss of SHIP-1 is associated with the increased proliferation seen in leukaemia when miR155 expression is increased. For example it has been shown that increased expression of miR155 silences SHIP-1 expression and encourages progression of preleukaemic B cells to leukaemia (420). This has also been demonstrated in natural killer cell leukaemias (421), whilst in macrophages, miR155 also mediates suppression of SHIP-1 expression (50). Interestingly, silencing of SHIP-1 expression using a retrovirus that mimics miR155 expression leads to a myeloproliferative disorder (50).

However, there are a number of possible explanations for the data found herein. Firstly, in SHIP-1$^{-/-}$ mice, the number of T cells is reported to be decreased. Some have attributed this to increased sensitivity of the T cells to FasL mediated apoptosis (264), but this is somewhat dubious. A more convincing explanation stems from the observation that SHIP-1$^{-/-}$ mice have an increase in the percentage of Tregs (184). Although this finding was not replicated in the T cell specific knockout mouse (183), it has been replicated using naive T cells from the whole animal knockout, which, in culture, are polarised more effectively to Tregs than their WT counterparts (186). Anergy and reduced proliferation are well known features of Treg cells, and therefore their phenotype was examined in more detail (see below).

An alternative explanation for the failure of SHIP-1 silenced cells to proliferate may lie in the fact that this is the only aberrant protein in these cells. During the cell cycle, a number of checkpoints ensure that proliferation is regulated and that cells with mutations are prevented from proliferating. In particular the G1 checkpoint allows a G1-S transition. This checkpoint can be overcome by actions of certain oncogenes in

cancer, however, in general, unhealthy cells will be prevented from proceeding further. It is possible that high levels of $PI(3,4,5)P_3$ present in the SHIP-1 shRNA cells indicate to them that they are not healthy and in order to reduced the chance of a leukaemia developing, these cells are prevented from proliferating. If this were the case then one would expect the loss of SHIP-1 that has been reported in some leukaemias, to occur at a late stage of oncogenesis, after the cell had acquired other mutations that will allow it to proceed through the G1 checkpoint. There is some evidence that SHIP-1 suppression is downstream of earlier oncogenic events (50). Furthermore, PI3K activity is key to progression through the G1 checkpoint, so a lack of its downstream product $PI(3,4)P_2$ generated in the SHIP-1 shRNA cells may also contribute to cell cycle arrest (422). A final explanation is that the high levels of disordered actin polymerisation seen in the SHIP-1 shRNA cells are inhibitory upon cell cycle progression. Well ordered polymerisation of actin filaments has been shown to be key for progression to S phase (423-425).

Since the completion of the experiments in this thesis, a recently published paper by Brooks *et al.* has shed further light of the decreased proliferation in SHIP-1-silenced cells (426). The authors identified 3 α-aminocholestane as an inhibitor of SHIP-1 in an isolated enzyme assay. They demonstrated that treatment of mice with the compound expanded myeloid immunoregulatory cell numbers. They also showed that inhibition of SHIP-1 reduced human and mouse allogenic responses in mixed leukocyte reactions, similar to that seen with genetic deletion of SHIP-1 (260). Inhibition of SHIP-1 caused increased granulocyte production, and upon irradiation recovery of neutrophils, platelet and red blood cell (RBC) numbers were increased by inhibition of SHIP-1.

Crucially, in contrast to genetic deletion of SHIP-1 (184), inhibition did not cause myeloid infiltration of the lung. However, the treatment of myeloid leukaemia cell lines with the compound resulted in increased apoptosis and reduced proliferation, and this could be reduced by exogenous $PI(3,4)P_2$. In an osteosarcoma cell line which lacked SHIP-1 expression, the compound had no effect.

Previous to this reduction of SHIP-1 was thought to contribute to survival and proliferation of leukaemic cells (50, 244), and this was the first evidence that it might

be detrimental. (Counterintuitively, activation of SHIP-1 using the allosteric modulator was identified as inhibiting proliferation and causing apoptosis of multiple myeloma cells (323)). However, the reduced proliferation observed using a SHIP-1 inhibitor correlated with the results herein using shRNA silencing of SHIP-1, and point to a crucial role of the phosphatase activity rather than the scaffolding/adaptor functions of the protein. The possible reasons for the reduced proliferation of cells upon silencing of SHIP-1 are summarised in Figure 9.1.

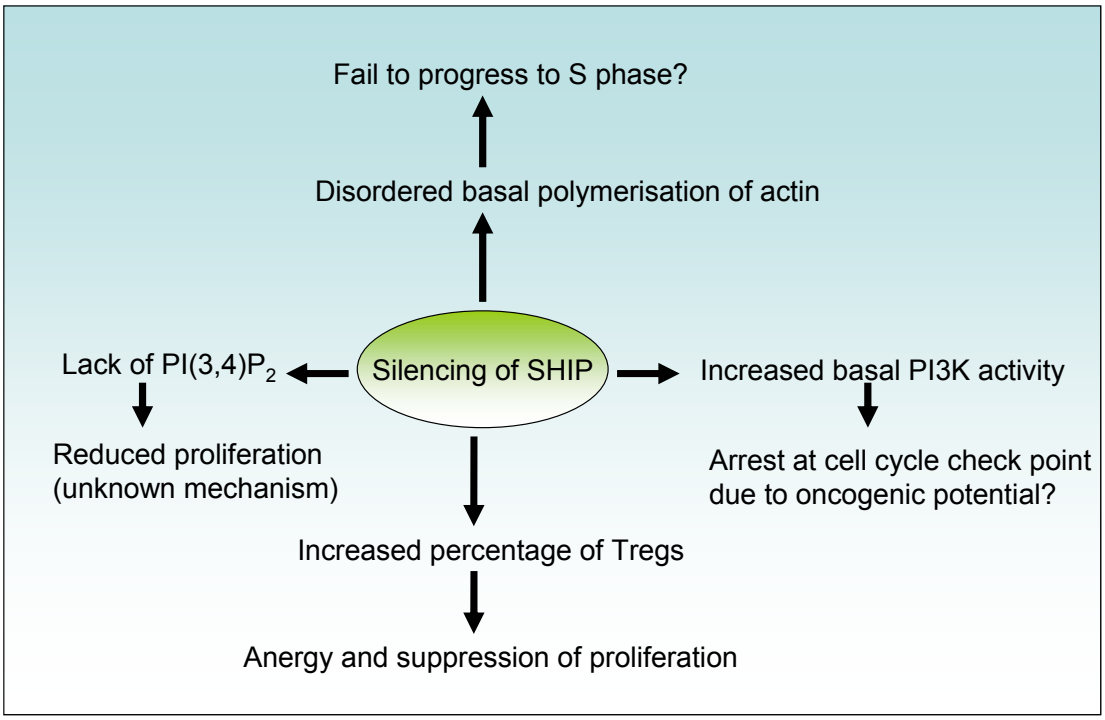

Figure 9.1 Model for decreased proliferation upon silencing of SHIP-1

9.9 PI3K signalling in the absence of stimulation and in response to the CD3 stimulatory antibody UCHT1 is increased by SHIP-1 silencing

In addition to the verification of SHIP-1 silencing at the protein and mRNA levels, the effects of SHIP-1 silencing were characterised by the effect of proximal targets, both basally and upon stimulation. The simulation used was UCHT1, an anti-TCR antibody, as this had been previously found to induce strong phosphorylation of SHIP-1. An optimal concentration of UCHT1 was determined by examining AKT phosphorylation by western blot, and a concentration of 10µg/ml was decided upon. To this end the effect of $PI(3,4,5)P_3$ levels was investigated, and it was found that silencing of SHIP-1 led to a basal increase in $PI(3,4,5)P_3$ levels, which were further increased upon TCR stimulation. This was a somewhat surprising finding, as previously it was thought that PTEN regulated the basal levels of PI3K activity, whereas SHIP-1 would influence the receptor induced PI3K response (136). However, close examination of western blots of phosphorylated SHIP-1 presented in the first results section reveals that there is a basal level of SHIP-1 phosphorylation which can be abrogated by use of the Src kinase inhibitor PP2. This would also suggest that there is some basal activity of SHIP-1. An analysis of basal levels of $PI(3,4)P_2$ was also attempted, however this was not possibly due to the anti-$PI(3,4)P_2$ antibody cross reacting with $PI(3,4,5)P_3$. An alternative approach would be to use a radioactivity based assay. However due to the methodology used to generate the SHIP-1 silenced cells, and their subsequent non-proliferation, it was deemed impractical to generate sufficient cells for this assay.

9.10 Phosphorylation of Akt and downstream targets is increased by silencing of SHIP-1

The next step was to investigate the effects of the increased $PI(3,4,5)P_3$ levels on the downstream signalling targets Akt, GSK3β and p70S6K. This was performed using an MSD mesoscale plate. It was decide to investigate signalling in response to TCR stimulation over a timecourse using the optimal concentration of UCHT1 decided upon in the previous experiment. Again it was observed that basal phosphorylation was increased in all three proteins, and they responded to TCR stimulation with a further increase in phosphorylation, but without changes in kinetics compared to the controls. Again this was in agreement with the results from the $PI(3,4,5)P_3$ assay, suggesting a major role for SHIP-1 in regulating basal PI3K activity. The timecourse

was confirmed in the novel assay (427) using a timecourse in control cells by western blot, which was found to be in agreement. This result was also verified by western blotting at single timepoints using SHIP-1 silenced cells, where again, levels of basal phosphorylation of Akt were found to be increased. The response to CXCL11 was also examined, and again the increase in Akt phosphorylation was observed to be at the basal state rather than further phosphorylation being induced upon receptor stimulation. ERK phosphorylation was also investigated as there is some evidence of cross regulation of MAPK pathways. There was evidence of a weak upregulation of basal ERK phosphorylation. It has been suggested that SHIP-1 could negatively regulate the MAPKp38 pathway and activation of SHIP-1 leads to a decrease in ERK phosphorylation (428). Furthermore, SHIP-1 has been shown to negatively regulate Tec, thus inhibiting the PLCγ pathway (429). SHIP-1 is thought to negatively regulate MAPK signalling independent of its phosphatase action on the PI3K pathway (430) and these results highlight the importance of SHIP-1 as an adaptor molecule. However, evidence from the T cell specific knockout mouse indicated that SHIP-$1^{-/-}$ T cells could signal normally in terms of ERK and Akt phosphorylation when stimulated with anti-CD3 or anti-CD3 plus anti-CD4. Calcium flux in response to CD3 was also unaffected. In contrast it was reported in using T cells from whole animal SHIP-$1^{-/-}$ mice that calcium flux in response to SDF was potentiated (360).

In agreement with findings in murine SHIP-$1^{-/-}$ neutrophils (293), splenocytes and thymocytes (360), basal polymerisation of actin was found to be increased when SHIP-1 was silenced in primary human T cells. Furthermore, the actin was not localised to discrete areas of the cell surface membrane as it was in the controls, lending further credence to the idea that SHIP-1 may by constitutively, if at low levels, present at the cell surface membrane, where it can regulate actin organisation, both through regulation of $PI(3,4,5)P_3$ levels and though its specific products. For example, TAPP1, which is recruited to $PI(3,4)P_2$ via its PH domain, binds synotrophins and controls actin polymerisation (431). This could have important repercussion for the cell as actin controls a range of processes from chemotaxis to cell division, to exocytosis. This would have serious implications for the functions of the cells, which were therefore investigated in the following results section.

9.11 Cell morphology and expression of adhesion molecules, but not adhesion, are altered by SHIP-1 silencing

The finding that SHIP-1 silenced cells lacked microvilli, as determined by SEM had important implications. Microvilli collapse has previously been reported in the literature in response to chemokine stimulation, a finding replicated here using CXCL11. The purpose of this has been hypothesised to be to allow firm adhesion and flattening of the cell during chemotaxis. Initial adhesion is due to adhesion molecules expressed on the tips of microvilli binding to their ligands. Upon stimulation, a Rac1 mediated dephosphorylation of ERM proteins occurs causing the dissociation of actin from the cell membrane. It would be logical that PI3K could drive the activation of Rac1 in this circumstance and therefore that silencing of SHIP-1, through an increase in PI3K signalling, would lead to microvilli collapse. It was therefore surprising that the morphology could not be rescued with LY294002. This suggested that SHIP-1 might further regulate the activation of Rac though its non catalytic actions (Figure 9.2). For example in B-cells and possibly T-cells, SHIP-1 binds Shc and in doing so prevents Shc's association with Grb2. In this way SHIP-1 inhibits Ras (432, 433) and thus could also downregulate Rac activation (434). Indeed, others have reported that SHIP-1 further regulates Rac activity though its non catalytic actions (435).

Rac activation has previously been shown to have both PI3K dependent and independent components (352, 354). It has also been shown that there are complex feedback loops between PI3K and Rac (436). In keeping with the idea that activation of PI3K signalling could lead to microvilli collapse, it was seen that LY294002 on its own did not affect cell morphology, but that bpVphen (which leads to an increase in $PI(3,4,5)P_3$ and $PI(3,4)P_2$ (338, 437-439)), did cause moderate loss of microvilli. However, it was seen that SHIP-1 silenced cells could polarise normally upon exposure to chemokine. Images captured at a lower magnification also revealed a diversity of cell morphologies within each treatment group, highlighting one of the drawbacks of SEM and confocal microscopy in that a "representative" cell is very much subject to interpretation.

To further investigate whether there was a Rac1 mediated ERM dephosphorylation occurring, confocal microscopy was undertaken with staining for both polymerised

actin and pERM. This allowed identification of pERM in microvilli tips and confirmed its loss from SHIP-1 silenced cells and those exposed to chemokine. The Rac1 inhibitor NSC23766 (440, 441) was then used in an attempt to restore ERM phosphorylation. This was moderately successful, as determined by the confocal microscopy and quantified by flow cytometry, confirming that Rac1 played a part in the loss of ERM phosphorylation seen in SHIP-1 silenced cells. However it did not fully restore levels to that of control cells, not did it restore microvilli. This leads to a number of possible hypotheses. Firstly the Rac inhibitor may not be at a high enough concentration to control Rac1 activity as tightly as in WT cells. Secondly, the Rac inhibitor on its own caused morphological defects in the control cells and over longer periods (results not shown) led to cell of an unhealthy appearance as assessed by flow cytometry, which may have adversely affected the cells' ability to reconstruct microvilli. Thirdly other SHIP-1 dependent processed may be required for not only preventing the loss of the microvilli but also their construction (or reconstruction) (149). Certainly, this assay revealed complex underlying defects in the SHIP-1 silenced cells under resting conditions, although again, their response to stimulation appeared normal.

A lack of phosphorylated ERM in SHIP-1 silenced cells, along with an inability to completely recover phosphorylation using a Rac inhibitor, indicated that expression of ERM at the protein level could have been reduced by silencing of SHIP-1. However, this was ruled out by confocal microscopy and flow cytometry for the total protein. Confocal microscopy indicated that the majority of ERM in control cells was located in microvilli on the cell surface, whereas in SHIP-1 silenced cells it was distributed throughout the cell. The observation that ERM was membrane localised and enriched at the leading edge and the uropod upon chemokine stimulation, has been previously reported in the literature (442) and this localisation is reported to aid polarisation of lymphocytes.

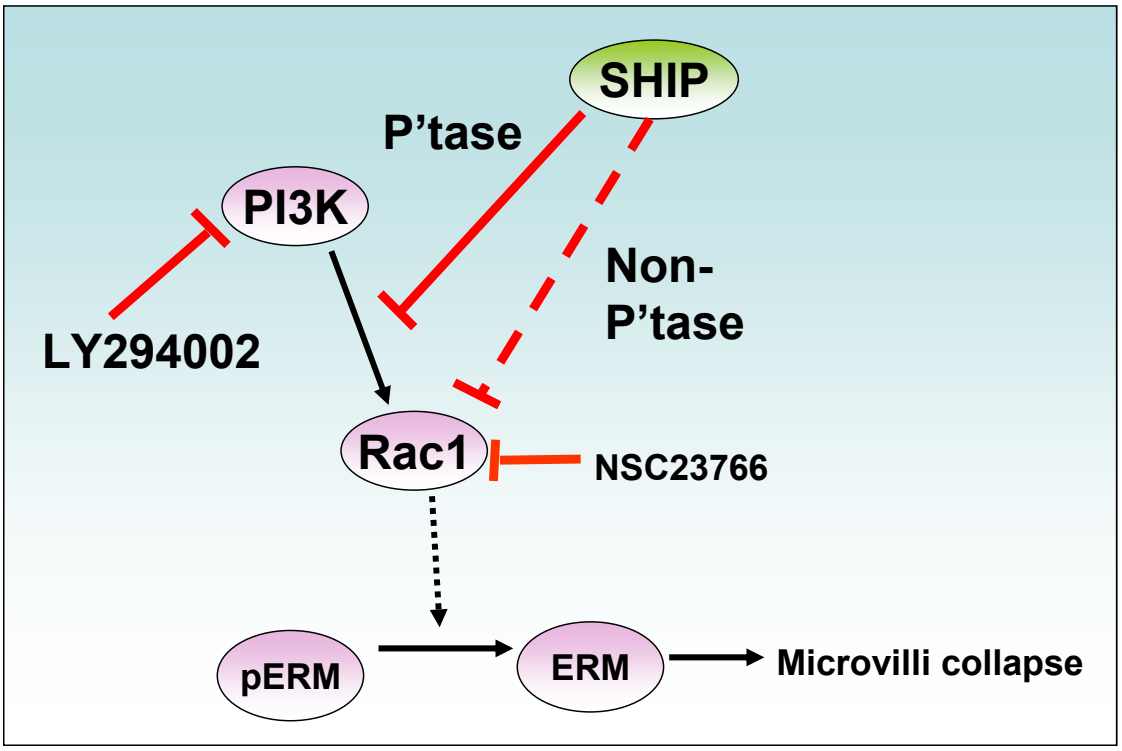

Figure 9.2 Model for microvilli loss

PI3K can activate Rac1 and lead to the dephosphorylation of ERM and hence microvilli collapse. SHIP-1 is an important regulator of basal PI3K activity through its phosphatase activity (P'tase). LY294002 can also inhibit PI3K activity and thus limit Rac1 activation. However, SHIP-1 can also regulate Rac1 activity through its non phosphatase functions (for example by competing for binding sites with other SH2 domain containing signalling proteins). Rac1 activity can also be inhibited by the compound NSC23766.

Following on from this it was decided to investigate further what effect the loss of microvilli might have on the cells, by examining the expression of two adhesion molecules. CD11a forms part of LFA-1, which binds to ICAM1-3, and is key in initial tethering of T cells during migration to sites on inflammation and in making initial contact with antigen presenting cells. It is capable of initiating inside out signalling and is also the target for Efalizumab. CD49d forms part of VLA-4 and binds to VCAM and fibronectin (356, 443). VLA-4 is preferentially localised to the microvilli tips and to membrane ruffles of lymphocytes (444, 445) and whilst there are some reports of LFA-1 having this localisation, it is generally agreed that it localises to the main cell body (446, 447). As it had been previously observed using SEM and confocal microscopy that microvilli were lost from the SHIP-1 silenced cells, it was therefore surprising that CD11a but not CD49d was downregulated, although defects in inside-out signalling may play a role (448) (350, 351, 449) (355). Other researchers have shown that overexpression of full length SHIP-1 had no effect of expression of LFA-1 but increased the activation of LFA-1, so that LFA-1-mediated adhesion to ICAM-1 was increased in a manner which was dependent upon SHIP-1's phosphatase activity (450).

Following on from this it was important to address whether SHIP-1 silenced cells could adhere normally. Two different surfaces were used: fibronectin (357) is a dimer that can be present in the plasma or as part of the extracellular matrix and can be adhered to by many different integrins including VLA-4 (α4β1) (358), whilst ICAM1 (CD54) is present of leukocytes and the endothelium and is bound by LFA-1 (αLβ2)(359). These two adhesion molecules were selected as they are thought to be important at different stages of adhesion during transendothelial migration. It was found that, despite lower levels of LFA-1 being expressed on the surface of the SHIP-1 silenced T cells, there was no difference in the adhesion to either fibronectin or ICAM1, and there was even a trend towards increased adhesion. Furthermore, the ability to adhere to fibronectin was similarly enhanced in control and SHIP-1 silenced cells when in the presence of either CXCL11 or UCHT1. The fact that a decrease in LFA-1 did not affect adhesion is probably due to the fact that a loss of microvilli allows easy adhesion of a large surface area of the cell body. Similarly, the results in the previous section have indicated that signalling in response to both CXCL11 and UCHT1 are largely intact following silencing of SHIP-1. Obviously, in physiological conditions, the cells would be attempting to extravasate under flow and shear stress, at which point, the absence of microvilli might become more relevant (87, 451). It is

worth noting that higher percentages of adhesion have been reported in the literature (331) in response to stimulation, however the assay in its present form was adequate for the purpose.

9.12 Expression of CXCR3 is unaffected by SHIP-1 silencing in CD4+ but is reduced in CD8+ T cells

It was thought desirable to investigate chemotaxis in light of the morphological changes observed in the cells and the known involvement of PI3K and Rac signalling in chemotaxis (286). In the T cell specific SHIP-1 KO, it was reported that levels of Tbet were increased in CD4+ (183). As PI3Kγ and the transcription factor Tbet have also been shown to drive expression of CXCR3 in both CD4 and CD8+ T cells (452), it was important to verify CXCR3 expression levels before proceeding with chemotaxis to CXCL11. However, flow cytometric analysis did not detect an increase in CXCR3 levels in CD4+ (consistent with observations in the next chapter that these CD4+ cells are not skewed towards Th1, nor do the CD8+ show an increase in toxicity). However, the CD8+ T cells did show a decrease in CXCR3 expression. It is less clear how CXCR3 expression is modulated on CD8+ T cells, as it is not driven by IFNγ and STAT1 signalling as it is in CD4+ T cells (453).

9.13 Basal motility but not chemotaxis, is reduced by SHIP-1 silencing.

Initial investigations into chemotaxis utilised the neuroprobe chemotaxis assay (286) in which cells migrate through pores in a membrane into a lower chamber with chemokine in it. By varying the concentration of chemokine in the chamber it is possible to get a classic bell shaped dose response curve. In addition, some of the cells will migrate in the absence of chemokine, due to their basal motility. By using a membrane with 5μm diameter pores, the T cells are required to actively distend as they move towards the chemokine, in the same way as when they pass between endothelial cells to exit the blood. In this assay it was noted that there was a defect in the basal motility of SHIP-1 silenced cells. The role of PI3K in chemotaxis has been debated; however it is known that PI3K signalling is biased towards the leading edge of chemotaxing cells where it is thought to contribute to the generation of pseudopods but not directional sensing (287). The reduction in basal motility found in SHIP-1 silenced T cells is in agreement with PTEN knockouts in *Dictyostelium* which can chemotax in response to stimuli, but lack basal motility because competition between emerging pseudopods cannot be resolved without $PI(3,4,5)P_3$ gradients

(454, 455). Furthermore, findings were in agreement with SHIP-1$^{-/-}$ neutrophils, which were reported to have a higher level of basal actin polymerisation and a reduction in basal motility but to chemotax normally to fMLP. In the neutrophils, SHIP-1 was required to regulate polarity and motility, but not directionality (344). This was in contrast to finding using SHIP-1$^{-/-}$ T cells, which exhibited normal basal motility but increased chemotaxis to CXCL12 (SDF-1) (360).

Chemotaxis is a complicated process, with PI3K signalling and other pathways frequently fulfilling redundant roles (456). Therefore it was not surprising that the cells could still detect the chemokine and move towards it in a concentration dependent manner. Indeed this was in agreement with the findings of others, whereby in freshly isolated T cells, PI3K is required for both basal migration and movement towards chemokine, but upon activation, only basal migration has a PI3K-dependent element (286) (chemotaxis of CD8+ T cells has been shown to be dependent on PI3Kγ (457)).

The next assay used to investigate chemotaxis used videomicroscopy as described elsewhere (206). In this assay cells chemotax across a fibronectin coated surface towards a chemokine gradient. It might be imagined that this would be more analogous to an earlier stage of chemotaxis *in vivo* when lymphocytes crawl or roll along the endothelium (451). However, this assay again replicated the findings of the neuroprobe assay, with a decrease in basal migration. Analysis of individual tracks allowed confirmation of findings in neutrophils (293) and the neuroprobe chemotaxis assay, as during basal motility both total and Euclidean distance were reduced as well as velocity. Therefore the effect of SHIP-1 silencing was on motility rather than directionality (i.e. the cells were not just going around in circles, which would have resulted in decreased Euclidean distance without affecting velocity or total path length). During chemotaxis to chemokine, this reduction in basal motility impinged upon the Euclidean distance and when the data were expressed as indices (fold change from respective basal figures), it was observed that the Euclidean Index was unaffected by silencing of SHIP-1, as had been observed with the chemotatic index in the Neuroprobe assay. Interestingly the accumulated distance and velocity during chemotaxis were not affected by silencing of SHIP-1 and therefore there were increases in the accumulated distance index and velocity index, possibly indicating a defect in directionality during chemotaxis. A logical next step for this assay would be to investigate under flow conditions (458) when, as mentioned previously, a lack of

microvilli might make a crucial difference to initial tethering the endothelial cells or fibronectin.

Use of the two systems for analysing chemotaxis was of benefit because not only could two different chemotactic behaviours be examined, but also, a balance could be struck between gaining information on a large number of cells, and being able to observe small changes in the behaviour of individual cells.

9.14 Localisation of fluorescent reporters and phosphorylated SHIP-1

The next results section examined the localisation of $PI(3,4)P_2$ by its ability to recruit a GFP tagged TAPP PH domain. It had been expected that some of the defects observed in the chemotaxing cells might be due to a lack of $PI(3,4)P_2$ in the polarised cell. Proteins with PH domains that preferentially bind $PI(3,4)P_2$, including TAPP1 TAPP2 and BAM32, have been shown to have key roles in B and T cells (459). For example, TAPP1 binds synotrophins and controls actin polymerisation (431).

It was somewhat surprising that the fluorescent TAPP PH domain proteins showed relatively weak localisation upon cell stimulation. bpVphen has been shown by others to cause the generation of $PI(3,4)P_2$ (388) and in the first results chapter, caused phosphorylation of SHIP-1 in primary human T cells. Therefore it would be expected to cause membrane recruitment of the probe. Similarly there are extensive reports of PI3K and SHIP-1 activity in motile cells, even when this pathway is not required for their movement (85). Moreover, SHIP-1 has been reported to localise to the sides of the chemotaxing cell, confining $PI(3,4,5)P_3$ to the leading edge and causing the accumulation of $PI(3,4)P_2$ at the sides of the cell (293), whilst TAPP1 and TAPP2 are localised to membrane ruffles in lymphocytes (460). Instead these experiments indicated that the $PI(3,4)P_2$ domain probe localised to the leading edge and emerging pseudopods. Due to the weak expression of the probes, a 1µm pinhole was used to capture fluorescence, and this may have been too broad to capture membrane localisation, particularly when cells were flattened during chemotaxis.

The finding that the mutant TAPP PH was excluded from the nucleus, whereas the WT TAPP PH appeared fairly uniform throughout the cell was unexpected. There is some evidence of nuclear localisation of $PI(3,4,5)P_3$, which may explain why the AKT PH domain probe was not excluded from the nucleus under resting conditions (461). Previous work has identifies $PI(3,4)P_2$ as being enriched at the cell surface membrane in response to growth factor stimulation of exposure to hydrogen peroxide, and it has also been identified on intracellular organelles such as the ER and endosomes. A small percentage was also detected on the nuclear envelope and in the nucleus (386). As this work was done in Swiss 3T3 cells (mouse embryonic fibroblasts), species and cell differences may account for the higher nuclear localisation of TAPP-PH seen in the primary human T cells. However, others have found that whilst TAPP reporter proteins can be detected in the nucleus in resting cells, they translocate to the membrane upon stimulation (460). An alternative explanation was that the GFP or RFP may be cleaved from the wildtype PH domain. This could be verified by western blotting for GFP at the expected molecular weight for the tag and PH domain. However, low levels of transient transfection meant that this was not an option. The alternative would be cloning of all reporters into a lentiviral expression vector.

The weak localisation of the $PI(3,4)P_2$ domain binding probes during chemotaxis was further investigated using confocal microscopy to identify the localisation of phosphorylated SHIP-1 in chemotaxing cells. Unexpectedly pY^{1020} SHIP-1 also lacked membrane localisation in cells exposed to CXCL11. These findings were in contrast to the results in the first results chapter, whereby H_2O_2 stimulation of CEMs led to a very convincing membrane localisation of phosphorylated SHIP-1. However, staining of phosphorylated SHIP-1 itself during chemotaxis (as opposed to its lipid product) has not been reported in the literature. There was some localisation of SHIP-1 to emerging pseudopods, in agreement with the distribution of the TAPP PH domain probe. There is some evidence that once phosphorylated, Akt can detach from the cell surface membrane, and translocated to the cytosol or the nucleus, where it retains its kinase function (462-464). It could be hypothesised that a similar process may occur with phosphorylated SHIP-1, or alternatively it may be trafficked along with other proteins that are bound by its adaptor domains.

9.15 Silencing of SHIP-1 leads to an increased percentage of iTreg cells

Exposure to lentivirus led to an increase in the percentage of cells that were CD25 positive. CD25 in the high affinity chain of the IL-2 receptor, which is upregulated upon T cell activation. It is also a marker for Tregs. As lentiviruses preferentially infect activated and rapidly proliferating T cells, it is likely that the puromycin selection of infected cells has selected for cells that are CD25 positive, explaining the increase in the percentage of CD25 positive cells seen in with shRNA control. The increase in CD25 expression per cell seen upon SHIP-1 silencing could have been an attempt to overcome reduced proliferation by increasing IL-2 signalling, or due to an increased percentage of Tregs. The situation regarding Tregs and SHIP-1 is not clear. In the original SHIP-1 knockout mice and increase in Tregs was observed and the Tregs were found to be functional. However, in the T cell specific knockout mouse no increase in Tregs was observed, and therefore the increase observed in the whole animal knockout was attributed to an attempt to inhibit the substantial inflammation that was caused by loss of SHIP-1 in other immune cells. However, a later study found an increase in T regs when naive cells from SHIP-1 knockout mice were culture *in vitro* indicating that a loss of SHIP-1 could predispose to Treg differentiation in a cell-intrinsic manner (194). Interestingly, there is also an increase in myeloid suppressor cell number *in vivo* upon loss of SHIP-1 (260).

Staining for foxp3 allowed the identification of the $CD25^{high}$ population as being iTregs, whose percentage was increased three fold by silencing of SHIP-1. This is probably why there is a decrease in proliferation of the SHIP-1 silenced cells as Tregs proliferate less than other Thelper cells an also inhibit the proliferation of other T cells. The exact role of iTregs in the human body has not been determined. *In vivo* they develop in response to suboptimal antigen presentation or in longstanding inflammation. The main role of iTregs is to establish tolerance, both to external and self antigens. It has been hypothesised that iTregs are key to maintaining a non-inflammatory environment in the gut and control of allergies, but may also prevent destruction of tumours (465).

iTreg differentiation is driven by IL-2, and can also be facilitated by TGFβ and retinoic acid (466). This allows the generation of iTregs to be in balance with Th17

differentiation in which TGFβ directs Th17 generation but only in combination with IL-6 (467). The balance between the two has been shown to be altered by the presence of SHIP-1, with SHIP-1$^{-/-}$ T cells being more prone to differentiation to Tregs *in vitro* and failing to become Th17s (186). Interestingly, inhibition of the mTOR pathway has been shown to increase the percentage of Treg cells in culture (468). Subsets of iTregs can produce IL-10 and TGFβ, although these do not express foxp3. However, much of the mechanisms for iTreg mediated suppression remain poorly defined although they are generally thought to be antigen independent but contact dependent (469). These include CTLA-4 expression, adenosine production, transfer of cAMP to target cells, and LFA-1 interaction with DCs (470, 471). It has also been postulated that they may compete for cytokines such as IL-2, thus depriving other cells and contributing to their reduced proliferation and even to apoptosis (472). However it has been demonstrated that human iTregs do not induce apoptosis of effector T cells (473) and in any case this would be unlikely to be a major mechanism in the experimental set up used here, as IL-2 is present in high quantities.

The results herein were therefore in keeping with those reported in murine T cells (186). Furthermore, the suppressive effects of Tregs probably account for the decrease in proliferation observed in SHIP-1 silenced cells. However, it was also observed that there was not a reciprocal decrease in cytokine production under Th0 conditions, which would have been an expected outcome of having a high percentage of Treg cells. It has been reported that Tregs' mechanism of suppression of cytokine production does not involve induction of anergy related genes in target cells which are known to inhibit TCR signalling (474). Therefore it is possible that human SHIP-1 silenced Tregs have some defects in their functions. In support of this was the finding that LFA-1 expression on the SHIP-1 silenced cells was in fact reduced, suggests that they were not fully effective in all capacities (470). Furthermore it has been demonstrated in several circumstances that foxp3^{+} cells can also secrete "effector" cytokines such as IL-17 (53). This possibility could be addressed through further dual staining experiments. It would be interesting to extend this study to cover skewing to Treg phenotype, and also to investigate the suppressive functions of these cells on target cells from the same donor.

An insight into the role of SHIP-1 in the generation of Tregs and Thelper populations can be gleaned from work done on miR155. In T cells, miR155 expression is high in

Tregs and activated T cells, but not in resting T cells. Bic/miR155$^{-/-}$ murine T cells can skew normally to Th1 and Th2, but under non-polarising conditions, produce more IL-4 and IL-10 but less IFNγ than WT cells (475). In Tregs expression of mir155 is regulated by foxp3 but conversely, a lack of miR155 causes a decrease in Treg numbers (476, 477). Loss of miR155 did not increase Treg activation induced cell death, but proliferation was decreased. These cells had a decrease in IL-2 signalling due to increased SOCS1 expression leading to attenuated STAT5 signalling (478). The fact that SHIP-1 is suppressed by miR155 contributes to an understanding of why high miR155 or loss of SHIP-1 both facilitate Treg generation.

9.16 Th1 cytokines are aberrantly controlled when SHIP-1 expression is silenced

IFNγ is considered to be the signature Th1 cytokine, responsible for many of the functions of Th1 cells, including their antiviral and anti-tumour activities. In the literature it is reported that knockout of SHIP-1 results in an increase in skewing towards a Th1 phenotype, due to increased levels of T-bet, the transcription factor required for Th1 differentiation. In agreement with this, in human cells it was observed that under Th1 conditions an increased percentage of cells stained positive for IFNγ. It was therefore unexpected that there was a trend towards a reduction in the levels of IFNγ in Th1 culture supernatants by silencing of SHIP-1. One possible explanation of this is a defect in secretion of IFNγ by SHIP-1 silenced cells. In general, cytokines are not thought to be stored by T helper cells (although they are stored in granules in CD8+ cells), however very little is known about their mechanisms of trafficking to the cell surface membrane and their release. Yet SHIP-1 has been recently identified as being present on the ER, where it facilitates glycosylation of CD95 (334). Similarly the non-significant reduced production of IL-1β, IL-8 and TNFα may also be attributable to defective release. However, it may also be due to decreased levels of IFNγ in the culture supernatant being insufficient to initiate production of these cytokines.

Defective secretion of IFNγ, rather than an inability to polarise successfully, or experimental error, is further supported by the observation that production of IL-12p70, a cytokine which initiates Tbet activation and skewing to Th1 as well as driving IFNγ production, is normal in SHIP-1 silenced cells. No firm conclusions as to

the effect of SHIP-1 silencing on IL-2 production could be drawn as the levels produced varied so much between donors. However, it did appear to be suppressed in Th2 conditions compared to Th0 or Th1 conditions.

9.17 Th2 cytokines are aberrantly controlled when SHIP-1 expression is silenced

Expression of IL-10 which may be produced by either Th2 or Treg populations, was unaffected by silencing of SHIP-1. Yet an apparent dichotomy was revealed with the other three Th2 cytokines, with increased production of IL-4 but a trend towards decreased production of IL-5 and IL-13. SHIP-1 knockout mice are prone to a Th2 type inflammation, with extensive leukocyte infiltration into the lungs (182). However in a study of mice with genetic ablation of SHIP-1 confined to the T cell compartment, Th2 responses were decreased, as the mice were skewed towards Th1 responses due to raised levels of Tbet (181). Therefore it was counterintuitive that IL-4 levels should be raised in human knockout, although the fact that the cells have been given the opportunity to develop in the thymus normally may have a bearing.

The genes for IL-4, IL-5 and IL-13 are located in a cluster on the same chromosome and are generally regulated together (479). However, in this case the effect also appeared to be promoter specific as levels of IL-5 and IL-13 were reduced. In support of this there is substantial evidence that IL-4, IL-5 and IL-13 are differentially regulated. It has been demonstrated that an NF-AT/AP-1 binding site is located in the IL-4 promoter, but additional elements are also required to drive IL-4 expression (480). Furthermore, c-maf has been shown to bind a c-maf response element in the IL-4 promoter (481). GATA3 has only a moderate effect on the proximal IL-4 promoter but acts on other genomic regions to enhance IL-4 transcription (482). IL-5 production can be driven by activation of GATA3 alone, and if GATA3 levels are reduced then that is sufficient to repress IL-5, but not IL-4 production (483). Other GATA-3 related factors are also involved in IL-5 expression (484). It has further been demonstrated that although IL-13 can also be induced by GATA-3, IL-13 is regulated by different pathway from IL-4, and that individual Th2 cells will not necessarily coexpress IL-4 and IL-13 (26).

9.18 Th17 cytokine production is aberrant upon silencing of SHIP-1

The role of PI3K in Th17 generation and IL-17 production has not been extensively assessed. However, we have found that genetic loss of PI3Kγ or its catalytic activity increases production of IL-17A and IL-17F in mice (Chapter 8), but that this effect was not reproducible using pharmacological inhibitors of PI3Kγ despite the reported plasticity of Th17 populations. In addition, Locke *et al.* reported that genetic knockout of SHIP-1 in mice leads to a block in Th17 development, and a reciprocal increase in Treg development due to defective IL-6 signalling, which was observable *in vitro*. This is in line with the findings of others, who report that IL-6 switches the signal of TGFβ from differentiation of Tregs to development of Th17s (485). Clearly this runs counter to the findings here, however, in a T cell specific SHIP-1 knockout, Tarasenko *et al.* found no increase in IL-17 production or in abundance of Th17s (183). In addition Locke *et al.* demonstrated that the naive SHIP-1 deficient T cells immediately showed a decreased ability to respond to IL-6 with STAT3 phosphorylation, indicating that SHIP-1 may play a role in the very early stages of skewing (186). Therefore the protocol required with human cells, whereby the cells are activate under skewing conditions and then infected with lentivirus, which takes several days to eliminate SHIP-1 at the protein level, may be too lengthy to influence Th17 skewing. Unfortunately, due to the endogenous presence of TGFβ in the culture media it would not be feasible to initiate Th17 skewing after SHIP-1 had been silenced, as in the absence of IL-6 it would bias towards the generation of Tregs. Furthermore, the exact role of TGFβ in human Th17 generation is very controversial (reviewed (486)) and for this reason it was not additionally supplemented to the culture media of Th17, although initial results in our lab have indicated that it can increase IL-17 production (not shown).

Locke *et al.* suggest that an increase in STAT5 phosphorylation and a concomitant block in STAT3 phosphorylation is responsible for decreased Th17 skewing in SHIP-1 silenced T cells (186). To further clarify the transcriptional events in the SHIP-1 silenced human T cells, STAT3 phosphorylation was therefore examined. However when STAT3 phosphorylation was assessed in SHIP-1 silenced T cells there was no difference in levels of STAT3 phosphorylation between shRNA control cells and SHIP-1 shRNA treated cells. Locke *et al.* demonstrated that in freshly isolated murine T cells, loss of SHIP-1 results in reduced STAT3 phosphorylation in response to IL-6,

and SHIP-1 has been shown to be a key regulator of IL-6 signaling (420). However, it should be noted that IL-6 signalling in activated T cells is somewhat controversial, as some groups have reported that whilst IL-6 receptor expression is reduced on activated T cells, they are still present at sufficient levels to initiate STAT3 phosphorylation (487), whereas others find that receptor levels are insufficient to support signalling, and that signalling relies upon soluble receptor (trans-signalling) (488-490). However, consistent with the notion that IL-6 receptor expression is lost upon activation of T cells and that responsiveness to IL-6 in these cells is due to IL-6 trans signalling, no increase in STAT 3 phosphorylation was seen in response to IL-6.

9.19 CD8+ cytotoxicity is not enhanced by silencing of SHIP-1

Under physiological conditions, CD8+ T cells that have been activated, develop the ability to kill other cells, i.e. they are cytotoxic T lymphocytes (CTLs). When the CTL's TCR recognises a target, it rapidly releases perforins and granzymes that have been stored in granules, and these kill the target cell. They can also initiate Fas-mediated killing of target cells (491). PI3K is involved in CTL degranulation but not Fas mediated killing (492). It thought that it contributes to degranulation via a PKCθ/ RasGRP/Ras/ERK/paxillin pathway. Paxillin is an adaptor protein that facilitates recruitment of proteins to actin at the cell surface membrane, although its exact role in cytotoxicity is unclear (493). Others have shown that PI3K does not play a role in CTL perforin mediated lysis but instead regulate FasL expression (370). These results correlate better to the findings in this thesis, where short (1 hour) preincubations of CD8+ T cells with wortmannin, LY294002 or ZSTK474 all failed to alter their ability to kill target A20 cells.

It has previously been reported in the literature that murine CD8+ T cells have increased cytotoxicity when SHIP-1 is knocked out. This is due to increased levels of Tbet leading to enhanced granzyme B activity (183). However, the same effect was not found when expression of SHIP-1 was silenced in human T cells. Instead, the percentage of target cells killed was slightly reduced. Whilst the set up of the assay appeared valid, with efficient killing of the cells only in the presence of both CD8+ T cells and UCHT1, the protocol is obviously substantially different from that used in murine cells and therefore the mechanisms may be different. In addition, it was observed that a higher proportion of the SHIP-1 silenced cells were staining positive

for annexin by the end of the assay. Therefore their cytotoxic function may have been compromised by their death. It is not clear what would have triggered the cell death, although it would possibly have been contents released from dying A20 target cells.

Interestingly, in murine NK cells, it has been found that loss of SHIP-1 decreases cytotoxic activity (494). However, this is due to disruption of their receptor repertoire, with expression of an inhibitory receptor, 2B4, being favoured and the situation is different in human NK cells (495), where 2B4 is an activating receptor.

9.20 Final discussion on the role of SHIP-1

The role of PI3Ks in cell function has been extensively investigated in recent years, particularly as they have shown much promise as drug targets in inflammation and cancer. Yet SHIP-1, despite its key function in the PI3K pathway in immune cells, remains poorly understood, with even less attention being paid to its scaffolding function. Whilst a whole mouse SHIP-1 knockout and a T cell specific knockout mouse have been generated, and some research has been done in human leukaemic cell lines, this thesis is the first investigation into the role of SHIP-1 in primary human cells, and focuses in particular on its role in T cells.

The first set of experiments examined and reconfirmed a variety of stimuli as activators of SHIP-1, and also extended previous work into the role of SHIP-1 in leukaemic cell lines. It was found that expression of the SHIP-1 catalytic core can protect against cell death in response to oxidative stress and TRAIL. The aim of the second set of experiments was to investigate the role of SHIP-1 in primary cells. This involved the setting up and validation of a lentiviral expression system which is described in the first section of the results. This allowed the silencing of SHIP-1 expression without the low efficacy and seen using chemical methods or electroporation. This method allowed the introduction of a constitutively active SHIP-1 construct into T cells, which unfortunately resulted in unviable cells which were not suitable for further study. However, silencing of SHIP-1 yielded a considerable amount of data. Key findings were that silencing of SHIP-1 expression results in:

- No change in viability
- Decreased proliferation due to G0/G1 cell cycle arrest

- Increased levels of basal and receptor induced $PI(3,4,5)P_3$ as well as increased levels of AKT, GSK3β and p70s6K phosphorylation and actin polymerisation
- Loss of microvilli on the cell surface, probably due to Rac1-mediated ERM dephosphorylation
- Reduced cell surface expression of CD11a but not CD49d
- Reduced basal motility, without affecting on chemotaxis
- Increased expression of CD25 and foxp3, i.e. increased Treg generation
- Non-significant changes in ability to skew to Th1
- Increased ability to produce and secrete IL-4, the signature Th2 cytokine, but without increased IL-5 and IL-13
- Increased skewing to a Th17 phenotype
- Reduced ability of CD8+ to kill target cells

In addition, to complement the work on T cell chemotaxis, localisation of fluorescent PH domain probes was examined. However, whilst the Akt PH domain could localise to the cell surface membrane, the TAPP PH domain failed to do so. Therefore, an insight into SHIP-1's localisation during chemotaxis was not obtained.

Whilst some of these findings were in line with data from murine models, others, such as the decreased proliferation ran contrary to the findings in mice, and serve to highlight the fact that there are often substantial differences between the immune systems of mice and humans, and the importance of studying the role of proteins in human cells, even if the assays available are somewhat limited compared to animal models.

SHIP-1 now stands at a crossroads, with the first inhibitor of SHIP-1 recently reported in the literature (426) and an allosteric modulator in preclinical development (320), and scheduled to enter clinical trials in Q1 2011. At this point it will become clear whether the differences between the role of SHIP-1 in murine and human T cells identified in this thesis will be important, or whether its key role as a modulator of PI3K signalling transcends species differences.

9.21 Future work on SHIP-1

The work in this thesis has revealed much about the roles of SHIP-1 in human T cells, however, there are a number of areas that were particularly interesting and would benefit from further study. Firstly, the finding that loss of SHIP-1 expression

was inhibitory on proliferation and resulted in cell cycle arrest was somewhat counterintuitive and would benefit from further study. Examination of proliferation using a tritiated thymidine assay may aid an understanding of the process, as would assessment of expression and activation of cell cycle proteins key to the G1-S transition, such as cyclin A and cyclin E and their inhibitors.

The role of SHIP-1 in controlling cytokine production would also benefit from being investigated in more detail. In particular the defects in secretion of IFNγ, along with the reduction in either production or secretion of IL-5 and IL-13 should be investigated in more detail. There is some evidence that SHIP-1 can localise to the endosomes and be involved in the trafficking of proteins to the membrane, but further experiments would be required to verify this and to discovery whether this is the reason for changes in secretion patterns of cytokines. Furthermore, Th22 and Th9 subsets of CD4+ T cells have recently been identified, and it would be interesting to extend the current work to include these novel cell types.

In terms of chemotaxis, the studies herein could be expanded by cloning of a fluorescent $PI(3,4)P_2$ reporter into the lentiviral expression vector in order to understand the localisation of SHIP-1 within the cell during chemotaxis.

Finally, the effects of activation of SHIP-1 should be studied in more detail. The constitutively active construct could be successfully expressed in cell lines using a Tet-off promoter, but expression in primary cells using the lentiviral promoter was unsuccessful. Small molecule allosteric modulators of SHIP-1 activity have been described in the literature but are not commercially available. However some have questioned the presence of a second $PI(3,4)P_2$ binding domain and others have been unable to show allosteric enzyme kinetics, instead demonstrating classic Michaelis-Menten characteristics. Furthermore experience with ATP- competitive kinase inhibitors tells us that it is preferable to have a genetic model in parallel to a pharmacological approach, in order to identify possible off target effects of compounds. It may be possible to clone the CD2:SHIP construct into a lentiviral vector with a weaker promoter, but it would also be beneficial to investigate in greater detail the effect of overexpression of full length SHIP-1, including its adapter domains.

9.21 Discussion of the role of PI3Kγ in murine IL-17 production

The role of PI3Kγ has been dissected in great detail in terms of its functions in the immune system and inflammation and these results show a novel role for it in the suppression of IL-17A and IL-17F production. Previous work by Matt Thomas had shown that a genetic loss of PI3Kγ resulted in increased IL-17A both *in vivo* and *in vitro*, and in response to various stimuli despite otherwise normal cytokine production and proliferation. Knock in of a catalytically inactive PI3Kγ also caused increased IL-17 production, demonstrating that the kinase function rather than the structural role (496) is required for control of IL-17 production. This is the first reported involvement of PI3Kγ in IL-17 production, despite evidence that SHIP-1 and mTOR are required for development of Th17s and that AKT signalling impairs their generation (186) (164, 497).

It was hypothesised that IL-17A may have been produced in higher quantities by PI3Kγ$^{-/-}$ cells because it was not functional, for example due to abberant post-translational modification (99, 498) and could not activate a negative feedback loop. IL-17 induces the production of IL-6, IL-8 GM-CSF, matrix metalloproteinases and chemokines from a variety of cells, e.g. fibroblasts, keratinocytes, eosinophils, airway smooth muscle and epithelial cells (30, 499). Therefore, an assay which involved the production of IL-6 by mouse dermal fibroblasts in response to IL-17 was used to measure IL-17 functionality. This ruled out the possibility of non-functional IL-17 as the IL-17 in the supernatant was effective in inducing IL-6 production by MDFs.

Others have found that IL-17A and IL-17F regulate both their own and each others' production (383, 500, 501). It was therefore hypothesised that an excess in IL-17A could be due to a decrease in IL-17F failing to suppress its production, or as an attempt to raise IL-17F production. However, this was found not to be the case, as IL-17F levels were also elevated in cultures of PI3Kγ$^{-/-}$ T cells.

There is some evidence that Th17 expansion is counteracted by PI3K signalling (497, 502). However the kinetics of IL-17 production was the same in both WT and PI3Kγ$^{-/-}$ cells and no increased percentage of IL-17 positive cells was found by intracellular staining. Therefore, despite having no more Th17 cells, PI3Kγ$^{-/-}$ cultures produced more IL-17, due to a higher output per cell. This was in line with other findings in IL-17RA knockout animals, where an increase in the Th17 population was not seen in response to ConA stimulation. Instead there was an increase in mean intracellular staining for IL-17 in liver cells, particularly CD4+ cells in these animals. *In vitro* these CD4+ cells secreted 10-100 times more IL-17 than WT CD4+ and also had an increase in IL-17F production (382).

IL-17RA is a type 1 transmembrane protein (503) which is reported (generally on the basis of mRNA levels) to be ubiquitously expressed (504). Levels of surface expression vary considerably (505) although both CD4+ and CD8+ T cells express IL-17RA (506). It has been reported that IL-17RA associates with IL-17RC during IL-17A signal transduction and that IL-17RC is an essential part of the IL-17 receptor signalling complex (507) in both mice and humans. However, others report that in mice IL-17RC binds only IL-17F and not IL-17A (508). IL-17RA and IL-17RC are reported to play a role in a negative feedback loop whereby IL-17F homodimers signal through them to reduce production of IL-17A and IL-17F by CD4+ cells (382, 509). Similarly IL-17A has been reported to inhibit production of IL-17F (500) and of IL-17A itself (383). However others have postulated that that IL-17A and IL-17F are regulated by distinct pathways during Th17 differentiation (40) and it has recently been reported that TCR signalling induces IL-17A but not IL-17F signalling, by usitlising an Itk/NFATc1 pathway Moreover, IL-17A production could be reduced in WT cells by suboptimal TCR stimulation (510).

IL-17A is reported to downregulate the IL-17RA (506), however it has also been reported that PI3K signalling limits the expression of IL-17 receptors (506). The experiments in this thesis were in agreement with the latter theory, with loss of PI3Kγ resulting in an increase in IL-17RA expression. Levels of IL-17RC expression in particular were low and in line with the findings of others. It has been hypothesized that the failure of splenocytes to respond to IL-17 is due to low expression of IL-17RC expression (506).

The increased levels of IL-17RA expression in freshly isolated PI3Kγ$^{-/-}$ cells despite high levels of IL-17A suggested there might be a possible defect in either the negative feedback loop signalling and/or internalisation of receptors. Relatively little is known about IL-17R signalling as the receptors bear little homology to other known cytokine receptors (511, 512). The IL-17RA is reported to contain a SEFs (similar expression to fibroblast growth factor (FGF) genes) and interleukin 17 (IL-17) receptor (SEFIR) domain which is hypothesised to recruit PI3K (512). Furthermore, IL-17 receptors have been shown to recruit Ras (513) and activate MAPK and ERK signalling (512) or alternatively to negatively regulate Ras activity (514) IL-17RA also signals to NFκB and C/EBPβ, the latter involving GSK3β signalling (515). Intriguingly, although PI3K signalling is generally upstream of GSK3β, in this setting PI3K inhibitors had no effect upon this element of IL-17RA signalling (512). Others have hypothesised a role for PI3K in IL-17 receptor signalling (512) with reports of JAK-mediated PI3K signalling in response to IL-17A in human airway epithelial cells (516) and synovial fibroblasts (517). However, others have questioned whether IL-17 receptors are expressed at high enough levels on T cells to initiate signalling (506). Therefore signalling in response to both IL-17A and IL-17F was examined. IL-17A induced Akt phosphorylation in WT but not PI3Kγ$^{-/-}$ cells, thus demonstrating a novel mechanism by which IL-17RA signals via PI3Kγ in response to IL-17A (although not IL-17F). The subsequent increased IL-17A and IL-17F levels in PI3Kγ$^{-/-}$ animals may therefore be due to a dysregulated negative feedback loop for IL-17 production dependent on effective signalling through the IL-17RA receptor. These findings, and the possible feedback loop are illustrated in Figure 9.3.

Th17 profiles are thought to be fairly plastic (518), and the kinase-dead knock-in mouse reproduced the phenotype of the knockout mouse, indicating that it was the catalytic function of PI3Kγ that is required to regulate IL-17 production. However, the phenotype could not be reproduced using PI3Kγ inhibitors (data not shown) over the timescales used for the other experiments shown here. This might suggest that the mechanism is PI3Kγ mediated, and that small molecule inhibitors do not have the required selectivity to avoid influencing other confounding stimulatory/inhibitory mechanisms. In addition, it is worth noting that the defects in the Itk$^{-/-}$ T cell production of IL-17A mentioned above, could also not be rescued using pharmacological intervention (510), leading to the hypothesis that chromatin

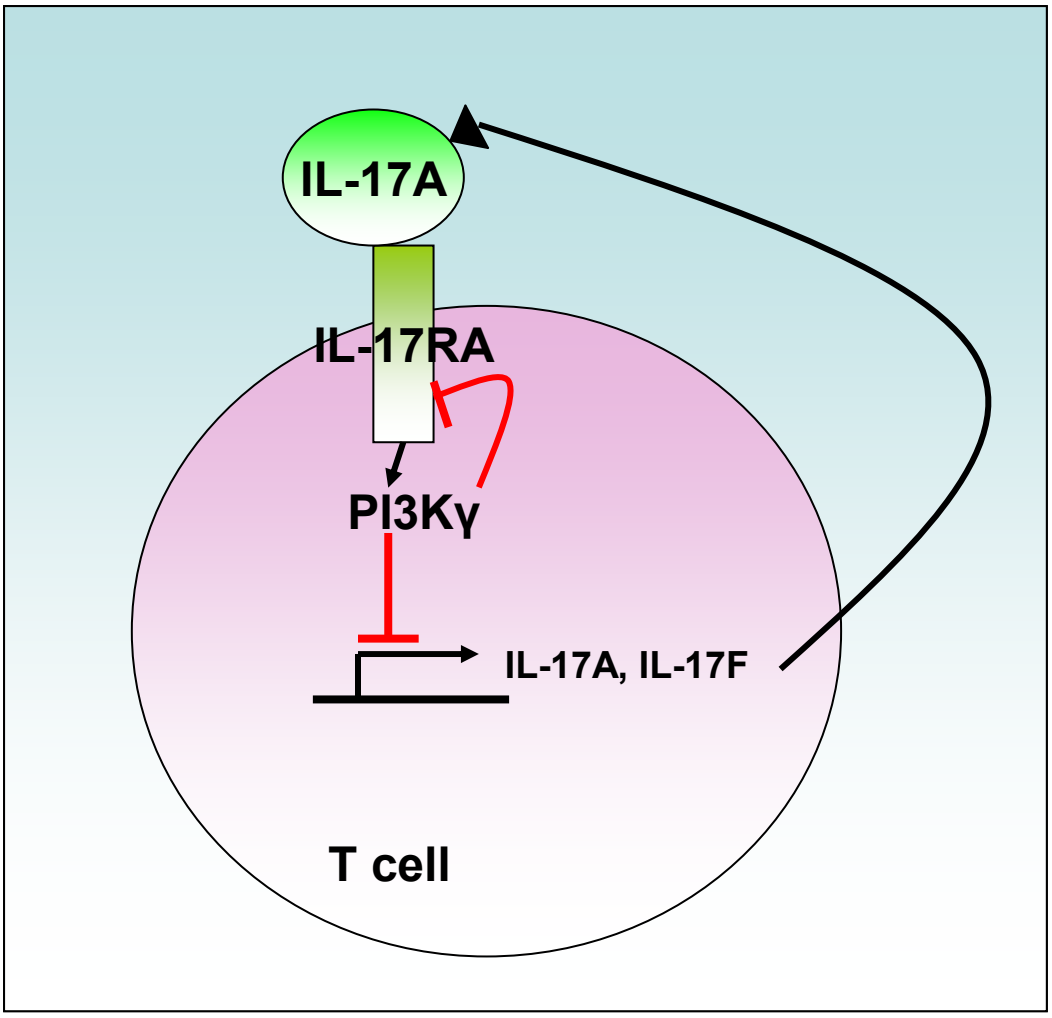

Figure 9.3 Model of the role of PI3Kγ in IL-17 signalling and production

In murine T cells, IL-17A signals, probably via the IL-17RA receptor, to activate PI3Kγ. PI3Kγ negatively regulates the expression of IL-17RA and also the production of both IL-17A and IL-17F, thus completing a negative feedback loop.

remodelling of the IL-17A locus by NFAT signalling during development may be important, as well as NFAT mediated IL-17A transcription (510, 519). Hence, the alternative explanation is that loss of PI3Kγ during development is important in determining IL-17 signalling in mature T cells. This would also be in line with findings that loss of PI3Kγ and PI3Kδ can cause defective Th1 and Th2 responses which cannot be fully replicated using inhibitors and which are due to defects during thymocyte development (168). Genetic loss of PI3Kγ has been previously demonstrated to result in reduced disease severity in models of conditions such as asthma and arthritis (175), due to the decreased migration of leukocytes to sites of infection and inflammation in PI3Kγ$^{-/-}$ animals (174, 177). However, overexpression of IL-17A (10) or IL-17F (520) has been reported to induce airway inflammation. Excess IL-17 generation may cause pro-inflammatory complications, particularly as IL-17 can act upon tissue cells to induce further inflammation (378, 499). IL-17 has been implicated in the suppression of T cell cytotoxicity, and inhibits clearance of persistent viral infections (521). Similarly, IL-17 is involved in the generation of an autoimmune response and multiple diseases in the airway, as it has roles in both innate and adaptive immunity (522). Furthermore, sustained high levels of Il-17A and Il-17F may favour tumour development (43). One concern therefore, is that chronic PI3Kγ inhibition as currently being explored in a range of inflammatory disease settings may lead to adverse effects as a result of elevated IL-17 production. However, this would be unlikely, due to the inability of PI3Kγ$^{-/-}$ cells to migrate to sites of inflammation (177).

In summary, this section of the results identified a novel mechanism of signalling downstream of Il-17RA in response to IL-17A (but not IL-17F) in which PI3Kγ is required for Akt phosphorylation. PI3Kγ was also required for maintenance of normal levels of IL-17 receptor expression. These defects may contribute to an increase in IL-17A and Il-17F levels observed both *in vitro* and *in vivo* upon knockout of PI3Kγ.

9.23 Future work on the role of PI3Kγ in IL-17 production

Future experiments will examine the expression of the IL-23 receptor, RORγ(t) and RORα in PI3Kγ$^{-/-}$ T cells. In addition the regulatory T cells will be charachterised by examination of foxp3 expression. The activation of PI3K γ downstream of IL-17 receptors will be investigated by western blotting and will also be examined in B cells.

In addition, the role of PI3Kγ in IL-17 production will be examined in human T cells using lentiviral delivery to silence expression of PI3Kγ.

9.24 General conclusions

In conclusion, the work in this thesis has examined two areas of PI3K signalling in T cells, firstly exploring the role of SHIP-1 in human T cells and secondly exploring the role of PI3Kγ in murine T cells. In both cases the findings contribute to an understanding of PI3K signalling which will be of relevance to the development of drugs targeting PI3K in the immune system.

References

1. Okkenhaug, K., K. Ali, and B. Vanhaesebroeck. 2007. Antigen receptor signalling: a distinctive role for the p110delta isoform of PI3K. *Trends Immunol* 28:80-87.
2. Iwasaki, A., and R. Medzhitov. Regulation of Adaptive Immunity by the Innate Immune System. *Science* 327:291-295.
3. Kindt, T. J., B. A. Osborne, and R. A. Goldsby. 2007. *Kuby Immunology* W.H. Freeman.
4. Jensen, K. D. C., and Y.-h. Chien. 2009. Thymic maturation determines [gamma][delta] T cell function, but not their antigen specificities. *Current Opinion in Immunology* 21:140-145.
5. Beetz, S., D. Wesch, L. Marischen, S. Welte, H. H. Oberg, and D. Kabelitz. 2008. Innate immune functions of human gammadelta T cells. *Immunobiology* 213:173-182.
6. Ju, X., G. Clark, and D. N. Hart. Review of human DC subtypes. *Methods Mol Biol* 595:3-20.
7. Zuniga-Pflucker, J. C. 2009. The original intrathymic progenitor from which T cells originate. *J Immunol* 183:3-4.
8. Mosmann, T. R., H. Cherwinski, M. W. Bond, M. A. Giedlin, and R. L. Coffman. 1986. Two types of murine helper T cell clone. I. Definition according to profiles of lymphokine activities and secreted proteins. *J Immunol* 136:2348-2357.
9. Zhu, J., H. Yamane, and W. E. Paul. 2009. Differentiation of Effector CD4 T Cell Populations. *Annual Review of Immunology* 28 445-489
10. Park, H., Z. Li, X. O. Yang, S. H. Chang, R. Nurieva, Y. H. Wang, Y. Wang, L. Hood, Z. Zhu, Q. Tian, and C. Dong. 2005. A distinct lineage of CD4 T cells regulates tissue inflammation by producing interleukin 17. *Nat Immunol* 6:1133-1141.
11. Harrington, L. E., R. D. Hatton, P. R. Mangan, H. Turner, T. L. Murphy, K. M. Murphy, and C. T. Weaver. 2005. Interleukin 17-producing CD4+ effector T cells develop via a lineage distinct from the T helper type 1 and 2 lineages. *Nat Immunol* 6:1123-1132.
12. Veldhoen, M., C. Uyttenhove, J. van Snick, H. Helmby, A. Westendorf, J. Buer, B. Martin, C. Wilhelm, and B. Stockinger. 2008. Transforming growth factor-[beta] 'reprograms' the differentiation of T helper 2 cells and promotes an interleukin 9-producing subset. *Nat Immunol* 9:1341-1346.
13. Dardalhon, V., A. Awasthi, H. Kwon, G. Galileos, W. Gao, R. A. Sobel, M. Mitsdoerffer, T. B. Strom, W. Elyaman, I. C. Ho, S. Khoury, M. Oukka, and V. K. Kuchroo. 2008. IL-4 inhibits TGF-[beta]-induced Foxp3+ T cells and, together with TGF-[beta], generates IL-9+ IL-10+ Foxp3- effector T cells. *Nat Immunol* 9:1347-1355.
14. Duhen, T., R. Geiger, D. Jarrossay, A. Lanzavecchia, and F. Sallusto. 2009. Production of interleukin 22 but not interleukin 17 by a subset of human skin-homing memory T cells. *Nat Immunol* 10:857-863.

15. Weaver, C. T., R. D. Hatton, P. R. Mangan, and L. E. Harrington. 2007. IL-17 family cytokines and the expanding diversity of effector T cell lineages. *Annu Rev Immunol* 25:821-852.
16. Jager, A., V. Dardalhon, R. A. Sobel, E. Bettelli, and V. K. Kuchroo. 2009. Th1, Th17, and Th9 effector cells induce experimental autoimmune encephalomyelitis with different pathological phenotypes. *J Immunol* 183:7169-7177.
17. Iwakura, Y., and H. Ishigame. 2006. The IL-23/IL-17 axis in inflammation. *The Journal of Clinical Investigation* 116:1218-1222.
18. O'Connor, W., Jr., M. Kamanaka, C. J. Booth, T. Town, S. Nakae, Y. Iwakura, J. K. Kolls, and R. A. Flavell. 2009. A protective function for interleukin 17A in T cell-mediated intestinal inflammation. *Nat Immunol* 10:603-609.
19. Szabo, S. J., S. T. Kim, G. L. Costa, X. Zhang, C. G. Fathman, and L. H. Glimcher. 2000. A Novel Transcription Factor, T-bet, Directs Th1 Lineage Commitment. *Cell* 100:655-669.
20. Lieberman, L. A., M. Banica, S. L. Reiner, and C. A. Hunter. 2004. STAT1 plays a critical role in the regulation of antimicrobial effector mechanisms, but not in the development of Th1-type responses during toxoplasmosis. *J Immunol* 172:457-463.
21. Suto, A., A. L. Wurster, S. L. Reiner, and M. J. Grusby. 2006. IL-21 inhibits IFN-gamma production in developing Th1 cells through the repression of Eomesodermin expression. *J Immunol* 177:3721-3727.
22. Constant, S. L., and K. Bottomly. 1997. Induction of Th1 and Th2 CD4+ T cell responses: the alternative approaches. *Annu Rev Immunol* 15:297-322.
23. Finkelman, F. D., T. Shea-Donohue, J. Goldhill, C. A. Sullivan, S. C. Morris, K. B. Madden, W. C. Gause, and J. F. Urban. 2003. Cytokine regulation of host defense against parasitic gastrointestinal nemotodes:Lessons from Studies with Rodent Models*1. *Annual Review of Immunology* 15:505-533.
24. Ansel, K. M., I. Djuretic, B. Tanasa, and A. Rao. 2006. Regulation of Th2 differentiation and il4 locus accessibility. *Annual Review of Immunology* 24:607-656.
25. Tykocinski, L. O., P. Hajkova, H. D. Chang, T. Stamm, O. Sozeri, M. Lohning, J. Hu-Li, U. Niesner, S. Kreher, B. Friedrich, C. Pannetier, G. Grutz, J. Walter, W. E. Paul, and A. Radbruch. 2005. A critical control element for interleukin-4 memory expression in T helper lymphocytes. *J Biol Chem* 280:28177-28185.
26. Kishikawa, H., J. Sun, A. Choi, S.-C. Miaw, and I. C. Ho. 2001. The Cell Type-Specific Expression of the Murine IL-13 Gene Is Regulated by GATA-3. *J Immunol* 167:4414-4420.
27. Mowen, K. A., and L. H. Glimcher. 2004. Signaling pathways in Th2 development. *Immunol Rev* 202:203-222.
28. Messi, M., I. Giacchetto, K. Nagata, A. Lanzavecchia, G. Natoli, and F. Sallusto. 2003. Memory and flexibility of cytokine gene expression as separable properties of human TH1 and TH2 lymphocytes. *Nat Immunol* 4:78-86.
29. Mangan, P. R., L. E. Harrington, D. B. O'Quinn, W. S. Helms, D. C. Bullard, C. O. Elson, R. D. Hatton, S. M. Wahl, T. R. Schoeb, and C. T. Weaver. 2006. Transforming growth factor-beta induces development of the T(H)17 lineage. *Nature* 441:231-234.

30. Korn, T., E. Bettelli, M. Oukka, and V. K. Kuchroo. 2009. IL-17 and Th17 Cells. *Annu Rev Immunol* 27:485-517.
31. Dong, C. 2008. Regulation and pro-inflammatory function of interleukin-17 family cytokines. *Immunol Rev* 226:80-86.
32. de Jong, E., T. Suddason, and G. M. Lord. Translational mini-review series on Th17 cells: development of mouse and human T helper 17 cells. *Clin Exp Immunol* 159:148-158.
33. Martinez, G. J., R. I. Nurieva, X. O. Yang, and C. Dong. 2008. Regulation and function of proinflammatory TH17 cells. *Ann N Y Acad Sci* 1143:188-211.
34. Chen, Z., A. Laurence, Y. Kanno, M. Pacher-Zavisin, B. M. Zhu, C. Tato, A. Yoshimura, L. Hennighausen, and J. J. O'Shea. 2006. Selective regulatory function of Socs3 in the formation of IL-17-secreting T cells. *Proc Natl Acad Sci U S A* 103:8137-8142.
35. Ivanov, II, B. S. McKenzie, L. Zhou, C. E. Tadokoro, A. Lepelley, J. J. Lafaille, D. J. Cua, and D. R. Littman. 2006. The orphan nuclear receptor RORgammat directs the differentiation program of proinflammatory IL-17+ T helper cells. *Cell* 126:1121-1133.
36. Fouser, L. A., J. F. Wright, K. Dunussi-Joannopoulos, and M. Collins. 2008. Th17 cytokines and their emerging roles in inflammation and autoimmunity. *Immunol Rev* 226:87-102.
37. Hirota, K., H. Yoshitomi, M. Hashimoto, S. Maeda, S. Teradaira, N. Sugimoto, T. Yamaguchi, T. Nomura, H. Ito, T. Nakamura, N. Sakaguchi, and S. Sakaguchi. 2007. Preferential recruitment of CCR6-expressing Th17 cells to inflamed joints via CCL20 in rheumatoid arthritis and its animal model. *J Exp Med* 204:2803-2812.
38. Laurence, A., C. M. Tato, T. S. Davidson, Y. Kanno, Z. Chen, Z. Yao, R. B. Blank, F. Meylan, R. Siegel, L. Hennighausen, E. M. Shevach, and J. O'Shea J. 2007. Interleukin-2 signaling via STAT5 constrains T helper 17 cell generation. *Immunity* 26:371-381.
39. Langrish, C. L., Y. Chen, W. M. Blumenschein, J. Mattson, B. Basham, J. D. Sedgwick, T. McClanahan, R. A. Kastelein, and D. J. Cua. 2005. IL-23 drives a pathogenic T cell population that induces autoimmune inflammation. *J Exp Med* 201:233-240.
40. Liang, S. C., A. J. Long, F. Bennett, M. J. Whitters, R. Karim, M. Collins, S. J. Goldman, K. Dunussi-Joannopoulos, C. M. Williams, J. F. Wright, and L. A. Fouser. 2007. An IL-17F/A heterodimer protein is produced by mouse Th17 cells and induces airway neutrophil recruitment. *J Immunol* 179:7791-7799.
41. Nakae, S., Y. Komiyama, A. Nambu, K. Sudo, M. Iwase, I. Homma, K. Sekikawa, M. Asano, and Y. Iwakura. 2002. Antigen-Specific T Cell Sensitization Is Impaired in IL-17-Deficient Mice, Causing Suppression of Allergic Cellular and Humoral Responses. *Immunity* 17:375-387.
42. Komiyama, Y., S. Nakae, T. Matsuki, A. Nambu, H. Ishigame, S. Kakuta, K. Sudo, and Y. Iwakura. 2006. IL-17 plays an important role in the development of experimental autoimmune encephalomyelitis. *J Immunol* 177:566-573.
43. Murugaiyan, G., and B. Saha. 2009. Protumor vs Antitumor Functions of IL-17. *J Immunol* 183:4169-4175.
44. Zheng, S. G., J. H. Wang, J. D. Gray, H. Soucier, and D. A. Horwitz. 2004. Natural and induced CD4+CD25+ cells educate CD4+CD25- cells to develop

suppressive activity: the role of IL-2, TGF-beta, and IL-10. *J Immunol* 172:5213-5221.

45. DiPaolo, R. J., C. Brinster, T. S. Davidson, J. Andersson, D. Glass, and E. M. Shevach. 2007. Autoantigen-specific TGFbeta-induced Foxp3+ regulatory T cells prevent autoimmunity by inhibiting dendritic cells from activating autoreactive T cells. *J Immunol* 179:4685-4693.
46. Sarah, E. A., X. S.-Z. George, A. Thomas, N. M. Alicia, and K. L. Megan. 2008. Inducible reprogramming of human T cells into Treg cells by a conditionally active form of FOXP3. *Eur J Immunol* 38:3282-3289.
47. Wildin, R. S., F. Ramsdell, J. Peake, F. Faravelli, J.-L. Casanova, N. Buist, E. Levy-Lahad, M. Mazzella, O. Goulet, L. Perroni, F. Dagna Bricarelli, G. Byrne, M. McEuen, S. Proll, M. Appleby, and M. E. Brunkow. 2001. X-linked neonatal diabetes mellitus, enteropathy and endocrinopathy syndrome is the human equivalent of mouse scurfy. *Nat Genet* 27:18-20.
48. Kohlhaas, S., O. A. Garden, C. Scudamore, M. Turner, K. Okkenhaug, and E. Vigorito. 2009. Cutting Edge: The Foxp3 Target miR-155 Contributes to the Development of Regulatory T Cells. *J Immunol* 182:2578-2582.
49. Rodriguez, A., E. Vigorito, S. Clare, M. V. Warren, P. Couttet, D. R. Soond, S. van Dongen, R. J. Grocock, P. P. Das, E. A. Miska, D. Vetrie, K. Okkenhaug, A. J. Enright, G. Dougan, M. Turner, and A. Bradley. 2007. Requirement of bic/microRNA-155 for Normal Immune Function. *Science* 316:608-611.
50. O'Connell, R. M., A. A. Chaudhuri, D. S. Rao, and D. Baltimore. 2009. Inositol phosphatase SHIP1 is a primary target of miR-155. *Proc Natl Acad Sci U S A* 106:7113-7118.
51. Xu, L., A. Kitani, I. Fuss, and W. Strober. 2007. Cutting edge: regulatory T cells induce CD4+CD25-Foxp3- T cells or are self-induced to become Th17 cells in the absence of exogenous TGF-beta. *J Immunol* 178:6725-6729.
52. Yang, X. O., R. Nurieva, G. J. Martinez, H. S. Kang, Y. Chung, B. P. Pappu, B. Shah, S. H. Chang, K. S. Schluns, S. S. Watowich, X. H. Feng, A. M. Jetten, and C. Dong. 2008. Molecular antagonism and plasticity of regulatory and inflammatory T cell programs. *Immunity* 29:44-56.
53. Voo, K. S., Y. H. Wang, F. R. Santori, C. Boggiano, K. Arima, L. Bover, S. Hanabuchi, J. Khalili, E. Marinova, B. Zheng, D. R. Littman, and Y. J. Liu. 2009. Identification of IL-17-producing FOXP3+ regulatory T cells in humans. *Proc Natl Acad Sci U S A* 106:4793-4798.
54. Koch, M. A., G. Tucker-Heard, N. R. Perdue, J. R. Killebrew, K. B. Urdahl, and D. J. Campbell. 2009. The transcription factor T-bet controls regulatory T cell homeostasis and function during type 1 inflammation. *Nat Immunol* 10:595-602.
55. Vazquez, F., S. R. Grossman, Y. Takahashi, M. V. Rokas, N. Nakamura, and W. R. Sellers. 2001. Phosphorylation of the PTEN Tail Acts as an Inhibitory Switch by Preventing Its Recruitment into a Protein Complex. *J Biol Chem* 276:48627-48630.
56. Intlekofer, A. M., A. Banerjee, N. Takemoto, S. M. Gordon, C. S. DeJong, H. Shin, C. A. Hunter, E. J. Wherry, T. Lindsten, and S. L. Reiner. 2008. Anomalous Type 17 Response to Viral Infection by CD8+ T Cells Lacking T-bet and Eomesodermin. *Science* 321:408-411.

57. Kondo, T., H. Takata, F. Matsuki, and M. Takiguchi. 2009. Cutting edge: Phenotypic characterization and differentiation of human CD8+ T cells producing IL-17. *J Immunol* 182:1794-1798.
58. Chowdhury, D., and J. Lieberman. 2008. Death by a Thousand Cuts: Granzyme Pathways of Programmed Cell Death. *Annual Review of Immunology* 26:389-420.
59. Johnson, B. J., E. O. Costelloe, D. R. Fitzpatrick, J. B. Haanen, T. N. Schumacher, L. E. Brown, and A. Kelso. 2003. Single-cell perforin and granzyme expression reveals the anatomical localization of effector CD8+ T cells in influenza virus-infected mice. *Proc Natl Acad Sci U S A* 100:2657-2662.
60. Pearce, E. L., A. C. Mullen, G. A. Martins, C. M. Krawczyk, A. S. Hutchins, V. P. Zediak, M. Banica, C. B. DiCioccio, D. A. Gross, C.-a. Mao, H. Shen, N. Cereb, S. Y. Yang, T. Lindsten, J. Rossant, C. A. Hunter, and S. L. Reiner. 2003. Control of Effector CD8+ T Cell Function by the Transcription Factor Eomesodermin. *Science* 302:1041-1043.
61. Sullivan, B. M., A. Juedes, S. J. Szabo, M. von Herrath, and L. H. Glimcher. 2003. Antigen-driven effector CD8 T cell function regulated by T-bet. *Proc Natl Acad Sci U S A* 100:15818-15823.
62. Liu, C. C., S. Rafii, A. Granelli-Piperno, J. A. Trapani, and J. D. Young. 1989. Perforin and serine esterase gene expression in stimulated human T cells. Kinetics, mitogen requirements, and effects of cyclosporin A. *J. Exp. Med.* 170:2105-2118.
63. Grujic, M., T. Braga, A. Lukinius, M. L. Eloranta, S. D. Knight, G. Pejler, and M. Abrink. 2005. Serglycin-deficient cytotoxic T lymphocytes display defective secretory granule maturation and granzyme B storage. *J Biol Chem* 280:33411-33418.
64. Stinchcombe, J. C., G. Bossi, S. Booth, and G. M. Griffiths. 2001. The Immunological Synapse of CTL Contains a Secretory Domain and Membrane Bridges. *Immunity* 15:751-761.
65. Keefe, D., L. Shi, S. Feske, R. Massol, F. Navarro, T. Kirchhausen, and J. Lieberman. 2005. Perforin Triggers a Plasma Membrane-Repair Response that Facilitates CTL Induction of Apoptosis. *Immunity* 23:249-262.
66. Shresta, S., T. A. Graubert, D. A. Thomas, S. Z. Raptis, and T. J. Ley. 1999. Granzyme A Initiates an Alternative Pathway for Granule-Mediated Apoptosis. *Immunity* 10:595-605.
67. Adrain, C., B. M. Murphy, and S. J. Martin. 2005. Molecular ordering of the caspase activation cascade initiated by the cytotoxic T lymphocyte/natural killer (CTL/NK) protease granzyme B. *J Biol Chem* 280:4663-4673.
68. Bromley, S. K., T. R. Mempel, and A. D. Luster. 2008. Orchestrating the orchestrators: chemokines in control of T cell traffic. *Nat Immunol* 9:970-980.
69. Alon, R., P. D. Kassner, M. W. Carr, E. B. Finger, M. E. Hemler, and T. A. Springer. 1995. The integrin VLA-4 supports tethering and rolling in flow on VCAM-1. *J Cell Biol* 128:1243-1253.
70. Kadono, T., G. M. Venturi, D. A. Steeber, and T. F. Tedder. 2002. Leukocyte Rolling Velocities and Migration Are Optimized by Cooperative L-Selectin and Intercellular Adhesion Molecule-1 Functions. *J Immunol* 169:4542-4550.

71. Kunkel, E. J., and E. C. Butcher. 2002. Chemokines and the tissue-specific migration of lymphocytes. *Immunity* 16:1-4.
72. Stein, J. V., A. Rot, Y. Luo, M. Narasimhaswamy, H. Nakano, M. D. Gunn, A. Matsuzawa, E. J. Quackenbush, M. E. Dorf, and U. H. von Andrian. 2000. The CC chemokine thymus-derived chemotactic agent 4 (TCA-4, secondary lymphoid tissue chemokine, 6Ckine, exodus-2) triggers lymphocyte function-associated antigen 1-mediated arrest of rolling T lymphocytes in peripheral lymph node high endothelial venules. *J Exp Med* 191:61-76.
73. Scimone, M. L., T. W. Felbinger, I. B. Mazo, J. V. Stein, U. H. Von Andrian, and W. Weninger. 2004. CXCL12 mediates CCR7-independent homing of central memory cells, but not naive T cells, in peripheral lymph nodes. *J Exp Med* 199:1113-1120.
74. Okada, T., and J. G. Cyster. 2007. CC chemokine receptor 7 contributes to Gi-dependent T cell motility in the lymph node. *J Immunol* 178:2973-2978.
75. Bajenoff, M., J. G. Egen, L. Y. Koo, J. P. Laugier, F. Brau, N. Glaichenhaus, and R. N. Germain. 2006. Stromal cell networks regulate lymphocyte entry, migration, and territoriality in lymph nodes. *Immunity* 25:989-1001.
76. Pham, T. H., T. Okada, M. Matloubian, C. G. Lo, and J. G. Cyster. 2008. S1P1 receptor signaling overrides retention mediated by G alpha i-coupled receptors to promote T cell egress. *Immunity* 28:122-133.
77. Chen, Q., D. T. Fisher, K. A. Clancy, J. M. Gauguet, W. C. Wang, E. Unger, S. Rose-John, U. H. von Andrian, H. Baumann, and S. S. Evans. 2006. Fever-range thermal stress promotes lymphocyte trafficking across high endothelial venules via an interleukin 6 trans-signaling mechanism. *Nat Immunol* 7:1299-1308.
78. Reiss, Y., A. E. Proudfoot, C. A. Power, J. J. Campbell, and E. C. Butcher. 2001. CC chemokine receptor (CCR)4 and the CCR10 ligand cutaneous T cell-attracting chemokine (CTACK) in lymphocyte trafficking to inflamed skin. *J Exp Med* 194:1541-1547.
79. Syrbe, U., J. Siveke, and A. Hamann. 1999. Th1/Th2 subsets: distinct differences in homing and chemokine receptor expression? *Springer Semin Immunopathol* 21:263-285.
80. Eyerich, S., K. Eyerich, D. Pennino, T. Carbone, F. Nasorri, S. Pallotta, F. Cianfarani, T. Odorisio, C. Traidl-Hoffmann, H. Behrendt, S. R. Durham, C. B. Schmidt-Weber, and A. Cavani. 2009. Th22 cells represent a distinct human T cell subset involved in epidermal immunity and remodeling. *The Journal of Clinical Investigation* 119:3573-3585.
81. Wei, S., I. Kryczek, and W. Zou. 2006. Regulatory T-cell compartmentalization and trafficking. *Blood* 108:426-431.
82. Mikhak, Z., C. M. Fleming, B. D. Medoff, S. Y. Thomas, A. M. Tager, G. S. Campanella, and A. D. Luster. 2006. STAT1 in peripheral tissue differentially regulates homing of antigen-specific Th1 and Th2 cells. *J Immunol* 176:4959-4967.
83. Balkwill, F. 2004. Cancer and the chemokine network. *Nat Rev Cancer* 4:540-550.
84. Ransohoff, R. M. 2009. Chemokines and Chemokine Receptors: Standing at the Crossroads of Immunobiology and Neurobiology. *Immunity* 31:711-721.

85. Ward, S. G., and F. M. Marelli-berg. 2009. Mechanisms of chemokine and antigen-dependent T-lymphocyte navigation. *Biochem J* 418:13-27.
86. Charo, I. F., and R. M. Ransohoff. 2006. The Many Roles of Chemokines and Chemokine Receptors in Inflammation. *N Engl J Med* 354:610-621.
87. Shulman, Z., V. Shinder, E. Klein, V. Grabovsky, O. Yeger, E. Geron, A. Montresor, M. Bolomini-Vittori, S. W. Feigelson, T. Kirchhausen, C. Laudanna, G. Shakhar, and R. Alon. 2009. Lymphocyte Crawling and Transendothelial Migration Require Chemokine Triggering of High-Affinity LFA-1 Integrin. *Immunity* 30:384-396.
88. Pruenster, M., L. Mudde, P. Bombosi, S. Dimitrova, M. Zsak, J. Middleton, A. Richmond, G. J. Graham, S. Segerer, R. J. Nibbs, and A. Rot. 2009. The Duffy antigen receptor for chemokines transports chemokines and supports their promigratory activity. *Nat Immunol* 10:101-108.
89. Mangalmurti, N. S., Z. Xiong, M. Hulver, M. Ranganathan, X. H. Liu, T. Oriss, M. Fitzpatrick, M. Rubin, D. Triulzi, A. Choi, and J. S. Lee. 2009. Loss of red cell chemokine scavenging promotes transfusion-related lung inflammation. *Blood* 113:1158-1166.
90. Pribila, J. T., A. C. Quale, K. L. Mueller, and Y. Shimizu. 2004. Integrins and T Cell Mediated Immunity. *Annual Review of Immunology* 22:157-180.
91. Jenkins, M. K., C. A. Chen, G. Jung, D. L. Mueller, and R. H. Schwartz. 1990. Inhibition of antigen-specific proliferation of type 1 murine T cell clones after stimulation with immobilized anti-CD3 monoclonal antibody. *J Immunol* 144:16-22.
92. Smith-Garvin, J. E., G. A. Koretzky, and M. S. Jordan. 2009. T Cell Activation. *Annual Review of Immunology* 27:591-619.
93. Van Seventer, G. A., Y. Shimizu, K. J. Horgan, and S. Shaw. 1990. The LFA-1 ligand ICAM-1 provides an important costimulatory signal for T cell receptor-mediated activation of resting T cells. *J Immunol* 144:4579-4586.
94. Morgan, D. A., F. W. Ruscetti, and R. Gallo. 1976. Selective in vitro growth of T lymphocytes from normal human bone marrows. *Science* 193:1007-1008.
95. Schuh, K., T. Twardzik, B. Kneitz, J. Heyer, A. Schimpl, and E. Serfling. 1998. The Interleukin 2 Receptor {alpha} Chain/CD25 Promoter Is a Target for Nuclear Factor of Activated T Cells. *J. Exp. Med.* 188:1369-1373.
96. Straus, D. B., and A. Weiss. 1993. The CD3 chains of the T cell antigen receptor associate with the ZAP-70 tyrosine kinase and are tyrosine phosphorylated after receptor stimulation. *J Exp Med* 178:1523-1530.
97. Sharpe, A. H., and A. K. Abbas. 2006. T-Cell Costimulation -- Biology, Therapeutic Potential, and Challenges. *N Engl J Med* 355:973-975.
98. Okamoto, N., K. Tezuka, M. Kato, R. Abe, and T. Tsuji. 2003. PI3-kinase and MAP-kinase signaling cascades in AILIM/ICOS- and CD28-costimulated T-cells have distinct functions between cell proliferation and IL-10 production. *Biochemical and Biophysical Research Communications* 310:691-702.
99. Tuettenberg, A., E. Huter, M. Hubo, J. Horn, J. Knop, B. Grimbacher, R. A. Kroczek, S. Stoll, and H. Jonuleit. 2009. The Role of ICOS in Directing T Cell Responses: ICOS-Dependent Induction of T Cell Anergy by Tolerogenic Dendritic Cells. *J Immunol* 182:3349-3356.

100. Parry, R., G. Smith, K. Reif, D. M. Sansom, and S. Ward. 1997. Activation of the PI3K effector protein kinase B following ligation of CD28 or Fas. *Biochem Soc Trans* 25:S589.
101. Galetic, I., S. M. Maira, M. Andjelkovic, and B. A. Hemmings. 2003. Negative regulation of ERK and Elk by protein kinase B modulates c-Fos transcription. *J Biol Chem* 278:4416-4423.
102. Martin-Cofreces, N. B., J. Robles-Valero, J. R. Cabrero, M. Mittelbrunn, M. Gordon-Alonso, C. H. Sung, B. Alarcon, J. Vazquez, and F. Sanchez-Madrid. 2008. MTOC translocation modulates IS formation and controls sustained T cell signaling. *J Cell Biol* 182:951-962.
103. Yokosuka, T., and T. Saito. The Immunological Synapse, TCR Microclusters, and T Cell Activation. *Curr Top Microbiol Immunol* 340:81-107.
104. Baker, R. G., C. J. Hsu, D. Lee, M. S. Jordan, J. S. Maltzman, D. A. Hammer, T. Baumgart, and G. A. Koretzky. 2009. The adapter protein SLP-76 mediates "outside-in" integrin signaling and function in T cells. *Mol Cell Biol* 29:5578-5589.
105. Wang, H., B. Wei, G. Bismuth, and C. E. Rudd. 2009. SLP-76-ADAP adaptor module regulates LFA-1 mediated costimulation and T cell motility. *Proc Natl Acad Sci U S A* 106:12436-12441.
106. Lafuente, E. M., A. A. van Puijenbroek, M. Krause, C. V. Carman, G. J. Freeman, A. Berezovskaya, E. Constantine, T. A. Springer, F. B. Gertler, and V. A. Boussiotis. 2004. RIAM, an Ena/VASP and Profilin ligand, interacts with Rap1-GTP and mediates Rap1-induced adhesion. *Dev Cell* 7:585-595.
107. Letschka, T., V. Kollmann, C. Pfeifhofer-Obermair, C. Lutz-Nicoladoni, G. J. Obermair, F. Fresser, M. Leitges, N. Hermann-Kleiter, S. Kaminski, and G. Baier. 2008. PKC-theta selectively controls the adhesion-stimulating molecule Rap1. *Blood* 112:4617-4627.
108. Medeiros, R. B., D. M. Dickey, H. Chung, A. C. Quale, L. R. Nagarajan, D. D. Billadeau, and Y. Shimizu. 2005. Protein Kinase D1 and the [beta]1 Integrin Cytoplasmic Domain Control [beta]1 Integrin Function via Regulation of Rap1 Activation. *Immunity* 23:213-226.
109. Moore, S. F., and A. B. MacKenzie. 2009. NADPH oxidase NOX2 mediates rapid cellular oxidation following ATP stimulation of endotoxin-primed macrophages. *J Immunol* 183:3302-3308.
110. Norell, H., T. Martins da Palma, A. Lesher, N. Kaur, M. Mehrotra, O. S. Naga, N. Spivey, S. Olafimihan, N. G. Chakraborty, C. Voelkel-Johnson, M. I. Nishimura, B. Mukherji, and S. Mehrotra. 2009. Inhibition of superoxide generation upon T-cell receptor engagement rescues Mart-1(27-35)-reactive T cells from activation-induced cell death. *Cancer Res* 69:6282-6289.
111. Klemke, C.-D., D. Brenner, E.-M. Weiss, M. Schmidt, M. Leverkus, K. Gulow, and P. H. Krammer. 2009. Lack of T-Cell Receptor-Induced Signaling Is Crucial for CD95 Ligand Up-regulation and Protects Cutaneous T-Cell Lymphoma Cells from Activation-Induced Cell Death. *Cancer Res* 69:4175-4183.
112. Temkin, V., and M. Karin. 2007. From death receptor to reactive oxygen species and c-Jun N-terminal protein kinase: the receptor-interacting protein 1 odyssey. *Immunol Rev* 220:8-21.

113. Lenardo, M. J. 1991. Interleukin-2 programs mouse alpha beta T lymphocytes for apoptosis. *Nature* 353:858-861.
114. Refaeli, Y., L. Van Parijs, C. A. London, J. Tschopp, and A. K. Abbas. 1998. Biochemical Mechanisms of IL-2-Regulated Fas-Mediated T Cell Apoptosis. *Immunity* 8:615-623.
115. Kaminski, M., M. Kiessling, D. Suss, P. H. Krammer, and K. Gulow. 2007. Novel Role for Mitochondria: Protein Kinase C{theta}-Dependent Oxidative Signaling Organelles in Activation-Induced T-Cell Death. *Mol. Cell. Biol.* 27:3625-3639.
116. Brenner, D., P. H. Krammer, and R. Arnold. 2008. Concepts of activated T cell death. *Critical Reviews in Oncology/Hematology* 66:52-64.
117. Ju, S. T., D. J. Panka, H. Cui, R. Ettinger, M. el-Khatib, D. H. Sherr, B. Z. Stanger, and A. Marshak-Rothstein. 1995. Fas(CD95)/FasL interactions required for programmed cell death after T-cell activation. *Nature* 373:444-448.
118. Sytwu, H.-K., R. S. Liblau, and H. O. McDevitt. 1996. The Roles of Fas/APO-1 (CD95) and TNF in Antigen-Induced Programmed Cell Death in T Cell Receptor Transgenic Mice. *Immunity* 5:17-30.
119. Sedger, L. M., A. Katewa, A. K. Pettersen, S. R. Osvath, G. C. Farrell, G. J. Stewart, L. J. Bendall, and S. I. Alexander. 2010 Extreme lymphoproliferative disease and fatal autoimmune thrombocytopenia in FasL- and TRAIL-double deficient mice. *Blood* 115 3258–3268.
120. Hildeman, D. A., Y. Zhu, T. C. Mitchell, P. Bouillet, A. Strasser, J. Kappler, and P. Marrack. 2002. Activated T Cell Death In Vivo Mediated by Proapoptotic Bcl-2 Family Member Bim. *Immunity* 16:759-767.
121. Tripathi, P., and D. Hildeman. 2004. Sensitization of T cells to apoptosis--a role for ROS? *Apoptosis* 9:515-523.
122. Hildeman, D. A. 2004. Regulation of T-cell apoptosis by reactive oxygen species. *Free Radic Biol Med* 36:1496-1504.
123. Hildeman, D. A., T. Mitchell, J. Kappler, and P. Marrack. 2003. T cell apoptosis and reactive oxygen species. *J Clin Invest* 111:575-581.
124. Courtneidge, S. A., and A. Heber. 1987. An 81 kd protein complexed with middle T antigen and pp60c-src: a possible phosphatidylinositol kinase. *Cell* 50:1031-1037.
125. Whitman, M., C. P. Downes, M. Keeler, T. Keller, and L. Cantley. 1988. Type I phosphatidylinositol kinase makes a novel inositol phospholipid, phosphatidylinositol-3-phosphate. *Nature* 332:644-646.
126. Hennessy, B. T., D. L. Smith, P. T. Ram, Y. Lu, and G. B. Mills. 2005. Exploiting the PI3K/AKT pathway for cancer drug discovery. *Nat Rev Drug Discov* 4:988-1004.
127. Rommel, C., M. Camps, and H. Ji. 2007. PI3Kdelta and PI3Kgamma: partners in crime in inflammation in rheumatoid arthritis and beyond? *Nat Rev Immunol* 7:191-201.
128. Ruckle, T., M. K. Schwarz, and C. Rommel. 2006. PI3Kgamma inhibition: towards an 'aspirin of the 21st century'? *Nat Rev Drug Discov* 5:903-918.
129. Deane, J. A., and D. A. Fruman. 2004. Phosphoinositide 3-kinase: diverse roles in immune cell activation. *Annu Rev Immunol* 22:563-598.

130. Ward, S. G., and D. A. Cantrell. 2001. Phosphoinositide 3-kinases in T lymphocyte activation. *Curr Opin Immunol* 13:332-338.
131. Suire, S., J. Coadwell, G. J. Ferguson, K. Davidson, P. Hawkins, and L. Stephens. 2005. p84, a New G[beta][gamma]-Activated Regulatory Subunit of the Type IB Phosphoinositide 3-Kinase p110[gamma]. *Current Biology* 15:566-570.
132. Voigt, P., M. B. Dorner, and M. Schaefer. 2006. Characterization of p87PIKAP, a Novel Regulatory Subunit of Phosphoinositide 3-Kinase {gamma} That Is Highly Expressed in Heart and Interacts with PDE3B. *J. Biol. Chem.* 281:9977-9986.
133. Guillermet-Guibert, J., K. Bjorklof, A. Salpekar, C. Gonella, F. Ramadani, A. Bilancio, S. Meek, A. J. Smith, K. Okkenhaug, and B. Vanhaesebroeck. 2008. The p110beta isoform of phosphoinositide 3-kinase signals downstream of G protein-coupled receptors and is functionally redundant with p110gamma. *Proc Natl Acad Sci U S A* 105:8292-8297.
134. Vanhaesebroeck, B., K. Ali, A. Bilancio, B. Geering, and L. C. Foukas. 2005. Signalling by PI3K isoforms: insights from gene-targeted mice. *Trends in Biochemical Sciences* 30:194-204.
135. Ward, S. G. 2004. Do phosphoinositide 3-kinases direct lymphocyte navigation? *Trends in immunology* 25:67-74.
136. Harris, S. J., R. V. Parry, J. Westwick, and S. G. Ward. 2008. Phosphoinositide lipid phosphatases: natural regulators of phosphoinositide 3-kinase signaling in T lymphocytes. *J Biol Chem* 283:2465-2469.
137. Crackower, M. A., G. Y. Oudit, I. Kozieradzki, R. Sarao, H. Sun, T. Sasaki, E. Hirsch, A. Suzuki, T. Shioi, J. Irie-Sasaki, R. Sah, H. Y. Cheng, V. O. Rybin, G. Lembo, L. Fratta, A. J. Oliveira-dos-Santos, J. L. Benovic, C. R. Kahn, S. Izumo, S. F. Steinberg, M. P. Wymann, P. H. Backx, and J. M. Penninger. 2002. Regulation of myocardial contractility and cell size by distinct PI3K-PTEN signaling pathways. *Cell* 110:737-749.
138. Patrucco, E., A. Notte, L. Barberis, G. Selvetella, A. Maffei, M. Brancaccio, S. Marengo, G. Russo, O. Azzolino, S. D. Rybalkin, L. Silengo, F. Altruda, R. Wetzker, M. P. Wymann, G. Lembo, and E. Hirsch. 2004. PI3K[gamma] Modulates the Cardiac Response to Chronic Pressure Overload by Distinct Kinase-Dependent and -Independent Effects. *Cell* 118:375-387.
139. Kok, K., G. E. Nock, E. A. Verrall, M. P. Mitchell, D. W. Hommes, M. P. Peppelenbosch, and B. Vanhaesebroeck. 2009. Regulation of p110delta PI 3-kinase gene expression. *PLoS One* 4:e5145.
140. Sawyer, C., J. Sturge, D. C. Bennett, M. J. O'Hare, W. E. Allen, J. Bain, G. E. Jones, and B. Vanhaesebroeck. 2003. Regulation of breast cancer cell chemotaxis by the phosphoinositide 3-kinase p110delta. *Cancer Res* 63:1667-1675.
141. Liu, Q., F. Shalaby, J. Jones, D. Bouchard, and D. J. Dumont. 1998. The SH2-Containing Inositol Polyphosphate 5-Phosphatase, Ship, Is Expressed During Hematopoiesis and Spermatogenesis. *Blood* 91:2753-2759.
142. Tanigaki, K., C. Mineo, I. S. Yuhanna, K. L. Chambliss, M. J. Quon, E. Bonvini, and P. W. Shaul. 2009. C-Reactive Protein Inhibits Insulin Activation of Endothelial Nitric Oxide Synthase via the Immunoreceptor Tyrosine-Based Inhibition Motif of Fc{gamma}RIIB and SHIP-1. *Circ Res* 104:1275-1282.

143. Pearce, L. R., D. Komander, and D. R. Alessi. The nuts and bolts of AGC protein kinases. *Nat Rev Mol Cell Biol* 11:9-22.
144. Casamayor, A., N. A. Morrice, and D. R. Alessi. 1999. Phosphorylation of Ser-241 is essential for the activity of 3-phosphoinositide-dependent protein kinase-1: identification of five sites of phosphorylation in vivo. *Biochem J* 342 287-292.
145. Calleja, V., D. Alcor, M. Laguerre, J. Park, B. Vojnovic, B. A. Hemmings, J. Downward, P. J. Parker, and B. Larijani. 2007. Intramolecular and intermolecular interactions of protein kinase B define its activation in vivo. *PLoS Biol* 5:e95.
146. Sarbassov, D. D., D. A. Guertin, S. M. Ali, and D. M. Sabatini. 2005. Phosphorylation and Regulation of Akt/PKB by the Rictor-mTOR Complex. *Science* 307:1098-1101.
147. Biondi, R. M., A. Kieloch, R. A. Currie, M. Deak, and D. R. Alessi. 2001. The PIF-binding pocket in PDK1 is essential for activation of S6K and SGK, but not PKB. *EMBO J* 20:4380-4390.
148. Le Good, J. A., W. H. Ziegler, D. B. Parekh, D. R. Alessi, P. Cohen, and P. J. Parker. 1998. Protein kinase C isotypes controlled by phosphoinositide 3-kinase through the protein kinase PDK1. *Science* 281:2042-2045.
149. Krugmann, S., K. E. Anderson, S. H. Ridley, N. Risso, A. McGregor, J. Coadwell, K. Davidson, A. Eguinoa, C. D. Ellson, P. Lipp, M. Manifava, N. Ktistakis, G. Painter, J. W. Thuring, M. A. Cooper, Z. Y. Lim, A. B. Holmes, S. K. Dove, R. H. Michell, A. Grewal, A. Nazarian, H. Erdjument-Bromage, P. Tempst, L. R. Stephens, and P. T. Hawkins. 2002. Identification of ARAP3, a novel PI3K effector regulating both Arf and Rho GTPases, by selective capture on phosphoinositide affinity matrices. *Mol Cell* 9:95-108.
150. Cully, M., H. You, A. J. Levine, and T. W. Mak. 2006. Beyond PTEN mutations: the PI3K pathway as an integrator of multiple inputs during tumorigenesis. *Nat Rev Cancer* 6:184-192.
151. Liu, P., H. Cheng, T. M. Roberts, and J. J. Zhao. 2009. Targeting the phosphoinositide 3-kinase pathway in cancer. *Nat Rev Drug Discov* 8:627-644.
152. Frech, M., M. Andjelkovic, E. Ingley, K. K. Reddy, J. R. Falck, and B. A. Hemmings. 1997. High affinity binding of inositol phosphates and phosphoinositides to the pleckstrin homology domain of RAC/protein kinase B and their influence on kinase activity. *J Biol Chem* 272:8474-8481.
153. Gray, A., J. Van Der Kaay, and C. P. Downes. 1999. The pleckstrin homology domains of protein kinase B and GRP1 (general receptor for phosphoinositides-1) are sensitive and selective probes for the cellular detection of phosphatidylinositol 3,4-bisphosphate and/or phosphatidylinositol 3,4,5-trisphosphate in vivo. *Biochem. J.* 344:929-936.
154. Dos, D. S., S. M. Ali, D.-H. Kim, D. A. Guertin, R. R. Latek, H. Erdjument-Bromage, P. Tempst, and D. M. Sabatini. 2004. Rictor, a Novel Binding Partner of mTOR, Defines a Rapamycin-Insensitive and Raptor-Independent Pathway that Regulates the Cytoskeleton. *Current Biology* 14:1296-1302.
155. Sarbassov, D. D., S. M. Ali, S. Sengupta, J.-H. Sheen, P. P. Hsu, A. F. Bagley, A. L. Markhard, and D. M. Sabatini. 2006. Prolonged Rapamycin

Treatment Inhibits mTORC2 Assembly and Akt/PKB. *Molecular Cell* 22:159-168.
156. Sancak, Y., and D. M. Sabatini. 2009. Rag proteins regulate amino-acid-induced mTORC1 signalling. *Biochem Soc Trans* 37:289-290.
157. Kim, D. H., D. D. Sarbassov, S. M. Ali, J. E. King, R. R. Latek, H. Erdjument-Bromage, P. Tempst, and D. M. Sabatini. 2002. mTOR interacts with raptor to form a nutrient-sensitive complex that signals to the cell growth machinery. *Cell* 110:163-175.
158. Peng, T., T. R. Golub, and D. M. Sabatini. 2002. The immunosuppressant rapamycin mimics a starvation-like signal distinct from amino acid and glucose deprivation. *Mol Cell Biol* 22:5575-5584.
159. Greg, M. D., and D. P. Jonathan. 2009. mTOR: taking cues from the immune microenvironment. *Immunology* 127:459-465.
160. Yang, Q., K. Inoki, E. Kim, and K. L. Guan. 2006. TSC1/TSC2 and Rheb have different effects on TORC1 and TORC2 activity. *Proc Natl Acad Sci U S A* 103:6811-6816.
161. Kamperschroer, C., J. P. Dibble, D. L. Meents, P. L. Schwartzberg, and S. L. Swain. 2006. SAP Is Required for Th Cell Function and for Immunity to Influenza. *J Immunol* 177:5317-5327.
162. Powell, J. D., C. G. Lerner, and R. H. Schwartz. 1999. Inhibition of cell cycle progression by rapamycin induces T cell clonal anergy even in the presence of costimulation. *J Immunol* 162:2775-2784.
163. Kang, J., S. J. Huddleston, J. M. Fraser, and A. Khoruts. 2008. De novo induction of antigen-specific CD4+CD25+Foxp3+ regulatory T cells in vivo following systemic antigen administration accompanied by blockade of mTOR. *J Leukoc Biol* 83:1230-1239.
164. Delgoffe, G. M., T. P. Kole, Y. Zheng, P. E. Zarek, K. L. Matthews, B. Xiao, P. F. Worley, S. C. Kozma, and J. D. Powell. 2009. The mTOR kinase differentially regulates effector and regulatory T cell lineage commitment. *Immunity* 30:832-844.
165. Fruman, D. A., and G. Bismuth. 2009. Fine tuning the immune response with PI3K. *Immunol Rev* 228:253-272.
166. Crabbe, T., M. J. Welham, and S. G. Ward. 2007. The PI3K inhibitor arsenal: choose your weapon! *Trends Biochem Sci* 32:450-456.
167. Ji, H., F. Rintelen, C. Waltzinger, D. Bertschy Meier, A. Bilancio, W. Pearce, E. Hirsch, M. P. Wymann, T. Ruckle, M. Camps, B. Vanhaesebroeck, K. Okkenhaug, and C. Rommel. 2007. Inactivation of PI3K{gamma} and PI3K{delta} distorts T-cell development and causes multiple organ inflammation. *Blood* 110:2940-2947.
168. Ji, H., F. Rintelen, C. Waltzinger, D. Bertschy Meier, A. Bilancio, W. Pearce, E. Hirsch, M. P. Wymann, T. Ruckle, M. Camps, B. Vanhaesebroeck, K. Okkenhaug, and C. Rommel. 2007. Inactivation of PI3Kgamma and PI3Kdelta distorts T-cell development and causes multiple organ inflammation. *Blood* 110:2940-2947.
169. Okkenhaug, K., A. Bilancio, J. L. Emery, and B. Vanhaesebroeck. 2004. Phosphoinositide 3-kinase in T cell activation and survival. *Biochemical Society Transactions* 32:332-335.

170. Parry, R. V., J. L. Riley, and S. G. Ward. 2007. Signalling to suit function: tailoring phosphoinositide 3-kinase during T-cell activation. *Trends in immunology* 28:161-168.
171. Garcon, F., D. T. Patton, J. L. Emery, E. Hirsch, R. Rottapel, T. Sasaki, and K. Okkenhaug. 2008. CD28 provides T-cell costimulation and enhances PI3K activity at the immune synapse independently of its capacity to interact with the p85/p110 heterodimer. *Blood* 111:1464-1471.
172. Samstag, Y., and G. Nebl. 2005. Ras initiates phosphatidyl-inositol-3-kinase (PI3K)/PKB mediated signalling pathways in untransformed human peripheral blood T lymphocytes. *Adv Enzyme Regul* 45:52-62.
173. Soond, D. R., E. Bjorgo, K. Moltu, V. Q. Dale, D. T. Patton, K. M. Torgersen, F. Galleway, B. Twomey, J. Clark, J. S. H. Gaston, K. Tasken, P. Bunyard, and K. Okkenhaug. PI3K p110{delta} regulates T-cell cytokine production during primary and secondary immune responses in mice and humans. *Blood* 115:2203-2213.
174. Thomas, M. J., A. Smith, D. H. Head, L. Milne, A. Nicholls, W. Pearce, B. Vanhaesebroeck, M. P. Wymann, E. Hirsch, A. Trifilieff, C. Walker, P. Finan, and J. Westwick. 2005. Airway inflammation: chemokine-induced neutrophilia and the class I phosphoinositide 3-kinases. *Eur J Immunol* 35:1283-1291.
175. Takeda, M., W. Ito, M. Tanabe, S. Ueki, H. Kato, J. Kihara, T. Tanigai, T. Chiba, K. Yamaguchi, H. Kayaba, Y. Imai, K. Okuyama, I. Ohno, T. Sasaki, and J. Chihara. 2009. Allergic airway hyperresponsiveness, inflammation, and remodeling do not develop in phosphoinositide 3-kinase [gamma]-deficient mice. *Journal of Allergy and Clinical Immunology* 123:805-812.
176. Sasaki, T., J. Irie-Sasaki, R. G. Jones, A. J. Oliveira-dos-Santos, W. L. Stanford, B. Bolon, A. Wakeham, A. Itie, D. Bouchard, I. Kozieradzki, N. Joza, T. W. Mak, P. S. Ohashi, A. Suzuki, and J. M. Penninger. 2000. Function of PI3K in Thymocyte Development, T Cell Activation, and Neutrophil Migration. *Science* 287:1040-1046.
177. Thomas, M. S., J. S. Mitchell, C. C. DeNucci, A. L. Martin, and Y. Shimizu. 2008. The p110{gamma} isoform of phosphatidylinositol 3-kinase regulates migration of effector CD4 T lymphocytes into peripheral inflammatory sites. *J Leukoc Biol* 84:814-823.
178. Alcazar, I., M. Marques, A. Kumar, E. Hirsch, M. Wymann, A. C. Carrera, and D. F. Barber. 2007. Phosphoinositide 3 kinase {gamma} participates in T cell receptor induced T cell activation. *J. Exp. Med.* 204:2977-2987.
179. Okkenhaug, K., A. Bilancio, G. Farjot, H. Priddle, S. Sancho, E. Peskett, W. Pearce, S. E. Meek, A. Salpekar, M. D. Waterfield, A. J. H. Smith, and B. Vanhaesebroeck. 2002. Impaired B and T Cell Antigen Receptor Signaling in p110delta PI 3-Kinase Mutant Mice. *Science* 297:1031-1034.
180. Okkenhaug, K., D. T. Patton, A. Bilancio, F. Garcon, W. C. Rowan, and B. Vanhaesebroeck. 2006. The p110{delta} Isoform of Phosphoinositide 3-Kinase Controls Clonal Expansion and Differentiation of Th Cells. *J Immunol* 177:5122-5128.
181. Jarmin, S. J. 2008. T cell receptor induced phosphoinositide-3-kinase p110delta activity is required for T cell localization to antigenic tissue in mice. *The Journal of Clinical Investigation* 118:1154-1164.

182. Patton, D. T., O. A. Garden, W. P. Pearce, L. E. Clough, C. R. Monk, E. Leung, W. C. Rowan, S. Sancho, L. S. Walker, B. Vanhaesebroeck, and K. Okkenhaug. 2006. Cutting edge: the phosphoinositide 3-kinase p110 delta is critical for the function of CD4+CD25+Foxp3+ regulatory T cells. *J Immunol* 177:6598-6602.
183. Tarasenko, T., H. K. Kole, A. W. Chi, M. M. Mentink-Kane, T. A. Wynn, and S. Bolland. 2007. T cell-specific deletion of the inositol phosphatase SHIP reveals its role in regulating Th1/Th2 and cytotoxic responses. *Proc Natl Acad Sci U S A* 104:11382-11387.
184. Helgason, C. D., J. E. Damen, P. Rosten, R. Grewal, P. Sorensen, S. M. Chappel, A. Borowski, F. Jirik, G. Krystal, and R. K. Humphries. 1998. Targeted disruption of SHIP leads to hemopoietic perturbations, lung pathology, and a shortened life span. *Genes Dev* 12:1610-1620.
185. Collazo, M. M., D. Wood, K. H. Paraiso, E. Lund, R. W. Engelman, C. T. Le, D. Stauch, K. Kotsch, and W. G. Kerr. 2009. SHIP limits immunoregulatory capacity in the T-cell compartment. *Blood* 113:2934-2944.
186. Locke, N. R., S. J. Patterson, M. J. Hamilton, L. M. Sly, G. Krystal, and M. K. Levings. 2009. SHIP regulates the reciprocal development of T regulatory and Th17 cells. *J Immunol* 183:975-983.
187. Li, J., C. Yen, D. Liaw, K. Podsypanina, S. Bose, S. I. Wang, J. Puc, C. Miliaresis, L. Rodgers, R. McCombie, S. H. Bigner, B. C. Giovanella, M. Ittmann, B. Tycko, H. Hibshoosh, M. H. Wigler, and R. Parsons. 1997. PTEN, a Putative Protein Tyrosine Phosphatase Gene Mutated in Human Brain, Breast, and Prostate Cancer. *Science* 275:1943-1947.
188. Maehama, T., and J. E. Dixon. 1998. The Tumor Suppressor, PTEN/MMAC1, Dephosphorylates the Lipid Second Messenger, Phosphatidylinositol 3,4,5-Trisphosphate. *J Biol Chem* 273:13375-13378.
189. Patton, D. T., O. A. Garden, W. P. Pearce, L. E. Clough, C. R. Monk, E. Leung, W. C. Rowan, S. Sancho, L. S. K. Walker, B. Vanhaesebroeck, and K. Okkenhaug. 2006. Cutting Edge: The Phosphoinositide 3-Kinase p110{delta} Is Critical for the Function of CD4+CD25+Foxp3+ Regulatory T Cells. *J Immunol* 177:6598-6602.
190. Rodriguez-Borlado, L., D. F. Barber, C. Hernandez, M. A. Rodriguez-Marcos, A. Sanchez, E. Hirsch, M. Wymann, C. Martinez-A, and A. C. Carrera. 2003. Phosphatidylinositol 3-Kinase Regulates the CD4/CD8 T Cell Differentiation Ratio. *J Immunol* 170:4475-4482.
191. Barber, D. F., A. Bartolome, C. Hernandez, J. M. Flores, C. Fernandez-Arias, L. Rodriguez-Borlado, E. Hirsch, M. Wymann, D. Balomenos, and A. C. Carrera. 2006. Class IB-Phosphatidylinositol 3-Kinase (PI3K) Deficiency Ameliorates IA-PI3K-Induced Systemic Lupus but Not T Cell Invasion. *J Immunol* 176:589-593.
192. Nombela-Arrieta, C., R. A. Lacalle, M. C. Montoya, Y. Kunisaki, D. Megías, M. Marqués, A. C. Carrera, S. Mañes, Y. Fukui, C. Martínez-A, and J. V. Stein. 2004. Differential Requirements for DOCK2 and Phosphoinositide-3-Kinase [gamma] during T and B Lymphocyte Homing. *Immunity* 21:429-441.
193. Oh, S.-Y., T. Zheng, M. L. Bailey, D. L. Barber, J. T. Schroeder, Y.-K. Kim, and Z. Zhu. 2007. Src homology 2 domain-containing inositol 5-phosphatase

1 deficiency leads to a spontaneous allergic inflammation in the murine lung. *Journal of Allergy and Clinical Immunology* 119:123-131.

194. Kashiwada, M., G. Cattoretti, L. McKeag, T. Rouse, B. M. Showalter, U. Al-Alem, M. Niki, P. P. Pandolfi, E. H. Field, and P. B. Rothman. 2006. Downstream of Tyrosine Kinases-1 and Src Homology 2-Containing Inositol 5'-Phosphatase Are Required for Regulation of CD4+CD25+ T Cell Development. *J Immunol* 176:3958-3965.
195. Di Cristofano, A., P. Kotsi, Y. F. Peng, C. Cordon-Cardo, K. B. Elkon, and P. P. Pandolfi. 1999. Impaired Fas Response and Autoimmunity in Pten+/ Mice. *Science* 285:2122-2125.
196. Lacalle, R. A., C. Gomez-Mouton, D. F. Barber, S. Jimenez-Baranda, E. Mira, C. Martinez-A, A. C. Carrera, and S. Manes. 2004. PTEN regulates motility but not directionality during leukocyte chemotaxis. *J Cell Sci* 117:6207-6215.
197. Johnson, T. A., S. Tsutsui, and F. R. Jirik. 2008. Antigen-Induced Pten Gene Deletion in T Cells Exacerbates Neuropathology in Experimental Autoimmune Encephalomyelitis. *Am J Pathol* 172:980-992.
198. Buckler, J. L., P. T. Walsh, P. M. Porrett, Y. Choi, and L. A. Turka. 2006. Cutting Edge: T Cell Requirement for CD28 Costimulation Is Due to Negative Regulation of TCR Signals by PTEN. *J Immunol* 177:4262-4266.
199. Zhang, T.-t., K. Okkenhaug, B. F. Nashed, K. D. Puri, Z. A. Knight, K. M. Shokat, B. Vanhaesebroeck, and A. J. Marshall. 2008. Genetic or pharmaceutical blockade of p110[delta] phosphoinositide 3-kinase enhances IgE production. *Journal of Allergy and Clinical Immunology* 122:811-819.e812.
200. Al-Alwan, M. M., K. Okkenhaug, B. Vanhaesebroeck, J. S. Hayflick, and A. J. Marshall. 2007. Requirement for Phosphoinositide 3-Kinase p110{delta} Signaling in B Cell Antigen Receptor-Mediated Antigen Presentation. *J Immunol* 178:2328-2335.
201. Tamir, I., J. C. Stolpa, C. D. Helgason, K. Nakamura, P. Bruhns, M. Daeron, and J. C. Cambier. 2000. The RasGAP-binding protein p62dok is a mediator of inhibitory FcgammaRIIB signals in B cells. *Immunity* 12:347-358.
202. Leung, W. H., T. Tarasenko, and S. Bolland. 2009. Differential roles for the inositol phosphatase SHIP in the regulation of macrophages and lymphocytes. *Immunol Res* 43:243-251.
203. Suzuki, A., T. Kaisho, M. Ohishi, M. Tsukio-Yamaguchi, T. Tsubata, P. A. Koni, T. Sasaki, T. W. Mak, and T. Nakano. 2003. Critical Roles of Pten in B Cell Homeostasis and Immunoglobulin Class Switch Recombination. *J. Exp. Med.* 197:657-667.
204. Randis, T. M., K. D. Puri, H. Zhou, and T. G. Diacovo. 2008. Role of PI3Kdelta and PI3Kgamma in inflammatory arthritis and tissue localization of neutrophils. *Eur J Immunol* 38:1215-1224.
205. Sarraj, B., S. Massberg, Y. Li, A. Kasorn, K. Subramanian, F. Loison, L. E. Silberstein, U. von Andrian, and H. R. Luo. 2009. Myeloid-Specific Deletion of Tumor Suppressor PTEN Augments Neutrophil Transendothelial Migration during Inflammation. *J Immunol* 182:7190-7200.
206. Heit, B., S. M. Robbins, C. M. Downey, Z. Guan, P. Colarusso, B. J. Miller, F. R. Jirik, and P. Kubes. 2008. PTEN functions to 'prioritize' chemotactic cues and prevent 'distraction' in migrating neutrophils. *Nat Immunol* 9:743-752.

207. Li, Y., Y. Jia, M. Pichavant, F. Loison, B. Sarraj, A. Kasorn, J. You, B. E. Robson, D. T. Umetsu, J. P. Mizgerd, K. Ye, and H. R. Luo. 2009. Targeted deletion of tumor suppressor PTEN augments neutrophil function and enhances host defense in neutropenia-associated pneumonia. *Blood* 113:4930-4941.
208. Thomas, M., M. J. Edwards, E. Sawicka, N. Duggan, E. Hirsch, M. P. Wymann, C. Owen, A. Trifilieff, C. Walker, J. Westwick, and P. Finan. 2009. Essential role of phosphoinositide 3-kinase gamma in eosinophil chemotaxis within acute pulmonary inflammation. *Immunology* 126:413-422.
209. Papakonstanti, E. A., O. Zwaenepoel, A. Bilancio, E. Burns, G. E. Nock, B. Houseman, K. Shokat, A. J. Ridley, and B. Vanhaesebroeck. 2008. Distinct roles of class IA PI3K isoforms in primary and immortalised macrophages. *J Cell Sci* 121:4124-4133.
210. Camps, M., T. Ruckle, H. Ji, V. Ardissone, F. Rintelen, J. Shaw, C. Ferrandi, C. Chabert, C. Gillieron, B. Francon, T. Martin, D. Gretener, D. Perrin, D. Leroy, P. A. Vitte, E. Hirsch, M. P. Wymann, R. Cirillo, M. K. Schwarz, and C. Rommel. 2005. Blockade of PI3Kgamma suppresses joint inflammation and damage in mouse models of rheumatoid arthritis. *Nat Med* 11:936-943.
211. Jones, G. E., E. Prigmore, R. Calvez, C. Hogan, G. A. Dunn, E. Hirsch, M. P. Wymann, and A. J. Ridley. 2003. Requirement for PI 3-kinase [gamma] in macrophage migration to MCP-1 and CSF-1. *Experimental Cell Research* 290:120-131.
212. Bishop, J. L., L. M. Sly, G. Krystal, and B. B. Finlay. 2008. The Inositol Phosphatase SHIP Controls Salmonella enterica Serovar Typhimurium Infection In Vivo. *Infect. Immun.* 76:2913-2922.
213. Nakamura, K., A. Malykhin, and K. M. Coggeshall. 2002. The Src homology 2 domain-containing inositol 5-phosphatase negatively regulates Fcgamma receptor-mediated phagocytosis through immunoreceptor tyrosine-based activation motif-bearing phagocytic receptors. *Blood* 100:3374-3382.
214. Kamen, L. A., J. Levinsohn, A. Cadwallader, S. Tridandapani, and J. A. Swanson. 2008. SHIP-1 Increases Early Oxidative Burst and Regulates Phagosome Maturation in Macrophages. *J Immunol* 180:7497-7505.
215. Ali, K., M. Camps, W. P. Pearce, H. Ji, T. Ruckle, N. Kuehn, C. Pasquali, C. Chabert, C. Rommel, and B. Vanhaesebroeck. 2008. Isoform-Specific Functions of Phosphoinositide 3-Kinases: p110{delta} but Not p110{gamma} Promotes Optimal Allergic Responses In Vivo. *J Immunol* 180:2538-2544.
216. Ali, K., A. Bilancio, M. Thomas, W. Pearce, A. M. Gilfillan, C. Tkaczyk, N. Kuehn, A. Gray, J. Giddings, E. Peskett, R. Fox, I. Bruce, C. Walker, C. Sawyer, K. Okkenhaug, P. Finan, and B. Vanhaesebroeck. 2004. Essential role for the p110[delta] phosphoinositide 3-kinase in the allergic response. *Nature* 431:1007-1011.
217. Kitaura, J., T. Kinoshita, M. Matsumoto, S. Chung, Y. Kawakami, M. Leitges, D. Wu, C. A. Lowell, and T. Kawakami. 2005. IgE- and IgE+Ag-mediated mast cell migration in an autocrine/paracrine fashion. *Blood* 105:3222-3229.
218. Laffargue, M., R. Calvez, P. Finan, A. Trifilieff, M. Barbier, F. Altruda, E. Hirsch, and M. P. Wymann. 2002. Phosphoinositide 3-Kinase [gamma] Is an Essential Amplifier of Mast Cell Function. *Immunity* 16:441-451.

219. Haddon, D. J., F. Antignano, M. R. Hughes, M.-R. Blanchet, L. Zbytnuik, G. Krystal, and K. M. McNagny. 2009. SHIP1 Is a Repressor of Mast Cell Hyperplasia, Cytokine Production, and Allergic Inflammation In Vivo. *J Immunol* 183:228-236.
220. Huber, M., C. D. Helgason, J. E. Damen, L. Liu, R. K. Humphries, and G. Krystal. 1998. The src homology 2-containing inositol phosphatase (SHIP) is the gatekeeper of mast cell degranulation. *Proc Natl Acad Sci U S A* 95:11330-11335.
221. Furumoto, Y., S. Brooks, A. Olivera, Y. Takagi, M. Miyagishi, K. Taira, R. Casellas, M. A. Beaven, A. M. Gilfillan, and J. Rivera. 2006. Cutting Edge: Lentiviral Short Hairpin RNA Silencing of PTEN in Human Mast Cells Reveals Constitutive Signals That Promote Cytokine Secretion and Cell Survival. *J Immunol* 176:5167-5171.
222. Saudemont, A., F. Garcon, H. Yadi, M. Roche-Molina, N. Kim, A. Segonds-Pichon, A. Martin-Fontecha, K. Okkenhaug, and F. Colucci. 2009. p110gamma and p110delta isoforms of phosphoinositide 3-kinase differentially regulate natural killer cell migration in health and disease. *Proc Natl Acad Sci U S A* 106:5795-5800.
223. Tassi, I., M. Cella, S. Gilfillan, I. Turnbull, T. G. Diacovo, J. M. Penninger, and M. Colonna. 2007. p110[gamma] and p110[delta] Phosphoinositide 3-Kinase Signaling Pathways Synergize to Control Development and Functions of Murine NK Cells. *Immunity* 27:214-227.
224. Wang, J.-W., J. M. Howson, T. Ghansah, C. Desponts, J. M. Ninos, S. L. May, K. H. T. Nguyen, N. Toyama-Sorimachi, and W. G. Kerr. 2002. Influence of SHIP on the NK Repertoire and Allogeneic Bone Marrow Transplantation. *Science* 295:2094-2097.
225. Kishimoto, H., T. Ohteki, N. Yajima, K. Kawahara, M. Natsui, S. Kawarasaki, K. Hamada, Y. Horie, Y. Kubo, S. Arase, M. Taniguchi, B. Vanhaesebroeck, T. W. Mak, T. Nakano, S. Koyasu, T. Sasaki, and A. Suzuki. 2007. The Pten/PI3K pathway governs the homeostasis of V{alpha}14iNKT cells. *Blood* 109:3316-3324.
226. Krishnamoorthy, N., T. B. Oriss, M. Paglia, M. Fei, M. Yarlagadda, B. Vanhaesebroeck, A. Ray, and P. Ray. 2008. Activation of c-Kit in dendritic cells regulates T helper cell differentiation and allergic asthma. *Nat Med* 14:565-573.
227. Del Prete, A., W. Vermi, E. Dander, K. Otero, L. Barberis, W. Luini, S. Bernasconi, M. Sironi, A. Santoro, C. Garlanda, F. Facchetti, M. P. Wymann, A. Vecchi, E. Hirsch, A. Mantovani, and S. Sozzani. 2004. Defective dendritic cell migration and activation of adaptive immunity in PI3Kgamma-deficient mice. *EMBO J* 23:3505-3515.
228. Neill, L., A. H. Tien, J. Rey-Ladino, and C. D. Helgason. 2007. SHIP-deficient mice provide insights into the regulation of dendritic cell development and function. *Experimental Hematology* 35:627-639.
229. Agrawal, A., S. Agrawal, J.-N. Cao, H. Su, K. Osann, and S. Gupta. 2007. Altered Innate Immune Functioning of Dendritic Cells in Elderly Humans: A Role of Phosphoinositide 3-Kinase-Signaling Pathway. *J Immunol* 178:6912-6922.

230. Vonakis, B. M., K. Vasagar, J. S. P. Gibbons, L. Gober, P. M. Sterba, H. Chang, and S. S. Saini. 2007. Basophil Fc[var epsilon]RI histamine release parallels expression of Src-homology 2-containing inositol phosphatases in chronic idiopathic urticaria. *Journal of Allergy and Clinical Immunology* 119:441-448.
231. Gericke, A., M. Munson, and A. H. Ross. 2006. Regulation of the PTEN phosphatase. *Gene* 374:1-9.
232. Leslie, N. R., D. Bennett, Y. E. Lindsay, H. Stewart, A. Gray, and C. P. Downes. 2003. Redox regulation of PI 3-kinase signalling via inactivation of PTEN. *Embo J* 22:5501-5510.
233. Lin, H. K., Y. C. Hu, D. K. Lee, and C. Chang. 2004. Regulation of androgen receptor signaling by PTEN (phosphatase and tensin homolog deleted on chromosome 10) tumor suppressor through distinct mechanisms in prostate cancer cells. *Molecular Endocrinology* 18:2409-2423.
234. Liu, F., S. Wagner, R. B. Campbell, J. A. Nickerson, C. A. Schiffer, and A. H. Ross. 2005. PTEN enters the nucleus by diffusion. *Journal of Cellular Biochemistry* 96:221-234.
235. Baker, S. J. 2007. PTEN enters the nuclear age. *Cell* 128:25-28.
236. Ginn-Pease, M. E., and C. Eng. 2003. Increased nuclear phosphatase and tensin homologue deleted on chromosome 10 is associated with G0-G1 in MCF-7 cells. *Cancer Res* 63:282-286.
237. Kavanaugh, W. M., D. A. Pot, S. M. Chin, M. Deuter-Reinhard, A. B. Jefferson, F. A. Norris, F. R. Masiarz, L. S. Cousens, P. W. Majerus, and L. T. Williams. 1996. Multiple forms of an inositol polyphosphate 5-phosphatase form signaling complexes with Shc and Grb2. *Current Biology* 6:438-445.
238. Tu, Z., J. M. Ninos, Z. Ma, J. W. Wang, M. P. Lemos, C. Desponts, T. Ghansah, J. M. Howson, and W. G. Kerr. 2001. Embryonic and hematopoietic stem cells express a novel SH2-containing inositol 5'-phosphatase isoform that partners with the Grb2 adapter protein. *Blood* 98:2028-2038.
239. Wolf, I., D. M. Lucas, P. A. Algate, and L. R. Rohrschneider. 2000. Cloning of the Genomic Locus of Mouse SH2 Containing Inositol 5-Phosphatase (SHIP) and a Novel 110-kDa Splice Isoform, SHIP[delta]. *Genomics* 69:104-112.
240. Damen, J. E., L. Liu, M. D. Ware, M. Ermolaeva, P. W. Majerus, and G. Krystal. 1998. Multiple forms of the SH2-containing inositol phosphatase, SHIP, are generated by C-terminal truncation. *Blood* 92:1199-1205.
241. Lucas, D. M., and L. R. Rohrschneider. 1999. A novel spliced form of SH2-containing inositol phosphatase is expressed during myeloid development. *Blood* 93:1922-1933.
242. Moody, J. L., and F. R. Jirik. 2004. Compound heterozygosity for Pten and SHIP augments T-dependent humoral immune responses and cytokine production by CD(4+) T cells. *Immunology* 112:404-412.
243. Luo, J. M., Z. L. Liu, H. L. Hao, F. X. Wang, Z. R. Dong, and R. Ohno. 2004. Mutation analysis of SHIP gene in acute leukemia. *Journal of Experimental Hematology / Chinese Association of Pathophysiology* 12:420-426.
244. Freeburn, R. W., K. L. Wright, S. J. Burgess, E. Astoul, D. A. Cantrell, and S. G. Ward. 2002. Evidence That SHIP-1 Contributes to Phosphatidylinositol 3,4,5-Trisphosphate Metabolism in T Lymphocytes and Can Regulate Novel Phosphoinositide 3-Kinase Effectors. *J Immunol* 169:5441-5450.

245. Suzuki, A., M. T. Yamaguchi, T. Ohteki, T. Sasaki, T. Kaisho, Y. Kimura, R. Yoshida, A. Wakeham, T. Higuchi, M. Fukumoto, T. Tsubata, P. S. Ohashi, S. Koyasu, J. M. Penninger, T. Nakano, and T. W. Mak. 2001. T cell-specific loss of Pten leads to defects in central and peripheral tolerance. *Immunity* 14:523-534.
246. Buckler, J. L., P. T. Walsh, P. M. Porrett, Y. Choi, and L. A. Turka. 2006. Cutting edge: T cell requirement for CD28 costimulation is due to negative regulation of TCR signals by PTEN. *J Immunol* 177:4262-4266.
247. Seminario, M. C., P. Precht, S. C. Bunnell, S. E. Warren, C. M. Morris, D. Taub, and R. L. Wange. 2004. PTEN permits acute increases in D3-phosphoinositide levels following TCR stimulation but inhibits distal signaling events by reducing the basal activity of Akt. *Eur J Immunol* 34:3165-3175.
248. Shan, X., M. J. Czar, S. C. Bunnell, P. Liu, Y. Liu, P. L. Schwartzberg, and R. L. Wange. 2000. Deficiency of PTEN in Jurkat T cells causes constitutive localization of Itk to the plasma membrane and hyperresponsiveness to CD3 stimulation. *Mol Cell Biol* 20:6945-6957.
249. Lee, K. S., S. R. Kim, S. J. Park, H. K. Lee, H. S. Park, K. H. Min, S. M. Jin, and Y. C. Lee. 2006. Phosphatase and tensin homolog deleted on chromosome 10 (PTEN) reduces vascular endothelial growth factor expression in allergen-induced airway inflammation. *Molecular Pharmacology* 69:1829-1839.
250. Kwak, Y. G., C. H. Song, H. K. Yi, P. H. Hwang, J. S. Kim, K. S. Lee, and Y. C. Lee. 2003. Involvement of PTEN in airway hyperresponsiveness and inflammation in bronchial asthma. *J Clin Invest* 111:1083-1092.
251. Thomas, C. C., S. Dowler, M. Deak, D. R. Alessi, and D. M. van Aalten. 2001. Crystal structure of the phosphatidylinositol 3,4-bisphosphate-binding pleckstrin homology (PH) domain of tandem PH-domain-containing protein 1 (TAPP1): molecular basis of lipid specificity. *Biochem. J.* 358:287-294.
252. Damen, J. E., M. D. Ware, J. Kalesnikoff, M. R. Hughes, and G. Krystal. 2001. SHIP's C-terminus is essential for its hydrolysis of PIP3 and inhibition of mast cell degranulation. *Blood* 97:1343-1351.
253. Sattler, M., S. Verma, Y. B. Pride, R. Salgia, L. R. Rohrschneider, and J. D. Griffin. 2001. SHIP1, an SH2 Domain Containing Polyinositol-5-phosphatase, Regulates Migration through Two Critical Tyrosine Residues and Forms a Novel Signaling Complex with DOK1 and CRKL. *J Biol Chem* 276:2451-2458.
254. Sattler, M., R. Salgia, G. Shrikhande, S. Verma, J. L. Choi, L. R. Rohrschneider, and J. D. Griffin. 1997. The phosphatidylinositol polyphosphate 5-phosphatase SHIP and the protein tyrosine phosphatase SHP-2 form a complex in hematopoietic cells which can be regulated by BCR/ABL and growth factors. *Oncogene* 15:2379-2384.
255. Chari, R., S. Kim, S. Murugappan, A. Sanjay, J. L. Daniel, and S. P. Kunapuli. 2009. Lyn, PKC-{delta}, SHIP-1 interactions regulate GPVI-mediated platelet-dense granule secretion. *Blood* 114:3056-3063.
256. Xiao, W., H. Hong, Y. Kawakami, C. A. Lowell, and T. Kawakami. 2008. Regulation of myeloproliferation and M2 macrophage programming in mice by Lyn/Hck, SHIP, and Stat5. *The Journal of Clinical Investigation* 118:924-934.
257. Zhang, J., S. F. Walk, K. S. Ravichandran, and J. C. Garrison. 2009. Regulation of the Src homology 2 domain-containing inositol 5'-phosphatase

(SHIP1) by the cyclic AMP-dependent protein kinase. *J Biol Chem* 284:20070-20078.

258. Dong, S., B. Corre, E. Foulon, E. Dufour, A. Veillette, O. Acuto, and F. Michel. 2006. T cell receptor for antigen induces linker for activation of T cell-dependent activation of a negative signaling complex involving Dok-2, SHIP-1, and Grb-2. *J Exp Med* 203:2509-2518.
259. Paraiso, K. H., T. Ghansah, A. Costello, R. W. Engelman, and W. G. Kerr. 2007. Induced SHIP deficiency expands myeloid regulatory cells and abrogates graft-versus-host disease. *J Immunol* 178:2893-2900.
260. Ghansah, T., K. H. T. Paraiso, S. Highfill, C. Desponts, S. May, J. K. McIntosh, J.-W. Wang, J. Ninos, J. Brayer, F. Cheng, E. Sotomayor, and W. G. Kerr. 2004. Expansion of Myeloid Suppressor Cells in SHIP-Deficient Mice Represses Allogeneic T Cell Responses. *J Immunol* 173:7324-7330.
261. Liu, Q., A. J. Oliveira-Dos-Santos, S. Mariathasan, D. Bouchard, J. Jones, R. Sarao, I. Kozieradzki, P. S. Ohashi, J. M. Penninger, and D. J. Dumont. 1998. The inositol polyphosphate 5-phosphatase ship is a crucial negative regulator of B cell antigen receptor signaling. *J Exp Med* 188:1333-1342.
262. Oh, S. Y., T. Zheng, M. L. Bailey, D. L. Barber, J. T. Schroeder, Y. K. Kim, and Z. Zhu. 2007. Src homology 2 domain-containing inositol 5-phosphatase 1 deficiency leads to a spontaneous allergic inflammation in the murine lung. *J Allergy Clin Immunol* 119:123-131.
263. Gloire, G., E. Charlier, S. Rahmouni, C. Volanti, A. Chariot, C. Erneux, and J. Piette. 2006. Restoration of SHIP-1 activity in human leukemic cells modifies NF-kappaB activation pathway and cellular survival upon oxidative stress. *Oncogene* 25:5485-5494.
264. Gloire, G., C. Erneux, and J. Piette. 2007. The role of SHIP1 in T-lymphocyte life and death. *Biochemical Society Transactions* 35:277-280.
265. Yagi, J., Y. Arimura, H. Takatori, H. Nakajima, I. Iwamoto, and T. Uchiyama. 2006. Genetic background influences Th cell differentiation by controlling the capacity for IL-2-induced IL-4 production by naive CD4+ T cells. *Int. Immunol.* 18:1681-1690.
266. Lapierre, P., K. Béland, I. Djilali-Saiah, and F. Alvarez. 2006. Type 2 autoimmune hepatitis murine model: The influence of genetic background in disease development. *Journal of Autoimmunity* 26:82-89.
267. Masnaya, N. V., A. A. Churin, O. S. Borsuk, and E. Y. Sherstoboev. 2002. Immune reactions in different mouse strains. *Bull Exp Biol Med* 134:376-378.
268. Gueders, M. M., G. Paulissen, C. Crahay, F. Quesada-Calvo, J. Hacha, C. Van Hove, K. Tournoy, R. Louis, J. M. Foidart, A. Noel, and D. D. Cataldo. 2009. Mouse models of asthma: a comparison between C57BL/6 and BALB/c strains regarding bronchial responsiveness, inflammation, and cytokine production. *Inflamm Res* 58:845-854.
269. Luo, J. M., H. Yoshida, S. Komura, N. Ohishi, L. Pan, K. Shigeno, I. Hanamura, K. Miura, S. Iida, R. Ueda, T. Naoe, Y. Akao, R. Ohno, and K. Ohnishi. 2003. Possible dominant-negative mutation of the SHIP gene in acute myeloid leukemia. *Leukemia* 17:1-8.
270. Fukuda, R., A. Hayashi, A. Utsunomiya, Y. Nukada, R. Fukui, K. Itoh, K. Tezuka, K. Ohashi, K. Mizuno, M. Sakamoto, M. Hamanoue, and T. Tsuji. 2005. Alteration of phosphatidylinositol 3-kinase cascade in the multilobulated

nuclear formation of adult T cell leukemia/lymphoma (ATLL). *Proc Natl Acad Sci U S A* 102:15213-15218.

271. Fukuda, R. I., K. Tsuchiya, K. Suzuki, K. Itoh, J. Fujita, A. Utsunomiya, and T. Tsuji. 2009. Human T-cell leukemia virus type I tax down-regulates the expression of phosphatidylinositol 3,4,5-trisphosphate inositol phosphatases via the NF-kappaB pathway. *J Biol Chem* 284:2680-2689.
272. Tony, C. T. L., M. B. Lisa, K. Youngjin, N. Elizabeth Ann, L. Y. Alice, and B. D. Mitchell. 2009. Inactivation of SHIP1 in T-cell acute lymphoblastic leukemia due to mutation and extensive alternative splicing. *Leukemia Research* 33:1562-1566.
273. Avota, E., H. Harms, and S. Schneider-Schaulies. 2006. Measles virus induces expression of SIP110, a constitutively membrane clustered lipid phosphatase, which inhibits T cell proliferation. *Cell Microbiol* 8 1826-1839.
274. Latour, S., G. Gish, C. D. Helgason, R. K. Humphries, T. Pawson, and A. Veillette. 2001. Regulation of SLAM-mediated signal transduction by SAP, the X-linked lymphoproliferative gene product. *Nat Immunol* 2:681-690.
275. Desponts, C., J. M. Ninos, and W. G. Kerr. 2006. s-SHIP associates with receptor complexes essential for pluripotent stem cell growth and survival. *Stem Cells Dev* 15:641-646.
276. Desponts, C., A. L. Hazen, K. H. Paraiso, and W. G. Kerr. 2006. SHIP deficiency enhances HSC proliferation and survival but compromises homing and repopulation. *Blood* 107:4338-4345.
277. Backers, K., D. Blero, N. Paternotte, J. Zhang, and C. Erneux. 2003. The termination of PI3K signalling by SHIP1 and SHIP2 inositol 5-phosphatases. *Advances in Enzyme Regulation* 43:15-28.
278. Dyson, J. M., A. M. Kong, F. Wiradjaja, M. V. Astle, R. Gurung, and C. A. Mitchell. 2005. The SH2 domain containing inositol polyphosphate 5-phosphatase-2: SHIP2. *Int J Biochem Cell Biol* 37:2260-2265.
279. Pesesse, X., S. Deleu, F. De Smedt, L. Drayer, and C. Erneux. 1997. Identification of a second SH2-domain-containing protein closely related to the phosphatidylinositol polyphosphate 5-phosphatase SHIP. *Biochem Biophys Res Commun* 239:697-700.
280. Habib, T., J. A. Hejna, R. E. Moses, and S. J. Decker. 1998. Growth factors and insulin stimulate tyrosine phosphorylation of the 51C/SHIP2 protein. *J Biol Chem* 273:18605-18609.
281. Tomlinson, M. G., V. L. Heath, C. W. Turck, S. P. Watson, and A. Weiss. 2004. SHIP Family Inositol Phosphatases Interact with and Negatively Regulate the Tec Tyrosine Kinase. *J Biol Chem* 279: 55089-55096.
282. Zhang, Y., A. S. Wavreille, A. R. Kunys, and D. Pei. 2009. The SH2 domains of inositol polyphosphate 5-phosphatases SHIP1 and SHIP2 have similar ligand specificity but different binding kinetics. *Biochemistry* 48:11075-11083.
283. Stephens, L., L. Milne, and P. Hawkins. 2008. Moving towards a Better Understanding of Chemotaxis. *Current Biology* 18:R485-R494.
284. Lu, M., J. M. Kinchen, K. L. Rossman, C. Grimsley, C. deBakker, E. Brugnera, A. C. Tosello-Trampont, L. B. Haney, D. Klingele, J. Sondek, M. O. Hengartner, and K. S. Ravichandran. 2004. PH domain of ELMO functions in trans to regulate Rac activation via Dock180. *Nat Struct Mol Biol* 11:756-762.

285. Andrews, S., L. R. Stephens, and P. T. Hawkins. 2007. PI3K Class IB Pathway in Neutrophils. *Sci. STKE* 2007:cm3.
286. Smith, L. D., E. S. Hickman, R. V. Parry, J. Westwick, and S. G. Ward. 2007. PI3K[gamma] is the dominant isoform involved in migratory responses of human T lymphocytes: Effects of ex vivo maintenance and limitations of non-viral delivery of siRNA. *Cellular Signalling* 19:2528-2539.
287. Andrew, N., and R. H. Insall. 2007. Chemotaxis in shallow gradients is mediated independently of PtdIns 3-kinase by biased choices between random protrusions. *Nat Cell Biol* 9:193-200.
288. Insall, R., and N. Andrew. 2007. Chemotaxis in Dictyostelium: how to walk straight using parallel pathways. *Current Opinion in Microbiology* 10:578-581.
289. Bagorda, A., and C. A. Parent. 2008. Eukaryotic chemotaxis at a glance. *J Cell Sci* 121:2621-2624.
290. Cantley, L. C. 2002. The Phosphoinositide 3-Kinase Pathway. *Science* 296:1655-1657.
291. Subramanian, K. K., Y. Jia, D. Zhu, B. T. Simms, H. Jo, H. Hattori, J. You, J. P. Mizgerd, and H. R. Luo. 2007. Tumor suppressor PTEN is a physiologic suppressor of chemoattractant-mediated neutrophil functions. *Blood* 109:4028-4037.
292. Gao, P., R. L. Wange, N. Zhang, J. J. Oppenheim, and O. M. Howard. 2005. Negative regulation of CXCR4-mediated chemotaxis by the lipid phosphatase activity of tumor suppressor PTEN. *Blood* 106:2619-2626.
293. Nishio, M., K. Watanabe, J. Sasaki, C. Taya, S. Takasuga, R. Iizuka, T. Balla, M. Yamazaki, H. Watanabe, R. Itoh, S. Kuroda, Y. Horie, I. Forster, T. W. Mak, H. Yonekawa, J. M. Penninger, Y. Kanaho, A. Suzuki, and T. Sasaki. 2007. Control of cell polarity and motility by the PtdIns(3,4,5)P3 phosphatase SHIP1. *Nat Cell Biol* 9:36-44.
294. Wain, C. M., J. Westwick, and S. G. Ward. 2005. Heterologous regulation of chemokine receptor signaling by the lipid phosphatase SHIP in lymphocytes. *Cellular Signalling* 17:1194-1202.
295. Yap, T. A., M. D. Garrett, M. I. Walton, F. Raynaud, J. S. de Bono, and P. Workman. 2008. Targeting the PI3K-AKT-mTOR pathway: progress, pitfalls, and promises. *Curr Opin Pharmacol* 8:393-412.
296. Stoyanova, S., G. Bulgarelli-Leva, C. Kirsch, T. Hanck, R. Klinger, R. Wetzker, and M. P. Wymann. 1997. Lipid kinase and protein kinase activities of G-protein-coupled phosphoinositide 3-kinase gamma: structure-activity analysis and interactions with wortmannin. *Biochem. J.* 324:489-495.
297. Vlahos, C. J., W. F. Matter, K. Y. Hui, and R. F. Brown. 1994. A specific inhibitor of phosphatidylinositol 3-kinase, 2-(4-morpholinyl)-8-phenyl-4H-1-benzopyran-4-one (LY294002). *J Biol Chem* 269:5241-5248.
298. Sadhu, C., B. Masinovsky, K. Dick, C. G. Sowell, and D. E. Staunton. 2003. Essential role of phosphoinositide 3-kinase delta in neutrophil directional movement. *J Immunol* 170:2647-2654.
299. Raynaud, F. I., S. A. Eccles, S. Patel, S. Alix, G. Box, I. Chuckowree, A. Folkes, S. Gowan, A. De Haven Brandon, F. Di Stefano, A. Hayes, A. T. Henley, L. Lensun, G. Pergl-Wilson, A. Robson, N. Saghir, A. Zhyvoloup, E. McDonald, P. Sheldrake, S. Shuttleworth, M. Valenti, N. C. Wan, P. A. Clarke, and P. Workman. 2009. Biological properties of potent inhibitors of class I

phosphatidylinositide 3-kinases: from PI-103 through PI-540, PI-620 to the oral agent GDC-0941. *Mol Cancer Ther* 8:1725-1738.

300. Harris, S. J., J. G. Foster, and S. G. Ward. 2009. PI3K isoforms as drug targets in inflammatory diseases: lessons from pharmacological and genetic strategies. *Curr Opin Investig Drugs* 10:1151-1162.
301. Doukas, J., W. Wrasidlo, G. Noronha, E. Dneprovskaia, R. Fine, S. Weis, J. Hood, A. Demaria, R. Soll, and D. Cheresh. 2006. Phosphoinositide 3-kinase gamma/delta inhibition limits infarct size after myocardial ischemia/reperfusion injury. *Proc Natl Acad Sci U S A* 103:19866-19871.
302. Nashed, N Zhang, TAl-Alwan, M Halayko, HJ Okkenhaug,K Vanhaesebroeck, B HayGlass, KT Marshall, AJ 2007. Role of the phosphoinositide 3-kinase p110&dgr; in generation of type 2 cytokine responses and allergic airway inflammation. *European Journal of Immunology* 37:416-424.

303. 2009. ClinicalTrials.gov Study to Investigate Effects of CAL-101 in Subjects With Allergic Rhinitis Exposed to Allergen in an Environmental Chamber.
304. Thomas, M. Edwards, M. J. Sawicka, E. Duggan, N. Hirsch, E. Wymann, M. P.Owen, C.Trifilieff, A.Walker, C.Westwick, J.Finan, P.2009. Essential role of phosphoinositide 3-kinase gamma in eosinophil chemotaxis within acute pulmonary inflammation. *Immunology* 126:413-422.

305. Lim, D. H., J. Y. Cho, D. J. Song, S. Y. Lee, M. Miller, and D. H. Broide. 2009. PI3K{gamma}-deficient mice have reduced levels of allergen-induced eosinophilic inflammation and airway remodeling. *Am J Physiol Lung Cell Mol Physiol* 296:L210-219.
306. Doukas, J., L. Eide, K. Stebbins, A. Racanelli-Layton, L. Dellamary, M. Martin, E. Dneprovskaia, G. Noronha, R. Soll, W. Wrasidlo, L. M. Acevedo, and D. A. Cheresh. 2009. Aerosolized Phosphoinositide 3-Kinase {gamma}/{delta} Inhibitor TG100-115 [3-[2,4-Diamino-6-(3-hydroxyphenyl)pteridin-7-yl]phenol] as a Therapeutic Candidate for Asthma and Chronic Obstructive Pulmonary Disease. *J Pharmacol Exp Ther* 328:758-765.
307. Ito, K., G. Caramori, and I. M. Adcock. 2007. Therapeutic Potential of Phosphatidylinositol 3-Kinase Inhibitors in Inflammatory Respiratory Disease. *J Pharmacol Exp Ther* 321:1-8.
308. Maus, U. A., M. Backi, C. Winter, M. Srivastava, M. K. Schwarz, T. Ruckle, J. C. Paton, D. Briles, M. Mack, T. Welte, R. Maus, R. M. Bohle, W. Seeger, C. Rommel, E. Hirsch, J. Lohmeyer, and K. T. Preissner. 2007. Importance of phosphoinositide 3-kinase gamma in the host defense against pneumococcal infection. *Am J Respir Crit Care Med* 175:958-966.
309. Park S Kyung, H. M. Yong, C. L. 2008. Phosphoinositide 3-kinase δ inhibitor as a novel therapeutic agent in asthma. *Respirology* 13:764-771.

310. B. J. Lannutti S. A. Meadows A. Kashishian B. Steiner H. Chen R. G. A. Yu k. D. Puri N.A. Giese 2009. The development of PI3K p110delta inhibitors for hematological malignancies and inflammation. *Keystone Symposia: PI 3-Kinase Signaling in Disease* Olympic Valley, California, USA.

311. 2009. Calistoga Pharmaceuticals Reports Additional Clinical Responses in Ongoing Clinical Trial of CAL-101, an Isoform-Selective PI3 Kinase Inhibitor, Under Evaluation in Patients with Hematologic Malignancies.
312. Flinn, I. W., J. C. Byrd, R. R. Furman, J. R. Brown, C. B. T. S. Lin, N. A. Giese, and A. S. Yu. 2009. Preliminary evidence of clinical activity in a phase I study of CAL-101, a selective inhibitor of the p1108 isoform of phosphatidylinositol 3-kinase (P13K), in patients with select hematologic malignancies. *J Clin Oncol* 27:suppl; abstr 3543.
313. Marone, R., V. Cmiljanovic, B. Giese, and M. P. Wymann. 2008. Targeting phosphoinositide 3-kinase--Moving towards therapy. *Biochimica et Biophysica Acta (BBA) - Proteins & Proteomics* 1784:159-185.
314. Kim, S. R., K. S. Lee, S. J. Park, K. H. Min, K. Y. Lee, Y. H. Choe, Y. R. Lee, J. S. Kim, S. J. Hong, and Y. C. Lee. 2007. PTEN Down-Regulates IL-17 Expression in a Murine Model of Toluene Diisocyanate-Induced Airway Disease. *J Immunol* 179:6820-6829.
315. Rosivatz, E. 2007. Inhibiting PTEN. *Biochemical Society Transactions* 35:257-259.
316. Rosivatz, E., J. G. Matthews, N. Q. McDonald, X. Mulet, K. K. Ho, N. Lossi, A. C. Schmid, M. Mirabelli, K. M. Pomeranz, C. Erneux, E. W. Lam, R. Vilar, and R. Woscholski. 2006. A small molecule inhibitor for phosphatase and tensin homologue deleted on chromosome 10 (PTEN). *ACS Chem Biol* 1:780-790.
317. Knobloch, J., I. Schmitz, K. Gotz, K. Schulze-Osthoff, and U. Ruther. 2008. Thalidomide Induces Limb Anomalies by PTEN Stabilization, Akt Suppression, and Stimulation of Caspase-Dependent Cell Death. *Mol. Cell. Biol.* 28:529-538.
318. Harris, S. J., R. V. Parry, J. Westwick, and S. G. Ward. 2008. Phosphoinositide Lipid Phosphatases: Natural Regulators of Phosphoinositide 3-Kinase Signaling in T Lymphocytes. *J. Biol. Chem.* 283:2465-2469.
319. Yang, L., D. E. Williams, A. Mui, C. Ong, G. Krystal, R. van Soest, and R. J. Andersen. 2005. Synthesis of pelorol and analogues: activators of the inositol 5-phosphatase SHIP. *Org Lett* 7:1073-1076.
320. Ong, C. J., A. Ming-Lum, M. Nodwell, A. Ghanipour, L. Yang, D. E. Williams, J. Kim, L. Demirjian, P. Qasimi, J. Ruschmann, L. P. Cao, K. Ma, S. W. Chung, V. Duronio, R. J. Andersen, G. Krystal, and A. L. Mui. 2007. Small molecule agonists of SHIP1 inhibit the phosphoinositide 3-kinase pathway in hematopoietic cells. *Blood* 110:1942-1949.
321. Ong, C. J., A. Ming-Lum, M. Nodwell, A. Ghanipour, L. Yang, D. E. Williams, J. Kim, L. Demirjian, P. Qasimi, J. Ruschmann, L. P. Cao, K. Ma, S. W. Chung, V. Duronio, R. J. Andersen, G. Krystal, and A. L. Mui. 2007. Small molecule agonists of SHIP1 inhibit the phosphoinositide 3-kinase pathway in hematopoietic cells. *Blood*. 110:1942-1949.
322. Ong, C. J., A. Ming-Lum, M. Nodwell, A. Ghanipour, L. Yang, D. E. Williams, J. Kim, L. Demirjian, P. Qasimi, J. Ruschmann, L.-P. Cao, K. Ma, S. W. Chung, V. Duronio, R. J. Andersen, G. Krystal, and A. L. F. Mui. 2007. Small-molecule agonists of SHIP1 inhibit the phosphoinositide 3-kinase pathway in hematopoietic cells. *Blood* 110:1942-1949.

323. Kennah, M., T. Y. Yau, M. Nodwell, G. Krystal, R. J. Andersen, C. J. Ong, and A. L. F. Mui. 2009. Activation of SHIP via a small molecule agonist kills multiple myeloma cells. *Experimental Hematology* 37:1274-1283.
324. Aquinox Pharmaceuticals selects AQX-1125 as lead clinical candidate http://aqxpharma.com/news/news-20091011.html.
325. Oh, S., S. Roongapinun, F. Wu, T. Zheng, and Z. Zhu. 2009. Deletion of SHIP-1 in Mice Leads to Diminished Th2 Responses to TCR Stimulation in vitro and Allergen Immunization in vivo. *Journal of Allergy and Clinical Immunology* 123:S124-S124.
326. Curnock, A. P., and S. G. Ward. 2003. Development and characterisation of tetracycline-regulated phosphoinositide 3-kinase mutants: assessing the role of multiple phosphoinositide 3-kinases in chemokine signaling. *Journal of Immunological Methods* 273:29-41.
327. Kahl, C. A., J. Marsh, J. Fyffe, D. A. Sanders, and K. Cornetta. 2004. Human immunodeficiency virus type 1-derived lentivirus vectors pseudotyped with envelope glycoproteins derived from Ross River virus and Semliki Forest virus. *J Virol* 78:1421-1430.
328. Lois, C., E. J. Hong, S. Pease, E. J. Brown, and D. Baltimore. 2002. Germline transmission and tissue-specific expression of transgenes delivered by lentiviral vectors. *Science* 295:868-872.
329. Varela-Rohena, A., C. Carpenito, E. E. Perez, M. Richardson, R. V. Parry, M. Milone, J. Scholler, X. Hao, A. Mexas, R. G. Carroll, C. H. June, and J. L. Riley. 2008. Genetic engineering of T cells for adoptive immunotherapy. *Immunol Res* 42:166-181.
330. Parish, C. R. 1999. Fluorescent dyes for lymphocyte migration and proliferation studies. *Immunol Cell Biol* 77:499-508.
331. Vielkind, S., M. Gallagher-Gambarelli, M. Gomez, H. J. Hinton, and D. A. Cantrell. 2005. Integrin Regulation by RhoA in Thymocytes. *J Immunol* 175:350-357.
332. Van Gool, S. W., M. de Boer, and J. L. Ceuppens. 1993. CD28 ligation by monoclonal antibodies or B7/BB1 provides an accessory signal for the cyclosporin A-resistant generation of cytotoxic T cell activity. *J Immunol* 150:3254-3263.
333. Thomas, M., M. J. Edwards, E. Sawicka, N. Duggan, E. Hirsch, M. P. Wymann, C. Owen, A. Trifilieff, C. Walker, J. Westwick, and P. Finan. 2009. Essential role of phosphoinositide 3-kinase gamma in eosinophil chemotaxis within acute pulmonary inflammation. *Immunology* 126:413-422.
334. Gloire, G., E. Charlier, S. Rahmouni, C. Volanti, A. Chariot, C. Erneux, and J. Piette. 2006. Restoration of SHIP-1 activity in human leukemic cells modifies NF-[kappa]B activation pathway and cellular survival upon oxidative stress. *Oncogene* 25:5485-5494.
335. Edmunds, C., R. V. Parry, S. J. Burgess, B. Reaves, and S. G. Ward. 1999. CD28 stimulates tyrosine phosphorylation, cellular redistribution and catalytic activity of the inositol lipid 5-phosphatase SHIP. *Eur J Immunol* 29:3507-3515.
336. Sato, T., T. Machida, S. Takahashi, S. Iyama, Y. Sato, K. Kuribayashi, K. Takada, T. Oku, Y. Kawano, T. Okamoto, R. Takimoto, T. Matsunaga, T. Takayama, M. Takahashi, J. Kato, and Y. Niitsu. 2004. Fas-mediated

apoptosome formation is dependent on reactive oxygen species derived from mitochondrial permeability transition in Jurkat cells. *J Immunol* 173:285-296.

337. Hao, J. H., M. Yu, F. T. Liu, A. C. Newland, and L. Jia. 2004. Bcl-2 inhibitors sensitize tumor necrosis factor-related apoptosis-inducing ligand-induced apoptosis by uncoupling of mitochondrial respiration in human leukemic CEM cells. *Cancer Research* 64:3607-3616.
338. Batty, I. H., J. van der Kaay, A. Gray, J. F. Telfer, M. J. Dixon, and C. P. Downes. 2007. The control of phosphatidylinositol 3,4-bisphosphate concentrations by activation of the Src homology 2 domain containing inositol polyphosphate 5-phosphatase 2, SHIP2. *Biochem J* 407:255-266.
339. Van der Kaay, J., M. Beck, A. Gray, and C. P. Downes. 1999. Distinct Phosphatidylinositol 3-Kinase Lipid Products Accumulate upon Oxidative and Osmotic Stress and Lead to Different Cellular Responses. *J. Biol. Chem.* 274:35963-35968.
340. Phee, H., A. Jacob, and K. M. Coggeshall. 2000. Enzymatic activity of the Src homology 2 domain-containing inositol phosphatase is regulated by a plasma membrane location. *J. Biol. Chem.* 275:19090-19097.
341. Baran, C. P., S. Tridandapani, C. D. Helgason, R. K. Humphries, G. Krystal, and C. B. Marsh. 2003. The inositol 5'-phosphatase SHIP-1 and the Src kinase Lyn negatively regulate macrophage colony-stimulating factor-induced Akt activity. *J. Biol. Chem.* 278:38628-38636.
342. Williams, M. S., and J. Kwon. 2004. T Cell Receptor Stimulation, Reactive Oxygen Species, and Cell Signaling. *Free Radical Biology and Medicine* 37:1144-1151.
343. Jaattela, M., and J. Tschopp. 2003. Caspase-independent cell death in T lymphocytes. *Nat Immunol* 4:416-423.
344. Nishio, M., K.-i. Watanabe, J. Sasaki, C. Taya, S. Takasuga, R. Iizuka, T. Balla, M. Yamazaki, H. Watanabe, R. Itoh, S. Kuroda, Y. Horie, I. Forster, T. W. Mak, H. Yonekawa, J. M. Penninger, Y. Kanaho, A. Suzuki, and T. Sasaki. 2007. Control of cell polarity and motility by the PtdIns(3,4,5)P3 phosphatase SHIP1. *Nat Cell Biol* 9:36-44.
345. Smith, L. D., E. S. Hickman, R. V. Parry, J. Westwick, and S. G. Ward. 2007. PI3Kgamma is the dominant isoform involved in migratory responses of human T lymphocytes: effects of ex vivo maintenance and limitations of non-viral delivery of siRNA. *Cell Signal* 19:2528-2539.
346. Goffinet, C., and O. T. Keppler. 2006. Efficient nonviral gene delivery into primary lymphocytes from rats and mice. *FASEB J.* 20:500-502.
347. Rozema, D. B., and D. L. Lewis. 2003. siRNA delivery technologies for mammalian systems. *TARGETS* 2:253-260.
348. Aagaard, L., and J. J. Rossi. 2007. RNAi therapeutics: Principles, prospects and challenges. *Advanced Drug Delivery Reviews* 59:75-86.
349. Auvinen, E., N. Kivi, and A. Vaheri. 2007. Regulation of ezrin localization by Rac1 and PIPK in human epithelial cells. *Experimental Cell Research* 313:824-833.
350. Bretscher, A., D. Chambers, R. Nguyen, and D. Reczek. 2003. ERM-Merlin and EBP50 protein families in plasma membrane organisation and function. *Annual Review of Cell and Developmental Biology* 16:113-143.

351. Brown, M. J., R. Nijhara, J. A. Hallam, M. Gignac, K. M. Yamada, S. L. Erlandsen, J. Delon, M. Kruhlak, and S. Shaw. 2003. Chemokine stimulation of human peripheral blood T lymphocytes induces rapid dephosphorylation of ERM proteins, which facilitates loss of microvilli and polarization. *Blood* 102:3890-3899.
352. Fleming, I. N., A. Gray, and C. P. Downes. 2000. Regulation of the Rac1-specific exchange factor Tiam1 involves both phosphoinositide 3-kinase-dependent and -independent components. *Biochem J* 351:173-182.
353. Sanchez-Martin, L., N. Sanchez-Sanchez, M. D. Gutierrez-Lopez, A. I. Rojo, M. Vicente-Manzanares, M. J. Perez-Alvarez, P. Sanchez-Mateos, X. R. Bustelo, A. Cuadrado, F. Sanchez-Madrid, J. L. Rodriguez-Fernandez, and C. Cabanas. 2004. Signaling through the leukocyte integrin LFA-1 in T cells induces a transient activation of Rac-1 that is regulated by Vav and PI3K/Akt-1. *J Biol Chem* 279:16194-16205.
354. Oki, S., A. Limnander, P. M. Yao, M. Niki, P. P. Pandolfi, and P. B. Rothman. 2005. Dok1 and SHIP act as negative regulators of v-Abl-induced pre-B cell transformation, proliferation and Ras/Erk activation. *Cell Cycle* 4:310-314.
355. Hogg, N., A. Smith, A. McDowall, K. Giles, P. Stanley, M. Laschinger, and R. Henderson. 2004. How T cells use LFA-1 to attach and migrate. *Immunology Letters* 92:51-54.
356. Shimizu, Y., W. Newman, T. V. Gopal, K. J. Horgan, N. Graber, L. D. Beall, G. A. van Seventer, and S. Shaw. 1991. Four molecular pathways of T cell adhesion to endothelial cells: roles of LFA-1, VCAM-1, and ELAM-1 and changes in pathway hierarchy under different activation conditions. *J Cell Biol* 113:1203-1212.
357. Pankov, R., and K. M. Yamada. 2002. Fibronectin at a glance. *J Cell Sci* 115:3861-3863.
358. Plow, E. F., T. A. Haas, L. Zhang, J. Loftus, and J. W. Smith. 2000. Ligand binding to integrins. *J Biol Chem* 275:21785-21788.
359. Muller, W. A. 2009. Mechanisms of Transendothelial Migration of Leukocytes. *Circ Res* 105:223-230.
360. Kim, C. H., G. Hangoc, S. Cooper, C. D. Helgason, S. Yew, R. K. Humphries, G. Krystal, and H. E. Broxmeyer. 1999. Altered responsiveness to chemokines due to targeted disruption of SHIP. *The Journal of Clinical Investigation* 104:1751-1759.
361. Dowler, S., R. A. Currie, D. G. Campbell, M. Deak, G. Kular, C. P. Downes, and D. R. Alessi. 2000. Identification of pleckstrin-homology-domain-containing proteins with novel phosphoinositide-binding specificities. *Biochem J* 351:19-31.
362. Rong, S. B., Y. Hu, I. Enyedy, G. Powis, E. J. Meuillet, X. Wu, R. Wang, S. Wang, and A. P. Kozikowski. 2001. Molecular modeling studies of the Akt PH domain and its interaction with phosphoinositides. *J Med Chem* 44:898-908.
363. Strieter, R. M., J. A. Belperio, and M. P. Keane. 2002. Cytokines in innate host defense in the lung. *The Journal of Clinical Investigation* 109:699-705.
364. Nelson, B. H. 2004. IL-2, Regulatory T Cells, and Tolerance. *J Immunol* 172:3983-3988.

365. Moore, K. W., R. de Waal Malefyt, R. L. Coffman, and A. O'Garra. 2001. Interleukin-10 and the interleukin-10 receptor. *Annu Rev Immunol* 19:683-765.
366. Egwuagu, C. E. 2009. STAT3 in CD4+ T helper cell differentiation and inflammatory diseases. *Cytokine* 47:149-156.
367. Sakaguchi, S. 2003. The origin of FOXP3-expressing CD4+ regulatory T cells: thymus or periphery. *J Clin Invest* 112:1310-1312.
368. Grant, M., F. Smaill, S. Muller, H. Kohler, and K. Rosenthal. 2000. The anti-idiotypic antibody 1F7 selectively inhibits cytotoxic T cells activated in HIV-1 infection. *Immunol Cell Biol* 78:20-27.
369. Sloan, D. D., G. Zahariadis, C. M. Posavad, N. T. Pate, S. J. Kussick, and K. R. Jerome. 2003. CTL Are Inactivated by Herpes Simplex Virus-Infected Cells Expressing a Viral Protein Kinase. *J Immunol* 171:6733-6741.
370. Harris, T. J., J. F. Grosso, H. R. Yen, H. Xin, M. Kortylewski, E. Albesiano, E. L. Hipkiss, D. Getnet, M. V. Goldberg, C. H. Maris, F. Housseau, H. Yu, D. M. Pardoll, and C. G. Drake. 2007. Cutting edge: An in vivo requirement for STAT3 signaling in TH17 development and TH17-dependent autoimmunity. *J Immunol* 179:4313-4317.
371. O'Brien, R. L., C. L. Roark, and W. K. Born. 2009. IL-17-producing gammadelta T cells. *Eur J Immunol* 39:662-666.
372. Hamada, H., L. Garcia-Hernandez Mde, J. B. Reome, S. K. Misra, T. M. Strutt, K. K. McKinstry, A. M. Cooper, S. L. Swain, and R. W. Dutton. 2009. Tc17, a unique subset of CD8 T cells that can protect against lethal influenza challenge. *J Immunol* 182:3469-3481.
373. Lockhart, E., A. M. Green, and J. L. Flynn. 2006. IL-17 Production Is Dominated by {gamma}{delta} T Cells rather than CD4 T Cells during Mycobacterium tuberculosis Infection. *J Immunol* 177:4662-4669.
374. Happel, K. I., M. Zheng, E. Young, L. J. Quinton, E. Lockhart, A. J. Ramsay, J. E. Shellito, J. R. Schurr, G. J. Bagby, S. Nelson, and J. K. Kolls. 2003. Cutting Edge: Roles of Toll-Like Receptor 4 and IL-23 in IL-17 Expression in Response to Klebsiella pneumoniae Infection. *J Immunol* 170:4432-4436.
375. Gao, H., T. A. Neff, L. M. Hoesel, R.-F. Guo, L. Sun, M. A. Flierl, J. V. Sarma, F. S. Zetoune, and P. A. Ward. 2007. Complement C5a signaling dependent production of IL-17 during sepsis. *Molecular Immunology* 44:175-175.
376. Ouyang, W., E. Filvaroff, Y. Hu, and J. Grogan. 2009. Novel therapeutic targets along the Th17 pathway. *Eur J Immunol* 39:670-675.
377. Ogawa, A., A. Andoh, Y. Araki, T. Bamba, and Y. Fujiyama. 2004. Neutralization of interleukin-17 aggravates dextran sulfate sodium-induced colitis in mice. *Clin Immunol* 110:55-62.
378. Lubberts, E., P. Schwarzenberger, W. Huang, J. R. Schurr, J. J. Peschon, W. B. van den Berg, and J. K. Kolls. 2005. Requirement of IL-17 receptor signaling in radiation-resistant cells in the joint for full progression of destructive synovitis. *J Immunol* 175:3360-3368.
379. Ruckle, T., M. K. Schwarz, and C. Rommel. 2006. PI3K[gamma] inhibition: towards an 'aspirin of the 21st century'? *Nat Rev Drug Discov* 5:903-918.
380. Walker, E. H., M. E. Pacold, O. Perisic, L. Stephens, P. T. Hawkins, M. P. Wymann, and R. L. Williams. 2000. Structural determinants of

phosphoinositide 3-kinase inhibition by wortmannin, LY294002, quercetin, myricetin, and staurosporine. *Mol Cell* 6:909-919.

381. Suire, S., P. Hawkins, and L. Stephens. 2002. Activation of Phosphoinositide 3-Kinase [gamma] by Ras. *Current Biology* 12:1068-1075.
382. Nagata, T., L. McKinley, J. J. Peschon, J. F. Alcorn, S. J. Aujla, and J. K. Kolls. 2008. Requirement of IL-17RA in Con A induced hepatitis and negative regulation of IL-17 production in mouse T cells. *J Immunol* 181:7473-7479.
383. Smith, E., M. A. Stark, A. Zarbock, T. L. Burcin, A. C. Bruce, D. Vaswani, P. Foley, and K. Ley. 2008. IL-17A inhibits the expansion of IL-17A-producing T cells in mice through "short-loop" inhibition via IL-17 receptor. *J Immunol* 181:1357-1364.
384. Blau, H. M., and F. M. Rossi. 1999. Tet B or not tet B: advances in tetracycline-inducible gene expression. *Proc Natl Acad Sci U S A* 96:797-799.
385. Rossi, F. M., and H. M. Blau. 1998. Recent advances in inducible gene expression systems. *Curr Opin Biotechnol* 9:451-456.
386. Watt, S. A., W. A. Kimber, I. N. Fleming, N. R. Leslie, C. P. Downes, and J. M. Lucocq. 2004. Detection of novel intracellular agonist responsive pools of phosphatidylinositol 3,4-bisphosphate using the TAPP1 pleckstrin homology domain in immunoelectron microscopy. *Biochem. J.* 377:653-663.
387. Brognard, J., and A. C. Newton. 2008. PHLiPPing the switch on Akt and protein kinase C signaling. *Trends in Endocrinology & Metabolism* 19:223-230.
388. Batty, I. H., J. van der kaay, A. Gray, J. F. Telfer, M. J. Dixon, and C. P. Downes. 2007. The control of phosphatidylinositol 3,4-bisphosphate concentrations by activation of the Src homology 2 domain containing inositol polyphosphate 5-phosphatase 2, SHIP2. *Biochem J* 407:255-266.
389. Cheung, S. M. S., J. C. Kornelson, M. Al-Alwan, and A. J. Marshall. 2007. Regulation of phosphoinositide 3-kinase signaling by oxidants: Hydrogen peroxide selectively enhances immunoreceptor-induced recruitment of phosphatidylinositol (3,4) bisphosphate-binding PH domain proteins. *Cellular Signalling* 19:902-912.
390. MacGlashan, D., Jr., and N. Vilarino. 2006. Nonspecific Desensitization, Functional Memory, and the Characteristics of SHIP Phosphorylation following IgE-Mediated Stimulation of Human Basophils. *J Immunol* 177:1040-1051.
391. Horn, S., J. Meyer, J. Heukeshoven, B. Fehse, C. Schulze, S. Li, J. Frey, S. Poll, C. Stocking, and M. Jucker. 2001. The inositol 5-phosphatase SHIP is expressed as 145 and 135 kDa proteins in blood and bone marrow cells in vivo, whereas carboxyl-truncated forms of SHIP are generated by proteolytic cleavage in vitro. *Leukemia* 15:112-120.
392. Alexandra, D., O. Ronald, D. Merle, G. Antje, A. Sebastian, U. Susanne, L. Reiner, W. Sebastian, and S. Björn. 2009. The Akt inhibitor triciribine sensitizes prostate carcinoma cells to TRAIL-induced apoptosis. *International Journal of Cancer* 125:932-941.
393. Rajaram, M. V. S., J. P. Butchar, K. V. L. Parsa, T. J. Cremer, A. Amer, L. S. Schlesinger, and S. Tridandapani. 2009. Akt and SHIP Modulate Francisella Escape from the Phagosome and Induction of the Fas-Mediated Death Pathway. *PLoS One* 4:e7919.

394. Daigle, I., S. Yousefi, M. Colonna, D. R. Green, and H.-U. Simon. 2002. Death receptors bind SHP-1 and block cytokine-induced anti-apoptotic signaling in neutrophils. *Nat Med* 8:61-67.
395. Hurez, V., R. Dzialo-Hatton, J. Oliver, R. J. Matthews, and C. T. Weaver. 2002. Efficient adenovirus-mediated gene transfer into primary T cells and thymocytes in a new coxsackie/adenovirus receptor transgenic model. *BMC Immunol* 3:4.
396. Chemnitz, J. M., R. V. Parry, K. E. Nichols, C. H. June, and J. L. Riley. 2004. SHP-1 and SHP-2 Associate with Immunoreceptor Tyrosine-Based Switch Motif of Programmed Death 1 upon Primary Human T Cell Stimulation, but Only Receptor Ligation Prevents T Cell Activation. *J Immunol* 173:945-954.
397. O'Doherty, U., W. J. Swiggard, and M. H. Malim. 2000. Human Immunodeficiency Virus Type 1 Spinoculation Enhances Infection through Virus Binding. *J. Virol.* 74:10074-10080.
398. Ramaswamy, S., N. Nakamura, I. Sansal, L. Bergeron, and W. R. Sellers. 2002. A novel mechanism of gene regulation and tumor suppression by the transcription factor FKHR. *Cancer Cell* 2:81-91.
399. Ramaswamy, S., N. Nakamura, F. Vazquez, D. B. Batt, S. Perera, T. M. Roberts, and W. R. Sellers. 1999. Regulation of G1 progression by the PTEN tumor suppressor protein is linked to inhibition of the phosphatidylinositol 3-kinase/Akt pathway. *Proc Natl Acad Sci U S A* 96:2110-2115.
400. Franke, T. F., C. P. Hornik, L. Segev, G. A. Shostak, and C. Sugimoto. 2003. PI3K/Akt and apoptosis: size matters. *Oncogene* 22:8983-8998.
401. Kisseleva, M. V., L. Cao, and P. W. Majerus. 2002. Phosphoinositide-specific inositol polyphosphate 5-phosphatase IV inhibits Akt/protein kinase B phosphorylation and leads to apoptotic cell death. *J Biol Chem* 277:6266-6272.
402. Zou, C. Y., K. D. Smith, Q. S. Zhu, J. Liu, I. E. McCutcheon, J. M. Slopis, F. Meric-Bernstam, Z. Peng, W. G. Bornmann, G. B. Mills, A. J. Lazar, R. E. Pollock, and D. Lev. 2009. Dual targeting of AKT and mammalian target of rapamycin: A potential therapeutic approach for malignant peripheral nerve sheath tumor. *Mol Cancer Ther*. 8: 1157-1162
403. Chen, J. S., L. J. Zhou, M. Entin-Meer, X. Yang, M. Donker, Z. A. Knight, W. Weiss, K. M. Shokat, D. Haas-Kogan, and D. Stokoe. 2008. Characterization of structurally distinct, isoform-selective phosphoinositide 3'-kinase inhibitors in combination with radiation in the treatment of glioblastoma. *Mol Cancer Ther* 7:841-850.
404. Carver, D. J., M. J. Aman, and K. S. Ravichandran. 2000. SHIP inhibits Akt activation in B cells through regulation of Akt membrane localization. *Blood* 96:1449-1456.
405. Kimber, W. A., M. Deak, A. R. Prescott, and D. R. Alessi. 2003. Interaction of the protein tyrosine phosphatase PTPL1 with the PtdIns(3,4)P2-binding adaptor protein TAPP1. *Biochem J* 376:525-535.
406. Kimber, W. A., L. Trinkle-Mulcahy, P. C. Cheung, M. Deak, L. J. Marsden, A. Kieloch, S. Watt, R. T. Javier, A. Gray, C. P. Downes, J. M. Lucocq, and D. R. Alessi. 2002. Evidence that the tandem-pleckstrin-homology-domain-containing protein TAPP1 interacts with Ptd(3,4)P2 and the multi-PDZ-domain-containing protein MUPP1 in vivo. *Biochem J* 361:525-536.

407. Costantini, J. L., S. M. S. Cheung, S. Hou, H. Li, S. K. Kung, J. B. Johnston, J. A. Wilkins, S. B. Gibson, and A. J. Marshall. 2009. TAPP2 links phosphoinositide 3-kinase signaling to B cell adhesion through interaction with the cytoskeletal protein utrophin: expression of a novel cell adhesion-promoting complex in B cell leukemia. *Blood* 114:4703-4712.
408. Horn, S., E. Endl, B. Fehse, M. M. Weck, G. W. Mayr, and M. Jucker. 2004. Restoration of SHIP activity in a human leukemia cell line downregulates constitutively activated phosphatidylinositol 3-kinase//Akt//GSK-3[beta] signaling and leads to an increased transit time through the G1 phase of the cell cycle. *Leukemia* 18:1839-1849.
409. http://www.clontech.com/products/detail.asp?tabno=2&product_id=172013.
410. Kafri, T., H. van Praag, F. H. Gage, and I. M. Verma. 2000. Lentiviral vectors: regulated gene expression. *Mol Ther* 1:516-521.
411. Gascón, S., J. A. Paez-Gomez, M. Díaz-Guerra, P. Scheiffele, and F. G. Scholl. 2008. Dual-promoter lentiviral vectors for constitutive and regulated gene expression in neurons. *Journal of Neuroscience Methods* 168:104-112.
412. Liu, L., J. E. Damen, M. R. Hughes, I. Babic, F. R. Jirik, and G. Krystal. 1997. The Src homology 2 (SH2) domain of SH2-containing inositol phosphatase (SHIP) is essential for tyrosine phosphorylation of SHIP, its association with Shc, and its induction of apoptosis. *J Biol Chem* 272:8983-8988.
413. Aman, M. J., S. F. Walk, M. E. March, H. P. Su, D. J. Carver, and K. S. Ravichandran. 2000. Essential role for the C-terminal noncatalytic region of SHIP in FcgammaRIIB1-mediated inhibitory signaling. *Mol Cell Biol* 20:3576-3589.
414. Morales, J. C., M. J. Ruiz-Magaña, and C. Ruiz-Ruiz. 2007. Regulation of the resistance to TRAIL-induced apoptosis in human primary T lymphocytes: Role of NF-[kappa]B inhibition. *Molecular Immunology* 44:2587-2597.
415. Luciano, F., J. E. Ricci, M. Herrant, C. Bertolotto, B. Mari, J. L. Cousin, and P. Auberger. 2002. T and B leukemic cell lines exhibit different requirements for cell death: correlation between caspase activation, DFF40/DFF45 expression, DNA fragmentation and apoptosis in T cell lines but not in Burkitt's lymphoma. *Leukemia* 16:700-707.
416. Last'ovicka, J., V. Budinský, R. Spísek, and J. Bartunková. 2009. Assessment of lymphocyte proliferation: CFSE kills dividing cells and modulates expression of activation markers. *Cellular Immunology* 256:79-85.
417. Li, J., C. Yen, D. Liaw, K. Podsypanina, S. Bose, S. I. Wang, J. Puc, C. Miliaresis, L. Rodgers, R. McCombie, S. H. Bigner, B. C. Giovanella, M. Ittmann, B. Tycko, H. Hibshoosh, M. H. Wigler, and R. Parsons. 1997. PTEN, a Putative Protein Tyrosine Phosphatase Gene Mutated in Human Brain, Breast, and Prostate Cancer. *Science* 275:1943-1947.
418. Metzner, A., C. Precht, B. Fehse, W. Fiedler, C. Stocking, A. Gunther, G. W. Mayr, and M. Jucker. 2009. Reduced proliferation of CD34+ cells from patients with acute myeloid leukemia after gene transfer of INPP5D. *Gene Ther* 16:570-573.
419. Xu, Q., S.-E. Simpson, T. J. Scialla, A. Bagg, and M. Carroll. 2003. Survival of acute myeloid leukemia cells requires PI3 kinase activation. *Blood* 102:972-980.

420. Costinean, S., S. K. Sandhu, I. M. Pedersen, E. Tili, R. Trotta, D. Perrotti, D. Ciarlariello, P. Neviani, J. Harb, L. R. Kauffman, A. Shidham, and C. M. Croce. 2009. Src homology 2 domain-containing inositol-5-phosphatase and CCAAT enhancer-binding protein {beta} are targeted by miR-155 in B cells of E{micro}-MiR-155 transgenic mice. *Blood* 114:1374-1382.
421. Yamanaka, Y., H. Tagawa, N. Takahashi, A. Watanabe, Y.-M. Guo, K. Iwamoto, J. Yamashita, H. Saitoh, Y. Kameoka, N. Shimizu, R. Ichinohasama, and K.-i. Sawada. 2009. Aberrant overexpression of microRNAs activate AKT signaling via down-regulation of tumor suppressors in natural killer-cell lymphoma/leukemia. *Blood* 114:3265-3275.
422. Gao, N., D. C. Flynn, Z. Zhang, X.-S. Zhong, V. Walker, K. J. Liu, X. Shi, and B.-H. Jiang. 2004. G1 cell cycle progression and the expression of G1 cyclins are regulated by PI3K/AKT/mTOR/p70S6K1 signaling in human ovarian cancer cells. *Am J Physiol Cell Physiol* 287:C281-291.
423. Lee, Y.-J., and P. Keng. 2005. Studying the effects of actin cytoskeletal destabilization on cell cycle by cofilin overexpression. *Molecular Biotechnology* 31:1-10.
424. Lohez, O. D., C. Reynaud, F. Borel, P. R. Andreassen, and R. L. Margolis. 2003. Arrest of mammalian fibroblasts in G1 in response to actin inhibition is dependent on retinoblastoma pocket proteins but not on p53. *J. Cell Biol.* 161:67-77.
425. Burkhardt, J. K., E. Carrizosa, and M. H. Shaffer. 2008. The actin cytoskeleton in T cell activation. *Annu Rev Immunol* 26:233-259.
426. Brooks, R., G. M. Fuhler, S. Iyer, M. J. Smith, M. Y. Park, K. H. Paraiso, R. W. Engelman, and W. G. Kerr. SHIP1 inhibition increases immunoregulatory capacity and triggers apoptosis of hematopoietic cancer cells. *J Immunol* 184:3582-3589.
427. Gowan, S. M., A. Hardcastle, A. E. Hallsworth, M. R. Valenti, L.-J. K. Hunter, A. K. de Haven Brandon, M. D. Garrett, F. Raynaud, P. Workman, W. Aherne, and S. A. Eccles. 2007. Application of Meso Scale Technology for the Measurement of Phosphoproteins in Human Tumor Xenografts. *ASSAY and Drug Development Technologies* 5:391-402.
428. Chang, C.-C., Z. Liu, G. Vlad, H. Qin, X. Qiao, D. M. Mancini, C. C. Marboe, R. Cortesini, and N. Suciu-Foca. 2009. Ig-Like Transcript 3 Regulates Expression of Proinflammatory Cytokines and Migration of Activated T Cells. *J Immunol* 182:5208-5216.
429. Tomlinson, M. G., V. L. Heath, C. W. Turck, S. P. Watson, and A. Weiss. 2004. SHIP family inositol phosphatases interact with and negatively regulate the Tec tyrosine kinase. *J Biol Chem* 279:55089-55096.
430. An, H., H. Xu, M. Zhang, J. Zhou, T. Feng, C. Qian, R. Qi, and X. Cao. 2005. Src homology 2 domain-containing inositol-5-phosphatase 1 (SHIP1) negatively regulates TLR4-mediated LPS response primarily through a phosphatase activity- and PI-3K-independent mechanism. *Blood* 105:4685-4692.
431. Hogan, A., Y. Yakubchyk, J. Chabot, C. Obagi, E. Daher, K. Maekawa, and S. H. Gee. 2004. The phosphoinositol 3,4-bisphosphate-binding protein TAPP1 interacts with syntrophins and regulates actin cytoskeletal organization. *J Biol Chem* 279:53717-53724.

432. Tridandapani, S., G. Chacko, J. Van Brocklyn, and K. Coggeshall. 1997. Negative signaling in B cells causes reduced Ras activity by reducing Shc-Grb2 interactions. *J Immunol* 158:1125-1132.
433. Pradhan, M., and K. M. Coggeshall. 1997. Activation-induced bi-dentate interaction of SHIP and Shc in B lymphocytes. *J Cell Biochem* 67:32-42.
434. Scita, G., P. Tenca, E. Frittoli, A. Tocchetti, M. Innocenti, G. Giardina, and P. P. Di Fiore. 2000. Signaling from Ras to Rac and beyond: not just a matter of GEFs. *EMBO J* 19:2393-2398.
435. Chaigne-Delalande, B., G. Anies, I. Kramer, and E. Genot. 2007. Nonadherent cells switch to a Rac-mediated, SHIP regulated, Akt activation mode for survival. *Oncogene* 27:1876-1885.
436. Inoue, T., and T. Meyer. 2008. Synthetic Activation of Endogenous PI3K and Rac Identifies an AND Gate Switch for Cell Polarization and Migration. *PLoS ONE* 3:e3068.
437. Van der Kaay, J., M. Beck, A. Gray, and C. P. Downes. 1999. Distinct phosphatidylinositol 3-kinase lipid products accumulate upon oxidative and osmotic stress and lead to different cellular responses. *J Biol Chem* 274:35963-35968.
438. Zhao, M. 2007. PTEN: a promising pharmacological target to enhance epithelial wound healing. *Br J Pharmacol* 152:1141-1144.
439. Lai, J. P., J. T. Dalton, and D. L. Knoell. 2007. Phosphatase and tensin homologue deleted on chromosome ten (PTEN) as a molecular target in lung epithelial wound repair. *Br J Pharmacol* 152:1172-1184.
440. Schore, R. J., Y. Zheng, D. A. Williams, and Y. Gu. 2005. Inhibition of the Rho GTPase, Rac, Differentially Inhibits Proliferation of AML Cell Lines and May Serve as a Novel Molecular Target. *ASH Annual Meeting Abstracts* 106:1205.
441. Gao, Y., J. B. Dickerson, F. Guo, J. Zheng, and Y. Zheng. 2004. Rational design and characterization of a Rac GTPase-specific small molecule inhibitor. *Proc Natl Acad Sci U S A* 101:7618-7623.
442. Lee, J.-H., T. Katakai, T. Hara, H. Gonda, M. Sugai, and A. Shimizu. 2004. Roles of p-ERM and Rho-ROCK signaling in lymphocyte polarity and uropod formation. *J. Cell Biol.* 167:327-337.
443. Shimizu, Y., G. A. van Seventer, K. J. Horgan, and S. Shaw. 1990. Costimulation of proliferative responses of resting CD4+ T cells by the interaction of VLA-4 and VLA-5 with fibronectin or VLA-6 with laminin. *J Immunol* 145:59-67.
444. Cui, L., K. Johkura, Y. Liang, R. Teng, N. Ogiwara, Y. Okouchi, K. Asanuma, and K. Sasaki. 2002. Biodefense function of omental milky spots through cell adhesion molecules and leukocyte proliferation. *Cell Tissue Res* 310:321-330.
445. Kohei, J., L. Yan, C. Li, O. Naoko, and S. Katsunori. 2001. Spatial distribution of cell adhesion molecules on the peritoneal surface in the cecal perforation-induced peritonitis. *The Anatomical Record* 264:219-227.
446. Neelamegham, S., A. D. Taylor, A. R. Burns, C. W. Smith, and S. I. Simon. 1998. Hydrodynamic Shear Shows Distinct Roles for LFA-1 and Mac-1 in Neutrophil Adhesion to Intercellular Adhesion Molecule-1. *Blood* 92:1626-1638.

447. Abitorabi, M. A., R. K. Pachynski, R. E. Ferrando, M. Tidswell, and D. J. Erle. 1997. Presentation of Integrins on Leukocyte Microvilli: A Role for the Extracellular Domain in Determining Membrane Localization. *J. Cell Biol.* 139:563-571.
448. Burkhardt, J. K. 2003. Microvillar loss: when your pERM won't hold. *Blood* 102:3856-3857.
449. Shulman, Z., R. Pasvolsky, E. Woolf, V. Grabovsky, S. W. Feigelson, N. Erez, Y. Fukui, and R. Alon. 2006. DOCK2 regulates chemokine-triggered lateral lymphocyte motility but not transendothelial migration. *Blood* 108:2150-2158.
450. Rey-Ladino, J. A., M. Huber, L. Liu, J. E. Damen, G. Krystal, and F. Takei. 1999. The SH2-Containing Inositol-5'-Phosphatase Enhances LFA-1-Mediated Cell Adhesion and Defines Two Signaling Pathways for LFA-1 Activation. *J Immunol* 162:5792-5799.
451. Ward, S. G. 2009. Millipede-like Lymphocyte Crawling: Feeling the Way with Filopodia. *Immunity* 30:315-317.
452. Barbi, J., H. E. Cummings, B. Lu, S. Oghumu, T. Ruckle, C. Rommel, W. Lafuse, C. C. Whitacre, and A. R. Satoskar. 2008. PI3Kgamma (PI3Kgamma) is essential for efficient induction of CXCR3 on activated T cells. *Blood* 112:3048-3051.
453. Barbi, J., S. Oghumu, C. M. Lezama-Davila, and A. R. Satoskar. 2007. IFN-gamma and STAT1 are required for efficient induction of CXC chemokine receptor 3 (CXCR3) on CD4+ but not CD8+ T cells. *Blood* 110:2215-2216.
454. Kay, R. R., P. Langridge, D. Traynor, and O. Hoeller. 2008. Changing directions in the study of chemotaxis. *Nat Rev Mol Cell Biol* 9:455-463.
455. Hoeller, O., and R. R. Kay. 2007. Chemotaxis in the absence of PIP3 gradients. *Curr Biol* 17:813-817.
456. Kolsch, V., P. G. Charest, and R. A. Firtel. 2008. The regulation of cell motility and chemotaxis by phospholipid signaling. *J Cell Sci* 121:551-559.
457. Martin, A. L., M. D. Schwartz, S. C. Jameson, and Y. Shimizu. 2008. Selective Regulation of CD8 Effector T Cell Migration by the p110{gamma} Isoform of Phosphatidylinositol 3-Kinase. *J Immunol* 180:2081-2088.
458. Rainger, G. E., A. Fisher, C. Shearman, and G. B. Nash. 1995. Adhesion of flowing neutrophils to cultured endothelial cells after hypoxia and reoxygenation in vitro. *Am J Physiol Heart Circ Physiol* 269:H1398-1406.
459. Allam, A., and A. J. Marshall. 2005. Role of the adaptor proteins Bam32, TAPP1 and TAPP2 in lymphocyte activation. *Immunol Lett* 97:7-17.
460. Marshall, A. J., A. K. Krahn, K. Ma, V. Duronio, and S. Hou. 2002. TAPP1 and TAPP2 are targets of phosphatidylinositol 3-kinase signaling in B cells: sustained plasma membrane recruitment triggered by the B-cell antigen receptor. *Mol Cell Biol* 22:5479-5491.
461. Lindsay, Y., D. McCoull, L. Davidson, N. R. Leslie, A. Fairservice, A. Gray, J. Lucocq, and C. P. Downes. 2006. Localization of agonist-sensitive PtdIns(3,4,5)P3 reveals a nuclear pool that is insensitive to PTEN expression. *J Cell Sci* 119:5160-5168.
462. Xuan Nguyen, T. L., J. W. Choi, S. B. Lee, K. Ye, S.-D. Woo, K.-H. Lee, and J.-Y. Ahn. 2006. Akt phosphorylation is essential for nuclear translocation and retention in NGF-stimulated PC12 cells. *Biochemical and Biophysical Research Communications* 349:789-798.

463. Burelout, C., P. H. Naccache, and S. G. Bourgoin. 2007. Dissociation between the translocation and the activation of Akt in fMLP-stimulated human neutrophils--effect of prostaglandin E2. *J Leukoc Biol* 81:1523-1534.
464. Ananthanarayanan, B., M. Fosbrink, M. Rahdar, and J. Zhang. 2007. Live-cell molecular analysis of Akt activation reveals roles for activation loop phosphorylation. *J Biol Chem* 282:36634-36641.
465. Curotto de Lafaille, M. A., and J. J. Lafaille. 2009. Natural and Adaptive Foxp3+ Regulatory T Cells: More of the Same or a Division of Labor? *Immunity* 30:626-635.
466. Piccirillo, C. A. 2008. Regulatory T cells in health and disease. *Cytokine* 43:395-401.
467. Ziegler, S. F., and J. H. Buckner. 2009. FOXP3 and the regulation of Treg/Th17 differentiation. *Microbes and Infection* 11:594-598.
468. Long, S. A., and J. H. Buckner. 2008. Combination of rapamycin and IL-2 increases de novo induction of human CD4+CD25+FOXP3+ T cells. *Journal of Autoimmunity* 30:293-302.
469. Domdey, A., A. H. Millner, K. Lund, I. Søndergaard, and P. A. Würtzen. 2007. Suppression Induced By In Vitro Expanded Human Tregs Is Antigen-independent And Is Partly Abrogated By GITR Signalling. *J Allergy Clin Immunol* 119:S309-S309.
470. Tran, D. Q., D. D. Glass, G. Uzel, D. A. Darnell, C. Spalding, S. M. Holland, and E. M. Shevach. 2009. Analysis of Adhesion Molecules, Target Cells, and Role of IL-2 in Human FOXP3+ Regulatory T Cell Suppressor Function. *J Immunol* 182:2929-2938.
471. Vignali, D. A. A., L. W. Collison, and C. J. Workman. 2008. How regulatory T cells work. *Nat Rev Immunol* 8:523-532.
472. Scheffold, A., K. M. Murphy, and T. Hofer. 2007. Competition for cytokines: Treg cells take all. *Nat Immunol* 8:1285-1287.
473. Vercoulen, Y., E. J. Wehrens, N. H. van Teijlingen, W. de Jager, J. M. Beekman, and B. J. Prakken. 2009. Human Regulatory T Cell Suppressive Function Is Independent of Apoptosis Induction in Activated Effector T Cells. *PLoS One* 4:e7183.
474. Oberle, N., N. Eberhardt, C. S. Falk, P. H. Krammer, and E. Suri-Payer. 2007. Rapid Suppression of Cytokine Transcription in Human CD4+CD25 T Cells by CD4+Foxp3+ Regulatory T Cells: Independence of IL-2 Consumption, TGF-beta, and Various Inhibitors of TCR Signaling. *J Immunol* 179:3578-3587.
475. Thai, T.-H., D. P. Calado, S. Casola, K. M. Ansel, C. Xiao, Y. Xue, A. Murphy, D. Frendewey, D. Valenzuela, J. L. Kutok, M. Schmidt-Supprian, N. Rajewsky, G. Yancopoulos, A. Rao, and K. Rajewsky. 2007. Regulation of the Germinal Center Response by MicroRNA-155. *Science* 316:604-608.
476. Marson, A., K. Kretschmer, G. M. Frampton, E. S. Jacobsen, J. K. Polansky, K. D. MacIsaac, S. S. Levine, E. Fraenkel, H. von Boehmer, and R. A. Young. 2007. Foxp3 occupancy and regulation of key target genes during T-cell stimulation. *Nature* 445:931-935.
477. Zheng, Y., S. Z. Josefowicz, A. Kas, T.-T. Chu, M. A. Gavin, and A. Y. Rudensky. 2007. Genome-wide analysis of Foxp3 target genes in developing and mature regulatory T cells. *Nature* 445:936-940.

478. Lu, L.-F., T.-H. Thai, D. P. Calado, A. Chaudhry, M. Kubo, K. Tanaka, G. B. Loeb, H. Lee, A. Yoshimura, K. Rajewsky, and A. Y. Rudensky. 2009. Foxp3-Dependent MicroRNA155 Confers Competitive Fitness to Regulatory T Cells by Targeting SOCS1 Protein. *Immunity* 30:80-91.
479. Kelly, B. L., and R. M. Locksley. 2000. Coordinate Regulation of the IL-4, IL-13, and IL-5 Cytokine Cluster in Th2 Clones Revealed by Allelic Expression Patterns. *J Immunol* 165:2982-2986.
480. Wenner, C. A., S. J. Szabo, and K. M. Murphy. 1997. Identification of IL-4 promoter elements conferring Th2-restricted expression during T helper cell subset development. *J Immunol* 158:765-773.
481. Ho, I. C., M. R. Hodge, J. W. Rooney, and L. H. Glimcher. 1996. The proto-oncogene c-maf is responsible for tissue-specific expression of interleukin-4. *Cell* 85:973-983.
482. Ranganath, S., W. Ouyang, D. Bhattarcharya, W. C. Sha, A. Grupe, G. Peltz, and K. M. Murphy. 1998. Cutting Edge: GATA-3-Dependent Enhancer Activity in IL-4 Gene Regulation. *J Immunol* 161:3822-3826.
483. Zhang, D.-H., L. Yang, and A. Ray. 1998. Cutting Edge: Differential Responsiveness of the IL-5 and IL-4 Genes to Transcription Factor GATA-3. *J Immunol* 161:3817-3821.
484. Lee, H. J., A. O'Garra, K.-i. Arai, and N. Arai. 1998. Characterization of cis-Regulatory Elements and Nuclear Factors Conferring Th2-Specific Expression of the IL-5 Gene: A Role for a GATA-Binding Protein. *J Immunol* 160:2343-2352.
485. Bettelli, E., Y. Carrier, W. Gao, T. Korn, T. B. Strom, M. Oukka, H. L. Weiner, and V. K. Kuchroo. 2006. Reciprocal developmental pathways for the generation of pathogenic effector TH17 and regulatory T cells. *Nature* 441:235-238.
486. Steinman, L. 2008. A rush to judgment on Th17. *J. Exp. Med.* 205:1517-1522.
487. Teague, T. K., B. C. Schaefer, D. Hildeman, J. Bender, T. Mitchell, J. W. Kappler, and P. Marrack. 2000. Activation-Induced Inhibition of Interleukin 6-Mediated T Cell Survival and Signal Transducer and Activator of Transcription 1 Signaling. *J. Exp. Med.* 191:915-926.
488. Jones, G. W., R. M. McLoughlin, V. J. Hammond, C. R. Parker, J. D. Williams, R. Malhotra, J. Scheller, S. Rose-John, N. Topley, and S. A. Jones. Loss of T-cell IL-6R expression during inflammation: IL-6 trans-signaling regulates T-cell trafficking and effector characteristics. *Cytokine* 48:126-127.
489. Nowell, M. A., P. J. Richards, S. Horiuchi, N. Yamamoto, S. Rose-John, N. Topley, A. S. Williams, and S. A. Jones. 2003. Soluble IL-6 Receptor Governs IL-6 Activity in Experimental Arthritis: Blockade of Arthritis Severity by Soluble Glycoprotein 130. *J Immunol* 171:3202-3209.
490. McLoughlin, R. M., B. J. Jenkins, D. Grail, A. S. Williams, C. A. Fielding, C. R. Parker, M. Ernst, N. Topley, and S. A. Jones. 2005. IL-6 trans-signaling via STAT3 directs T cell infiltration in acute inflammation. *Proc Natl Acad Sci U S A* 102:9589-9594.
491. Barry, M., and R. C. Bleackley. 2002. Cytotoxic T lymphocytes: all roads lead to death. *Nat Rev Immunol* 2:401-409.

492. Fuller, C. L., K. S. Ravichandran, and V. L. Braciale. 1999. Phosphatidylinositol 3-Kinase-Dependent and -Independent Cytolytic Effector Functions. *J Immunol* 162:6337-6340.
493. Robertson, L. K., L. R. Mireau, and H. L. Ostergaard. 2005. A Role for Phosphatidylinositol 3-Kinase in TCR-Stimulated ERK Activation Leading to Paxillin Phosphorylation and CTL Degranulation. *J Immunol* 175:8138-8145.
494. Wahle, J. A., K. H. T. Paraiso, R. D. Kendig, H. R. Lawrence, L. Chen, J. Wu, and W. G. Kerr. 2007. Inappropriate Recruitment and Activity by the Src Homology Region 2 Domain-Containing Phosphatase 1 (SHP1) Is Responsible for Receptor Dominance in the SHIP-Deficient NK Cell. *J Immunol* 179:8009-8015.
495. Vaidya, S. V., and P. A. Mathew. 2006. Of mice and men: Different functions of the murine and human 2B4 (CD244) receptor on NK cells. *Immunology Letters* 105:180-184.
496. Hirsch, E., L. Braccini, E. Ciraolo, F. Morello, and A. Perino. 2009. Twice upon a time: PI3K's secret double life exposed. *Trends in Biochemical Sciences* 34:244-248.
497. Pierau, M., S. Engelmann, D. Reinhold, T. Lapp, B. Schraven, and U. H. Bommhardt. 2009. Protein Kinase B/Akt Signals Impair Th17 Differentiation and Support Natural Regulatory T Cell Function and Induced Regulatory T Cell Formation. *J Immunol* 183:6124-6134.
498. Fuson, K. L., M. Zheng, M. Craxton, A. Pataer, R. Ramesh, S. Chada, and R. B. Sutton. 2009. Structural mapping of post-translational modifications in human interleukin-24: role of N-linked glycosylation and disulfide bonds in secretion and activity. *J Biol Chem* 284:30526-30533.
499. Rahman, M. S., A. Yamasaki, J. Yang, L. Shan, A. J. Halayko, and A. S. Gounni. 2006. IL-17A induces eotaxin-1/CC chemokine ligand 11 expression in human airway smooth muscle cells: role of MAPK (Erk1/2, JNK, and p38) pathways. *J Immunol* 177:4064-4071.
500. von Vietinghoff, S., and K. Ley. 2009. IL-17A controls IL-17F production and maintains blood neutrophil counts in mice. *J Immunol* 183:865-873.
501. Yang, X. O., S. H. Chang, H. Park, R. Nurieva, B. Shah, L. Acero, Y.-H. Wang, K. S. Schluns, R. R. Broaddus, Z. Zhu, and C. Dong. 2008. Regulation of inflammatory responses by IL-17F. *J. Exp. Med.* 205:1063-1075.
502. Nasso, M., G. Fedele, F. Spensieri, R. Palazzo, P. Costantino, R. Rappuoli, and C. M. Ausiello. 2009. Genetically detoxified pertussis toxin induces Th1/Th17 immune response through MAPKs and IL-10-dependent mechanisms. *J Immunol* 183:1892-1899.
503. Yao, Z., M. K. Spriggs, J. M. Derry, L. Strockbine, L. S. Park, T. VandenBos, J. D. Zappone, S. L. Painter, and R. J. Armitage. 1997. Molecular characterization of the human interleukin (IL)-17 receptor. *Cytokine* 9:794-800.
504. Moseley, T. A., D. R. Haudenschild, L. Rose, and A. H. Reddi. 2003. Interleukin-17 family and IL-17 receptors. *Cytokine Growth Factor Rev* 14:155-174.
505. Shen, F., Z. Hu, J. Goswami, and S. L. Gaffen. 2006. Identification of common transcriptional regulatory elements in interleukin-17 target genes. *J Biol Chem* 281:24138-24148.

506. Lindemann, M. J., Z. Hu, M. Benczik, K. D. Liu, and S. L. Gaffen. 2008. Differential regulation of the IL-17 receptor by gammac cytokines: inhibitory signaling by the phosphatidylinositol 3-kinase pathway. *J Biol Chem* 283:14100-14108.
507. Toy, D., D. Kugler, M. Wolfson, T. V. Bos, J. Gurgel, J. Derry, J. Tocker, and J. Peschon. 2006. Cutting Edge: Interleukin 17 Signals through a Heteromeric Receptor Complex. *J Immunol* 177:36-39.
508. Kuestner, R. E., D. W. Taft, A. Haran, C. S. Brandt, T. Brender, K. Lum, B. Harder, S. Okada, C. D. Ostrander, J. L. Kreindler, S. J. Aujla, B. Reardon, M. Moore, P. Shea, R. Schreckhise, T. R. Bukowski, S. Presnell, P. Guerra-Lewis, J. Parrish-Novak, J. L. Ellsworth, S. Jaspers, K. E. Lewis, M. Appleby, J. K. Kolls, M. Rixon, J. W. West, Z. Gao, and S. D. Levin. 2007. Identification of the IL-17 receptor related molecule IL-17RC as the receptor for IL-17F. *J Immunol* 179:5462-5473.
509. Hymowitz, S. G., E. H. Filvaroff, J. Yin, J. Lee, L. Cai, P. Risser, M. Maruoka, W. Mao, J. Foster, R. F. Kelley, G. Pan, A. L. Gurney, A. M. de Vos, and M. A. Starovasnik. 2001. IL-17s adopt a cystine knot fold: structure and activity of a novel cytokine, IL-17F, and implications for receptor binding. *EMBO J* 20:5332-5341.
510. Gomez-Rodriguez, J., N. Sahu, R. Handon, T. S. Davidson, S. M. Anderson, M. R. Kirby, A. August, and P. L. Schwartzberg. 2009. Differential expression of interleukin-17A and -17F is coupled to T cell receptor signaling via inducible T cell kinase. *Immunity* 31:587-597.
511. Chen, S., F. Lin, M. E. Shin, F. Wang, L. Shen, and H. E. Hamm. 2008. RACK1 regulates directional cell migration by acting on G betagamma at the interface with its effectors PLC beta and PI3K gamma. *Mol Biol Cell* 19:3909-3922.
512. Gaffen, S. L. 2009. Structure and signalling in the IL-17 receptor family. *Nat Rev Immunol* 9:556-567.
513. Li, T.-S., X.-N. Li, Z.-J. Chang, X.-Y. Fu, and L. Liu. 2006. Identification and functional characterization of a novel interleukin 17 receptor: A possible mitogenic activation through ras/mitogen-activated protein kinase signaling pathway. *Cellular Signalling* 18:1287-1298.
514. Tsang, M., R. Friesel, T. Kudoh, and I. B. Dawid. 2002. Identification of Sef, a novel modulator of FGF signalling. *Nat Cell Biol* 4:165-169.
515. Shen, F., N. Li, P. Gade, D. V. Kalvakolanu, T. Weibley, B. Doble, J. R. Woodgett, T. D. Wood, and S. L. Gaffen. 2009. IL-17 Receptor Signaling Inhibits C/EBP{beta} by Sequential Phosphorylation of the Regulatory 2 Domain. *Sci. Signal.* 2:ra8-.
516. Huang, F., C. Y. Kao, S. Wachi, P. Thai, J. Ryu, and R. Wu. 2007. Requirement for both JAK-mediated PI3K signaling and ACT1/TRAF6/TAK1-dependent NF-kappaB activation by IL-17A in enhancing cytokine expression in human airway epithelial cells. *J Immunol* 179:6504-6513.
517. Kim, H. R., M. L. Cho, K. W. Kim, J. Y. Juhn, S. Y. Hwang, C. H. Yoon, S. H. Park, S. H. Lee, and H. Y. Kim. 2007. Up-regulation of IL-23p19 expression in rheumatoid arthritis synovial fibroblasts by IL-17 through PI3-kinase-, NF-kappaB- and p38 MAPK-dependent signalling pathways. *Rheumatology* 46:57-64.

518. Nurieva, R., X. O. Yang, Y. Chung, and C. Dong. 2009. Cutting edge: in vitro generated Th17 cells maintain their cytokine expression program in normal but not lymphopenic hosts. *J Immunol* 182:2565-2568.
519. Berg, L. J. 2009. Strength of T cell receptor signaling strikes again. *Immunity* 31:529-531.
520. Yang, X. O., S. H. Chang, H. Park, R. Nurieva, B. Shah, L. Acero, Y.-H. Wang, K. S. Schluns, R. R. Broaddus, Z. Zhu, and C. Dong. 2008. Regulation of inflammatory responses by IL-17F. *J. Exp. Med.*: 205 1063-1075
521. Hou, W., H. S. Kang, and B. S. Kim. 2009. Th17 cells enhance viral persistence and inhibit T cell cytotoxicity in a model of chronic virus infection. *J Exp Med* 206:313-328.
522. Hsu, H. C., P. Yang, J. Wang, Q. Wu, R. Myers, J. Chen, J. Yi, T. Guentert, A. Tousson, A. L. Stanus, T. V. Le, R. G. Lorenz, H. Xu, J. K. Kolls, R. H. Carter, D. D. Chaplin, R. W. Williams, and J. D. Mountz. 2008. Interleukin 17-producing T helper cells and interleukin 17 orchestrate autoreactive germinal center development in autoimmune BXD2 mice. *Nat Immunol* 9:166-175.